Actuarial and Financial Risk Management in Networks

Von der Fakultät für Mathematik und Physik
der Gottfried Wilhelm Leibniz Universität Hannover

zur Erlangung des akademischen Grades
Doktorin der Naturwissenschaften
Dr. rer. nat.

genehmigte Dissertation von

M.Sc. Kerstin Awiszus

2020

Referent: Prof. Dr. Stefan Weber
Korreferent: Prof. Dr. Agostino Capponi
Korreferent: Prof. Dr. Ralf Korn
Korreferentin: Prof. Dr. Luitgard A. M. Veraart
Tag der Promotion: 17. Juli 2020

Actuarial and Financial Risk Management in Networks

M.Sc. Kerstin Awiszus
Leibniz Universität Hannover

Abstract

Interconnectedness constitutes a key characteristic of actuarial and financial systems. In regular times, it facilitates the provision of the systems' important services to society. In times of crisis, however, it enables the spread of contagious distress that may adversely affect the overall economy and amplify crisis situations. In this thesis, we introduce and analyze two financial and one actuarial network model representing three particular risk management problems that arise from different forms of interconnectedness.

First, we consider the spread of financial losses and defaults in a comprehensive model of a banking network. Distress therein may propagate through various forms of connections such as direct financial obligations, bankruptcy costs, fire sales, and cross-holdings. For the integrated financial market, we prove the existence of a price-payment equilibrium and design an algorithm for its computation. The corresponding number of defaults is analyzed in several comparative case studies. These illustrate the individual and joint impact of the considered interaction channels on systemic risk.

Second, we study the problem of minimizing market inefficiencies, defined as deviations of realized asset prices from fundamental values, as a function of the network of banks' overlapping asset portfolios. Prices are pressured from trading actions of the leverage targeting banks, which rebalance their portfolios in response to exogenous asset shocks. We prove the existence of a network of efficient asset holdings and characterize its properties and sensitivities. In particular, we find that the standard paradigm of asset portfolio diversification may cause tremendous market inefficiencies, especially during crisis situations.

Third, we consider insurance against cyber epidemics. Infectious cyber threats, such as viruses and worms, diffuse within a network of possibly insured parties. Since the infection may affect many different agents at the same time, a provider of cyber insurance is exposed to significant accumulation risk. We build and analyze a stochastic model of losses generated by infectious cyber threats based on interacting particle systems and marked point processes. Together with a novel polynomial and mean-field approximation, our approach allows to explicitly compute prices for different forms of cyber insurance contracts. Numerical case studies demonstrate the impact of the network topology and indicate that higher order approximations are indispensable for the analysis of non-linear contracts.

Keywords: Risk Management, Networks, Systemic Risk, Financial Contagion, Cross-Holdings, Fire Sales, Bankruptcy Costs, Systemic Significance, Price Pressure, Leverage Targeting, Market Efficiency, Cyber Insurance, Emerging Risks, Mean-Field Approximation.

Contents

1 Introduction **1**

2 The Joint Impact of Bankruptcy Costs, Fire Sales, and Cross-Holdings on Systemic Risk in Financial Networks **7**

2.1 An Integrated Financial Network Model 10
2.1.1 Assets and Liabilities 10
2.1.2 Net Worth 13
2.1.3 Price of the Illiquid Asset 13
2.1.4 Payment Vector 14
2.2 Existence of Equilibria and an Algorithm for their Computation 16
2.3 Case Studies 19
2.3.1 Erdős–Rényi Random Networks 20
2.3.2 Core-Periphery Random Networks 32
2.4 Conclusion 39
2.5 Proofs 40
2.6 Appendix: Price-Payment Equilibria Example 47
2.7 Appendix: Cross-Holdings with Price Impact 48

3 Market Efficient Portfolios in a Systemic Economy **51**

3.1 Model Specification 55
3.1.1 The Banking Sector 56
3.1.2 The Nonbanking Sector 57
3.1.3 Asset Prices 58
3.2 Market Inefficiencies and Systemic Significance 59
3.2.1 Market Capitalization and Deviation from Efficiency 59
3.2.2 Systemic Significance 60
3.3 f-Efficient Holdings 61
3.3.1 Characterization of f-Efficient Holdings 62
3.3.2 When is Diversification f-Efficient? 65
3.4 Comparative Statics and Examples 66
3.4.1 The Case $N = K = 2$ 67

3.4.2 The Case $N = K = 3$ . . . 70
3.4.3 Systemic Significance, Market Scenarios, and Asset Holdings . . 71
3.5 Conclusion . . . 76
3.6 Appendix: Proofs . . . 77
3.6.1 Proofs of Section 3.1 . . . 77
3.6.2 Proofs of Section 3.3 . . . 78
3.6.3 Proofs of Section 3.4 . . . 86
3.7 Appendix: Non-Uniqueness of Asset Holdings . . . 88
3.8 Appendix: f-Efficient Liquidation Strategies . . . 90
3.8.1 General Derivation . . . 90
3.8.2 Liquidation Strategy Example . . . 92
3.9 Appendix: Majorization and Diversity vs. Diversification . . . 93

4 Pricing of Cyber Insurance Contracts in a Network Model 97
4.1 Exact Loss Model . . . 101
4.1.1 Spread Process . . . 102
4.1.2 Claims Processes . . . 103
4.2 Approximations . . . 104
4.2.1 Polynomial Approximation of Non-Linear Claim Functions . . . 104
4.2.2 Mean-Field Approximation of Moments . . . 108
4.3 Case Studies . . . 122
4.3.1 Model Setting . . . 122
4.3.2 Model Results . . . 124
4.4 Conclusion . . . 129
4.5 Appendix: Proofs . . . 129
4.6 Appendix: Basic ODE Theory . . . 134
4.7 Appendix: Matrix Form of the n-th Order Mean-Field Approximation . . 135
4.8 Appendix: Adjacency Matrices . . . 139

Bibliography 141

List of Figures 151

List of Tables 155

Publications 157

Acknowledgment 159

1 Introduction

Interconnectedness constitutes a key characteristic of financial and actuarial systems. Banks and insurance companies are directly connected through financial and other contractual obligations, such as lending agreements, engagement in joint projects, and/or indirectly connected through, e.g., similarities in their asset portfolios. Connections arise naturally as they facilitate the provision of the systems' important financial and actuarial services to society: Liquidity can be provided, collaboration may yield symbiotic effects, and risks can be transferred, shared, and appropriately diversified. However, in times of distress, it is this interconnectedness that may trigger and amplify financial crises through *contagion effects*: If one firm gets into trouble, distress may spread via the connections within the system, possibly affecting many different firms at the same time.

Different forms of connections may serve as channels for the spread of various forms of contagious distress. For example, in the 2007-2009 financial crisis, the default of Lehman Brothers triggered *financial losses and defaults* among many market participants worldwide. In addition to direct promised payments that could not be fulfilled, many financial institutions were indirectly connected through their asset portfolios by holding large amounts of credit default obligation derivatives that lost dramatically in value as a consequence of the US house price decline. This created *market inefficiencies* as asset prices did not reflect the fundamental asset values anymore. Similar contagion and amplification effects can also be observed in other situations, for example, when considering the spread of *(cyber) epidemics* caused by, e.g., (computer) viruses.

In order to manage such risks, it is necessary to gain a deeper understanding of the driving factors behind contagion effects in interconnected systems. Effective risk management requires the development of suitable tools and models. From a mathematical perspective, interconnectedness can adequately be captured by the concept of networks. A network $G = (N, E)$ consists of a set of nodes N connected through (possibly weighted and/or directed) edges E. In this thesis, we study three different risk management problems that arise from interconnectedness. They are represented by three different types of networks illustrated in Figure 1.1:

- As the first topic of this thesis, we consider the propagation of *financial losses and defaults* in a banking network comprising different interaction channels. We ana-

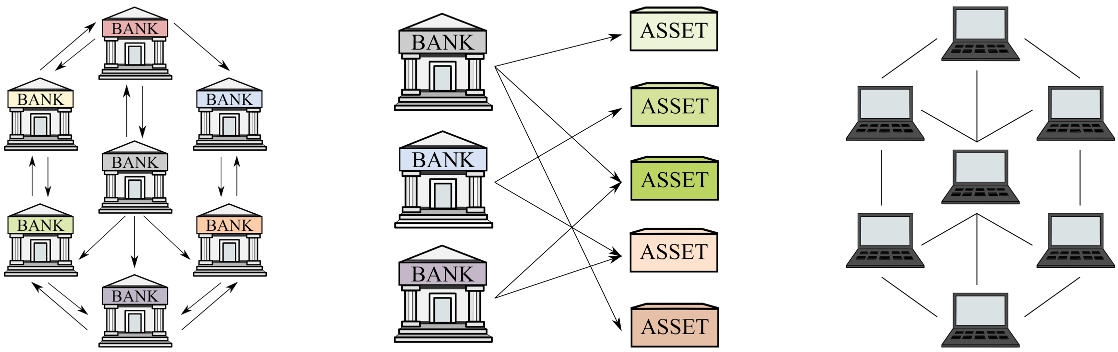

(a) Chapter 2 **(b) Chapter 3** **(c) Chapter 4**

Figure 1.1: Example networks for the models in the three chapters of this thesis.

lyze, for the first time from a joint perspective, the impact of direct financial obligations between market participants, indirect connections through one commonly held illiquid asset (posing the threat of so-called fire sales), cross-holdings, and bankruptcy costs on the risk of financial system failure. If one bank is unable to repay its debt to other banks, distress may spread throughout the system. This effect may be amplified by fire sales and frictions like bankruptcy costs. The underlying basic financial system is modeled as a directed weighted network, where the nodes are banks and the edges represent directed financial obligations, see Figure 1.1 (a). This topic is covered in Chapter 2.

- Second, we study the influence of the structure of banks' asset holdings on *market inefficiencies*. When banks hold similar types of assets and, in response to exogenous asset shocks, are forced to purchase or sell them at the same time (e.g., to maintain a certain leverage requirement), this may push asset prices away from their fundamental values, i.e., create market inefficiencies. We develop an explicit expression for the matrix of those asset holdings that minimize market inefficiencies. This matrix can be represented as a bipartite weighted network in which the edges capture the size of the banks' holdings in the given assets, see Figure 1.1 (b). The problem is analyzed in Chapter 3.

- The third and last topic of this thesis is insurance against *cyber epidemics*. We focus on cyber threats that spread out in a data network, e.g., viruses, worms or Trojans. Possibly affecting many different agents at the same time, these threats facilitate cyber attacks that involve a large proportion of the insured network. An insurance company covering losses generated by infectious cyber risks is thus faced with significant accumulation risk. We provide a method to explicitly calculate prices for different forms of cyber insurance contracts against infectious cyber threats. The underlying interconnectedness is modeled using an undirected network, where a node may represent an insured party, e.g., an entire firm, a business division or a single computer that is connected to other agents via, e.g., business contacts, e-mail correspondence or physical wiring, see Figure 1.1 (c). This topic is analyzed in Chapter 4.

Network theory thus serves as a unified approach to modeling and analyzing the three different risk management problems that constitute this thesis. All chapters of this thesis are self-contained. A review of the related literature is given in each chapter. We provide the following main contributions.

Contributions of Chapter 2. In Chapter 2, we construct a comprehensive model of a banking system that integrates multiple interaction channels. Banks interact with each other directly through credit contracts and cross-shareholdings as well as indirectly through similarities in asset portfolios (here, modeled by a single illiquid asset). Through these connections, financial distress may propagate. Bankruptcy costs may additionally amplify the interaction effects.

(i) To the best of our knowledge, the chapter presents the first joint financial network model that integrates all of the above mentioned interaction and amplification effects at the same time.

(ii) In the model, we are able to prove the existence of a (non-necessarily unique) clearing vector that describes the payments made in a hypothetical clearing scenario. Clearing payments as well as the clearing price of the commonly held illiquid asset are characterized as fixed points in a clearing equilibrium and constructed via a fictitious default algorithm.

(iii) In numerical case studies, we analyze the impact of all single interaction channels on clearing payments and on the number of defaults. We find that bankruptcy costs as well as overlapping asset portfolios may trigger and amplify systemic crises. Cross-shareholdings, in contrast, may possess a stabilizing effect, if they can be liquidated without any costs.

(iv) Since we provide a joint model, we are able to include multiple interaction channels at the same time. This allows us, firstly, to assess the robustness of conclusions regarding the impact of single interaction channels from a general perspective. Secondly, regulatory policies can be studied in a robust manner. In particular, we analyze the efficiency of capital requirements. We find that classical capital adequacy ratios based on risk-weighted assets may be misleading since they may suggest the same capital requirement for parameter values that are associated with completely different levels of risk. In contrast, in our model, the more sophisticated approach of systemic risk measures is shown to be a much better alternative.

Contributions of Chapter 3. Chapter 3 focuses in detail on one particular interaction channel in the financial system: overlapping asset portfolios. As seen in Chapter 2, similarities in banks' asset holdings may create a strong impact on asset prices. In Chapter 3, prices are now pressured from trading actions of leverage targeting banks, which rebalance their portfolios in response to exogenous asset shocks.

(i) We study market inefficiency, defined as the deviation of asset prices from their fundamental values, as a function of the structure of banks' asset portfolios. The smaller the deviation, the more efficient the financial market. This view complements the traditional analysis of systemic risk in financial markets, as also done in Chapter 2, that solely focuses on risk statistics such as the number of defaults or quantitative measures of the downside risk.

(ii) We identify the key driving factors and characterize the structure of those banks' asset portfolios that minimize market inefficiency. We prove existence, study uniqueness, and investigate the distance to diversification of such efficient holdings.

(iii) In particular, we show that the standard paradigm of diversification of asset portfolios might lead to tremendous market inefficiencies, if the underlying assets are not completely homogeneous. This effect is even stronger during times of crisis.

(iv) We analyze the role of leverage targets, liquidation strategies, price elasticities of a nonbanking sector for various assets, and asset shocks. We identify two key sufficient statistics determining banks' efficient holdings: systemic significance and the moments of the distribution of asset shocks. A bank possesses a high systemic significance, e.g., if it targets a high leverage ratio or liquidates less liquid assets. Consistent with intuition, we show that in efficient holding situations, a systemically more significant bank is assigned less risky assets.

(v) Finally, we detect an important tradeoff between bank diversity and asset diversification: Heterogeneity in the systemic significances across banks moves efficient holdings closer to diversification, while heterogeneity of the moments of asset shock distributions moves efficient holdings away from diversification.

Contributions of Chapter 4. The final Chapter 4 of this thesis complements our analysis by extending network risk management to an actuarial context. Firms interact with each other in different ways, e.g., through e-mail contacts. This creates the possibility of the spread of certain cyber threats, e.g., viruses, worms or Trojans, which facilitate attacks throughout the firm network and, thus, may cause and amplify financial losses. No matter how elaborate self-protection and risk management strategies of individual firms against such infectious cyber threats become, some residual risks will remain that require insurance solutions.

(i) To the best of our knowledge, Chapter 4 develops the first mathematical model of insured losses generated by infectious cyber threats. The stochastic model consists of two key ingredients: a Markov process modeling the spread of the cyber infection, and a marked point process that captures the number of attacks and loss sizes at attack times.

(ii) For the spread process, we build on the well-known SIS model in networks and develop a novel general framework for n-th order mean-field approximations of its moments. We analyze special cases and properties such as the accuracy of the approximation.

(iii) From an actuarial perspective, we provide a new methodology to explicitly calculate an insurance company's expected aggregate losses. The method is applicable to a large variety of contract designs and can thus be used for pricing decisions.

(iv) In numerical case studies, we analyze the role of the topology of the network of insured firms. We show that this structure possesses a significant impact on the size of expected aggregate losses. Our findings suggest that the infection and healing parameters of the spread process as well as the network topology are key ingredients for the pricing of cyber insurance contracts.

2 The Joint Impact of Bankruptcy Costs, Fire Sales, and Cross-Holdings on Systemic Risk in Financial Networks

The original version of this chapter was previously published in *Probability, Uncertainty and Quantitative Risk*, 2(9):1–38, 2017, see Weber and Weske (2017).

"Systemic risk refers to the risk that a financial system as a whole is susceptible to failures initiated by the characteristics of the system itself."[1] If strong links between financial institutions are present, a shock to only a small number of entities might propagate through the system and trigger substantial financial losses. Significant dependence can thus increase the risk of a system-wide breakdown.

Financial institutions influence each other via direct or indirect channels such as credit contracts, similar asset portfolios that are jointly exposed to price impact in market crises, and cross-shareholdings. Frictions like, e.g., bankruptcy costs may amplify the impact of the effect of the firms' interaction. The aim of the current chapter consists in constructing and analyzing a comprehensive model that integrates all effects mentioned above. This multi-factor setting allows to assess regulatory policies in a robust manner. To the best of our knowledge, such a contribution is still missing in the literature.

1. We prove the existence of a clearing equilibrium that is not necessarily unique and provide an algorithm for the computation of the greatest and the least equilibrium. The equilibrium is characterized by the vector of clearing payments and the price of the commonly held illiquid asset that is exposed to price effects.

2. We study the impact of bankruptcy costs, fire sales, and cross-holdings on systemic risk in numerical experiments. We demonstrate that fire sales and bankruptcy costs can trigger and amplify financial crises. Policies that mitigate their impact might significantly enhance the resilience of the financial system. Cross-holdings do, in contrast, have a stabilizing effect, if they can be exchanged for liquid assets. Central banks that engage in such a market can reduce the number of defaults in the system.

3. We study policy implications and regulatory instruments, including central bank

[1] See Feinstein et al. (2017)

guarantees, quantitative easing, the significance of last wills of financial institutions, and the efficiency of capital requirements. We find that capital adequacy ratios based on risk-weighted assets reduce systemic risk, if they are sufficiently high. However, they do not rely on any statistics that capture systemic risk in a proper way. Comparative statics show that capital adequacy ratios can be equal for varying parameters of our model that are associated with completely different levels of systemic risk. This demonstrates that classical capital adequacy ratios are a very rough instrument. A much better alternative are systemic risk measures that we analyze in the last section.

Previous papers do not allow an assessment of the robustness of their conclusions since they only focus on particular aspects of systemic risk neglecting all other driving factors. Our model, in contrast, shows to what extent causal relations that were previously discovered are preserved within a general framework; it also detects the differences that might occur. In summary, we find that many of our qualitative results are quite robust across different network structures and for a large number of driving factors. However, the relative importance of interacting contagion channels can only be characterized in the joint model. This justifies—for the first time from a general perspective—the relevance of previous approaches, but indicates at the same time that quantitative predictions and the design of regulatory policies require a more sophisticated analysis.

Literature

Our approach extends the equilibrium approach of Eisenberg and Noe (2001). Their seminal paper models interbank contagion within a network of nominal liabilities and proves the existence and uniqueness of a clearing payment vector that endogenously captures losses given default. At the same time, they construct an efficient algorithm for the computation of the clearing vector. Closely related empirical studies can, e.g., be found in Cont et al. (2013), Elsinger et al. (2006), Glasserman and Young (2015), and Upper (2011). These cast doubt that empirical patterns of contagious defaults can solely be explained by networks of nominal liabilities.

In this chapter, we integrate multiple interaction channels and amplifying mechanisms of contagion, including bankruptcy costs, fire sales, and cross-holdings. While we investigate their joint impact, up to now the literature has only been studying these factors separately: Bankruptcy costs are, for example, considered by Rogers and Veraart (2013), Elliott et al. (2014), Elsinger (2009), and Glasserman and Young (2015); cross-holdings, e.g., by Suzuki (2002), Elsinger (2009), Elliott et al. (2014), Fischer (2014), and Karl and Fischer (2014). Cifuentes, Ferrucci, and Shin (2005) incorporate fire sales into the setting of Eisenberg and Noe (2001); their approach is further extended by Gai and Kapadia

(2010), Nier et al. (2007), Amini et al. (2013), Chen et al. (2016), and Feinstein (2017). Most of these papers consider only one extension of the basic framework.[2] For a detailed review of the literature see also Staum (2013).

All of these mechanisms are important channels of contagion. In contrast to direct liabilities and cross-holdings that are described by network structures, fire sales are a global transmission mechanism. It is, for example, defined in Shleifer and Vishny (2011):

> "A fire sale is essentially a forced sale of an asset at a dislocated price. The asset sale is forced in the sense that the seller cannot pay creditors without selling assets. The price is dislocated because the highest potential bidders are typically involved in a similar activity as the seller, and are therefore themselves indebted and cannot borrow more to buy the asset. Indeed, rather than bidding for the asset, they might be selling similar assets themselves. Assets are then bought by nonspecialists who, knowing that they have less expertise with the assets in question, are only willing to buy at valuations that are much lower."

Evidence is discussed in several papers including Brunnermeier (2009), Cont and Wagalath (2016), Coval and Stafford (2007), Jotikasthira et al. (2012), Khandani and Lo (2011), and Shleifer and Vishny (1992). In real markets, fire sales typically refer to the liquidation of portfolios. Empirical data show that this is related to increased correlations as well as price impact. A single representative illiquid asset can thus be used as a first approximation. This is the approach that we take in our model in order to keep the suggested framework simple. For an analysis of market inefficiencies as a function of the banks' holding network of multiple (illiquid) assets, we refer to Chapter 3 of this thesis.

Outline

This chapter is organized as follows. In Section 2.1, we present our model of the financial system and provide a preliminary analysis of net worth, price impact, and clearing payment vectors. The existence of a price-payment equilibrium consisting of a clearing payment vector and a clearing price of the illiquid asset is demonstrated in Section 2.2. Moreover, we provide an extension of the *fictitious default algorithm* of Eisenberg and Noe (2001) in order to compute the greatest and least equilibrium. Section 2.3 focuses

[2] Elliott et al. (2014) and Elsinger (2009) consider both cross-holdings and bankruptcy costs. However, the underlying network model of Elliott et al. (2014) does not explicitly feature direct liabilities, but aggregates instead all dependencies linearly including cross-holdings. Elsinger (2009) uses a modified Eisenberg–Noe model, but only includes a stylized form of bankruptcy costs. This is primarily done in order to illustrate that the profitability of bailouts depends on these costs.

on numerical case studies which constitute a key part of this chapter. These illustrate the individual and joint impact of bankruptcy costs, fire sales, and cross-holdings on systemic risk, measured as the number of defaults in the greatest price-payment equilibrium. We describe various regulatory policies and analyze their efficiency. The main conclusions and questions for future research are discussed in Section 2.4. All proofs of the results in Sections 2.1 and 2.2 are presented in Section 2.5.

2.1 An Integrated Financial Network Model

We analyze default in a one-period interbank market model in which banks are connected to each other via three different channels:

- **Direct liabilities**: Banks have nominal liabilities against each other. These liabilities are promises that will only partially be fulfilled if some of the banks default.
- **Fire sales**: If the portfolios of different banks include common assets, changes in asset prices simultaneously influence the net worths of these banks. Common holdings may give rise to substantial systemic risk, if illiquid assets are sold in large quantities and prices decrease significantly. For simplicity, our model assumes the existence of a single (representative) illiquid asset.
- **Cross-holdings**: Banks may, in addition, hold shares of each other. In this case, the net worths of banks depends on the net worths of other banks due to these cross-holdings.

The single period is interpreted as a snapshot of a banking system that continues to exist afterwards. The net worth of each bank in the financial network depends on the realized payments, the price of the commonly held illiquid asset, and the net worths of the other banks. In the first step, we will describe how the value of asset holdings of an individual bank can be computed if these three key factors are exogenously fixed. In the second step, we will construct and analyze an equilibrium model that allows an endogenous computation of the net worths of all banks, a clearing payment vector, and a realized average price of the illiquid asset.

2.1.1 Assets and Liabilities

Letting $\mathcal{N} = \{1, \dots, n\}$ be the set of banks in the financial system, we denote by $p \in \mathbb{R}^n_+$ the realized payments of the banks, by $w \in \mathbb{R}^n_+$ the vector of net worths of the banks, and by $q \in \mathbb{R}_+$ the price of the representative illiquid asset. In the first step, we suppose that these quantities are exogenously specified.

External Assets. As suggested by Cifuentes et al. (2005), we consider banks that hold two assets which are external to the banking system: an amount of $r \in \mathbb{R}^n_+$ shares of a liquid asset (e.g., cash) and $s \in \mathbb{R}^n_+$ shares of an illiquid asset. Assuming that the liquid asset's price remains constant at one monetary unit, the value of bank i's external assets is given by $r_i + s_i q$, if the price of the illiquid asset is q.

Liabilities. Each bank has nominal liabilities to the other banks for the considered time horizon. Analogous to Eisenberg and Noe (2001), we suppose that these liabilities are represented by a *nominal liabilities matrix* $L \in \mathbb{R}^{n \times n}$: for all $i, j \in \mathcal{N}$, $L_{ij} \geq 0$ describes the nominal obligation of bank i towards bank j; no bank may hold a liability against itself, i.e., $L_{ii} = 0$ for all $i \in \mathcal{N}$. In addition, banks may have further liabilities $l \in \mathbb{R}^n_+$ to entities outside the banking system; here, the component l_i is interpreted as the liability of bank i to the outside.

The *vector of total liabilities* $\bar{p}$ captures all liabilities of the banks in the system; i.e., its component $\bar{p}_i$ equals the total liabilities of bank i and is given by $\bar{p}_i = \sum_{j \in \mathcal{N}} L_{ij} + l_i$, for $i \in \mathcal{N}$. If all banks are able to fulfill their total obligations, $\bar{p}$ indeed equals the realized payments p of the banks. If, in contrast, some banks do not possess sufficient resources to meet their obligations, then $p \leq \bar{p}$, where the inequality is interpreted componentwise.

Following Eisenberg and Noe (2001), we assume that in case of bank i's default, its realized payments $p_i < \bar{p}_i$ will be distributed proportionally among its creditors according to the size of each creditor's claim. Therefore, we define the *relative liabilities matrix* $\Pi \in \mathbb{R}^{n \times n}$ by $\Pi_{ij} = L_{ij}/\bar{p}_i$, if $\bar{p}_i > 0$, and $\Pi_{ij} = 0$, otherwise. Thus, the entry Π_{ij} captures the size of the interbank obligations of bank i towards bank j in proportion to the size of i's total liabilities. This implies that for a given vector of realized payments p, the value of bank i's interbank claims is given by $\sum_{j \in \mathcal{N}} \Pi_{ji} p_j$.

Cross-Holdings. Each bank may hold shares of the other banks. Following Elsinger (2009), these holdings will be captured by a *cross-holdings matrix* $C \in \mathbb{R}^{n \times n}$: the component C_{ij} denotes the fraction of bank i's equity that is held by bank j. We assume that the cross-holdings are nonnegative, i.e., $C_{ij} \geq 0$ for all $i, j \in \mathcal{N}$, and that a bank is not allowed to hold shares of itself, i.e., $C_{ii} = 0$ for all $i \in \mathcal{N}$. The technical assumption $\sum_{j \in \mathcal{N}} C_{ij} < 1$, $i \in \mathcal{N}$, guarantees that the net worth of each bank, as introduced below, is well-defined. If both a cross-holdings matrix C and a vector of positive net worths w are given, the contribution of bank i's cross-holdings to its net worth is equal to $\sum_{j \in \mathcal{N}} C_{ji} w_j$. We also suppose limited liability of cross-holdings, i.e., if bank j's net worth w_j is negative, cross-holdings of bank j do not negatively affect the net worths of other banks.

It is well-known that cross-holdings inflate the value of the financial system, see Brioschi et al. (1989), Fedenia et al. (1994), and Elliott et al. (2014). This, in particular, refers to the fact that the aggregated net worth of all banks will be larger than the value of total assets if cross-holdings are present. As argued in Brioschi et al. (1989), Fedenia et al. (1994), and Elliott et al. (2014), net worths need to be adjusted by an auxiliary factor that guarantees the conservation of value in the system. The *market value* of bank i should thus be computed as $(1 - \sum_{j \in \mathcal{N}} C_{ij}) w_i$ for $w_i \geq 0$.

Total Net Worth. We will now describe how each bank's net worth is calculated. In order to fulfill its obligation $\bar{p}_i$, bank i will first use its liquid external assets r_i and its interbank revenues $\sum_{j \in \mathcal{N}} \Pi_{ji} p_j$. If these are insufficient, the bank is left with its illiquid asset and cross-holdings. We assume that bank i's cross-holdings $\sum_{j \in \mathcal{N}} C_{ji} w_j$ can be exchanged against cash (possibly involving central banks or governments). However, we suppose that bank i can only realize a fraction of $\lambda_i \in [0,1]$. An alternative way to model price impact of cross-holdings liquidation via inverse demand functions is presented in Appendix 2.7.

Each bank decides on the order of liquidation. This decision is captured by an indicator variable $\mathbb{I}_i \in \{0,1\}$, where $\mathbb{I}_i = 1$ represents the case that bank i exchanges its total cross-holdings against cash before it starts selling the illiquid asset; $\mathbb{I}_i = 0$ refers to the reversed order of liquidation. Banks liquidate their cross-holdings proportionally, i.e., the percentage of cross-holdings that are exchanged against cash can be computed as

$$\nu_i(p,q,w) := \min\left(\frac{\max(\bar{p}_i - r_i - \sum_{j \in \mathcal{N}} \Pi_{ji} p_j - (1 - \mathbb{I}_i) s_i q, 0)}{\lambda_i \sum_{j \in \mathcal{N}} C_{ji} \max(w_j, 0)}, 1 \right) \in [0,1].$$

The remaining share $1 - \nu_i(p,q,w)$ remains on the bank's balance sheet and is not subject to the price impact modeled by the factor λ_i. Setting $\mu_i(p,q,w) := \nu_i(p,q,w)\lambda_i + 1 - \nu_i(p,q,w)$, $i \in \mathcal{N}$, the net worth of bank i is given by

$$w_i = r_i + s_i q + \sum_{j \in \mathcal{N}} \Pi_{ji} p_j + \mu_i(p,q,w) \sum_{j \in \mathcal{N}} C_{ji} \max(w_j, 0) - \bar{p}_i.$$

The bank is *in default* if it cannot cover its liabilities, i.e., if $w_i < 0$.

As mentioned before, due to cross-holdings, the net worths of the banks differ from their market values, see Brioschi et al. (1989), Fedenia et al. (1994), and Elliott et al. (2014). We will, however, focus on default count statistics which can be computed in terms of the vector of net worths. Market values will only be considered explicitly in the numerical case studies.

As defined above, the net worth of bank i depends on the realized payments p, the price q of the illiquid asset, and all other banks' net worths w. In the following sections, we provide a method to derive these three key quantities *endogenously*.

2.1.2 Net Worth

Suppose first that p and q are fixed. In this situation, our aim is to define an equilibrium vector of the net worths of the banks. To simplify the notation, we write $\mathbf{0} := (0,\ldots,0)^T, \mathbf{1} := (1,\ldots,1)^T \in \mathbb{R}^n$, set $a \vee b := (\max(a_1,b_1),\ldots,\max(a_n,b_n))$ for $a,b \in \mathbb{R}^n$, and denote by $\mathrm{Diag}(\mu(p,q,w))$ the diagonal matrix whose diagonal entries are given by the vector $\mu(p,q,w) := (\mu_1(p,q,w),\ldots,\mu_n(p,q,w))^T$.

Definition 2.1.1. For $p \in \mathbb{R}^n_+,\ q \in \mathbb{R}_+$, an *essential net worths vector* is a fixed-point vector $w^*(p,q) \in \mathbb{R}^n$ such that

$$w^*(p,q) = \Psi(w^*(p,q)), \tag{2.1}$$

where the function $\Psi : \mathbb{R}^n \to \mathbb{R}^n$ is defined by

$$\Psi(w) := r + sq + \Pi^T p + \mathrm{Diag}(\mu(p,q,w))C^T(w \vee \mathbf{0}) - \bar{p}. \tag{2.2}$$

The essential net worths vector is defined as a solution of the non-linear fixed-point problem (2.1). The following lemma shows that this equation always possesses a unique solution. A proof of this result is given in Section 2.5.

Lemma 2.1.2. *For all $p \in \mathbb{R}^n_+,\ q \in \mathbb{R}_+$:*

(a) The essential net worths vector $w^*(p,q)$ exists and is unique.

(b) The essential net worths vector is increasing in payments and prices:

$$\begin{aligned} p^1 \geq p^2 \quad &\Longrightarrow \quad w^*(p^1,q) \geq w^*(p^2,q), \\ q^1 \geq q^2 \quad &\Longrightarrow \quad w^*(p,q^1) \geq w^*(p,q^2). \end{aligned}$$

2.1.3 Price of the Illiquid Asset

We will now explain how the clearing vector p and the price q of the illiquid asset can endogenously be derived. The presence of the illiquid asset enables us to incorporate the effect of *fire sales* into the model. As described in the introduction, the basic economic idea is that, if a bank is unable to pay its outstanding debt in the considered period using its shares of the liquid asset and interbank payments, it can sell a proportion of its illiquid asset holdings at the current market price. This triggers an increase in the supply of the asset that can decrease its market price during times of crisis. Consequently, other banks holding the same asset are also affected by such a price decline. In particular, if they need to sell an amount of the illiquid asset themselves, the proceeds from this transaction are diminished. At the same time, the price is further pushed down.

To integrate this idea into our model, we assume that there exists an exogenously given positive continuous *inverse demand function* for the illiquid asset $f : [0, \sum_{i \in \mathcal{N}} s_i] \to (0, \infty)$, such that the price q of one unit of the illiquid asset is given by $q = f(\theta)$, where θ denotes the quantity of the illiquid asset that is sold in the market. We assume that $f(0) = q_0$ and that $\theta \mapsto f(\theta)$ is monotonically decreasing which indicates that the illiquid asset's price is decreasing in its supply. A fixed-point problem is present, since the amount sold depends on the price of the illiquid asset itself:

$$q = f(\theta(p,q))$$

for a given payment vector p and where

$$\theta(p,q) := \sum_{i \in \mathcal{N}} \min\left(\frac{\max[\bar{p}_i - r_i - \sum_{j \in \mathcal{N}} \Pi_{ji} p_j - \mathbb{I}_i \lambda_i \sum_{j \in \mathcal{N}} C_{ji} \max(w_j^*(p,q), 0), 0]}{q}, s_i\right)$$

signifies the total amount of the illiquid asset that is sold. If $\mathbb{I}_i = 1$, bank i exchanges its total cross-holdings against cash before selling the illiquid asset and, obviously, this decreases the asset's supply θ; here, $w^*(p,q)$ denotes the unique vector of essential net worths as introduced in Definition 2.1.1. We assume that all illiquid asset holdings are marked-to-market at the resulting price. Note that due to our assumptions, the price of the illiquid asset is both bounded from above by q_0 and from below by $q_{\min} := f(\sum_{i \in \mathcal{N}} s_i)$, since banks may at most sell their total holdings of the illiquid asset $\sum_{i \in \mathcal{N}} s_i$.

2.1.4 Payment Vector

In the final step, we define a *price-payment equilibrium* that endogenously derives the price of the illiquid asset as well as a corresponding clearing vector. We integrate one more effect that influences the clearing process, namely *bankruptcy costs*. In reality, a fraction of the recovery value of the assets will be lost to the obligors in case of default due to, e.g., legal and administrative expenses. Observe that bankruptcy costs and fire sales impact systemic risk differently. Firstly, bankruptcy costs are only incurred in the case of a default, while fire sales may also occur if there are no defaults in the system. Secondly, a fire sale may affect banks that are not connected to the triggering bank via direct credit contracts. Fire sales are a global channel of contagion, while bankruptcy costs are an amplifier of credit risk.

Following Rogers and Veraart (2013), we introduce two new parameters $0 \leq \alpha \leq 1$ and $0 \leq \beta \leq 1$, such that $1 - \alpha$ and $1 - \beta$ determine the frictional costs due to bankruptcy: A defaulting bank will only realize a fraction α of its external asset value, i.e., the value of the liquid and illiquid asset, and a fraction β of its interbank asset value, i.e., the value of interbank claims and cross-holdings. We further postulate that the clearing process satisfies the criteria of proportionality, limited liability, and absolute priority of debt, as outlined by Eisenberg and Noe (2001). Finally, we define a *price-payment equilibrium* as follows.

Definition 2.1.3. A *price-payment equilibrium* is a pair $(p^*, q^*) \in [\mathbf{0}, \bar{p}] \times [q_{\min}, q_0] \subseteq \mathbb{R}^{n+1}$, consisting of a *clearing payment vector* p^* and a *clearing price* q^*, such that

$$(p^*, q^*) = \Phi(p^*, q^*),$$

where $\Phi : \mathbb{R}^{n+1} \to \mathbb{R}^{n+1}$ is the function defined by

$$\Phi_i(p,q) := \begin{cases} \chi_i(p,q), & \text{for } i = 1, \ldots, n, \\ f(\theta(p,q)), & \text{for } i = n+1, \end{cases}$$

with

$$\chi_i(p,q) := \begin{cases} \bar{p}_i, & \text{if } r_i + s_i q + \eta_i(p,q) \geq \bar{p}_i, \\ \alpha[r_i + s_i q] + \beta\left[\eta_i(p,q)\right], & \text{otherwise}, \end{cases}$$

$$\eta_i(p,q) := \sum_{j \in \mathcal{N}} \Pi_{ji} p_j + \mu_i(p,q) \sum_{j \in \mathcal{N}} C_{ji} \max(w_j^*(p,q), 0),$$

$$\mu_i(p,q) = \nu_i(p,q)\lambda_i + 1 - \nu_i(p,q),$$

$$\nu_i(p,q) = \min\left(\frac{\max(\bar{p}_i - r_i - \sum_{j \in \mathcal{N}} \Pi_{ji} p_j - (1 - \mathbb{I}_i) s_i q, 0)}{\lambda_i \sum_{j \in \mathcal{N}} C_{ji} \max(w_j^*(p,q), 0)}, 1\right),$$

and

$$\theta(p,q) := \sum_{i \in \mathcal{N}} \min\left(\frac{\max(\bar{p}_i - r_i - \sum_{j \in \mathcal{N}} \Pi_{ji} p_j - \mathbb{I}_i \lambda_i \sum_{j \in \mathcal{N}} C_{ji} \max(w_j^*(p,q), 0), 0)}{q}, s_i\right).$$

In the combined equilibrium, the banks' clearing payments p^* are given as the fixed point of the function χ, and a clearing price of the illiquid asset q^* is found as a fixed point of the inverse demand function f. Hence, bank i pays its total liabilities $\bar{p}_i$, if its total asset value consisting of its external asset value $r_i + s_i q^*$ and interbank asset value $\eta_i(p^*, q^*)$ exceeds its liabilities. If this is not the case, bank i is in default and receives (and due to absolute priority of debt also pays out) only the given fractions α and β of its external and interbank asset value, respectively. The interbank asset value of bank i, $\eta_i(p^*, q^*)$, depends on the proportion of cross-holdings that are exchanged against liquid assets, $\nu_i(p^*, q^*)$, and this proportion is multiplied by $\lambda_i \in [0,1]$ as defined in $\mu_i(p^*, q^*)$. Finally, the amount of the illiquid asset that is sold in equilibrium is given by $\theta(p^*, q^*)$.

The price-payment equilibrium provides a solution to an *integrated financial system* which is characterized by $(\Pi, \bar{p}, r, s, \alpha, \beta, \lambda, f, C, \mathbb{I})$; here, $\lambda = (\lambda_1, \ldots, \lambda_n) \in [0,1]^n$ and $\mathbb{I} = (\mathbb{I}_1, \ldots, \mathbb{I}_n) \in \{0,1\}^n$. It admits a joint analysis of a network of liabilities, bankruptcy costs, cross-holdings, and fire sales as well as an analysis of models that incorporate only some of these effects. Namely, by choosing $\alpha = \beta = 1$, $s = \mathbf{0}$, or C as the zero $n \times n$ matrix, we can simply exclude the corresponding extensions from our system. This shows that the models of, e.g., Eisenberg and Noe (2001), Rogers and Veraart (2013), Cifuentes et al. (2005), and Elsinger (2009) are special cases of our integrated financial system.

2.2 Existence of Equilibria and an Algorithm for their Computation

The current section analyzes the existence and computation of equilibria. All proofs are provided in Section 2.5. We consider the ordered vector space $\langle \mathbb{R}^{n+1}, \leq \rangle$ equipped with the partial order $x \leq y :\Leftrightarrow x_i \leq y_i \ \forall i = 1, \ldots, n+1$ and use the notation $x < y :\Leftrightarrow (x \leq y \text{ and } \exists i : x_i \neq y_i)$. We will also use this ordering on linear subspaces. The following lemma states elementary properties of the function Φ, see Definition 2.1.3.

Lemma 2.2.1. *The function Φ has the following properties:*

(a) Φ is bounded: For all $(p,q) \in [\mathbf{0}, \bar{p}] \times [q_{\min}, q_0]$: $\Phi(p,q) \geq (\mathbf{0}, q_{\min})$ and $\Phi(p,q) \leq (\bar{p}, q_0)$,

(b) Φ is monotone: For $(p^1, q^1) \leq (p^2, q^2)$: $\Phi(p^1, q^1) \leq \Phi(p^2, q^2)$.

Lemma 2.2.1 enables us to apply Tarski's fixed-point theorem (Tarski, 1955, Theorem 1) to the function Φ proving the existence of equilibria.

Theorem 2.2.2. *Let $(\Pi, \bar{p}, r, s, \alpha, \beta, \lambda, C, \mathbb{I})$ be an integrated financial system. Then, there always exist a unique greatest and least price-payment equilibrium (p^+, q^+) and (p^-, q^-), i.e., for every price-payment equilibrium (p^*, q^*) it holds that*

$$(p^-, q^-) \leq (p^*, q^*) \leq (p^+, q^+).$$

Remark 2.2.3. While the clearing payment vector is unique within the basic setting of Eisenberg and Noe (2001) under certain technical conditions, extensions allowing separately for bankruptcy costs or fire sales may lead to multiple clearing vectors, see (Rogers and Veraart, 2013, Example 3.3) and (Chen et al., 2016, Example 7). This observation applies, in particular, to our integrated financial system as shown by an example in Appendix 2.6. The example also demonstrates that the set of equilibria is not necessarily connected.

Amini et al. (2016) prove uniqueness of price-payment equilibria in a model with fire sales under the additional condition on the inverse demand function f that $x \mapsto xf(x)$ is strictly increasing. They provide the following rational for their assumption: If there exists a subinterval $I := (x_0, x_1)$ with $I \ni x \mapsto xf(x)$ decreasing, rational banks would never choose to sell a suboptimal amount $x \in I$ of the illiquid asset; they would instead liquidate less, i.e., only the quantity x_0.

The argument of Amini et al. (2016) relies on implicit assumptions. First, it requires that banks understand both the mechanism of price formation as well as their own price impact. Second, the price of the illiquid asset depends on the total quantity that is sold which would have to be known; it does not only depend on the amount that is sold by an individual bank. However, in contrast to the price, the total quantity sold is hardly observable in reality. Third, Amini et al. (2016) interpret the one-stage model literally; the latter could also be seen as a simplified static picture of the true dynamic processes of prices sliding down the slide while banks continue to liquidate their holdings over time. For simplicity, we decided to model banks as price takers and do not impose the additional condition of Amini et al. (2016).

We now explain how equilibria can be determined, generalizing the *fictitious default algorithm* of Eisenberg and Noe (2001), and the procedures of Rogers and Veraart (2013), and Amini et al. (2013). Our method allows the computation of the greatest and least price-payment equilibrium, see Algorithm 2.2.4 and Remark 2.2.6 below.

Algorithm 2.2.4. Set $k = 0$, $(p^{(0)}, q^{(0)}) := (\bar{p}, q_0)$, $\mathcal{D}_{-1} := \emptyset$ and determine the starting essential net worths vector $w^{(0)} := w^*(p^{(0)}, q^{(0)})$ using fixed-point iteration. Determine the sets of initially defaulting and surviving banks

$$\mathcal{D}_0 := \{i \in \mathcal{N} \mid w_i^{(0)} < 0\} \quad \text{and} \quad \mathcal{S}_0 := \{i \in \mathcal{N} \mid w_i^{(0)} \geq 0\}.$$

If $\mathcal{D}_0 = \mathcal{D}_{-1}$ and no bank has to liquidate its illiquid asset holdings, i.e., for all $i \in \mathcal{N}$:

$$r_i + \sum_{j \in \mathcal{N}} \Pi_{ji} p_j^{(0)} + \mathbb{I}_i \lambda_i \sum_{j \in \mathcal{N}} C_{ji} \max(w_j^{(0)}, 0) \geq \bar{p}_i, \tag{2.3}$$

terminate. Otherwise, go to Step 2.

Step 1: Determine the sets of defaulting and surviving banks

$$\mathcal{D}_k := \{i \in \mathcal{N} \mid w_i^{(k)} < 0\} \quad \text{and} \quad \mathcal{S}_k := \{i \in \mathcal{N} \mid w_i^{(k)} \geq 0\}.$$

If $\mathcal{D}_k = \mathcal{D}_{k-1}$, terminate. Otherwise, go to Step 2.

Step 2: Set $p_i^{(k+1)} = \bar{p}_i$ for all $i \in \mathcal{S}_k$, $p_i^{(k+1)} = x_i$ for all $i \in \mathcal{D}_k$, $q^{(k+1)} = y$, and $w^{(k+1)} = w^*(x,y)$, where (x,y) is determined as the maximal solution to the following system of equations:

$$x_i = \alpha\,[r_i + s_i y] + \beta\left[\sum_{j\in\mathcal{D}_k}\Pi_{ji}x_j + \sum_{j\in\mathcal{S}_k}[\Pi_{ji}\bar{p}_j + \lambda_i C_{ji}\max(w_j^*(x,y),0)]\right],\quad \forall i\in\mathcal{D}_k, \tag{2.4}$$

$$y = f\left(\sum_{i\in\mathcal{D}_k}s_i + \sum_{i\in\mathcal{S}_k}\min\left(\frac{\zeta_i^{(k)}(x,y)}{y}, s_i\right)\right), \tag{2.5}$$

$$\zeta_i^{(k)}(x,y) := \max\left(\bar{p}_i - r_i - \sum_{j\in\mathcal{D}_k}\Pi_{ji}x_j - \sum_{j\in\mathcal{S}_k}[\Pi_{ji}\bar{p}_j + \mathbb{I}_i\lambda_i C_{ji}\max(w_j^*(x,y),0)], 0\right),\quad \forall i\in\mathcal{S}_k. \tag{2.6}$$

The (sloppy) notation $w^*(x,y)$ refers to the essential net worths vector corresponding to the payment vector $p^{(k+1)}$; its components are equal to x_i for the defaulting banks $i \in \mathcal{D}_k$ and equal to $\bar{p}_i$ for the surviving banks $i \in \mathcal{S}_k$.

Set $k \to k+1$ and go to Step 1.

The algorithm works as follows. Starting with the total liabilities vector for the payments and the initial price of the illiquid asset q_0, it calculates the set of those banks that will default even if all other banks pay their liabilities in full. This is the set of initially defaulting banks. If there are no initially defaulting banks and, in addition, no bank has to liquidate parts of its illiquid asset holdings, we immediately arrive at the end of the clearing process and terminate. Note that leaving out the extra condition (2.3) in the initial step may lead to an incorrect result if the contagion cascade is solely triggered by the asset price effect. This is due to the fact that the price of the illiquid asset and the corresponding payments must be adjusted if there are banks forced to sell the illiquid asset. The adjustment is made in Step 2 by solving the fixed-point equations (2.4) and (2.5) simultaneously. Using the adjusted price-payment pair, in Step 1 of the next round, we calculate the set of defaulting banks that corresponds to it. If this default set equals the default set from the previous round, the algorithm terminates with the current pair of payments and price of the illiquid asset. Otherwise, the procedure continues until the set of defaulting banks does not change anymore.

The following theorem extends (Rogers and Veraart, 2013, Theorem 3.7) to the case of cross-holdings and fire sales.

Theorem 2.2.5. *Algorithm 2.2.4 produces a sequence of price-payment pairs $(p^{(k)}, q^{(k)})$ that decreases to the greatest price-payment equilibrium in at most $n+1$ iterations.*

Remark 2.2.6. Algorithm 2.2.4 computes the least price-payment equilibrium, if we make the following changes:

- In the initial step: Set $(p^{(0)}, q^{(0)}) = (\mathbf{0}, q_{\min})$, $\mathcal{D}_{-1} = \mathcal{N}$, and terminate the algorithm if $\mathcal{D}_0 = \mathcal{D}_{-1}$, i.e., condition (2.3) can be eliminated.

- In Step 2: Compute the minimal solution to the system of equations.

The iterations of the procedure that computes the least price-payment equilibrium can be viewed[3] as a process in which financial health spreads throughout a system that is initially in default. The iterations of the algorithm that determines the greatest price-payment equilibrium describe, in contrast, how defaults spread in a system that initially is completely healthy. As we expect the latter situation to be more likely in real world financial markets, we focus on the greatest equilibrium when conducting our numerical case studies.

The greatest price-payment equilibrium (p^+, q^+) corresponds to a set of defaulting banks

$$\mathcal{D}(p^+, q^+) := \{i \in \mathcal{N} \mid w_i^*(p^+, q^+) < 0\} = \{i \in \mathcal{N} \mid p_i^+ < \bar{p}_i\}$$

that is directly provided by Algorithm 2.2.4. The cardinality of this set is a simple measure of systemic risk. In the following section, we will investigate how this quantity is affected by bankruptcy costs, cross-holdings, and fire sales—separately and jointly.

2.3 Case Studies

The integrated financial system is characterized by a 10-tuple, $(\Pi, \bar{p}, r, s, \alpha, \beta, \lambda, f, C, \mathbb{I})$. The relative liabilities matrix Π and the cross-holdings matrix C will be modeled as random quantities. In contrast to a deterministic approach, a probabilistic mechanism allows for an identification of the structure of a class of networks on the basis of appropriate statistical quantities. We choose two settings: Erdős–Rényi random networks (Erdős and Rényi (1959)), and a two-tiered (core-periphery) random graph model adapted to German interbank market data (extracted from Craig and von Peter (2014)). We also analyze an extension to multi-layer networks that capture heterogeneous business models.

[3]This interpretation is due to Rogers and Veraart (2013).

2.3.1 Erdős–Rényi Random Networks

2.3.1.1 Simulation Methodology

We use a simulation procedure similar to Elliott et al. (2014). Specifically, we choose two parameters $c_\Pi \in [0,1]$ and $d_\Pi \in [0, n-1]$ describing the level of integration and diversification of the relative liabilities network. The parameter c_Π refers to the proportion of total liabilities that are spread across the interbank market while d_Π describes the expected number of creditors of a bank therein. We generate a homogeneous weighted random network for Π with n nodes as follows:

1. Construct an adjacency matrix $A \in \mathbb{R}^{n\times n}$ by letting A_{ij}, $i \neq j \in \mathcal{N}$, be i.i.d. Bernoulli random variables, taking the value 1 with probability $d_\Pi/(n-1)$ and 0 with probability $1 - d_\Pi/(n-1)$. Set $A_{ii} = 0$ for all $i \in \mathcal{N}$.
2. For all banks $i \in \mathcal{N}$, set $d_i^{out} = \sum_{j\in\mathcal{N}} A_{ij}$, and let $\Pi_{ij} = c_\Pi/d_i^{out}$ if $A_{ij} = 1$, otherwise $\Pi_{ij} = 0$, $j \in \mathcal{N}$.

The parameter d_Π is the average out-degree of the corresponding directed network, the parameter c_Π is the row sum of the matrix A.

The cross-holdings matrix C describes an interbank network as well and can be modeled according to an analogous mechanism. We denote by $c \in [0,1)$ the corresponding level of integration, and by $d \in [0, n-1]$ the level of diversification of the cross-holdings matrix. The parameter c refers to the fraction of net worth that banks sell as cross-holdings to other banks, d describes the expected number of shareholders within the interbank market. We assume that banks can liquidate cross-holdings at their market value, possibly reduced to a fraction $\kappa \in [0,1)$. We thus set $\lambda_i = (1-c)\kappa$, $i \in \mathcal{N}$. Buyers could either be market participants or a central bank that tries to stabilize the financial system.

The number of shares r of the liquid asset and the number of shares s of the illiquid asset are specified in terms of two parameters δ and ρ; δ denotes the size of a capital buffer, and ρ the proportion of the illiquid asset:

1. Compute the random vector of the minimal value of assets that prevent the banks from defaulting (not considering cross-holdings): $h := (\bar{p} - \Pi^T \bar{p}) \vee \mathbf{0}$.
2. Given a capital buffer $\delta > 0$, set the overall external assets to be $e := (1+\delta)h$.
3. Given a proportion $\rho \in [0,1]$ of the illiquid asset, let $r = (1-\rho)e$ and $s = \rho e$.

For simplicity, we use the parametric exponential inverse demand function

$$f(x) = \exp(-\gamma x);$$

alternative inverse demand functions can also be implemented within our framework. We assume that all banks follow the same rule regarding the order of liquidation. This means that either all banks exchange their total cross-holdings against cash before selling the illiquid asset (i.e., $\mathbb{I} = \mathbf{1}$), or that all banks first liquidate their total holdings of the illiquid asset before using cross-holdings (i.e., $\mathbb{I} = \mathbf{0}$).

Setting $n = 100$ and $\bar{p} = \mathbf{1}$, the following parameters govern the simulation model:

$$(c_\Pi, d_\Pi, \delta, \alpha, \beta, \rho, \gamma, c, d, \kappa, \mathbb{I}).$$

We fix $c_\Pi = 0.15$, $d_\Pi = 10$, and $\delta = 0.01$, and vary the other parameters as indicated in Table 2.1.[4]

Table 2.1: Extension parameters

Parameter	Description	Range of variation
α	Realized fraction of external asset value in case of bankruptcy	[0.5,1]
β	Realized fraction of interbank asset value in case of bankruptcy	[0,1]
ρ	Proportion of the illiquid asset	[0,0.05]
γ	Exponent of the inverse demand function	[0,1]
c	Integration of the cross-holdings matrix	[0,0.9]
d	Diversification of the cross-holdings matrix	[1,90]
κ	Realized fraction of cross-holdings' market value	[0,1]
$\mathbb{I}$	Order of liquidation	$\{\mathbf{0}, \mathbf{1}\}$

Methodological Remark 2.3.1. The numerical case studies are conducted as follows: Π and C are randomly sampled; the derived random quantities r and s are computed from the samples. One bank $i \in \mathcal{N}$ is uniformly sampled at random; its external asset holdings r_i and s_i are set to zero. This corresponds to a local shock to a single bank. For the resulting scenario, the greatest price-payment equilibrium and the corresponding number of defaulting firms is calculated. The simulation is repeated a large number of times, and

[4]The choice of $c_\Pi = 0.15$ is consistent with empirical findings for developed countries reported in Upper (2007) (with data from 2005), in Drehmann and Tarashev (2011) for the 20 largest internationally active banks, and with integration values for European countries computed in Glasserman and Young (2015).

sample averages and standard deviations are computed. The exact number of the simulations that were conducted is mentioned below for each case study. We use the following notation: Parameters corresponding to a basic Eisenberg–Noe model are denoted by EN, B signifies the incorporation of bankruptcy costs, C cross-holdings, and F fire sales.

2.3.1.2 Separate Effects

First, we focus on the separate impact of individual model ingredients, leaving all other parameters as in the EN model. Section 2.3.1.3 investigates joint effects.

Bankruptcy Costs and Fire Sales. As expected, both bankruptcy costs and fire sales amplify the threat of contagion to the system. This is shown in Figure 2.1. Increasing

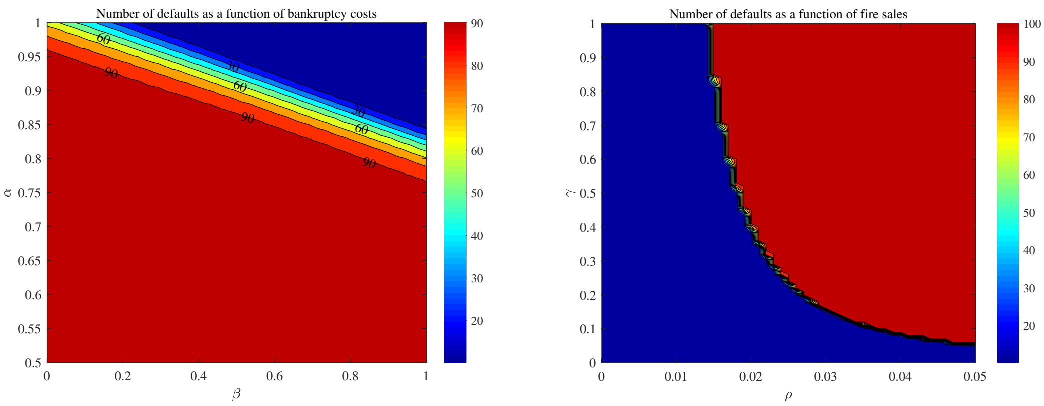

(a) (b)

Figure 2.1: Contour plots of the number of defaults for $n = 100$ banks as a function of (a) bankruptcy costs and (b) fire sales, averaged over 1000 simulations of Π. The simulation procedure is explained in Remark 2.3.1.

bankruptcy costs, i.e., decreasing α and β, increases the number of defaults quite quickly, as shown by Figure 2.1 (a). Part (b) of Figure 2.1 shows a similar phenomenon when both fire sales parameters are increased. Additionally, a clear threshold effect can be observed that separates an area of many defaults from an area of few defaults. For low parameter values of ρ and γ, the financial system exhibits the EN number of defaults (around 11). Increasing ρ and γ beyond a certain threshold boundary *causes defaults of all banks in the system*. The threshold curve can approximately be described by the following power-law function: $\rho = \exp(-4.3183) \cdot \gamma^{-0.4528}$.

From a policy point of view, these findings have two important implications:

1. Bankruptcy costs increase the instability of the financial system significantly. These costs are mainly incurred due to the impaired operations of financial institutions in default. Administrative and legal expenses increase significantly for such institutions. Policies that improve the efficiency of managing defaults and restructuring institutions would mitigate the consequences of financial crises. This could, for example, be achieved by limiting the complexity of financial products and the operations of financial institutions. Another promising instrument are last wills of financial institutions, approved by the regulator during their lifetime, that simplify the processes in default.

2. Illiquidity, i.e., the joint consequences of limited funding and price impact, decreases market stability. When markets dry up, the value of financial institutions that need short-term funding might be significantly impaired. Quantitative easing would, in this case, be an appropriate instrument to stabilize the banking sector. This should include the purchase of temporarily illiquid assets.

The simulations also exhibit a sharp boundary between the regimes with few and many defaults. This indicates that regulatory policies should aim for substantial safety margins in order to create a resilient system.

Cross-Holdings. Cross-holdings significantly impact the number of defaults. This has implications for the policies of regulators that we will discuss below.

Integration c generally reduces the expected number of defaults. The dependence on c is, however, non-monotonic. As shown in Figure 2.2 (a), increasing c to approximately 0.8 decreases their number at a nearly constant rate; beyond this point the number of defaults increases again. A second observation concerns diversification. For $d \geq 10$, the average number of defaults is largely independent of the value of d. This is also confirmed in Figure 2.2 (b). In addition to integration and diversification, the number of defaults also depends on the realized fraction κ of the market value of cross-holdings. Figure 2.3 presents the expected monotonic effect.

Cross-ownership in the banking sector may stabilize the financial system. However, this finding relies on the existence of a market with substantial demand for cross-holdings. Our results show that regulators and central banks might use cross-holdings in order to stabilize financial markets during financial crises. Regulatory policies that provide incentives to cross-ownership in the financial market as well as a credible promise that these shares will be purchased, e.g., by the central bank would decrease systemic risk in our model.

The benefits of cross-holdings rely on the fact that they can be exchanged against cash. This effect becomes, of course, less significant if the realized fraction κ is smaller. At

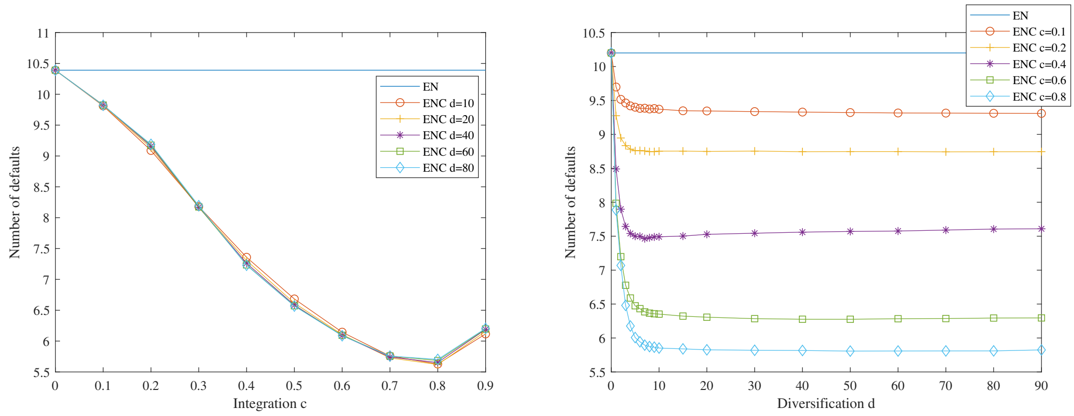

(a) (b)

Figure 2.2: Number of defaults for $n = 100$ banks as a function of (a) integration and (b) diversification of the cross-holdings matrix C, realized fraction of cross-holdings' market value $\kappa = 0.8$, averaged over 100 simulations of Π, each averaged over 100 simulations of C. The simulation procedure is explained in Remark 2.3.1.

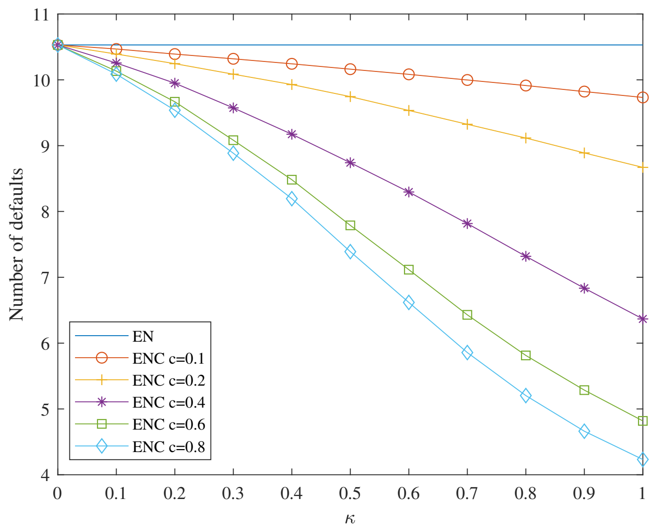

Figure 2.3: Number of defaults as a function of the realized fraction κ of cross-holdings' market value, varying integration and diversification $d = 10$, averaged over 100 simulations of Π, each averaged over 100 simulations of C. The simulation procedure is explained in Remark 2.3.1.

the same time, there might be an inverse effect on the financial institution whose shares are sold. If a large sale of its shares decreases its equity price, its solvency is not directly affected: Solvency is a function of the book value of equity—the latter being computed from a market consistent balance sheet. The book value of equity may deviate from its market value. But a decreased equity price may increase the cost of capital and thereby negatively affect the bank's solvency indirectly. The closely related topic of the impact of equity valuation on credit supply to the real economy is, e.g., discussed in Boucinha et al. (2017).

Random Fluctuations. The preceding sections described the average behavior of the system. The actual outcomes, however, might significantly deviate from these averages. Two examples are provided in Figure 2.4. The figures display the standard deviation[5] of the number of defaults as (a) a function of the bankruptcy costs parameters α and β, and (b) as a function of the level c of integration of the cross-holdings matrix. A comparison

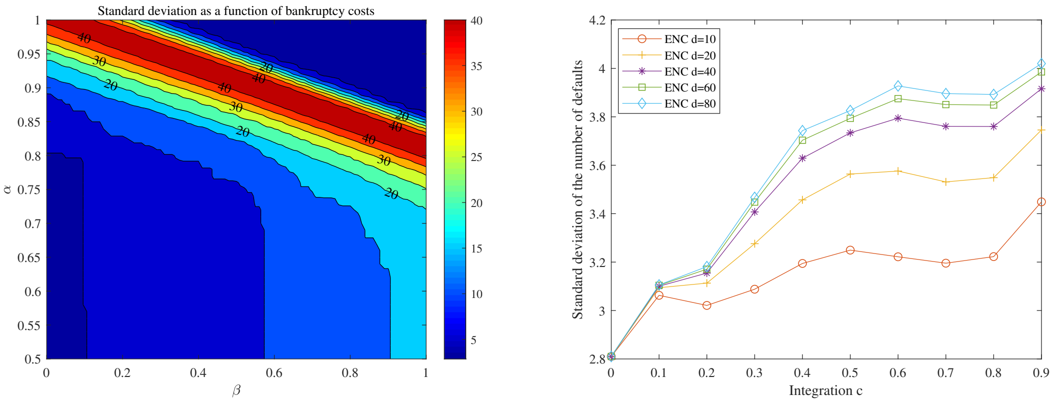

(a) **(b)**

Figure 2.4: Standard deviation of the number of defaults for $n = 100$ banks (a) as a function of both parameters of bankruptcy costs for 1000 simulations of Π, and (b) as a function of integration of the cross-holdings matrix C for 100 simulations of Π, each averaged over 100 simulations of C. The simulation procedure is explained in Remark 2.3.1.

of Figure 2.4 (a) and Figure 2.1 (a) leads to the following observation: For values of α and β that lead to outcomes of either a very low number of defaults (i.e., EN-level) or the total breakdown of the system, the corresponding standard deviation is relatively low. However, in the transition area between these regimes, we observe a very high standard

[5] In the ENC scenario, we computed the standard deviation on the basis of the Π samples and continue to average over the C simulations, since the conditional variance given Π is relatively low.

deviation. We observed a similar behavior when analyzing fire sales: while regimes with a very low or a very high average number of defaults exhibited low standard deviations, regimes with an intermediate average number of defaults were associated with significant fluctuations around the averages and thus with significant risk. A refined analysis[6] shows that the empirical distribution of defaults is mainly concentrated on the extreme scenarios of few or many defaults. Medium levels of bankruptcy costs or fire sales may, on average, seem acceptable, but are in fact associated with an unstable financial system. This shows that gradual improvements of the efficiency of the operations of distressed banks or light quantitative easing do not lead to resilience. Regulatory rules and interventions must be sufficiently forceful in order to achieve the desired effect of creating a stable financial system.

In the case of cross-holdings, an analysis of the average number of defaults is not sufficient. Comparing Figure 2.4 (b) with Figure 2.2 (a) shows that increasing integration has an overall beneficial effect on the average number of defaults, but increases the standard deviation within the considered parameter range. Features of the network thus have a quite complex impact on how financial stability and instability spread within the system. Moreover, Figure 2.4 (b) demonstrates that increasing diversification increases the standard deviation, while diversification does almost not affect the average number of defaults for $d > 10$. A diversification of $d = 10$ (i.e., $\sqrt{n}$) seems to be an optimal level. It would be interesting to investigate if such a statement holds more generally. Regulatory incentives for cross-ownership in the banking sector must therefore be very carefully designed. This requires substantial future research on the exact magnitude of the impact of cross-holdings in real financial networks.

2.3.1.3 Joint Effects

In the current section, we investigate the joint impact of network effects, bankruptcy costs, fire sales, and cross-holdings in our integrated model and study the robustness of the results of the previous section. We focus on the following three questions: (i) Is quantitative easing in the joint model an appropriate policy for limiting systemic risk? How is this affected by other model drivers? (ii) Are the results modified by the change of the order of liquidation? (iii) Do cross-holdings have a beneficial effect on the stability of the financial system if bankruptcy costs and fire sales are included in the model? Which regulatory policies are appropriate?

(i) First, consider an integrated financial system with $\alpha = 0.9$, $\beta = 0.9$, $c = 0.5$,

[6] We include an analysis of the empirical distribution in the joint model in Figure 2.8. These findings were also confirmed in multiple other case studies for other parameter constellations.

$d = 10$, and $\kappa = 0.8$. The resulting average number of defaults as a function of the fire sales parameters is displayed in Figure 2.5.[7]

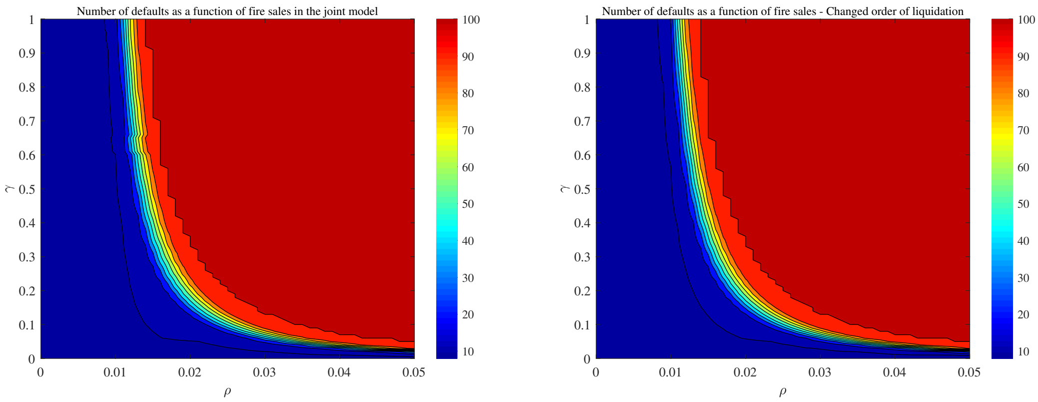

(a) $\mathbb{I} = \mathbf{1}$ **(b)** $\mathbb{I} = \mathbf{0}$

Figure 2.5: Contour plot of the number of defaults for $n = 100$ banks as a function of both parameters of fire sales, ρ and γ, for $\alpha = 0.9$, $\beta = 0.9$, $c = 0.5$, $d = 10$, $\kappa = 0.8$, $\mathbb{I} = \mathbf{1}$ in (a) and $\mathbb{I} = \mathbf{0}$ in (b), averaged over 100 simulations of Π, each averaged over 100 simulations of C. The simulation procedure is explained in Remark 2.3.1.

A comparison of Figures 2.1 (b) and 2.5 (a) reveals that the general structure of the influence of price impact is preserved if bankruptcy costs and cross-holdings are added. However, the number of defaults increases and the sharp transition between the area of few defaults and the area of the breakdown of the system disappears. Similar qualitative results were all also confirmed in additional case studies based on both the ENBF and ENCF models. The results indicate that quantitative easing continues to be a suitable instrument in order to contain the number of defaults in this case.

(ii) Second, Figures 2.5 (b) and 2.6 deal with the impact of changing the order of liquidation on the number of defaults and the price of the illiquid asset as a function of the fire sales parameters ρ and γ. These figures show that, regardless of whether cross-holdings or illiquid asset shares are liquidated first, the observed behavior is very similar.

(iii) Third, we analyze the effects of integration of cross-holdings in the joint model. This leads to rather complex, but very interesting features. We investigate a network

[7] Kinks in the boundary are numerical artifacts. Note that the simulations still took several days to complete on the RRZN computing cluster.

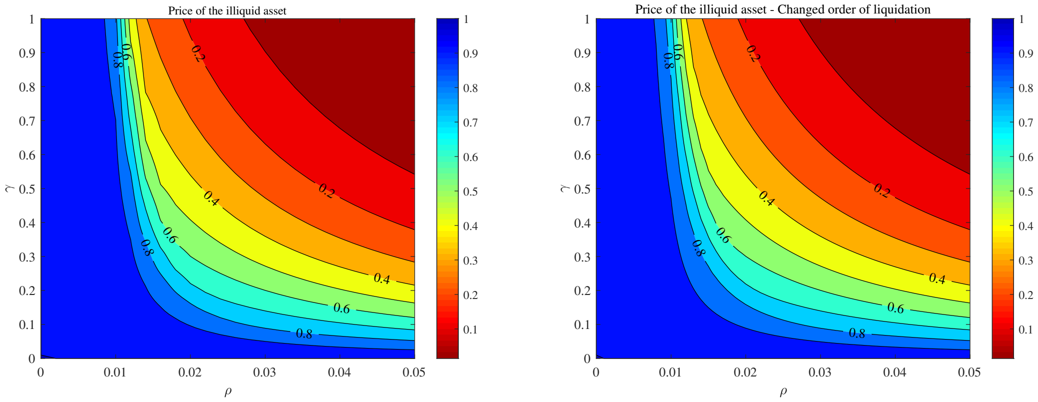

(a) $\mathbb{I} = \mathbf{1}$ **(b)** $\mathbb{I} = \mathbf{0}$

Figure 2.6: Contour plot of the price of the illiquid asset for $n = 100$ banks as a function of both parameters of fire sales, ρ and γ, for $\alpha = 0.9$, $\beta = 0.9$, $c = 0.5$, $d = 10$, $\kappa = 0.8$, $\mathbb{I} = \mathbf{1}$ in (a) and $\mathbb{I} = \mathbf{0}$ in (b), averaged over 100 simulations of Π, each averaged over 100 simulations of C. The simulation procedure is explained in Remark 2.3.1.

model with $d = 10$, $\kappa = 0.8$, $\beta = 0.9$, $\gamma = 0.2$, $\rho = 0.02$, and varying α. Within the considered parameter range, increasing integration decreases the average number of defaults, cf. Figure 2.7 (a). The non-monotonicity observed in Figure 2.2 (a) disappears. As expected, the higher the realized fraction α, the lower the number of defaults. However, for $\alpha \leq 0.8$ cross-holdings cannot prevent the total breakdown of the system. Observe that for the chosen value of $\beta = 0.9$, the value $\alpha = 0.8$ corresponds roughly to the critical boundary between the regimes of a very high ($\alpha \leq 0.8$) and a very low ($\alpha \geq 0.9$) number of defaults in Figure 2.1 (a).

Figure 2.7 (b) displays standard deviations. These are comparatively small for extreme regimes of the default count statistics, i.e., $\alpha \in \{0.8, 0.85, 0.95\}$. For regimes with an intermediate average number of defaults, i.e., $\alpha \in \{0.9, 0.925\}$, the standard deviations are large. For fixed $\alpha \leq 0.9$, the standard deviation increases as a function of integration c; for $\alpha \geq 0.925$, the standard deviation is decreasing.

This different behavior can easily be understood when analyzing the empirical cumulative distribution functions (CDFs) of the number of defaults. It turns out that the distributions of the numbers of defaults are very close to Bernoulli distributions. In this case, the standard deviation is maximal for a success probability of 0.5 and monotonously decreasing if the success probability is either increased or decreased. As illustrated in Figure 2.8, for $\alpha = 0.9$, the distribution of defaults for $c = 0.3$ roughly corresponds to a success probability of $0.2 - 0.3$; for $c = 0.7$, to

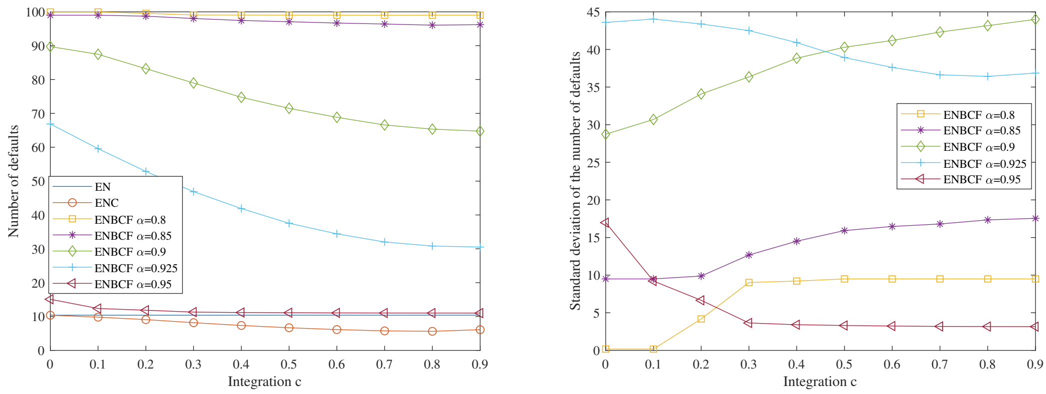

(a) **(b)**

Figure 2.7: Average (a) and standard deviation (b) of the number of defaults for $n = 100$ banks as a function of integration c for $d = 10$, and for different bankruptcy costs parametrized by α in an integrated financial system with $\beta = 0.9$, $\gamma = 0.2$, $\rho = 0.02$, $\kappa = 0.8$, $\mathbb{I} = \mathbf{1}$ averaged over 100 simulations of Π, each averaged over 100 simulations of C. The simulation procedure is explained in Remark 2.3.1.

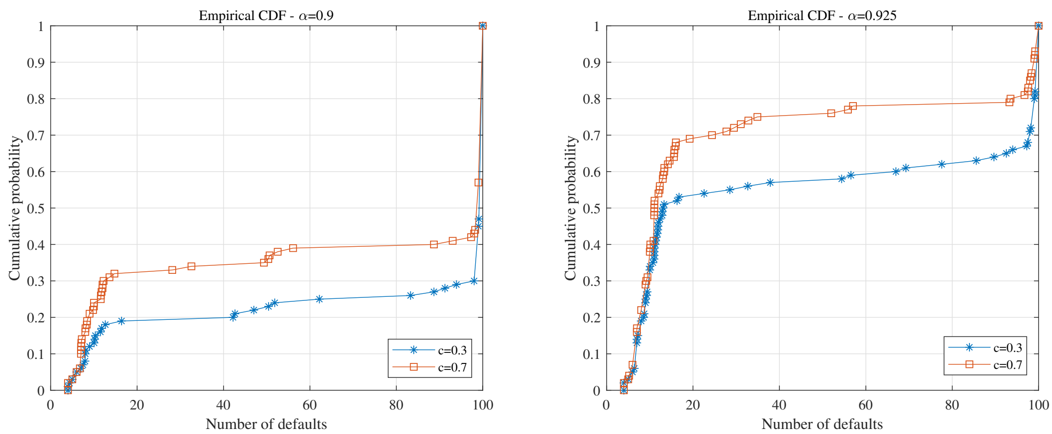

(a) **(b)**

Figure 2.8: Empirical cumulative distribution functions of the number of defaults in 100 simulations of the relative liabilities matrix Π each averaged over 100 simulations of C, for two integration values $c = 0.3$ and $c = 0.7$ for $\alpha = 0.9$ (a) and $\alpha = 0.925$ (b).

a success probability of 0.3 – 0.4. Thus, the standard deviation increases in c. In contrast, for $\alpha = 0.925$, the distribution of defaults for $c = 0.3$ roughly corresponds to a success probability of 0.5 – 0.6; for $c = 0.7$, to a success probability of 0.7 – 0.8. Thus, the standard deviation decreases in c.

The approximate Bernoulli distributions are supported by the EN number of defaults and a total breakdown of the system. This shows that the system *essentially randomizes between extreme states*. While the probability of the negative outcome can be controlled by cross-holdings for the chosen level of bankruptcy costs and fire sales, the number of defaults in this adverse scenario is not mitigated.

From a policy point of view, our numerical case studies again indicate the fundamental role played by bankruptcy costs, emphasizing the importance of efficient procedures for managing defaults and restructuring institutions. Regulators should thus implement policies that lower the costs of bankruptcy. Moreover, if bankruptcy costs are not too large, a higher integration c of cross-holdings decreases both the average number of defaults and their variance. More integrated systems are thus more resilient. These results, of course, rely on the existence of a sufficiently deep and liquid market for cross-holdings. If this market dries up during a crisis, central banks might buy cross-holdings or provide guarantees for their purchase in order to stabilize the financial system. In our model, such a policy, however, does not seem to be efficient anymore if bankruptcy costs are too high.

2.3.1.4 Capital Adequacy Ratios

Capital requirements are a powerful instrument for the regulation of financial institutions. We investigate these in Section 2.3.2.4 in more detail. For surveys of the literature on monetary risk measures, we refer to Föllmer and Schied (2011) and Föllmer and Weber (2015). A less sophisticated approach than monetary risk measures are capital adequacy ratios (CAR) based on risk-weighted assets. In the current section, we show in the context of our model that these are not always well-adopted for regulatory purposes.

We consider a stylized definition of CAR and ignore cross-holdings. For each bank i, capital C_i is computed as the sum of external asset holdings e_i and promised interbank holdings $\sum_{j\in\mathcal{N}} \Pi_{ji}\bar{p}_j$ less its liabilities $\bar{p}_i$. We assume that risk-weights[8] are 100% and calculate risk-weighted assets RA_i of bank i as the sum of its illiquid assets s_i and its interbank holdings $\sum_{j\in\mathcal{N}} \Pi_{ji}\bar{p}_j$. The capital adequacy ratio of bank i is defined by $CAR_i = C_i/RA_i$.

[8]The specific risk-weight that is chosen is irrelevant to our findings.

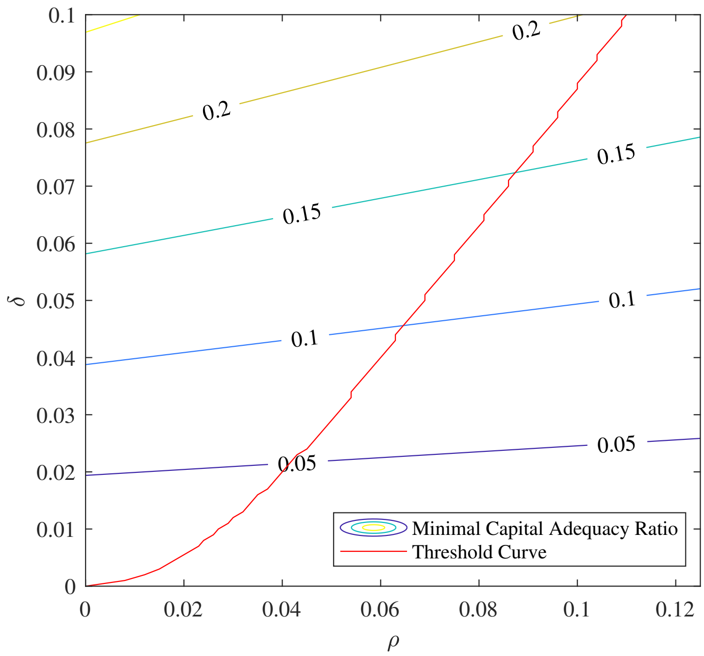

Figure 2.9: Level sets of the lowest capital adequacy ratio in the banking system $CAR := \min_{i\in\mathcal{N}} CAR_i$ as a function of the buffer δ and the proportion ρ of the illiquid asset in an ENBF-model with $\alpha = 0.925, \beta = 0.9$, and $\gamma = 0.2$. The solid line is the boundary between many (lower right) and few (upper left) defaults. Results are averaged over 100 simulations of Π. The simulation procedure is explained in Remark 2.3.1.

For a model including bankruptcy costs and fire sales, but no cross-holdings (ENBF), Figure 2.9 displays the level sets of the lowest capital adequacy ratio in the banking system, CAR, as a function of the buffer δ and the proportion ρ of the illiquid asset. At the same time, the boundary between the extreme default scenario (lower right corner) and few defaults (upper left corner) is shown.

A sufficiently high CAR can indeed prevent default cascades. However, in our case study, CAR appears to be an inefficient regulatory tool that does not properly measure the driving forces behind extreme default scenarios. Apparently, the barrier between many and few defaults and the level sets of CAR are not collinear. While for small values of ρ a small CAR is sufficient, for large values of ρ a large CAR is necessary in order to stabilize the system. The results indicate that regulators should base capital regulation on more sophisticated statistics than risk-weighted assets.

2.3.2 Core-Periphery Random Networks

So far, we considered homogeneous random network topologies. Recent research on financial networks, however, suggests that core-periphery network models capture the structure of the interbank market (see, e.g., Craig and von Peter (2014) for the German interbank market, and van Lelyveld and in 't Veld (2014) for the Netherlands): These consist of a few highly connected nodes (making up the *core*) and a larger number of only sparsely connected nodes (referred to as the *periphery*). Figure 2.10 shows both a sample of the homogeneous Erdős–Rényi network as well as the hierarchical core-periphery network.

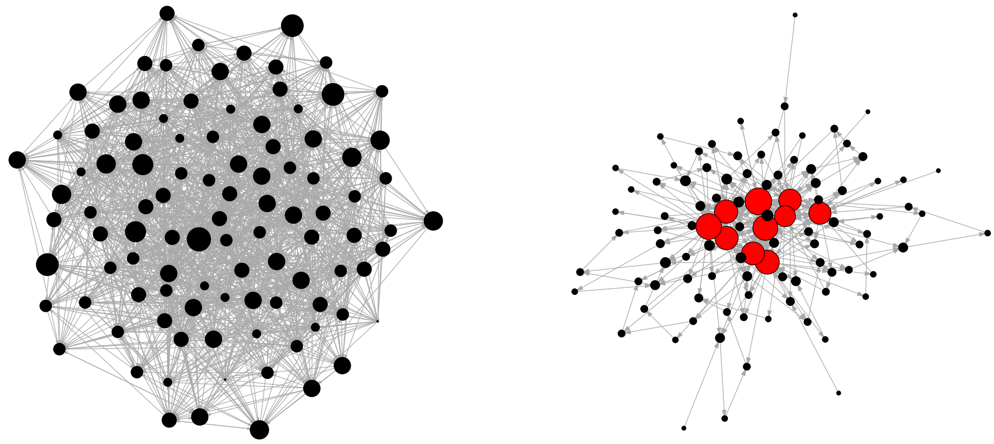

(a) Erdős–Rényi **(b)** Core-Periphery

Figure 2.10: Sample of (a) an Erdős–Rényi random network as described in Section 2.3.1.1 and (b) a core-periphery random network as described in Section 2.3.2.1; here, the highly connected core nodes are highlighted in red.

In this section, we simulate the relative liabilities matrix Π as a core-periphery random network and observe how this affects the impact of bankruptcy costs, cross-holdings, and fire sales on the number of defaults.

2.3.2.1 Simulation Methodology

We divide the set of banks $\mathcal{N}$ into a subset of core banks, $\mathcal{C}$, and a subset of periphery banks, $\mathcal{P}$, with cardinalities n^C and n^P, with $n^C + n^P = n$, respectively. We assume that a core-periphery relative liabilities matrix Π can be represented by a random block matrix

$$\Pi = \begin{pmatrix} CC & CP \\ PC & PP \end{pmatrix} \in \mathbb{R}^{n \times n}, \tag{2.7}$$

where, for example, the block $CP \in \mathbb{R}^{n^C \times n^P}$ represents the core banks' liabilities towards the periphery banks. This matrix is constructed as follows.

1. *Adjacency matrix:* We first simulate an adjacency matrix $A \in \mathbb{R}^{n \times n}$, using exogenously specified connection probabilities p^{CC}, p^{CP}, p^{PC}, and p^{PP} for each block.

2. *Weights:* Second, we fix the value of total liabilities ℓ of all banks. A fraction c_Π is allocated to the total interbank liabilities; the remaining share models external liabilities that are uniformly distributed among all banks, i.e., $l_i = \frac{(1-c_\Pi)\cdot\ell}{n}$, $i \in \mathcal{N}$. Total interbank liabilities $c_\Pi \cdot \ell$ are allocated to the four matrix blocks in fractions of x^{CC}, x^{PC}, x^{CP}, and x^{PP} with $x^{CC} + x^{PC} + x^{CP} + x^{PP} = 1$. The resulting interbank liabilities per block are uniformly distributed among all existing links within the block. This is, denoting by $l^{CP} = \sum_{i \in \mathcal{C}} \sum_{j \in \mathcal{P}} A_{ij}$ the random number of total links in the CP-block, the corresponding entries of the nominal liabilities matrix L are $L_{ij} = \frac{x^{CP} \cdot c_\Pi \cdot \ell}{l^{CP}}, i \in \mathcal{C}, j \in \mathcal{P}$, if $A_{ij} > 0$, and $L_{ij} = 0$, otherwise. The other blocks are computed analogously. Finally, with $\bar{p}_i = \sum_{j \in \mathcal{N}} L_{ij} + l_i$, the entries of the relative liabilities matrix Π are given by $\Pi_{ij} = \frac{L_{ij}}{\bar{p}_i}$.

As in the other case studies, we set $n = 100$, $c_\Pi = 0.15$, and $\ell = 100$. In addition, following Craig and von Peter (2014) who analyzed data from the German interbank market, we choose core-periphery parameters

$$\begin{aligned} &p^{CC} = 0.66, \quad p^{CP} = 0.15, \quad p^{PC} = 0.07, \quad p^{PP} = 0.001, \\ &x^{CC} = 0.35, \quad x^{CP} = 0.16, \quad x^{PC} = 0.47, \quad x^{PP} = 0.02. \end{aligned}$$

We fix the number of core banks as $n^C = 10$.[9] The simulation methodology is analogous to Section 2.3.1.1. Note, however, that simulation results will depend on whether a core or periphery bank is hit by an initial shock.

[9] This number is consistent with the empirical results of van Lelyveld and in 't Veld (2014), who find a core of around 10 banks in the Dutch interbank network, where the total number of banks is around our chosen number of 100.

2.3.2.2 Results

We focus on three case studies: the separate impact of a) bankruptcy costs and b) fire sales as well as c) the joint impact of all ingredients while varying the parameters that govern the fire sales.

Figure 2.11 shows the effects of bankruptcy costs and fire sales in the core-periphery network, given that initially a core bank is shocked.[10] The qualitative results for an initial periphery shock are similar; however, the total average number of defaults tends to be higher as an initially shocked core bank may survive the shock due to a high and possibly stabilizing level of interconnectedness. Comparing Figure 2.11 to Figure 2.1, we observe

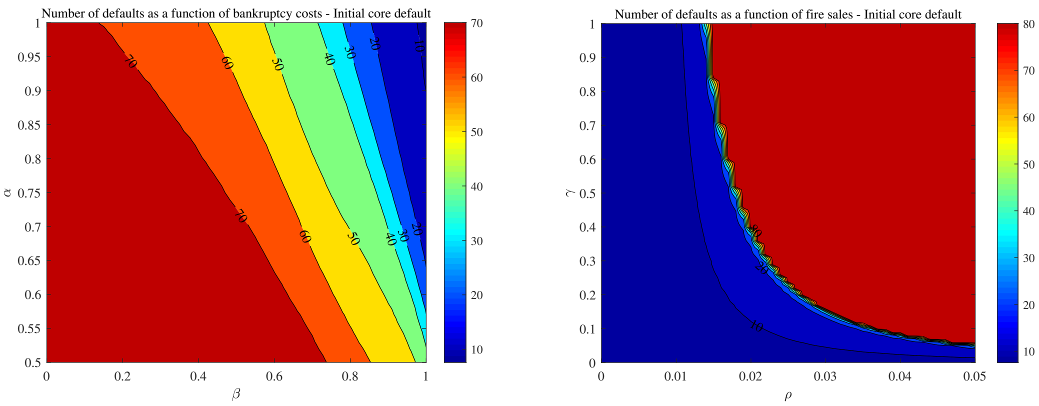

(a) **(b)**

Figure 2.11: Contour plots of the number of defaults for $n = 100$ banks as a function of (a) bankruptcy costs and (b) fire sales, conditional on an initial core shock, averaged over 100 simulations of Π, simulated as a core-periphery random network. The simulation procedure is explained in Remark 2.3.1.

that bankruptcy costs and fire sales have a similar impact as in the Erdős–Rényi network: as expected, an increase in the number of defaults for increasing bankruptcy costs and fire sales; a clear threshold boundary separating an area of many defaults from an area of few defaults. The exact numbers are, of course, different. For example, in Figure 2.11 (a) the impact of parameter β on defaults is stronger than before.

Figure 2.12 shows the average number of defaults as a function of both fire sales parameters in an ENBCF core-periphery model given that initially a core bank's external assets lose their total value. Again, our observations resemble the findings within Erdős–Rényi random networks.

[10]Observe that rough boundaries are artifacts of the numerical implementation. Still, computing time on the RRZN cluster was several days.

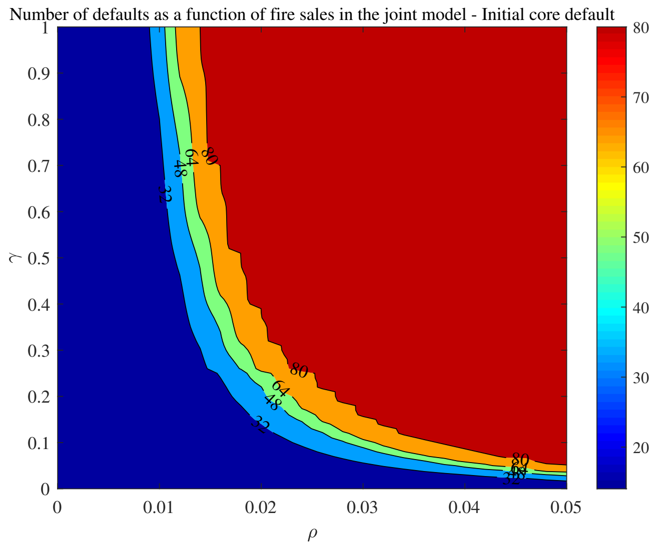

Figure 2.12: Contour plot of the number of defaults for $n = 100$ banks as a function of fire sales in the joint model ($\alpha = 0.9, \beta = 0.9, c = 0.5, d = 10, \kappa = 0.8, \mathbb{I} = \mathbf{1}$), conditional on an initial core default, averaged over 100 simulations of Π, simulated as a core-periphery random network, each averaged over 100 simulations of C simulated as an Erdős–Rényi random network. The simulation procedure is explained in Remark 2.3.1.

The considered core-periphery structure was calibrated to German interbank market data and presents a good description of a real world interbank market. Overall, the above comparisons indicate that the results we obtained are qualitatively similar to those within simpler Erdős–Rényi random networks. This shows that the simplified setting is already representative and relevant for the analysis of systemic risk. The policy implications discussed in the context of Erdős–Rényi random networks remain valid for the considered core-periphery structure.

2.3.2.3 Multi-Layer Networks

Our model can be extended to more than two layers and is capable of modeling heterogenous agents. We will illustrate this with three types of agents: banks, depositors, and borrowers. Depositors hold deposits at banks. Borrowers receive credit from the banks that act as intermediaries. For simplicity, we neglect bankruptcy costs and cross-holdings and assume that the banking system consists of 20 banks that form an Erdős–Rényi random network with $d_\Pi = 2$ and $\delta = 0.2$. We add depositors and borrowers to the system. The total liabilities of all banks (to other banks and to the depositors) within the considered time-period are normalized to the total number of banks, i.e., 20. Liabilities within the banking system are set to 15% of total liabilities, i.e., $c_\Pi = 0.15$.

The remaining 85% are liabilities to depositors. The number of depositors is 90, and each depositor is linked to exactly two banks that are uniformly sampled at random. Each link is associated with the same liability. We assume that all liabilities are immediately due. This scenario can be interpreted as a bank run.

There are 90 borrowers outside the banking system. Each borrower is linked to two banks that are sampled uniformly at random. Borrowers' short-term liabilities over the considered time-period are 1/100 per link. Borrowers hold external assets which amount to $1 + \delta$ of their total short-term liabilities; 40% of these are allocated to the illiquid asset.

All quantities are then computed as in Section 2.3.1.1. Figure 2.13 displays the average defaults in the banking system as a function of the fire sales parameters. Qualitatively, the graph resembles previous results and emphasizes their robustness. This shows again that quantitative easing can stabilize the banking system.

2.3.2.4 Capital Requirements

Another important regulatory tool are capital requirements for banks. In financial networks, the financial situation of a bank, of course, does not only depend on its own capital endowment, but also on the capital of other financial institutions with which it interacts directly or indirectly. Within a core-periphery network, we discuss the role of capital on

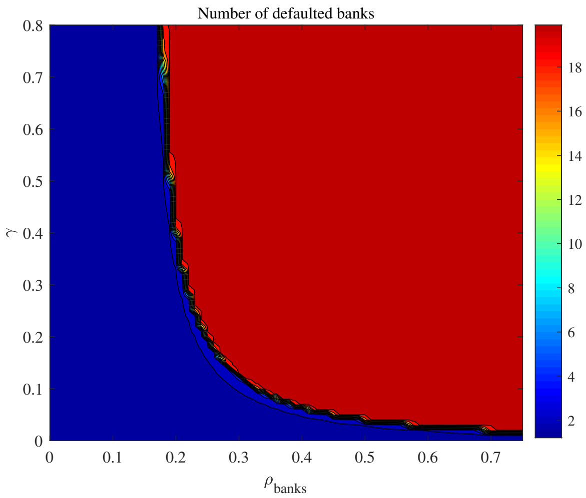

Figure 2.13: Contour plot of the average number of bank defaults as a function of fire sales parameters ρ_{banks} and γ in an ENF-model, averaged over 100 simulations of Π and periphery link choices. The simulation procedure is explained in Remark 2.3.1.

the basis of a framework suggested in Feinstein et al. (2017). We refer to this paper for further details on systemic risk measures.

In the current case study, all simulations are conducted according to the same methodology as described in Section 2.3.2.1. However, we introduce two further parameters k^C and k^P which signify *additional* capital on top of the originally computed external assets e that is held by the core and periphery banks, respectively. As before, the updated amount of the external assets is then divided into liquid and illiquid assets according to the parameter ρ, and the simulations are run.

In order to evaluate the effect of the additional capital encoded by the vector $k = (k^C, k^P)$ on the system, we use the following approach. Given k, we compute the greatest clearing vector $p^*(k)$ in our system. The clearing vector is a random quantity. The total random losses from direct liabilities are then given by:

$$L(k) = \sum_{i \in \mathcal{N}} (1 - \sum_{j \in \mathcal{N}} \Pi_{ij}) \cdot (p_i^*(k) - \bar{p}_i).$$

Observe that losses are considered negative. If there are no losses, $L(k)$ is equal to 0. Since financial institutions provide services to society, we assume that a regulator accepts a small loss or cost of up to t, but higher losses only with probability α. We define the set R of all $k = (k^C, k^P) \in \mathbb{R}^2$ that are compatible with this requirement:

$$R := \{k \in \mathbb{R}^2 : P(L(k) \leq -t) \leq \alpha\} = \{k \in \mathbb{R}^2 : V@R_\alpha(L(k)) \leq t\}.$$

The set R is a systemic risk measure in the sense of Feinstein et al. (2017).

We now consider an ENBF model and a core-periphery network as described in Section 2.3.2.1 and choose $t = 1/20$ and $\alpha = 10\%$. Figure 2.14 (a) displays the boundary of the set-valued systemic risk measures for varying fractions ρ of the illiquid asset without bankruptcy costs. Note that by definition, the systemic risk measure is an upper set in the sense that all points above the boundary are acceptable. As expected, we find that the higher the proportion of the illiquid asset in the external asset portfolio, i.e., the higher the ρ, the higher the capital requirement for both core and periphery banks is. The figure also shows that capital requirements tighten in a similar way for both core and periphery banks if the proportion of the illiquid asset is increased. This indicates, that according to our model, regulators should pay attention to the capital requirements of all banks if price impact is an important factor during crises.

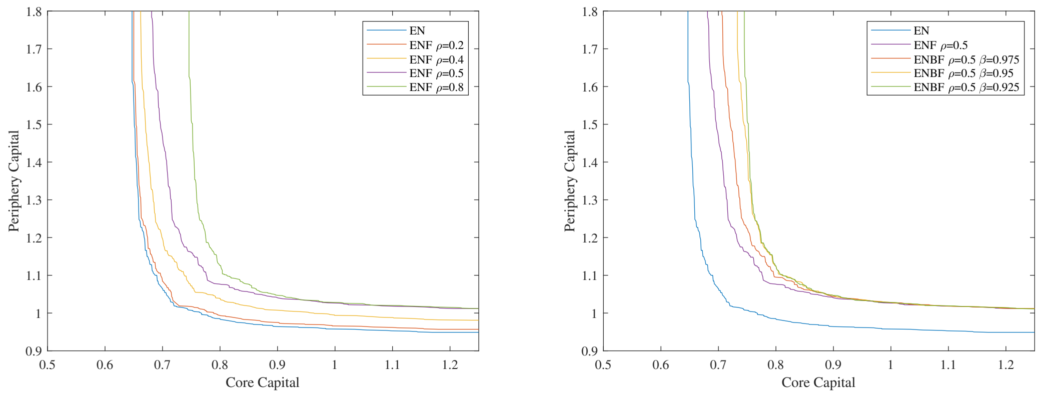

(a) **(b)**

Figure 2.14: Capital requirements for core and periphery banks as a function of fire sales (varying ρ and fixed $\gamma = 0.2$) (a) separately and (b) together with different levels of bankruptcy costs (varying β and fixed $\alpha = 1$).

Figure (b) includes bankruptcy costs for varying β with $\rho = 0.5$ fixed. While the capital requirements for the periphery banks are barely affected by decreasing β, the requirements for the core banks increase strongly. Since core banks are more connected than periphery banks, the impact of defaults and resulting interbank bankruptcy costs on core banks is more significant than on periphery banks. In the context of the chosen model, a regulator would be well advised if she particularly focused on strengthening the capital endowments of core banks. These can serve as a buffer that reduces systemic risk even if considerable bankruptcy costs are present.

2.4 Conclusion

The chapter presents a comprehensive model of a financial system that integrates network effects, bankruptcy costs, fire sales, and cross-holdings. For the integrated financial market, we prove the existence of a price-payment equilibrium and design an algorithm for the computation of the greatest and the least equilibrium. The number of defaults corresponding to the greatest price-payment equilibrium was analyzed in several comparative case studies for both simple Erdős–Rényi and more realistic core-periphery and multi-layer random networks:

1. Systemic risk was studied by shocking the system and computing the average number of defaults, its variance, and distribution. Outcomes are centered on extreme scenarios. The risk of extreme adverse events is present, even if averages indicate a relatively safe system. Regulatory policies should provide substantial safety margins in order to guarantee stability.

2. Fire sales strongly increase systemic risk, while cross-holdings may improve the resilience of the banking sector. Central banks might mitigate the risk of default cascades by purchasing illiquid assets and cross-holdings. Quantitative easing strengthens the system.

3. Bankruptcy costs are a main driver of systemic risk. Regulators should improve the efficiency of bankruptcy procedures and limit the associated deadweight losses. Policies might include reducing the complexity of financial products as well as operational procedures and requiring last wills of financial institutions.

4. Capital requirements are a powerful instrument, but capital adequacy ratios based on risk-weighted assets are an extremely rough measure of systemic risk. Instead, modern systemic risk measures that use capital efficiently could be implemented.

5. We analyzed different interbank network structures and heterogeneous business models. Our qualitative results were robust. Quantitative predictions, however, require a precise specification of all driving mechanisms.

The suggested model can be used as a framework for testing the impact of regulatory policies and their robustness. It can also provide insights into the significance of the financial market architecture for systemic risk, e.g., the pros and cons of CCPs. From a statistical point of view, our comparative statics show that default cascades can be triggered by a combination of various mechanisms. In particular, bankruptcy costs and fire sales exhibit similar consequences. Their statistical estimation is a challenging issue for future research that requires further data on historical bankruptcy procedures and price impact during crises.

2.5 Proofs

Proof of Lemma 2.1.2.

(a) This follows directly from Banach's fixed-point theorem applied to the function Ψ.

(b) We prove that the essential net worths vector is increasing in the payments p. The corresponding claim for the illiquid asset's price q can be proven analogously. To simplify the notation, we suppress the dependence on q and write $w^*(p)$ instead of $w^*(p,q)$ in the following. Now, for each given payment vector p, we define the following recursive sequence: Starting with $w^{(0)}(p) := r + sq + \Pi^T p - \bar{p}$, we set $w^{(n)}(p) = \Psi(w^{(n-1)}(p))$, for $n = 1, 2, \ldots$. Due to part (a), this sequence converges with $\lim_{n\to\infty} w^{(n)}(p) = w^*(p)$.

For two given payment vectors $p^1 \geq p^2$, it holds that $w^{(n)}(p^1) \geq w^{(n)}(p^2)$ for all n. We prove this statement by induction. For $n = 0$,

$$w^{(0)}(p^1) = r + sq + \Pi^T p^1 - \bar{p} \geq r + sq + \Pi^T p^2 - \bar{p} = w^{(0)}(p^2),$$

since $p^1 \geq p^2$. For the induction step, $n \to n+1$, it holds that

$$\begin{aligned} w^{(n+1)}(p^1) &= r + sq + \Pi^T p^1 + \mathrm{Diag}(\mu(p^1, w^{(n)}(p^1))C^T(w^{(n)}(p^1) \vee \mathbf{0}) - \bar{p} \\ &\geq r + sq + \Pi^T p^2 + \mathrm{Diag}(\mu(p^2, w^{(n)}(p^2))C^T(w^{(n)}(p^2) \vee \mathbf{0}) - \bar{p} \\ &= w^{(n+1)}(p^2), \end{aligned}$$

exploiting the induction hypothesis and the fact that $\mu_i(p, w)$ is by definition increasing in both components. Hence, $w^{(n)}(p^1) \geq w^{(n)}(p^2)$ for all n, and this yields

$$w^*(p^1) = \lim_{n\to\infty} w^{(n)}(p^1) \geq \lim_{n\to\infty} w^{(n)}(p^2) = w^*(p^2).$$

Proof of Lemma 2.2.1.

(a) It holds by definition that $\Phi_i(p,q) = \chi_i(p,q) \geq 0$ and $\Phi_i(p,q) \leq \bar{p}_i$ for all $i = 1, \ldots, n$, since the banks will pay at most their total liabilities. For $i = n+1$, the boundedness follows from the definition of the inverse demand function.

(b) Let $(p^1, q^1) \leq (p^2, q^2)$. We have that $\theta(p^1, q^1) \geq \theta(p^2, q^2)$, because the essential net worths vector is monotone in the price-payment pairs due to Lemma 2.1.2 (b).

Hence,

$$\Phi_{n+1}(p^1,q^1) = f(\theta(p^1,q^1)) \leq f(\theta(p^2,q^2)) = \Phi_{n+1}(p^2,q^2),$$

since f is monotonically decreasing. For $i = 1,\ldots,n$, monotonicity follows from a case-by-case analysis extending the arguments of Rogers and Veraart (2013) and Amini et al. (2013). First, assume that bank i is in default under (p^2,q^2). This implies that it is in default under (p^1,q^1) and that

$$\Phi_i(p^2,q^2) = \alpha[r_i + s_i q^2] + \beta\eta_i(p^2,q^2) \geq \alpha[r_i + s_i q^1] + \beta\eta_i(p^1,q^1) = \Phi_i(p^1,q^1),$$

due to Lemma 2.1.2 (b). Next, assume that bank i does not default under (p^2,q^2). Then, bank i can either survive or default under (p^1,q^1). In the first case, monotonicity of Φ_i directly follows from $\Phi_i(p^2,q^2) = \bar{p}_i = \Phi_i(p^1,q^1)$. In the second case, if bank i defaults under (p^1,q^1) but not under (p^2,q^2), it follows that

$$\Phi_i(p^2,q^2) = \bar{p}_i > r_i + s_i q^1 + \eta_i(p^1,q^1) \geq \alpha[r_i + s_i q^1] + \beta\eta_i(p^1,q^1) = \Phi_i(p^1,q^1).$$

Here, the first inequality holds true, since bank i defaults under (p^1,q^1). The second inequality follows from $\alpha,\beta \leq 1$.

Proof of Theorem 2.2.2.

Let $\mathcal{F} := \{(p,q) \in [\mathbf{0},\bar{p}] \times [q_{\min},q_0] \mid \Phi(p,q) = (p,q)\}$ denote the set of fixed points of Φ. Lemma 2.2.1 establishes that Φ is an increasing function on the complete lattice $\langle [\mathbf{0},\bar{p}] \times [q_{\min},q_0], \leq \rangle$ with the componentwise $\leq$-relation. Hence, Tarski's fixed-point theorem (Tarski, 1955, Theorem 1) states that $\mathcal{F}$ is not empty and, moreover, that $\langle \mathcal{F}, \leq \rangle$ constitutes a complete lattice itself. In particular, this yields the existence of a unique greatest and least element of $\mathcal{F}$. Since the elements of $\mathcal{F}$ constitute by definition the price-payment equilibria, this completes the proof.

Proof of Theorem 2.2.5.

This proof is an extension of the proof provided by Rogers and Veraart (2013) and proceeds in three steps. First, we show that the sequence of price-payment pairs $(p^{(k)},q^{(k)})$ decreases. Second, we demonstrate that each pair in this sequence is larger than or equal to the greatest price-payment equilibrium. Third, we observe that when the algorithm terminates, the calculated price-payment pair equals the greatest price-payment equilibrium.

1. For the first step, we claim that

$$(p^{(k+1)},q^{(k+1)}) \leq (p^{(k)},q^{(k)}) \quad \forall k = 0,1,\ldots,n-1. \tag{2.8}$$

We prove this statement by induction.

(B.S.) For the base step, $k = 0$, we need to prove that $p^{(1)} \leq p^{(0)} = \bar{p}$ and that $q^{(1)} \leq q^{(0)} = q_0$. Regarding the payments, this clearly holds for all $i \in \mathcal{S}_0$, since then $p_i^{(1)} = \bar{p}_i = p_i^{(0)}$. Thus, it remains to examine the payments of the defaulting banks in $\mathcal{D}_0$ and the corresponding price of the illiquid asset, which are jointly given by the maximal solution to the equations (2.4) and (2.5). In order to calculate this maximal solution, we propose the following recursive procedure: Start with $(x^{(0)}, y^{(0)})$, where $x_i^{(0)} = p_i^{(0)} = \bar{p}_i$ for $i \in \mathcal{D}_0$ and $y^{(0)} = q^{(0)} = q_0$, and define the sequence $(x^{(\nu)}, y^{(\nu)})$ recursively by

$$x_i^{(\nu+1)} = \alpha\left[r_i + s_i y^{(\nu)}\right] + \beta\left[\sum_{j\in\mathcal{D}_0}\Pi_{ji}x_j^{(\nu)} + \sum_{j\in\mathcal{S}_0}[\Pi_{ji}\bar{p}_j + \lambda C_{ji}\max(w_j^*(x^{(\nu)}, y^{(\nu)}), 0)]\right]$$

for $i \in \mathcal{D}_0$ and

$$y^{(\nu+1)} = f\left(\sum_{i\in\mathcal{D}_0} s_i + \sum_{i\in\mathcal{S}_0}\min\left(\frac{\zeta_i^{(0)}(x^{(\nu)}, y^{(\nu)})}{y^{(\nu)}}, s_i\right)\right),$$

with $\zeta_i^{(0)}(x, y)$ for all $i \in \mathcal{S}_0$ defined as in Equation (2.6), substituting k with 0. Next, we have to show that

$$(x^{(\nu+1)}, y^{(\nu+1)}) \leq (x^{(\nu)}, y^{(\nu)}) \quad \forall \nu = 0, 1, \ldots, \tag{2.9}$$

which we will prove by induction. First, for the base case, $\nu = 0$, we observe that for $i \in \mathcal{D}_0$:

$$\begin{aligned}
x_i^{(1)} &= \alpha\left[r_i + s_i y^{(0)}\right] + \beta\left[\sum_{j\in\mathcal{D}_0}\Pi_{ji}x_j^{(0)} + \sum_{j\in\mathcal{S}_0}[\Pi_{ji}\bar{p}_j + \lambda C_{ji}\max(w_j^*(x^{(0)}, y^{(0)}), 0)]\right] \\
&\leq r_i + s_i q^{(0)} + \sum_{j\in\mathcal{D}_0}\Pi_{ji}p_j^{(0)} \\
&\quad + \sum_{j\in\mathcal{S}_0}\Pi_{ji}\bar{p}_j + \lambda\sum_{j\in\mathcal{S}_0}C_{ji}\max(w_j^*(p^{(0)}, q^{(0)}), 0) \\
&= r_i + s_i q^{(0)} + \sum_{j=1}^{n}\Pi_{ji}p_j^{(0)} + \lambda\sum_{j=1}^{n}C_{ji}\max(w_j^*(p^{(0)}, q^{(0)}), 0) \\
&< \bar{p}_i = p_i^{(0)} = x_i^{(0)}.
\end{aligned}$$

Here, the first inequality is satisfied because $0 \leq \alpha, \beta \leq 1$. The second step follows from $p_j^{(0)} = \bar{p}_j$ on $\mathcal{S}_0$ and $w_j^*(p^{(0)}, q^{(0)}) < 0$ for $j \in \mathcal{D}_0$. The last step holds according to the definition of $\mathcal{D}_0$ and due to the fact that $0 \leq \lambda \leq \mu_i(p^{(0)}) \leq 1$.

Moreover,

$$\sum_{i \in \mathcal{D}_0} s_i + \sum_{i \in \mathcal{S}_0} \min\left(\frac{\zeta_i^{(0)}(x^{(0)}, y^{(0)})}{y^{(0)}}, s_i\right) \geq 0,$$

by definition of $\zeta_i^{(0)}(x^{(0)}, y^{(0)})$. Thus, since f is monotonically decreasing and $f(0) = q_0$, it follows that $y^{(1)} \leq q_0 = y^{(0)}$. Now, suppose that inequality (2.9) is satisfied up to some ν. Then, one obtains:

$$\begin{aligned}
\zeta_i^{(0)}(x^{(\nu)}, y^{(\nu)}) = \max\Bigg(\bar{p}_i - r_i - &\sum_{j \in \mathcal{D}_0} \Pi_{ji} x_j^{(\nu)} \\
&- \sum_{j \in \mathcal{S}_0} [\Pi_{ji}\bar{p}_j + \mathbb{I}_i \lambda C_{ji} \max(w_j^*(x^{(\nu)}, y^{(\nu)}), 0)], 0\Bigg) \\
\geq\ &\zeta_i^{(0)}(x^{(\nu-1)}, y^{(\nu-1)}),
\end{aligned}$$

by the induction hypothesis and Lemma 2.1.2 (b). This yields $y^{(\nu+1)} \leq y^{(\nu)}$, again exploiting the induction hypothesis together with the fact that f is monotonically decreasing.

Analogously, it follows from the recursive definition that $x_i^{(\nu+1)} \leq x_i^{(\nu)}$ for all $i \in \mathcal{D}_0$. Thus, the sequence continues to decrease for all ν. Hence, the limit $(x, y) := \lim\limits_{\nu \to \infty}(x^{(\nu)}, y^{(\nu)})$ exists and solves Equations (2.4) and (2.5). Moreover, (x, y) is the maximal solution to these equations by construction. This completes the base step of the induction argument for the proof of (2.8).

(I.S.) For the induction step, $k \to k+1$, we first observe that by the induction hypothesis we have that $\mathcal{D}_k \supseteq \mathcal{D}_{k-1}$ or, equivalently, $\mathcal{S}_k \subseteq \mathcal{S}_{k-1}$. Hence, for all $i \in \mathcal{S}_k$: $p_i^{(k+1)} = \bar{p}_i = p_i^{(k)}$. Thus, we have to investigate the payments of the defaulting banks and the corresponding price of the illiquid asset, defined by the maximal solution to Equations (2.4) and (2.5). Analogous to the base step, we propose the following recursive principle to calculate this maximal solution. Start with $(x^{(0)}, y^{(0)})$, where $x_i^{(0)} = p_i^{(k)}$ for $i \in \mathcal{D}_k$ and $y^{(0)} = q^{(k)}$, and define $(x^{(\nu)}, y^{(\nu)})$ by the obvious modification of the above recursive principle:

$$x_i^{(\nu+1)} = \alpha\left[r_i + s_i y^{(\nu)}\right] + \beta\Bigg[\sum_{j\in\mathcal{D}_k}\Pi_{ji}x_j^{(\nu)} + \sum_{j\in\mathcal{S}_k}[\Pi_{ji}\bar{p}_j + \lambda C_{ji}\max(w_j^*(x^{(\nu)},y^{(\nu)}),0)]\Bigg] \tag{2.10}$$

for $i \in \mathcal{D}_k$ and

$$y^{(\nu+1)} = f\left(\sum_{i\in\mathcal{D}_k} s_i + \sum_{i\in\mathcal{S}_k}\min\left(\frac{\zeta_i^{(k)}(x^{(\nu)},y^{(\nu)})}{y^{(\nu)}}, s_i\right)\right), \tag{2.11}$$

with $\zeta_i^{(k)}(x,y)$ for all $i \in \mathcal{S}_k$ defined as in Equation (2.6). Again, we want to prove that

$$(x^{(\nu+1)}, y^{(\nu+1)}) \leq (x^{(\nu)}, y^{(\nu)}), \quad \nu = 0, 1, \ldots. \tag{2.12}$$

First, note that for $\nu = 0$,

$$\begin{aligned}\sum_{j\in\mathcal{D}_k}\Pi_{ji}x_j^{(0)} = \sum_{j\in\mathcal{D}_k}\Pi_{ji}p_j^{(k)} &= \sum_{j\in\mathcal{S}_{k-1}\backslash\mathcal{S}_k}\Pi_{ji}p_j^{(k)} + \sum_{j\in\mathcal{D}_{k-1}}\Pi_{ji}p_j^{(k)}\\ &= \sum_{j\in\mathcal{S}_{k-1}\backslash\mathcal{S}_k}\Pi_{ji}\bar{p}_j + \sum_{j\in\mathcal{D}_{k-1}}\Pi_{ji}p_j^{(k)},\end{aligned}$$

observing $\mathcal{D}_k = (\mathcal{S}_{k-1}\backslash\mathcal{S}_k) \cup \mathcal{D}_{k-1}$ and $p_j^{(k)} = \bar{p}_j$ for all $j \in \mathcal{S}_{k-1}$. Second,

$$\sum_{j\in\mathcal{S}_k} C_{ji}\max(w_j^*(x^{(0)},y^{(0)}),0) = \sum_{j\in\mathcal{S}_{k-1}} C_{ji}\max(w_j^*(p^{(k)},q^{(k)}),0),$$

since $w_j^*(p^{(k)},q^{(k)}) < 0$ for all $j \in \mathcal{S}_{k-1}\backslash\mathcal{S}_k \subseteq \mathcal{D}_k$. We thus obtain that

$$\begin{aligned}x_i^{(1)} &= \alpha\left[r_i + s_i y^{(0)}\right] + \beta\Bigg[\sum_{j\in\mathcal{D}_k}\Pi_{ji}x_j^{(0)}\\ &\quad + \sum_{j\in\mathcal{S}_k}[\Pi_{ji}\bar{p}_j + \lambda C_{ji}\max(w_j^*(x^{(0)},y^{(0)}),0)]\Bigg]\\ &= \alpha\left[r_i + s_i q^{(k)}\right] + \beta\Bigg[\sum_{j\in\mathcal{D}_{k-1}}\Pi_{ji}p_j^{(k)}\\ &\quad + \sum_{j\in\mathcal{S}_{k-1}}[\Pi_{ji}\bar{p}_j + \lambda C_{ji}\max(w_j^*(p^{(k)},q^{(k)}),0)]\Bigg].\end{aligned} \tag{2.13}$$

For $i \in \mathcal{D}_{k-1}$ this shows that $x_i^{(1)} = p_i^{(k)} = x_i^{(0)}$. For the remaining case $i \in \mathcal{D}_k \backslash \mathcal{D}_{k-1}$, we have

$$\begin{aligned}
x_i^{(1)} &\leq r_i + s_i q^{(k)} + \sum_{j\in\mathcal{D}_{k-1}} \Pi_{ji} p_j^{(k)} + \sum_{j\in\mathcal{S}_{k-1}} [\Pi_{ji}\bar{p}_j + \lambda C_{ji} \max(w_j^*(p^{(k)}, q^{(k)}), 0)] \\
&= r_i + s_i q^{(k)} + \sum_{j=1}^{n} \Pi_{ji} p_j^{(k)} + \lambda \sum_{j=1}^{n} C_{ji} \max(w_j^*(p^{(k)}, q^{(k)}), 0) < \bar{p}_i = p_i^{(k)} \\
&= x_i^{(0)}.
\end{aligned}$$

Here, the first inequality holds because $0 \leq \alpha, \beta \leq 1$. The first stated equality follows from $p_j^{(k)} = \bar{p}_j$ for $j \in \mathcal{S}_{k-1}$ and the fact that $w_j^*(p^{(k)}, q^{(k)}) < 0$ for all $j \in \mathcal{D}_{k-1} \subseteq \mathcal{D}_k$. The last inequality results from $i \in \mathcal{D}_k \backslash \mathcal{D}_{k-1} \subseteq \mathcal{S}_{k-1}$.

For the price of the illiquid asset, we first observe that for all $i \in \mathcal{S}_k$,

$$\zeta_i^{(k)}(x^{(0)}, y^{(0)}) = \zeta_i^{(k-1)}(p^{(k)}, q^{(k)})$$

by using the same arguments as for Equation (2.13). From this it follows that

$$\begin{aligned}
y^{(1)} &= f\left(\sum_{i\in\mathcal{D}_{k-1}} s_i + \sum_{i\in\mathcal{S}_{k-1}\backslash\mathcal{S}_k} s_i + \sum_{i\in\mathcal{S}_k} \min\left(\frac{\zeta_i^{(k-1)}(p^{(k)}, q^{(k)})}{q^{(k)}}, s_i\right)\right) \\
&\leq f\left(\sum_{i\in\mathcal{D}_{k-1}} s_i + \sum_{i\in\mathcal{S}_{k-1}} \min\left(\frac{\zeta_i^{(k-1)}(p^{(k)}, q^{(k)})}{q^{(k)}}, s_i\right)\right) = q^{(k)} = y^{(0)},
\end{aligned}$$

because f is monotonically decreasing and the last step follows from the definition of $q^{(k)}$. This proves (2.12) for $\nu = 0$; the arguments for $\nu > 0$ are analogous. This implies that $(p^{(k+1)}, q^{(k+1)}) = \lim_\nu (x^{(\nu)}, y^{(\nu)}) \leq (x^{(0)}, y^{(0)}) = (p^{(k)}, q^{(k)})$. This finishes the induction step $k \to k+1$, and thus completes the first step of the proof, i.e., the sequence of price-payment pairs $(p^{(k)}, q^{(k)})$ decreases.

2. In the second step, we need to show that $(p^{(k)}, q^{(k)}) \geq (p^+, q^+)$ for all $k = 0, 1, \ldots, n$. Again, this will be established by induction. For $k = 0$ the assertion is obvious, since $(p^{(0)}, q^{(0)}) = (\bar{p}, q_0) \geq (p^+, q^+)$ by Lemma 2.2.1 (a).

   For the induction step $k \to k+1$, we observe that by the induction hypothesis a bank that defaults under $(p^{(k)}, q^{(k)})$ does also default under (p^+, q^+), thus $\mathcal{D}(p^+, q^+) \supseteq \mathcal{D}_k$. Now, for $i \in \mathcal{S}_k$, one has $p_i^{(k+1)} = \bar{p}_i \geq p_i^+$. It again remains to analyze the entries of $p^{(k+1)}$ belonging to banks in $\mathcal{D}_k$. Therefore, we reuse the recursive principle stated in Equation (2.10) together with (2.11), and prove that for all $\nu =$

$0,1,\ldots: x_i^{(\nu)} \geq p_i^+ \ (i \in \mathcal{D}_k)$, $y^{(\nu)} \geq q^+$. Now, starting again with $x_i^{(0)} = p_i^{(k)}$ for $i \in \mathcal{D}_k$ and $y^{(0)} = q^{(k)}$, we obtain for $i \in \mathcal{D}_k$ that

$$
\begin{aligned}
x_i^{(1)} &= \alpha \left[r_i + s_i q^{(k)}\right] + \beta \left[\sum_{j\in\mathcal{D}_k} \Pi_{ji} p_j^{(k)} + \sum_{j\in\mathcal{S}_k} [\Pi_{ji}\bar{p}_j + \lambda C_{ji} \max(w_j^*(p^{(k)}, q^{(k)}), 0)]\right] \\
&\geq \alpha \left[r_i + s_i q^+\right] + \beta \left[\sum_{j\in\mathcal{D}_k} \Pi_{ji} p_j^+ + \sum_{j\in\mathcal{S}_k} [\Pi_{ji}\bar{p}_j + \lambda C_{ji} \max(w_j^*(p^+, q^+), 0)]\right] \\
&\geq \alpha \left[r_i + s_i q^+\right] + \beta \left[\sum_{j=1}^{n} \Pi_{ji} p_j^+ + \lambda \sum_{j=1}^{n} C_{ji} \max(w_j^*(p^+, q^+), 0)\right] = p_i^+.
\end{aligned}
$$

Here, the first inequality holds because of the induction hypothesis and Lemma 2.1.2 (b). The second inequality follows from $\bar{p} \geq p^+$ and $w_j^*(p^+, q^+) < 0$ for all $j \in \mathcal{D}_k \subseteq \mathcal{D}(p^+, q^+)$. Finally, (p^+, q^+) is a price-payment equilibrium by assumption; thus, the last equality holds for $i \in \mathcal{D}_k \subseteq \mathcal{D}(p^+, q^+)$ according to Definition 2.1.3.

Regarding the price of the illiquid asset, we first obtain by the induction hypothesis that $\zeta_i^{(k)}(p^{(k)}, q^{(k)}) \leq \zeta_i^{(k)}(p^+, q^+)$, for all $i \in \mathcal{S}_k$. This leads to

$$
\begin{aligned}
y^{(1)} &= f\left(\sum_{i\in\mathcal{D}_k} s_i + \sum_{i\in\mathcal{S}_k} \min\left(\frac{\zeta_i^{(k)}(p^{(k)}, q^{(k)})}{q^{(k)}}, s_i\right)\right) \\
&\geq f\left(\sum_{i\in\mathcal{D}(p^+,q^+)} s_i + \sum_{i\in\mathcal{S}(p^+,q^+)} \min\left(\frac{\zeta_i^{(k)}(p^+, q^+)}{q^+}, s_i\right)\right) = q^+,
\end{aligned}
$$

using similar arguments as before. Hence, by the recursive definition of the sequence $(x^{(\nu)}, y^{(\nu)})$, we see that every element of this sequence will be larger than or equal to the corresponding entries of the greatest price-payment equilibrium. Overall, this yields $(p^{(k)}, q^{(k)}) \geq (p^+, q^+)$ for all $k = 0, 1, \ldots, n$, as desired.

3. To finish this proof, we combine all previous arguments. By our first step, the payment vectors are decreasing with each iteration of the algorithm and hence, $\mathcal{D}_{k+1} \supseteq \mathcal{D}_k$, which leads to two possible cases. The first is $\mathcal{D}_{k+1} = \mathcal{D}_k$. In this case, the algorithm terminates and due to the fixed-point construction, $(p^{(k)}, q^{(k)})$ is a price-payment equilibrium as in Definition 2.1.3. Moreover, as (p^+, q^+) is the unique greatest price-payment equilibrium and by our second step $(p^{(k)}, q^{(k)}) \geq (p^+, q^+)$, the algorithm terminates with the greatest price-payment equilibrium. The second possibility for the sequence of default sets is that it is strictly increasing from one round to another, i.e., $\mathcal{D}_{k+1} \supset \mathcal{D}_k$. This means that a new bank joined

the default set, and payments and prices have to be adjusted. But since there are at most n banks that can join the default set, after at most $n+1$ iterations[11] the default set does not change anymore. Thus, we eventually end up in the first possible case, finding the greatest price-payment equilibrium.

2.6 Appendix: Price-Payment Equilibria Example

Price-payment equilibria are non-unique and, moreover, the set of equilibria is not necessarily connected. In the following example, we will construct a financial system in which for some $p \in \mathbb{R}^n$ with $p^- < p < p^+$ there does not exist a $q \in [q^-, q^+]$ such that (p, q) is a price-payment equilibrium. We will also show that for given $q \in \mathbb{R}$ with $q^- < q < q^+$ it is not always possible to find $p \in [p^-, p^+]$ such that (p, q) is a price-payment equilibrium.

For the analysis of the counterexample, we recall two necessary conditions for price-payment equilibria (p^*, q^*) from Definition 2.1.3:

1. For a given clearing price q^*, the clearing payment vector p^* satisfies the relation
$$p^* = \chi(p^*, q^*). \tag{2.14}$$
For any fixed $q \in [q_{\min}, q_0]$, we call a corresponding fixed point of equation (2.14) a *clearing vector for* q, denoted by p^{*q}. Its existence is established by Tarski's fixed-point theorem, analogous to the proof of Theorem 2.2.2.

2. Analogously, for fixed $p \in [\mathbf{0}, \bar{p}]$, we define a *clearing price for* p by
$$q^{*p} = f(\theta(p, q^{*p})). \tag{2.15}$$
Its existence follows again from Tarski's fixed-point theorem.

Consider the following financial system:

$$\Pi = \begin{pmatrix} 0 & 0.4 \\ 0.4 & 0 \end{pmatrix}, r = \begin{pmatrix} 0.5 \\ 0.5 \end{pmatrix}, s = \begin{pmatrix} 1 \\ 2 \end{pmatrix}, \bar{p} = \begin{pmatrix} 1 \\ 1 \end{pmatrix},$$

$\alpha = \beta = 0.5$, with cross-holdings C set to zero, and the inverse demand function $f(x) = \exp(-x)$. We obtain the greatest and least price-payment equilibrium by Algorithm 2.2.4 and Remark 2.2.6:

$$(p^-, q^-) \approx \left(\begin{pmatrix} 0.3488 \\ 0.3695 \end{pmatrix}, 0.0498 \right), \quad (p^+, q^+) \approx \left(\begin{pmatrix} 1 \\ 1 \end{pmatrix}, 0.7717 \right).$$

[11] In the first round, $k = 0$, the default set can be empty as the contagion process may solely be triggered by the asset price effect.

We first demonstrate that there is no price-payment equilibrium (p,q) with payments $p = (0.4, 0.5)^T$, although $p^- < p < p^+$. If $p = (0.4, 0.5)^T$ was a clearing vector, then by (2.14)

$$p_i = \chi_i(p,q) = \alpha(r_i + s_i q) + \beta\Big(\sum_{j \in \mathcal{N}} \Pi_{ji} p_j\Big), \quad i = 1,2.$$

This follows since both banks are in default and faced with bankruptcy costs. However, there is no q solving both equations simultaneously. Hence, there is no $q \in [q^-, q^+]$ such that $p = (0.4, 0.5)^T$ becomes a clearing vector for q.

Second, we demonstrate that there is no price-payment equilibrium (p,q) with $q = 0.05$, although $q^- < q < q^+$. If q was a clearing price, then by (2.15):

$$0.05 = q = f(\theta(p, 0.05)) = \exp(-\theta(p, 0.05)) = \exp(-3) = 0.0498,$$

since $\theta(p, 0.05) = 3$ for all $p \in [p^-, p^+]$. This is a contradiction.

2.7 Appendix: Cross-Holdings with Price Impact

As explained in Section 2.1, we assume that the liquidation of cross-holdings is subject to price impact. So far, this was simply encoded by the parameter $\lambda \in \mathbb{R}^n$ which referred to a fixed fraction that can be realized. A more sophisticated approach consists in specifying an inverse demand function for cross-holdings. Letting $q^C \in \mathbb{R}^n$ be the vector of net worth prices for the cross-holdings in the n banks and $\theta^C[w, q^C] \in \mathbb{R}^n$ the amount of cross-holdings liquidated for a net worth vector $w \in \mathbb{R}^n$, the price vector q^C is given as a fixed point of the inverse demand function $f^C : \mathbb{R}^n \to [0,1]^n = [\mathbf{0}, \mathbf{1}] \subset \mathbb{R}^n$, i.e.,

$$q^C = f^C(\theta^C[w, q^C]),$$

with $f^C(\mathbf{0}) = \mathbf{1}$ and $x \mapsto f^C(x)$ monotonically decreasing. In case of liquidation, the value of bank i's cross-holdings is given by $\sum_{j \in \mathcal{N}} C_{ji} \max(w_j, 0) q_j^C$.

As before, we suppose that banks liquidate their cross-holdings proportionally; i.e., each bank $j \in \mathcal{N}$ calculates the proportion of cross-holdings it needs to liquidate:

$$v_j^C[w, q^C] = \min\left(\frac{\max\left[\bar{p}_j - r_j - \sum_{k \in \mathcal{N}} \Pi_{kj} p_k - (1 - \mathbb{I}_j) s_j q\ , 0\right]}{\sum_{k \in \mathcal{N}} C_{kj} \max(w_k, 0) q_k^C}, 1 \right);$$

thus, the total quantity of bank i's shares that is liquidated by other banks equals

$$\theta_i^C[w, q^C] = \sum_{j \in \mathcal{N}} C_{ij}\, v_j^C[w, q^C].$$

The net worth price vector q^C depends on the banks' net worths vector w and vice versa. We characterize these values as a combined equilibrium:

Definition 2.7.1. For fixed payments $p \in \mathbb{R}^n_+$ and a price of the illiquid asset $q \in \mathbb{R}_+$, a *net worth equilibrium* $[w^*, q^{C*}] \in \mathbb{R}^n \times \mathbb{R}^n$ is a fixed point of the function $\Psi^C : \mathbb{R}^n \times \mathbb{R}^n \to \mathbb{R}^n \times \mathbb{R}^n$ defined by:

$$\begin{aligned}
&\Psi^C[w, q^C] \\
&= \{r + sq + \Pi^T p + \mathrm{Diag}(v^C)C^T \,\mathrm{Diag}(q^C)(w \vee \mathbf{0}) + (I - \mathrm{Diag}(v^C))C^T(w \vee \mathbf{0})\} \\
&\quad \times \{f^C(\theta^C[w, q^C])\}.
\end{aligned}$$

The existence of a greatest and least net worth equilibrium follows again from Tarski's fixed-point theorem, now applied to the function Ψ^C.

Note that the modeling framework that we consider in the numerical case studies above is a special case of the general inverse demand function. Setting $\lambda_i = (1 - c)\kappa$ with $0 \leq \kappa \leq 1$, the corresponding inverse demand function f^C is defined by its components $f^C_j(x) = (1 - c)\kappa$, $j \in \mathcal{N}$.

3 Market Efficient Portfolios in a Systemic Economy

The original version of this chapter was previously published as a working paper, see Awiszus, Capponi, and Weber (2020).

Forced asset sales and purchases have been widely observed in financial markets. The most popular form of forced trading is that of fire sales which has been extensively implemented by hedge funds and broker dealers during the global 2007-2009 financial crisis; see Brunnermeier and Pedersen (2008) and Khandani and Lo (2011) for empirical evidence.

An asset is sold at a depressed price by a seller who faces financial constraints that become binding, i.e., when the seller becomes unable to pay his own creditors without liquidating the asset. For example, members of a clearinghouse need to post additional collateral if the value of their portfolios drops by a significant amount (Pirrong (2011)). Similarly, a mutual fund may need to liquidate assets at discounted prices if it faces heavy redemption requests from its investors and does not have enough cash reserves at disposal (Chen et al. (2010)). Banks manage their leverage based on internal value at risk models (Adrian and Shin (2014); Greenlaw et al. (2008)) and may need to liquidate (or purchase) assets if negative (or positive) shocks hit their balance sheets.

Forced purchases, despite less emphasized, are also important in financial markets. For instance, empirical evidence (see Coval and Stafford (2007)) suggests that equity mutual funds substantially increase their existing positions if they experience large inflows, thus creating upward pressure in the price of stocks held by these funds. Such inflow-driven purchases produce trading opportunities for outsiders, who would be able to sell their assets and earn a significant premium.

Asset purchases and sales triggered by financial constraints push asset prices away from fundamental values (Shleifer and Vishny (1992)), a form of inefficiency that we analyze in a systemic economy. Typically, when a firm must sell assets to fulfill a financial constraint, the potential buyers with the highest valuation for the asset are other firms belonging to the same industry or investors with appropriate expertise. Those firms are likely to be in a similar financial situation and thus unable to supply liquidity. The buyers of these assets are then outsiders, who value these assets less. A symmetric argument holds if the firm executes inflow-driven purchases.

When a firm impacts asset prices through its trading actions, other market participants who happen to hold the same assets on their balance sheets are also affected and may in turn violate their financial constraints, making it necessary for them to take trading actions. Through this process, the trading risk becomes *systemic*, i.e, it imposes cascading effects on asset prices and recursively impacts the equity of market participants through common asset ownership.

We consider an economy consisting of leveraged institutions (henceforth, called *banks*) that track a fixed leverage ratio. Empirically, this behavior has been well documented for commercial banks in the United States, see, e.g., Adrian and Shin (2010). After a shock hits an asset class, prices change and so does the bank's leverage ratio. To fulfill the financial constraint of targeting its leverage, the bank must then liquidate or purchase assets, depending on whether the experienced shock was positive or negative. Banks trade assets with other non-banking institutions that we model collectively as a representative nonbanking sector, assumed to have a downward sloping demand function as in Capponi and Larsson (2015). The equilibrium price of the asset is uniquely pinned down by the point at which the demand of the banking and nonbanking sector intersect.

We study market efficiency, measured by the mean squared deviation of fundamental capitalization, where all banks' portfolios are valued at the fundamental values, from market capitalization, where banks' portfolios are valued at the market prices. The latter prices internalize the pressure imposed by trading activities, as banks leverage or deleverage in response to exogenous shocks to asset values. Clearly, the closer prices are to their fundamental values, the more efficient the market is.

We consider the problem of maximizing efficiency from a centralized planner's perspective. This objective can be micro-founded in terms of increasing the information content of prices and as a result, better guiding the resource allocation in the economy. Brunnermeier et al. (2018) provide a simple economic setting, in which maximizing social welfare is consistent with the objectives of minimizing the deviation of asset prices from fundamentals and of reducing asset market volatility.[1]

We develop an explicit characterization of the distribution of banks' holdings that ex-ante maximize market efficiency. We refer to those as the *f-efficient holdings*[2]. The key

[1]The important role of prices in aggregating information that is dispersed in the economy has also been considered in the early work of Hayek (1945). Prices thereby facilitate the efficient allocation of scarce resources. In the context of secondary markets, this issue is, e.g., discussed in Leland (1992), Dow and Gorton (1997), Subrahmanyam and Titman (2001), Dow and Rahi (2003), and Goldstein and Guembel (2008).

[2]The terminology f-efficient is used to emphasize that the notion of efficiency we consider is related to fundamentals.

insight resulting from our approach is the identification of a sufficient statistic, the *systemic significance* vector, which captures the contribution of each bank to increased price pressures.

The systemic significance depends on the banks' target leverage, the banks' trading strategies, and the illiquidity characteristics of the assets. We adopt an "aggregate first then allocate" procedure to construct a solution to the quadratic minimization problem yielding f-efficient holdings. First, using the statistics of asset shocks, we construct a vector of auxiliary weighted holdings. Then, we distribute the holdings to the banks based on their contributions to market inefficiency, which is directly proportional to their systemic significances.

We show that portfolio diversification is f-efficient if asset price shocks are homogeneous and banks are heterogeneous in terms of their systemic significance. Our analysis suggests that as the shocks hitting an asset class become (statistically) larger, it is beneficial to transfer the holdings of such an asset from a more systemically significant to a less systemically significant bank to raise efficiency. We demonstrate that the more homogeneous the economy is in terms of banks' systemic significances, the further away the matrix of f-efficient holdings is from the matrix of full asset diversification.

Literature

There is, by now, a large number of studies that have analyzed the systemic implications of leverage and risk taking in an economy of leveraged institutions. Existing literature has identified two main channels through which banks are interlinked. The first channel is through the liability side of the balance sheet. Banks have claims on their debtors and once they are hit by shocks, they may become unable to honor their liabilities, potentially triggering negative feedback loops from reduced payments through the system. Seminal contributions in this direction include Eisenberg and Noe (2001), which provides an algorithm to measure contagion triggered by sequential defaults in the network of obligations, and Acemoglu et al. (2015), who analyze the stability of various network structures and their resilience to shocks of different sizes.[3]

The second channel is through the asset side of the balance sheet, as banks are interlinked through common portfolio holdings. Financial contagion arises when banks take hits on their balance sheets, typically because the price of their assets is subject to pressure due to forced purchases or sales (see also the discussion in the beginning of this chapter).

[3]Other related works include Elliott et al. (2014) and Gai and Kapadia (2010). Glasserman and Young (2015), Capponi et al. (2016), and Rogers and Veraart (2013) account for the impact of bankruptcy costs at defaults in a counterparty network model of financial contagion. Measures of systemic downside risk are analyzed in the works by Chen et al. (2013), Feinstein et al. (2017), and Biagini et al. (2019).

The present chapter contributes to this stream of literature. Our study is related to the study of Greenwood et al. (2015), who calibrate a model of fire-sale spillovers, assuming an economy of leverage targeting banks. Their work has been extended by Capponi and Larsson (2015), who consider the higher order effects of fire-sales externalities in a similar leverage targeting model. Duarte and Eisenbach (2019) construct and empirically valuate a measure of systemic risk generated by fire-sales externalities. The main components of their measure, namely banks' sizes, leverages, and illiquidity concentration, also constitute the primary determinants of the systemic significance vector in our model. Other works have considered models where contagion happens both through the asset and liability side of the balance sheet; see, for instance, the earlier work of Cifuentes et al. (2005) and the more recent works of Amini et al. (2013), Chen et al. (2016), and Weber and Weske (2017) (cf. Chapter 2 of this thesis). The models used in these papers build on the clearing payment framework of Eisenberg and Noe (2001) and further assume that banks sell illiquid assets when their available cash holdings plus payments received from other banks in the network are insufficient.

The analytical infrastructure of our model builds on the work of Greenwood et al. (2015) and Capponi and Larsson (2015). As in Greenwood et al. (2015), we restrict attention to the first-order effects of price pressures, i.e., those caused by the first round of banks' trading actions in response to shocks. As in Capponi and Larsson (2015), price impact is endogenous in our model and is determined by the capacity of the unconstrained nonbanking sector to absorb the trading pressure of the constrained banks. While Greenwood et al. (2015), Duarte and Eisenbach (2019), and Capponi and Larsson (2015) consider an ex-post model of asset contagion, where banks manage their assets after the shock has occurred, this chapter conducts an ex-ante analysis of balance sheet holdings.

A related study by Cont and Schaaning (2017) develops a systemic stress testing model and compares the asset pricing implications of threshold based versus target leveraging. Wagner (2011) analyzes the tradeoff between diversity on the systemic level and diversification at the banking level. While we focus on the centralized problem of maximizing market efficiency, Wagner (2011) considers the privately optimal solution. Specifically, he analyzes the Nash equilibrium of portfolio holdings in an economy consisting of a continuum of infinitesimally small investors with limited liability, each of them suffering liquidation costs only if he is not the only one to liquidate assets.[4]

Finally, our work is related to a branch of literature that has analyzed the stability of portfolio allocations, diversification, and heavy tail risks of portfolios. Using a general-

[4]Portfolio similarity has also been considered in other industry sectors than banking. In the insurance industry, Girardi et al. (2019) find a strong positive relationship between the portfolio similarity of pairs of insurance companies and their quarterly common sales during the following year.

ized branching process approach, Caccioli et al. (2014) identify a critical threshold for leverage which separates stable from unstable portfolio allocations (see also Raffestin (2014)). In a risk-sharing context, Ibragimov et al. (2011) analyze the tradeoff of diversity and diversification for heavy-tailed risk portfolio distributions. They show that the incentives of intermediaries (for diversification) and society (for diversity) are not necessarily aligned. Their findings are confirmed by results of Beale et al. (2011), who analyze the individually and systemically optimal allocations in a simplified loss model consisting of a small number of banks and assets.

Outline

The chapter is organized as follows. Section 3.1 summarizes the asset price contagion model. Our main contributions start from Section 3.2, where we define the quantitative measure of market efficiency and identify key drivers of this measure such as the vector of banks' systemic significances. In Section 3.3, we characterize f-efficient allocations. Section 3.4 provides case studies for a calibrated version of our model, which highlight the trade-off between diversification and diversity. Section 3.5 concludes. All proofs are delegated to Appendix 3.6.

3.1 Model Specification

To begin with, we introduce a few notations and definitions used throughout the chapter. For two (column) vectors $u = (u_1, \ldots, u_n)^\top$ and $v = (v_1, \ldots, v_n)^\top$, we let $u \circ v = (u_1 v_1, \ldots, u_n v_n)^\top$ denote the componentwise product. Similarly, $\frac{u}{v} = (u_1/v_1, \ldots, u_n/v_n)^\top$ denotes the componentwise ratio. We use $\mathrm{Diag}(u)$ to denote the diagonal matrix with vector u on the diagonal. The identity matrix is denoted by $\boldsymbol{I}$, the vector or matrix of ones is denoted by $\mathbf{1}$, and the vector or matrix of zeros is denoted by $\mathbf{0}$, where the dimension is either specified explicitly, e.g., $\mathbf{1}_K \in \mathbb{R}^K$, or clear from the context.

Our analysis is developed within the one-period version of the price contagion model by Capponi and Larsson (2015), which we briefly review in this section. They consider a financial market that consists of two sectors: a banking sector and a nonbanking sector. Each bank manages its asset portfolio to track a fixed leverage ratio, consistently with empirical evidence reported in the seminal contribution of Adrian and Shin (2010).[5] The

[5] In practice, banks do not immediately revert to the target leverage. Duarte and Eisenbach (2019) estimate the speed of leverage adjustment and find that leverage adjustment speed is roughly constant until 2006, before increasing by over 50% and spiking in 2008 due to the greater delevering through balance sheet contraction. Because we consider a one period snapshot of the economy, we may simply view the target leverage as a short-term target leverage.

nonbanking sector consists of institutions that are primarily equity funded (e.g., mutual funds, money market funds, insurances, and pension funds) and thus do not engage in leverage targeting.

There are K types of assets available, whose market prices at time $t = 0, 1$ are denoted by P_t^k. We write

$$P_t = (P_t^1, P_t^2, \dots, P_t^K)^\top$$

for the column vector of asset prices. The aggregate supply of each asset is fixed and given by $Q_{\text{tot}} = (Q_{\text{tot}}^1, \dots, Q_{\text{tot}}^K)^\top$. Each asset k is hit by an exogenous shock Z^k, which is modeled as a random variable. We use $Z = (Z^1, \dots, Z^K)^\top$ to denote the vector of shocks. The vector of *fundamental values* of the assets at time 1 is $P_0 + Z$, while we use P_1 to denote the vector of equilibrium prices which internalize banks' responses to shocks.

3.1.1 The Banking Sector

The economy consists of N banks, whose stylized balance sheets consist of assets, debt, and equity. Banks manage their balance sheets by buying or selling assets so to keep their leverage ratios (debt to equity ratios) at specified target levels. Banks hold a portfolio of assets at time 0. Then, price shocks occur and banks purchase or sell assets to restore leverage. These actions impose pressure on prices and as a result, the market value of bank portfolios at time 1 deviates from its fundamental value.

The quantity (number of units) of asset k held by bank i at time t is denoted by Q_t^{ki}. We use $Q_t^i = (Q_t^{1i}, Q_t^{2i}, \dots, Q_t^{Ki})^\top \in \mathbb{R}^K$ to denote the vector of bank i's holdings at t and $\boldsymbol{Q} := (Q_0^{ki})_{k=1,\dots,K, i=1,\dots,N} \in \mathbb{R}^{K \times N}$ to denote the matrix of banks' holdings at time zero. We write $A_t^i = (A_t^{1i}, A_t^{2i}, \dots, A_t^{Ki})^\top$, where $A_t^{ki} = P_t^k Q_t^{ki}$ is the market value of the i'th bank's holdings in asset k at t. The total market value of the i'th bank is given by $\mathbf{1}^\top A_t^i = \sum_{k=1}^K A_t^{ki}$.

Banks finance purchases by issuing debt. We use D_t^i to denote the total amount of debt issued by bank i at time t and assume that the interest rate on the debt is zero.[6] The main behavioral assumption in the model is that each bank i targets a fixed leverage ratio (debt to equity ratio) κ^i, i.e.,

$$\frac{D_t^i}{\mathbf{1}^\top A_t^i - D_t^i} = \kappa^i, \quad t = 0, 1, \quad i = 1, \dots, N. \tag{3.1}$$

Each bank executes an exogenously specified strategy $\alpha^i \in \mathbb{R}^K$, which specifies how a change in the amount of debt is offset by purchases or sales of the different assets

[6] Accounting for an exogenous nonzero interest rate would not qualitatively affect the results. Because our focus is on the price inefficiencies caused by banks' trading responses to shocks, we opt for a simpler model that highlights these effects.

in the portfolio. Hence, it holds that $\sum_{k=1}^{K} \alpha^{ki} = 1$. For future purposes, let $\boldsymbol{\alpha} := (\alpha^{ki})_{k=1,\ldots,K,i=1,\ldots,N} \in \mathbb{R}^{K\times N}$ denote the trading strategy matrix and let $L^i = \kappa^i/(1+\kappa^i)$. Hence, by the leverage equation (3.1), it always holds that $D_t^i = L^i \mathbf{1}^\top A_t^i$ for $t = 0, 1$.

The banks' demand curves, where $\Delta Q^{ki} := Q_1^{ki} - Q_0^{ki}$ denotes the change in quantities from period 0 to period 1, admit an explicit expression.

Proposition 3.1.1 (Capponi and Larsson (2015)). *The incremental demand of bank i for asset k is given by*

$$\Delta Q^{ki} = \alpha^{ki}\kappa^i Q_0^{i\top}\frac{\Delta P}{P_1^k}. \tag{3.2}$$

3.1.2 The Nonbanking Sector

Nonbanking institutions trade the same assets as the banking sector. This gives rise to additional demand, which we refer to as the *nonbanking demand*, and model it in a reduced form. We assume that demand curves are decoupled across assets, i.e., the nonbanking demand for asset k only depends on the price of asset k and not on the prices of other assets.[7]

At time 0, the nonbanking sector holds a quantity $Q_0^{k,\mathrm{nb}}$ of asset k and we write $A_0^{k,\mathrm{nb}} = P_0^k Q_0^{k,\mathrm{nb}}$ for the corresponding asset value. Unlike the banking sector whose demand function is upward sloping, the nonbanking sector has a downward sloping demand curve: it sells an asset if its price is above the fundamental value and purchases an asset if its price is below its fundamental value. Hence, the nonbanking sector acts as the liquidity provider when there are shocks and exerts a stabilizing force on the pressure imposed by banks. The demand for asset k is given by

$$\Delta Q^{k,\mathrm{nb}} = -\gamma_k Q_0^{k,\mathrm{nb}}\frac{\Delta P^k - Z^k}{P_1^k}, \tag{3.3}$$

where γ_k is a positive constant. This choice of demand function admits the following interpretation. Assume no shock occurs, i.e., $Z^k = 0$. Then

$$\frac{\Delta Q^{k,\mathrm{nb}}}{Q_0^{k,\mathrm{nb}}} = -\gamma_k \frac{\Delta P^k}{P_1^k}. \tag{3.4}$$

The parameter γ_k can thus be interpreted as the elasticity of the nonbanking demand for asset k, similar to $\kappa^i\alpha^{ki}$ in (3.2) for the banking sector. We refer to γ_k as the illiquidity characteristic of asset k. Unlike equation (3.4), (3.3) includes the correction term Z_k,

[7] This modeling choice allows us to focus only on the price impact caused by the banks' needs of tracking their leverage requirements.

because nonbanking demand is due to deviations from fundamental values. We write $Q_t^{\mathrm{nb}} = (Q_t^{1,\mathrm{nb}}, \ldots, Q_t^{K,\mathrm{nb}})^\top$, and denote by $\gamma = (\gamma_1, \ldots, \gamma_K)^\top$ the vector of illiquidity characteristics.

3.1.3 Asset Prices

In this section, we review the mechanism used to determine prices. The market-clearing condition is given by

$$Q_t^{\mathrm{nb}} + \sum_{i=1}^{N} Q_t^i = Q_{\mathrm{tot}}, \qquad t = 0, 1, \tag{3.5}$$

where the vector Q_{tot} of aggregate supply is constant through time. Capponi and Larsson (2015) identify the systemicness matrix $\boldsymbol{S}$ defined by $\boldsymbol{S} = \sum_{i=1}^{N} \frac{\alpha^i}{\gamma \circ Q_0^{\mathrm{nb}}} \kappa^i Q_0^{i\top} \in \mathbb{R}^{K \times K}$, or, in component-wise form,

$$S^{k\ell} = \sum_{i=1}^{N} \alpha^{ki} \frac{\kappa^i Q_0^{\ell i}}{\gamma_k Q_0^{k,\mathrm{nb}}}, \quad k, \ell = 1, \ldots, K, \tag{3.6}$$

as the primary determinant of market prices. This matrix captures how a shock to asset ℓ propagates to asset k through the banks' deleveraging activities.

Proposition 3.1.2 (Proposition 2.1. in Capponi and Larsson (2015))**.** *The dynamics of asset prices are given by*

$$\Delta P = (\boldsymbol{I} - \boldsymbol{S})^{-1} Z, \tag{3.7}$$

assuming that the matrix inverse exists.

Assumption 3.1.3. We will assume that the spectral radius of $\boldsymbol{S}$ is smaller than one. This yields invertibility of the matrix $\boldsymbol{I} - \boldsymbol{S}$, as needed in Proposition 3.1.2, with $(\boldsymbol{I} - \boldsymbol{S})^{-1} = \sum_{j=0}^{\infty} \boldsymbol{S}^j$. The spectral radius $\rho(\boldsymbol{S})$ for non-negative $\boldsymbol{S}$ is bounded from above by (cf. Capponi and Larsson (2015) and Horn and Johnson (1985), Corollary 8.1.29):

$$\rho(\boldsymbol{S}) \leq \max_{k=1,\ldots,K} \frac{\sum_{i=1}^{N} \kappa^i \alpha^{ki} \sum_{\ell=1}^{K} Q_0^{\ell i}}{\gamma_k Q^{k,\mathrm{nb}}}.$$

The spectral radius is small if the size of the nonbanking sector is large in comparison to the size of the leverage targeting banking sector, leverage targets are not too large, and price elasticities are not too small.

3.2 Market Inefficiencies and Systemic Significance

In this section, we introduce the measure used to quantify price deviation from fundamentals and characterize the key quantities that determine market efficiency. Section 3.2.1 derives an explicit expression for the price deviation from fundamentals and states the objective function of minimizing market efficiency in a systemic economy. Section 3.2.2 introduces a key sufficient statistic, a bank's systemic significance, that quantifies the contribution to price pressures of each bank in the economy.

3.2.1 Market Capitalization and Deviation from Efficiency

Banks actively manage their balance sheets in response to shocks and this imposes a pressure on asset prices, pushing them away from fundamental values. The value of market capitalization at the end of period 1 is given by

$$\begin{aligned} MC^e &:= Q_{\text{tot}}^\top P_1 = Q_{\text{tot}}^\top (P_0 + \Delta P) \\ &= Q_{\text{tot}}^\top \left(P_0 + (\boldsymbol{I} - \boldsymbol{S})^{-1} Z\right), \end{aligned} \tag{3.8}$$

where we recall that Z is the vector of exogenous price shocks (cf. equation (3.7)). In the absence of leverage-tracking banks, changes in prices are driven solely by changes in fundamentals, i.e., by the exogenous shocks. The resulting market capitalization is denoted by MC^f and given by

$$MC^f := Q_{\text{tot}}^\top (P_0 + Z).$$

The contribution to realized asset prices arising from the presence of leverage targeting banks, denoted by $D := MC^e - MC^f$, is a measure of market inefficiency.

Under the conditions discussed in Assumption 3.1.3, we obtain the first order approximation to market capitalization given by

$$MC^a := Q_{\text{tot}}^\top \left(P_0 + (\boldsymbol{I} + \boldsymbol{S})Z\right),$$

where we consider only the first term in the power series expansion of $(\boldsymbol{I} - \boldsymbol{S})^{-1}$. Recall that the i'th column of the matrix $\boldsymbol{Q}$ denotes the initial asset holdings of bank i. We then obtain the following first order approximation for the fire-sales externalities:

$$D \approx MC^a - MC^f = Q_{\text{tot}}^\top (\boldsymbol{S}Z) = (\boldsymbol{Q}v)^\top Z, \tag{3.9}$$

where

$$v := \text{Diag}(\kappa)\boldsymbol{\alpha}^\top \frac{Q_{\text{tot}}}{\gamma \circ Q_0^{\text{nb}}} \in \mathbb{R}^N. \tag{3.10}$$

We refer to the vector v as the *systemic significance* of the N banks and discuss its properties and economic implications in Section 3.2.2. The vector $\boldsymbol{Q}v$, i.e., the initial allocation of assets within the banking sector weighted by the banks' systemic significances, is a *network multiplier*: it describes how an initial price shock Z is amplified through the network of balance sheet holdings due to the leverage targeting actions of the banks.

Deviation from Efficiency: We use the mean squared deviation criterion

$$\mathbb{E}[D^2] \approx \mathbb{E}[(MC^a - MC^f)^2] =: MSD(\boldsymbol{Q}),$$

to quantify *ex-ante* these inefficiencies. We use the average of the squares of price deviation from fundamentals, i.e., we penalize equally positive and negative deviations of market prices from fundamental values.

We use μ and Σ to denote, respectively, the expected value and covariance matrix of shocks, i.e., $\mathbb{E}[Z] = \mu = (\mu_1, \dots, \mu_K)^\top$ and $\mathrm{Cov}[Z] = \boldsymbol{\Sigma} \in \mathbb{R}^{K \times K}$. Henceforth, we impose the following assumption on the distribution of asset shocks.

Assumption 3.2.1. Price shocks Z_k, $k = 1, 2, \dots, K$, are uncorrelated with variances $\sigma^2 = (\sigma_1^2, \dots, \sigma_K^2)^\top$, i.e., $\boldsymbol{\Sigma} = \mathrm{Diag}(\sigma^2)$, $\sigma_k > 0$, and the initial asset prices are normalized to $P_0^k = 1$, $k = 1, \dots, K$.

Assumption 3.2.1 allows us to focus solely on the endogenous correlation, i.e., linkages between prices arising from the leverage targeting actions of the banks due to overlapping portfolios.

3.2.2 Systemic Significance

This section discusses the properties of the systemic significance of a bank and its dependence on the model primitives. We start observing that, for any bank i, its systemic significance equals

$$v^i \quad = \quad \kappa^i \sum_{k=1}^{K} \frac{\alpha^{ki}}{\gamma_k} \cdot \frac{Q_{\text{tot}}^k}{Q_0^{k,\text{nb}}},$$

as it easily follows from Eq. (3.10). The systemic significance v^i depends on the targeted leverage κ^i, banks' strategies α^{ki}, the vector γ of price elasticities, and the initial proportion of assets held by the nonbanking sector $\frac{Q_0^{k,\text{nb}}}{Q_{\text{tot}}^k}$. If bank i liquidates a large fraction of an illiquid asset (i.e., $\frac{\alpha^{ki}}{\gamma_k}$ is high), then it creates a larger price pressure, especially if it is targeting a high leverage κ^i. If the nonbanking sector holds a significant fraction of the assets in the economy, then it will be able to better absorb the aggregate demand of the banking sector and thus the systemic significance of any bank in the system will be reduced.

Remark 3.2.2. Observe that both D and the square-root of the mean squared deviation $\sqrt{\mathbb{E}[D^2]} \approx \sqrt{\mathbb{E}[(MC^a - MC^f)^2]}$ are positively homogeneous, when viewed as functions of the systemic significance vector v. In particular, price pressures vanish and the market becomes efficient when v approaches zero; conversely, as v gets large, inefficiencies are higher.

The mean and variance of market capitalization can be uniquely characterized by the matrix of asset holdings and the systemic significances of the banks in the system, as stated next.

Lemma 3.2.3. *It holds that*

$$\mathbb{E}[D] \approx (\boldsymbol{Q}v)^\top \mu, \qquad \mathrm{Var}[D] \approx (\boldsymbol{Q}v)^\top \boldsymbol{\Sigma}\, (\boldsymbol{Q}v).$$

Moreover, the mean squared deviation of price pressures equals

$$\begin{aligned}\mathbb{E}[D^2] &= \mathrm{Var}[D] + \mathbb{E}[D]^2 \\ &\approx (\boldsymbol{Q}v)^\top \underbrace{(\mu\mu^\top + \mathrm{Diag}(\sigma^2))}_{=:\boldsymbol{G}\in\mathbb{R}^{K\times K}}(\boldsymbol{Q}v) = MSD(\boldsymbol{Q}). \qquad (3.11)\end{aligned}$$

The formulas above indicate that the mean squared deviation is a function of $\boldsymbol{Q}v$, i.e., the initial allocation of assets within the banking sector weighted by the banks' systemic significances and of statistics about fundamental shocks collected in the matrix $\boldsymbol{G}$. This is consistent with intuition: larger shocks require banks to trade a higher amount of assets to restore their leverage targets. As a result, through the network multiplier $\boldsymbol{Q}v$, these shocks are amplified more and lead to a higher pressure on prices.

3.3 f-Efficient Holdings

In this section, we study the impact of banks' portfolio holdings on market efficiency and develop an explicit construction of holding matrices which minimize the deviation of market capitalization from its fundamental value. We refer to those matrices as *f-efficient holdings*. Section 3.3.1 introduces a two-step procedure, "aggregate first then allocate" to construct f-efficient holdings. Section 3.3.2 discusses the relation between f-efficient holdings and the diversification benchmark where each bank fully diversifies its portfolio holdings.

3.3.1 Characterization of f-Efficient Holdings

Taking the initial budget of the banks as fixed, we compute the matrix $\boldsymbol{Q}$ of initial holdings which is f-efficient, i.e., which minimizes the mean squared deviation $MSD(\boldsymbol{Q})$.[8]

Let $q \in \mathbb{R}^K$ be the vector of total initial holdings of the banking sector and $b \in \mathbb{R}^N$ the vector of banks' initial budgets. The set of initially feasible asset allocations within the banking sector is then given by

$$\mathcal{D} = \mathcal{D}(q, b) := \{\boldsymbol{Q} \in \mathbb{R}^{K \times N} \mid \boldsymbol{Q}\mathbf{1}_N = q \quad \text{and} \quad \mathbf{1}_K^\top \boldsymbol{Q} = b^\top\},$$

where we have assumed that the initial prices of all assets are normalized (see Assumption 3.2.1). We then obtain

$$\sum_{k=1}^{K} q_k = \sum_{i=1}^{N} b_i =: T.$$

Example 3.3.1. Full portfolio diversification corresponds to the holding matrix

$$\boldsymbol{Q}^{\text{diversified}} := \frac{1}{T} q b^\top = \begin{pmatrix} \frac{b_1 q_1}{T} & \cdots & \frac{b_N q_1}{T} \\ \vdots & \ddots & \vdots \\ \frac{b_1 q_K}{T} & \cdots & \frac{b_N q_K}{T} \end{pmatrix} \in \mathcal{D}. \tag{3.12}$$

In the special case that initial aggregate holdings are the same for all assets, i.e., $q_1 = q_2 = \ldots = q_K$, full diversification is characterized by the holding matrix

$$\boldsymbol{Q}^{\text{diversified}} = \begin{pmatrix} \frac{b_1}{K} & \cdots & \frac{b_N}{K} \\ \vdots & \ddots & \vdots \\ \frac{b_1}{K} & \cdots & \frac{b_N}{K} \end{pmatrix}.$$

Definition 3.3.2. A feasible allocation matrix $\boldsymbol{Q}^* \in \mathcal{D}$ such that

$$\boldsymbol{Q}^* \in \operatorname*{argmin}_{\boldsymbol{Q} \in \mathcal{D}} \quad \underbrace{(\boldsymbol{Q}v)^\top \boldsymbol{G}(\boldsymbol{Q}v)}_{=MSD(\boldsymbol{Q})} \tag{3.13}$$

is called *f-efficient*.

f-efficient holdings are those which minimize, ex-ante, the mean squared deviation of asset prices from fundamentals among all feasible allocations. To exclude trivial cases and make the problem interesting, we make the following assumption, which is typically satisfied in practice.

[8] In Appendix 3.8, we study the sensitivity of market inefficiencies to the matrix $\boldsymbol{\alpha}$ of banks' trading strategies, taking the initial holdings as given. Consistent with intuition, we find that it is f-efficient for banks to sell solely the most liquid asset.

Assumption 3.3.3. There exist some $i, j \in \{1, \ldots, N\}$ such that $v_i \neq v_j$ and it holds that $b^\top v \neq 0$.

Remark 3.3.4. If $v_1 = \ldots = v_N$ then, for each given asset, it does not matter how it is distributed across the banks because all have the same systemic significance. As a result, $MSD(\boldsymbol{Q})$ is constant for all $\boldsymbol{Q} \in \mathcal{D}$, taking into account the constraint $\boldsymbol{Q}\mathbf{1} = q$. The requirement that systemic significance is not identical across banks is satisfied by any economy, which is not fully homogeneous in terms of targeted leverage and trading strategy. Empirically, Duarte and Eisenbach (2019), see Table 4 therein, find substantial variation in banks' leverage targets, with a size-weighted average of 13.6, an equal-weighted average of 11.5, and a standard deviation of 3.9.[9] If $b^\top v = 0$, there must exist banks in the system which are short some of the assets. Then, the negative price pressure imposed by some banks in the system would be compensated by a positive price pressure created by other banks. In this case, diversification would be f-efficient and lead to zero deviation of asset prices from fundamental values, i.e., $MSD(\boldsymbol{Q}^{\text{diversified}}) = (\frac{1}{T} q b^\top v)^\top \boldsymbol{G} (\frac{1}{T} q b^\top v) = 0$. In practice, however, $b^\top v > 0$ because the budget and the systemic significance of any bank in the system are both positive. Banks are long their assets, including consumer loans, agency and non-agency securities, municipal securities, etc.; see, again, Table 4 in Duarte and Eisenbach (2019).

We next describe the two-step procedure used to construct f-efficient holding matrices:

- **Step 1: Aggregation.** In this step, we find the network multiplier y that minimizes the mean squared deviation and which is consistent with the market structure. Concretely, let $\mathcal{D}_y := \{y \in \mathbb{R}^K \mid \mathbf{1}_K^\top y = b^\top v\}$. Such a multiplier is obtained from banks' initial holdings (and budgets), weighted with the systemic significance vector, i.e.,

$$y^* \in \underset{y \in \mathcal{D}_y}{\operatorname{argmin}} \quad y^\top \boldsymbol{G} y. \tag{3.14}$$

  Because of this weighting, the multiplier accounts for the banks' leverage tracking behavior, their liquidation strategies, and illiquidity characteristics of the assets. We refer to the minimizing vector y^* as the aggregate v-weighted holdings.

- **Step 2: Allocation.** In this step, we identify an allocation of asset holdings to banks, which is consistent with the vector of aggregate v-weighted holdings obtained from the previous step. Specifically, we denote by $\boldsymbol{Q}^* \in \mathcal{D}$ the matrix, consistent with the

[9] Their sample includes the largest 100 banks by assets every quarter, in a sample period from the third quarter of 1999 to the third quarter of 2016 at the quarterly frequency. They also find that 5% and 95% of the leverage target distribution are, respectively, 6.8 and 16.9 and that there is more cross-sectional than time-series variation.

budget and supply constraints, which distributes the aggregate v-weighted holdings to individual banks according to their systemic significance, i.e., $\boldsymbol{Q}^* v = y^*$.

The decomposition discussed above presents both conceptual and computational advantages. From a conceptual perspective, observe that the matrix $\boldsymbol{G}$ of shock statistics and the vector v of banks' systemic significances are "sufficient statistics" for the problem. In the aggregation step, the minimized functional only depends on $\boldsymbol{G}$, while v only enters into the constraint set. The allocation step instead, takes the aggregate holdings computed from the previous step as given and determines the holding matrix only on the basis of v. From a computational point of view, observe that finding the f-efficient holdings requires solving a $K \times N$ dimensional quadratic problem with linear constraints. Using the proposed decomposition, we first solve a K dimensional quadratic problem with one linear constraint and subsequently solve a simple $K \times N$ dimensional unconstrained linear system.

The following proposition states that the two-step procedure described above identifies f-efficient holdings.

Proposition 3.3.5. *Let $N \geq 2, K \geq 1$. The following statements are equivalent:*

(i) $\boldsymbol{Q}^* \in \mathcal{D}$ *is f-efficient.*

(ii) $y^* = \boldsymbol{Q}^* v$ *for some* $\boldsymbol{Q}^* \in \mathcal{D}$ *and* y^* *solves the problem* (3.14).

In the rest of the section, we discuss in more detail each step of the procedure above and highlight the key economic insights.

3.3.1.1 Step 1: Aggregation

We start showing that the minimization problem (3.14) admits a unique solution.

Lemma 3.3.6. *The unique solution to problem* (3.14) *is given by*

$$y^* := \frac{b^\top v}{\mathbf{1}_K^\top z} \cdot z,$$

where $z := \boldsymbol{G}^{-1}\mathbf{1}_K \in \mathbb{R}^K$.

The above expression indicates that aggregate v-weighted holdings are determined by the vector v, capturing the systemic significances of banks, weighted by the budget each bank is endowed with, and by the inverse of the matrix $\boldsymbol{G}$ which captures the size of the exogenous price shocks. Specifically, the aggregate systemically weighted budget vector

$b^\top v$ is split into the K available assets through the inverse of $\boldsymbol{G}$.

Example 3.3.7. Consider the special case of zero mean shocks, i.e., set $\mu = 0$. Then $y_k^* = (b^\top v) \cdot \frac{1/\sigma_k^2}{\sum_{\ell=1}^K 1/\sigma_\ell^2}$. Hence, the higher the variance of price shocks σ_k^2, the lower the fraction of asset k in the aggregate v-weighted holdings portfolio y^*. This is intuitive: an asset that creates high price pressure when banks manage their assets to restore their target leverage should, in aggregate, be invested less.

3.3.1.2 Step 2: Allocation

In the second step, the aggregate v-weighted holdings $y^* \in \mathbb{R}^K$ are allocated to the individual banks.

Proposition 3.3.8. *For every $N \geq 2, K \geq 1$, there exists a matrix $\boldsymbol{Q}^* \in \mathcal{D}$ satisfying $\boldsymbol{Q}^* v = y^*$.*

In the proof of the proposition, we construct a particular solution $\boldsymbol{Q}^*$ and describe the structure of the linear subspace of solutions. The following theorem shows existence, quantifies the mean squared deviation achieved by a matrix of f-efficient holdings, and addresses the uniqueness of the allocation.

Theorem 3.3.9. *Let $N, K \geq 2$.*

a) There exists an f-efficient holding matrix $\boldsymbol{Q}^*$ with mean squared deviation

$$MSD(\boldsymbol{Q}^*) = \frac{(b^\top v)^2}{\mathbf{1}_K^\top \boldsymbol{G}^{-1} \mathbf{1}_K}. \tag{3.15}$$

b) The f-efficient holding matrix is unique, if and only if there are exactly $N = 2$ banks. In this case, the unique f-efficient holding matrix is given by

$$\boldsymbol{Q}^{N=2} := \frac{1}{v_2 - v_1} \begin{pmatrix} v_2 q - y^* & y^* - v_1 q \end{pmatrix} \in \mathbb{R}^{K \times 2}. \tag{3.16}$$

3.3.2 When is Diversification f-Efficient?

In this subsection, we provide the conditions under which full diversification is f-efficient.

Theorem 3.3.10. *Full diversification $\boldsymbol{Q}^{\text{diversified}}$ is f-efficient, if and only if q and $z = \boldsymbol{G}^{-1} \mathbf{1}_K$ are linearly dependent.*

A direct consequence of the above theorem is that full diversification is f-efficient if the system is completely homogeneous, i.e., all asset shocks have the same mean and variance, and the total initial holdings of the banks are the same. Full diversification is no longer f-efficient if a little amount of heterogeneity is introduced in the system.

Corollary 3.3.11. *If either*

a) $q_1 = \ldots = q_K$, $\sigma_1^2 = \ldots = \sigma_K^2$, $\mu_1 = \ldots = \mu_{K-1}$, *and* $\mu_K = \mu_1 + \varepsilon$ *with* $\varepsilon \neq -K\mu_1$, *or*

b) $\mu_1 = \ldots = \mu_K$, $\sigma_1^2 = \ldots = \sigma_K^2$, $q_1 = \ldots = q_{K-1}$, *and* $q_K = q_1 + \varepsilon$, *or*

c) $q_1 = \ldots = q_K$, $\mu_1 = \ldots = \mu_K$, $\sigma_1^2 = \ldots = \sigma_{K-1}^2$, *and* $\sigma_K^2 = \sigma_1^2 + \varepsilon$,

then $\boldsymbol{Q}^{\text{diversified}}$ *is f-efficient, if and only if* $\varepsilon = 0$.

The result in the above corollary is consistent with intuition. If assets are fully homogeneous and the total holdings of the banking sector in each asset are the same, there is no reason to prefer one asset over the other. In this case, full diversification minimizes the portfolio liquidation risk and is optimal. However, as soon as assets no longer have identical characteristics, an f-efficient allocation requires to allocate assets to banks in accordance with their systemic significances. An alternative proof of Corollary 3.3.11 using the concept of matrix majorization, together with an analysis of the diversity vs. diversification tradeoff in homogeneous systems, is provided in Appendix 3.9.

3.4 Comparative Statics and Examples

In this section, we construct case studies to analyze the structure of f-efficient holdings. In the first part of this section, we consider the stylized case $N = K = 2$ and study the distance of f-efficient holdings from diversification as a function of key model parameters. For any matrix $\boldsymbol{Q} \in \mathbb{R}^{K \times N}$, we measure the distance from full diversification by the Frobenius norm

$$d(\boldsymbol{Q}) := \|\boldsymbol{Q} - \boldsymbol{Q}^{\text{diversified}}\|_F.$$

In the second part of the section, we study the minimal distance of f-efficient holdings from full diversification for the case $N = K = 3$. In the third part, we compare the impact of f-efficiency and diversification on the distribution of market capitalization under different economic scenarios.

3.4.1 The Case $N = K = 2$

According to Theorem 3.3.9 b), the f-efficient holding matrix for $N = K = 2$ is unique and given by

$$\boldsymbol{Q}^{2\times 2} := \frac{1}{v_2 - v_1} \begin{pmatrix} v_2 q_1 - y_1^* & y_1^* - v_1 q_1 \\ v_2 q_2 - y_2^* & y_2^* - v_1 q_2 \end{pmatrix}. \tag{3.17}$$

We normalize the total supply of assets within the banking sector and the budgets of banks to $q_1 = q_2 = b_1 = b_2 =: x > 0$; following Capponi and Larsson (2015), we choose $x = 0.08$, where the total supply is normalized to 1 for each asset. Hence, the the total size of the banking sector is 8% of the total size of the system.

3.4.1.1 Systemic Significance and Asset Riskiness

We start with an exploratory analysis, where we plot the f-efficient holdings of bank 1 and the distance of f-efficient holdings from diversification $d(\boldsymbol{Q}^{2\times 2})$ as a function of the riskiness of the first asset. Consistent with Corollary 3.3.11, full diversification is f-efficient

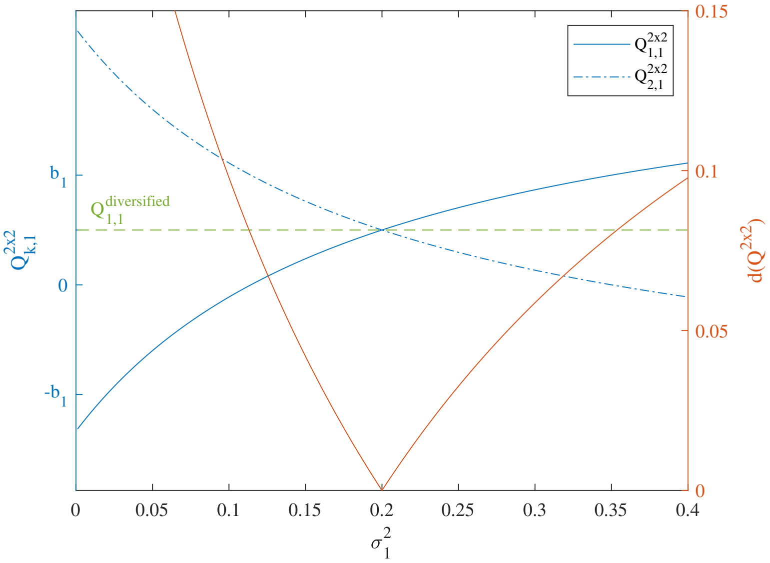

Figure 3.1: f-efficient holdings of bank 1 $\boldsymbol{Q}^{2\times 2}_{k,1}$ for assets $k = 1, 2$ and distance from diversification, $d(\boldsymbol{Q}^{2\times 2}) = \|\boldsymbol{Q}^{2\times 2} - \boldsymbol{Q}^{\text{diversified}}\|_F$, as a function of σ_1^2. We fix $\sigma_2^2 = 0.2$, $\mu = (0,0)^\top$, $v = (0.04, 0.07)^\top$, $q = b = (0.08, 0.08)^\top$.

if and only if $\sigma_1^2 = \sigma_2^2 = 0.2$. Figure 3.1 additionally suggests that a systemically more significant bank would have lower f-efficient holdings in the riskier asset than a systemically less significant bank: As σ_1 increases, bank 2 decreases its holdings in asset 1, while bank 1 increases it holdings in that asset. We rigorously formalize these observations in the following lemma.

Lemma 3.4.1. *Let* $q_1 = q_2 = b_1 = b_2 = x > 0$ *and* $\mu_1 = \mu_2$.

a) For $\sigma_1 > 0$, *we have*

$$\frac{\partial}{\partial \sigma_1} d(\boldsymbol{Q}^{2\times 2}) \begin{cases} < 0, & \textit{if } \sigma_1^2 < \sigma_2^2, \\ > 0, & \textit{if } \sigma_1^2 > \sigma_2^2. \end{cases}$$

b) If $v_2 > v_1 > 0$, *then* $\frac{\partial \boldsymbol{Q}_{1,1}^{2\times 2}}{\partial \sigma_1} > 0$ *for* $\sigma_1 > 0$.

3.4.1.2 Systemic Significance and Shock Sizes

As in the previous subsection, we start with a graphical illustration of the sensitivity of bank 1's f-efficient holdings and their distance from diversification to changes in the expected shock size μ. Figure 3.2 indicates that, as the expected (absolute) size of price

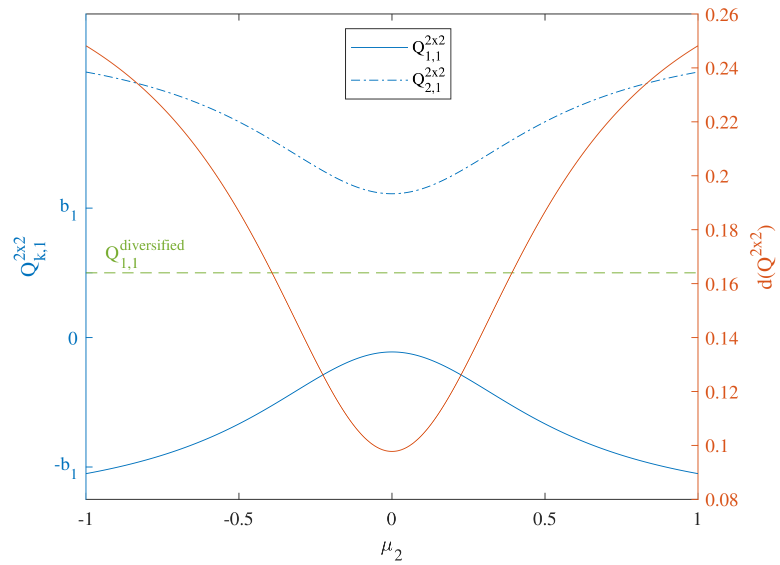

Figure 3.2: F-efficient holdings of bank 1 $\boldsymbol{Q}_{k,1}^{2\times 2}$ for assets $k = 1,2$ and distance from diversification $d(\boldsymbol{Q}^{2\times 2}) = \|\boldsymbol{Q}^{2\times 2} - \boldsymbol{Q}^{\text{diversified}}\|_F$ as a function of μ_2 for fixed $\sigma^2 = (0.1, 0.2)^\top$, $\mu_1 = 0$, $v = (0.04, 0.07)^\top$, $q = b = (0.08, 0.08)^\top$.

shocks for asset 2 increases, the f-efficient holdings of the least systemically significant bank (i.e., bank 1) increase. This can be, again, understood in terms of the banks' systemic significances: a more systemically significant bank, i.e., one that tracks a higher leverage ratio or which trades a larger fraction of illiquid assets, should reduce its holdings of asset 2, because the trading actions in response to the shock impose a higher pressure on the price and hence a large deviation of prices from fundamentals.

The distance from a full diversification strategy is minimal when the system achieves the highest possible degree of homogeneity, i.e., $\mu_2 = \mu_1$. As the system becomes more heterogeneous, the distance increases. As shown in Corollary 3.3.11, the minimal distance converges to zero as the system becomes fully homogeneous, i.e., $\sigma_1 = \sigma_2$. We formalize these observations via the following lemma.

Lemma 3.4.2. *Let $q_1 = q_2 = b_1 = b_2 = x > 0$, $\sigma_1^2 = \sigma_2^2$ and $\mu_1 = 0$.*

a) It holds that

$$\frac{\partial}{\partial \mu_2} d(\boldsymbol{Q}^{2\times 2}) \begin{cases} < 0, & \text{if } \mu_2 < 0, \\ = 0, & \text{if } \mu_2 = 0, \\ > 0, & \text{if } \mu_2 > 0. \end{cases}$$

b) If $v_2 > v_1 > 0$, then

$$\frac{\partial \boldsymbol{Q}_{1,1}^{2\times 2}}{\partial \mu_2} \begin{cases} > 0, & \text{if } \mu_2 < 0, \\ = 0, & \text{if } \mu_2 = 0, \\ < 0, & \text{if } \mu_2 > 0. \end{cases}$$

3.4.1.3 The Influence of Systemic Significance on f-Efficient Holdings

We analyze how heterogeneity in systemic significances impacts the degree of diversification of banks' holdings. Figure 3.3 highlights that, as the two banks become closer in terms of systemic significance, the distance of f-efficient holdings from diversification increases. This highlights the fundamental role of systemic significance on banks' f-efficient holdings: if two banks are similar in terms of systemic significance (for instance because they adopt similar trading strategies), then it is beneficial to sacrifice diversification benefits to reduce portfolio overlapping and thus price pressures. These intuitions can be formalized via the following lemma.

Lemma 3.4.3. *Let $q_1 = q_2 = b_1 = b_2 = x > 0$, $v_1 > 0$ and $|z_1| \neq |z_2|$[10]. For $0 < v_2 \neq v_1$, it holds that*

$$\frac{\partial}{\partial v_2} d(\boldsymbol{Q}^{2\times 2}) \begin{cases} > 0, & \text{if } v_2 < v_1, \\ < 0, & \text{if } v_2 > v_1. \end{cases}$$

[10] A sufficient condition for $|z_1| \neq |z_2|$ is that $\mu_1 = \mu_2$ and $\sigma_1^2 \neq \sigma_2^2$.

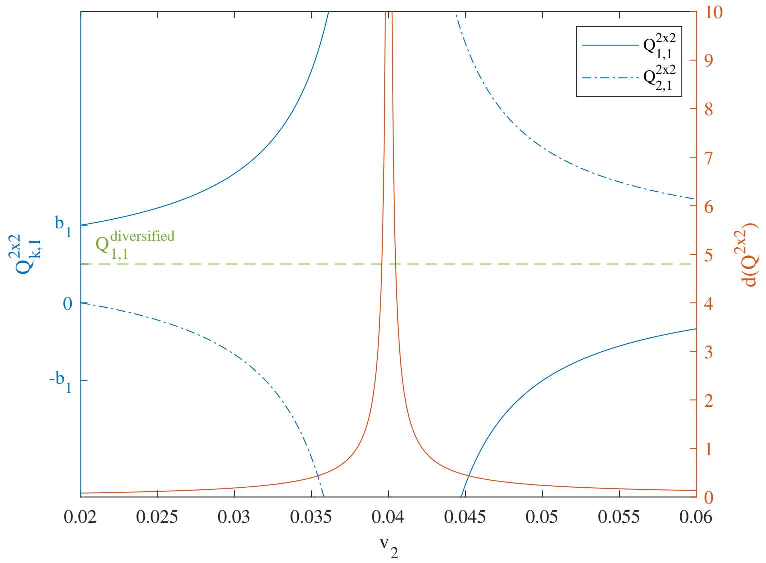

Figure 3.3: F-efficient holdings of bank 1 $\boldsymbol{Q}^{2\times2}_{k,1}$ for assets $k = 1,2$ and distance from diversification $d(\boldsymbol{Q}^{2\times2}) = \|\boldsymbol{Q}^{2\times2} - \boldsymbol{Q}^{\text{diversified}}\|_F$ as a function of systemic significance v_2 for fixed $\sigma^2 = (0.1, 0.2)^\top$, $\mu = (0,0)^\top$, $v_1 = 0.04$, $q = b = (0.08, 0.08)^\top$.

3.4.2 The Case $N = K = 3$

Having established the results for a system consisting of two banks and two assets, we analyze numerically how the findings would change for a larger economy. If the number of banks is $N > 2$, f-efficient holdings are no longer unique (see Theorem 3.3.9 b)). We then consider the f-efficient holdings whose Frobenius distance from diversification is minimal. Figure 3.4 plots the minimal distance of f-efficient holdings from diversification for the case $N = K = 3$. Noticeably, the qualitative findings remain similar to the setting $N = K = 2$. The f-efficient holdings get farther away from a full diversification strategy if heterogeneity in banks' systemic significances decreases. The intuition behind the result remains unchanged, i.e., in a system where banks are systemically very close, a full diversification strategy for each bank may lead to larger price pressures because all banks rebalance their portfolios in a similar fashion to meet their leverage targets.

In Appendix 3.7, we analyze the f-efficient holdings in an economy with more than two banks. We find that any f-efficient allocation prescribes the most systemically significant bank to have higher holdings of the less risky asset and the least systemically significant bank to have higher holdings of the more risky asset. We also show that for a system of three banks, given a fixed f-efficient allocation, any other f-efficient allocation is obtained by shifting the holdings within each bank based on the difference in systemic significances of the other two banks.

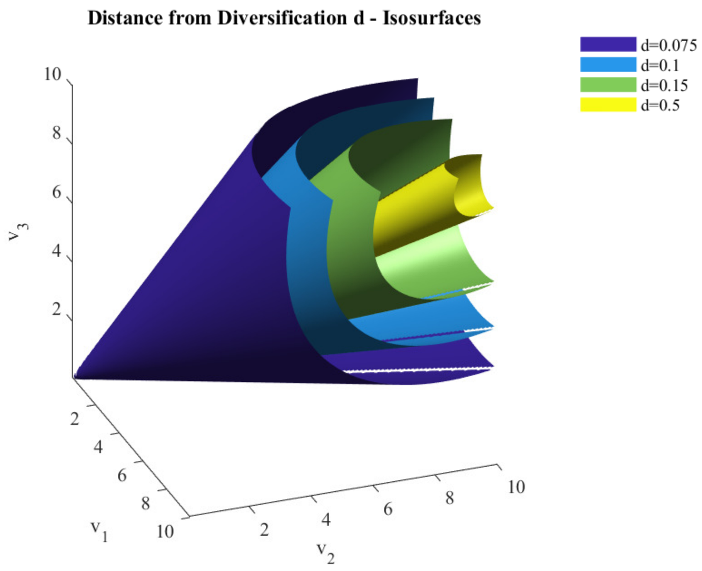

Figure 3.4: Isosurface plot of the Frobenius distance $d(\boldsymbol{Q}^{\min})$ from diversification for the f-efficient holding matrix $\boldsymbol{Q}^{\min}$ with the smallest distance to diversification. We vary the systemic significance parameters v_1, v_2, and v_3, and keep fixed shock characteristics, i.e., $\mu = (0.1, 0.125, 0.15)^\top$ and $\sigma^2 = (0.1, 0.15625, 0.225)^\top$. To ensure comparability with the results of Section 3.4.1, we choose $q_k = b_i = 0.08$, $i,k = 1,2,3$, and normalize the total supply of each asset to 1.

3.4.3 Systemic Significance, Market Scenarios, and Asset Holdings

In this section, we analyze how the distribution of banks' holdings depends on banks' systemic significances, heterogeneity in the distributions of initial shocks, and illiquidity characteristics of the assets. We also validate the accuracy of the first order approximation of market capitalization used throughout the chapter. Our results indicate that the mean squared deviation of the *actual* market capitalization from its fundamental value is low if the matrix of bank holdings coincides with the f-efficient holdings. This indicates that the solution to the (approximate) optimization problem, i.e., where the first-order approximation of the systemicness matrix is used, yields a low value for the actual objective function where the exact expression of the systemicness matrix is used.

In the analysis below, we consider three asset classes, each consisting of assets with identical characteristics, for a total of ten assets. As a result, we demonstrate that the methodology proposed in this chapter scales well to economies larger than those considered (analytically) in earlier sections.

3.4.3.1 Market Setting

We consider a financial market consisting of $N = 2$ banks. We choose $K = 10$ assets, normalize the total supply of each asset to 1, and set the holdings of banks in each asset to 0.08.[11] The two banks are assumed to have the same budget ($b_1 = b_2 = 0.8$) and the vector of leverage targets is $\kappa = (9, 10)^\top$.

Banks are assumed to follow a proportional liquidation strategy, i.e., $\alpha^{ki} = 1/10$ for all assets $k = 1, \ldots, 10$ and both banks $i = 1, 2$. The assets belong to three different groups: Assets 1 and 2 belong to group 1, assets 3 through 8 to group 2, and assets 9 and 10 to group 3. Within each of the three asset groups, the illiquidity characteristics of the assets and the expectation and variance of asset price shocks are equal.

We consider three economic scenarios, each characterized by a certain value of the shock variance and liquidity of the assets. We refer to the three scenarios as liquidity, intermediate crisis, and high risk high illiquidity scenarios. Across all scenarios, we set $\mu = (0.1, 0.1, 0.2, 0.2, 0.2, 0.2, 0.2, 0.2, 0.3, 0.3)^\top$.

The numerical values of the asset illiquidity characteristics should be interpreted as normalized to the corresponding characteristics of a reference asset and are broadly consistent with the estimates reported in Table 4 of Duarte and Eisenbach (2019).[12] Consistent with empirical evidence, the higher the illiquidity of the asset (i.e., the lower γ), the larger the variance of the exogenous asset price shocks, capturing the fact that more illiquid securities have a higher volatility than liquid ones.

(L) **Liquidity Scenario:**
Banks invest in liquid assets, i.e, assets with high price elasticities, or equivalently, low illiquidity characteristics. The first asset class has the highest price elasticity and the lowest shock variance and the third asset class has the lowest price elasticity and the highest variance. The second asset class has an intermediate value for those two quantities. Specifically, we choose

$$\gamma^L = (9, 9, 8, 8, 8, 8, 8, 8, 7, 7)^\top, \quad \sigma^L = (0.1, 0.1, 0.2, 0.2, 0.2, 0.2, 0.2, 0.2, 0.3, 0.3)^\top.$$

(I) **Intermediate Crisis Scenario:**
In contrast to scenario (L), the third asset class is significantly more illiquid (i.e., lower price elasticity) and has higher shock variance. This situation is typical of

[11] All parameters in this section are consistent with Capponi and Larsson (2015).

[12] Their estimates are based on the Net Stable Funding Ratio of the Basel III regulatory framework. Their illiquidity parameter is the reciprocal of ours, i.e., in their setting a larger value corresponds to a higher illiquidity of the asset. They take US Treasuries as the reference asset, i.e., the price impact of U.S. Treasuries is normalized to 1.

the beginning of a crisis period, where one asset may experience a severe shock and then becomes hard to sell quickly due to the lack of outside investors (the nonbanking sector in our model) willing to purchase the asset.[13] The parameters corresponding to the other asset classes are not altered. This scenario is specified by

$$\gamma^I = (9,9,8,8,8,8,8,8,1,1)^\top, \quad \sigma^I = (0.1,0.1,0.2,0.2,0.2,0.2,0.2,0.2,1,1)^\top.$$

(H) **High Risk High Illiquidity Scenario:**
Banks invest in assets with high illiquidity and volatility. This captures, for instance, a situation where banks invest in securities such as non-agency based mortgage, municipal bonds, or commercial and industry loans. All asset classes are thus characterized by a lower price elasticity and higher shock variance compared to the previous two scenarios:

$$\gamma^H = (3,3,2,2,2,2,2,2,1,1)^\top, \quad \sigma^H = (0.9,0.9,1.1,1.1,1.1,1.1,1.1,1.1,1.2,1.2)^\top.$$

Next, we compute the f-efficient holdings and banks' systemic significances for each of the above defined scenarios.

- In the liquidity scenario (L), the systemic significances of the banks equal $v_1^L \approx 1.23 < 1.37 \approx v_2^L$. The second bank—tracking a higher leverage ratio—is systemically more significant than the first bank. f-efficient holdings are given by

$$\boldsymbol{Q}^{*,L} \approx \begin{pmatrix} -3.79 & -3.79 & 0.87 & 0.87 & 0.87 & 0.87 & 0.87 & 0.87 & 1.37 & 1.37 \\ 3.87 & 3.87 & -0.79 & -0.79 & -0.79 & -0.79 & -0.79 & -0.79 & -1.29 & -1.29 \end{pmatrix}^\top.$$

  The systemically more significant bank 2 is endowed with a higher number of assets of class 1 (high elasticity, low variance); the least significant bank 1 holds a larger portion of the other assets (smaller elasticity, higher variance).

- In scenario (I), bank 2 is still systemically more significant than bank 1, i.e., $v_1^I \approx 2.91 < 3.23 \approx v_2^I$; in comparison to scenario (L), both banks' systemic significances increase due to the increased illiquidity and shock variances of assets from group 3. The f-efficient holdings are given by:

$$\boldsymbol{Q}^{*,I} \approx \begin{pmatrix} -3.87 & -3.87 & 1.07 & 1.07 & 1.07 & 1.07 & 1.07 & 1.07 & 0.87 & 0.87 \\ 3.95 & 3.95 & -0.99 & -0.99 & -0.99 & -0.99 & -0.99 & -0.99 & -0.79 & -0.79 \end{pmatrix}^\top.$$

  Again, the higher the systemic significance of the bank, the lower its holdings of the safer asset relative to the riskier asset.

[13] For instance, the volume of agency mortgage backed securities, typically highly liquid assets, declined substantially from 2008 to 2014, which is an indicator of worsening liquidity.

- In scenario (H), bank 2 remains systemically more significant than bank 1, with $v_1^H \approx 5.54 < 6.16 \approx v_2^H$, and the significance parameters are higher than in the two other scenarios. The f-efficient holdings are:

$$\boldsymbol{Q}^{*,H} \approx \begin{pmatrix} -0.41 & -0.41 & 0.10 & 0.10 & 0.10 & 0.10 & 0.10 & 0.10 & 0.31 & 0.31 \\ 0.49 & 0.49 & -0.02 & -0.02 & -0.02 & -0.02 & -0.02 & -0.02 & -0.23 & -0.23 \end{pmatrix}^\top .$$

  In this scenario, there is little heterogeneity in the riskiness of the assets and high heterogeneity in banks' systemic significances. As a result, the f-efficient holdings are more evenly distributed, i.e., closer to full diversification (see also the values of the distances given in Table 3.1 below).

3.4.3.2 Diversification and f-Efficiency

In this section, we compute the *exact* market capitalization, i.e.,

$$MC^e = Q_{\text{tot}}^\top (P_0 + (\boldsymbol{I} - \boldsymbol{S})^{-1} Z),$$

both under f-efficient ($\boldsymbol{Q}^{*,\cdot}$) and fully diversified ($\boldsymbol{Q}^{\text{diversified}}$) holding matrices. We suppose that the vector of shocks Z follows a multivariate normal distribution with mean vector μ, which is the same across all scenarios, and covariance matrix $\text{Diag}(\sigma^2)$, where σ depends on the considered scenario. In each scenario, we draw 100,000 independent samples of the shock vector Z.

We report the relevant statistics in Table 3.1. Figure 3.5 also provides a comparison of the probability density functions of market inefficiency and the corresponding box plots across all three scenarios. Consistent with intuition, the variance of market capitalization is the smallest in the liquidity scenario and the highest in the high risk high illiquidity scenario. We find that diversification results in a higher variance than f-efficiency across all market scenarios. While this difference is not very significant in the liquidity scenario, it becomes considerable in the crisis scenarios, especially if (as in the intermediate crisis scenario) the assets are shocked heterogeneously.

Observe, from the first row of the table, that the distance between f-efficient and fully diversified holding matrices is the lowest in the scenario (H). Nevertheless, the mean squared deviation criterion and variance of the exact market capitalization is the highest (in absolute terms) in such a scenario. Taken together, these two observations imply that if banks invest in high risk high illiquid assets, it suffices to only slightly distort the holdings from f-efficiency to induce large increases in the variance and mean squared deviation of market capitalization from its fundamental value. This is because holdings that are not f-efficient, such as fully diversified holdings, create a price pressure which becomes increasingly larger as we move towards balance sheets with highly volatile and illiquid assets.

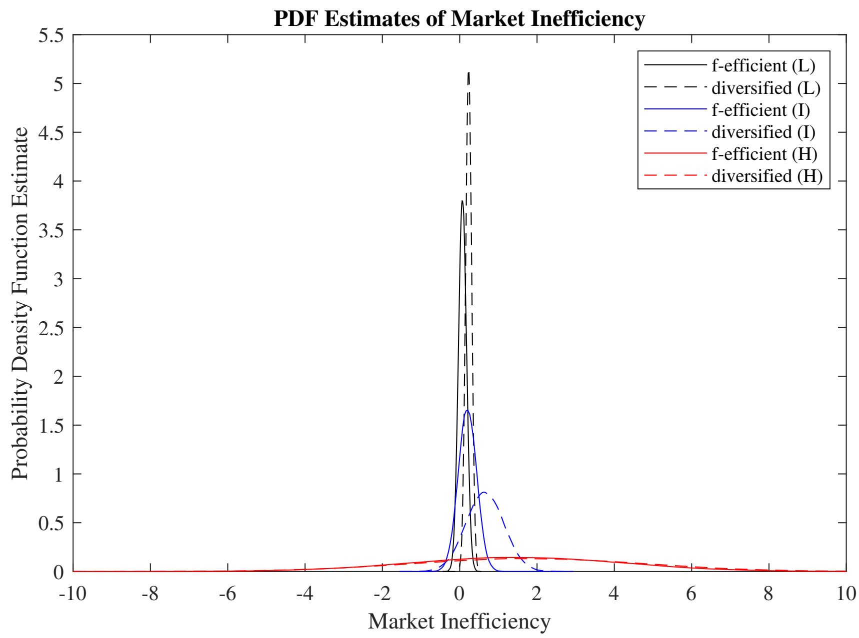

(a)

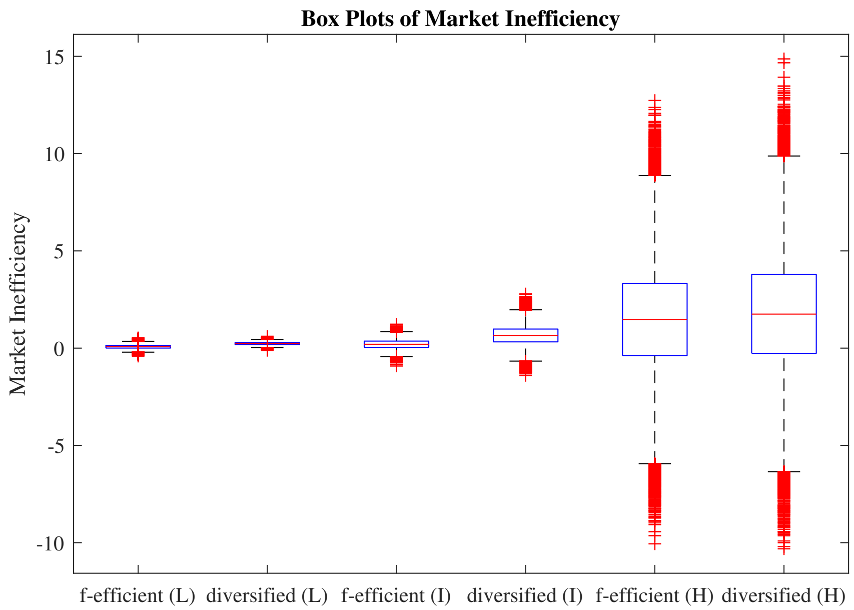

(b)

Figure 3.5: Probability density function estimates (a) and box plots (b) of market inefficiency $MC^e - MC^f$ for f-efficient ($\boldsymbol{Q}^{*,\cdot}$) and fully diversified ($\boldsymbol{Q}^{\text{diversified}}$) holdings, generated from 100,000 samples of $Z \sim \mathcal{N}_{10}(\mu, \text{Diag}((\sigma^{\cdot})^2))$, in the three considered scenarios: (L) liquidity, (I) intermediate crisis, and (H) high risk high illiquidity.

	L	I	H	I/L	H/L
$d(\boldsymbol{Q}^{*,\cdot})$	8.61	8.74	1.08	1.02	0.13
$\mathbb{E}(MC^e)$ for $\boldsymbol{Q}^{*,\cdot}$	12.07	12.20	13.45	1.01	1.11
$\mathbb{E}(MC^e)$ for $\boldsymbol{Q}^{\text{diversified}}$	12.23	12.65	13.74	1.03	1.12
$\text{Var}(MC^e)$ for $\boldsymbol{Q}^{*,\cdot}$	0.44	2.23	37.20	5.07	84.55
$\text{Var}(MC^e)$ for $\boldsymbol{Q}^{\text{diversified}}$	0.55	3.95	41.39	7.18	75.25
$\mathbb{E}[(MC^e - MC^f)^2]$ for $\boldsymbol{Q}^{*,\cdot}$	0.02	0.10	9.66	5.00	483.00
$\mathbb{E}[(MC^e - MC^f)^2]$ for $\boldsymbol{Q}^{\text{diversified}}$	0.06	0.66	12.14	11.00	202.33

Table 3.1: Statistics from the Monte Carlo simulation used to estimate the exact market capitalization. The Frobenius distance $d(\boldsymbol{Q}^{*,\cdot})$ measures the difference between diversified and f-efficient holdings. The last two columns present the numbers relative to the liquidity scenario.

3.5 Conclusion

We developed a model to examine the ex-ante asset holdings which minimize market inefficiency in a systemic multi-asset economy. Price pressure arises in our model from the exogenous trading actions of banks which manage their portfolios to target specific leverage ratios. In the model, we quantify inefficiency in terms of the mean squared deviation of market capitalization from capitalization measured using fundamental values. We find that inefficiencies are low if banks are not systemically significant, but become substantial if the overall systemic significance is high and banks are not sufficiently heterogeneous in systemic significance. We develop a procedure which constructs f-efficient holdings and show that these depend on two key sufficient statistics, namely the banks' systemic significances and the first two moments of exogenous asset shocks. Our analysis reveals that increasing heterogeneity in banks' systemic significances moves f-efficient holdings closer to full diversification, while heterogeneity in the distributions (expectation and variance) of exogenous asset value shocks moves f-efficient holdings away from diversification. In balance sheet scenarios characterized by high risk and illiquidity, deviating from f-efficient holdings would result in high inefficiencies and large variance of market capitalization.

3.6 Appendix: Proofs

3.6.1 Proofs of Section 3.1

3.6.1.1 Proof of Proposition 3.1.1

This proof is obtained by specializing Proposition 1.1 in Capponi and Larsson (2015) to a setting with only one period and assuming zero revenue shocks therein, i.e., $\Delta R^i = 0$. The fundamental cash-flow equation is given by:

$$P_1^k \Delta Q^{ki} = \alpha^{ki} \Delta D^i, \quad k = 1, \ldots, K. \tag{3.18}$$

Writing the cash-flow equation (3.18) in vector form yields

$$\mathrm{Diag}(P_1)\Delta Q^i = \alpha^i \Delta D^i.$$

Substituting for D_t^i in the above equation the expressions for L^i, we obtain

$$\begin{aligned} \mathrm{Diag}(P_1)\Delta Q^i &= \alpha^i \left(L_1^i \mathbf{1}^\top A_1^i - L_0^i \mathbf{1}^\top A_0^i\right) \\ &= \alpha^i \left(L_1^i \mathbf{1}^\top (A_1^i - A_0^i) + (L_1^i - L_0^i)\mathbf{1}^\top A_0^i\right). \end{aligned} \tag{3.19}$$

Rearranging the above expression leads to

$$\left(\mathrm{Diag}(P_1) - L^i \alpha^i P_1^\top\right) \Delta Q^i = \alpha^i L^i Q_0^{i\top} \Delta P. \tag{3.20}$$

The matrix multiplied by ΔQ^i can be inverted using the Sherman-Morrison formula. First, since $\mathbf{1}^\top \alpha^i = 1$, we have

$$1 - L^i P_1^\top \,\mathrm{Diag}(P_1)^{-1} \alpha^i = 1 - L^i \mathbf{1}^\top \alpha^i = 1 - L^i \neq 0,$$

so invertibility is guaranteed. The inverse is given by

$$\mathrm{Diag}(P_1)^{-1} + \kappa^i \,\mathrm{Diag}(P_1)^{-1} \alpha^i P_1^\top \,\mathrm{Diag}(P_1)^{-1},$$

which simplifies to $\mathrm{Diag}(P_1)^{-1}(I + \kappa^i \alpha^i \mathbf{1}^\top)$. From (3.20), we therefore obtain

$$\begin{aligned} \mathrm{Diag}(P_1)\Delta Q^i &= (I + \kappa^i \alpha^i \mathbf{1}^\top) \left(\alpha^i L^i Q_0^{i\top} \Delta P\right) \\ &= (1 + \kappa^i)\alpha^i \left(L^i Q_0^{i\top} \Delta P\right), \end{aligned}$$

where the second equality uses the identity $(I + \kappa^i \alpha^i \mathbf{1}^\top)\alpha^i = (1 + \kappa^i)\alpha^i$, which follows from $\mathbf{1}^\top \alpha^i = 1$. Noting that $(1 + \kappa^i)L^i = \kappa^i$, we obtain

$$\mathrm{Diag}(P_1)\Delta Q^i = \kappa^i \alpha^i Q_0^{i\top} \Delta P,$$

and the stated expression (3.2) follows.

3.6.1.2 Proof of Proposition 3.1.2

This proof is obtained by specializing Proposition 2.1 in Capponi and Larsson (2015) to a setting with only one period and assuming zero revenue shocks therein, i.e., $\Delta R^i = 0$. First, we use the market-clearing condition (3.5) and then the expressions (3.2) and (3.3) for the demand functions to get

$$\begin{aligned}\mathbf{0} &= P_1 \circ \Delta Q^{\mathrm{nb}} + \sum_{i=1}^{N} P_1 \circ \Delta Q^i \\ &= \operatorname{Diag}(\gamma \circ Q_0^{\mathrm{nb}})\,(Z - \Delta P) + \sum_{i=1}^{N} \alpha^i \kappa^i Q_0^{i\top} \Delta P.\end{aligned}$$

Multiplying from the left by $\operatorname{Diag}(\gamma \circ Q_0^{\mathrm{nb}})^{-1}$ and rearranging yields

$$\left[\boldsymbol{I} - \sum_{i=1}^{N} \frac{\alpha^i}{\gamma \circ Q_0^{\mathrm{nb}}} \kappa^i Q_0^{i\top}\right] \Delta P = Z. \tag{3.21}$$

The left-hand side is thus equal to $(\boldsymbol{I} - \boldsymbol{S})\Delta P$. We now simply multiply both sides of the equality (3.21) from the left by $(\boldsymbol{I} - \boldsymbol{S})^{-1}$ to arrive at the stated price change (3.7).

3.6.2 Proofs of Section 3.3

3.6.2.1 Proof of Proposition 3.3.5

- We first prove the direction (i)⇒(ii): Let $\boldsymbol{Q}^* \in \operatorname*{argmin}_{\boldsymbol{Q} \in \mathcal{D}} (\boldsymbol{Q}v)^\top \boldsymbol{G}(\boldsymbol{Q}v)$ be an f-efficient holding matrix. Since the objective function does only depend on the vector $\boldsymbol{Q}v \in \mathbb{R}^K$, the following statements are equivalent:

$$\boldsymbol{Q}^* \in \operatorname*{argmin}_{\boldsymbol{Q} \in \mathcal{D}} \; (\boldsymbol{Q}v)^\top \boldsymbol{G}(\boldsymbol{Q}v) \;\Leftrightarrow\; \widetilde{y} := \boldsymbol{Q}^* v \in \operatorname*{argmin}_{y \in \widetilde{\mathcal{D}}} \; y^\top \boldsymbol{G} y, \tag{3.22}$$

where $\widetilde{\mathcal{D}} := \{y \in \mathbb{R}^K \mid \exists\, \boldsymbol{Q} \in \mathcal{D} \text{ s.t. } y = \boldsymbol{Q}v\}$. Since every vector of the form $y = \boldsymbol{Q}v$ for one $\boldsymbol{Q} \in \mathcal{D}$ satisfies

$$\mathbf{1}_K^\top y = \mathbf{1}_K^\top \boldsymbol{Q} v = b^\top v,$$

it obviously holds that $\widetilde{\mathcal{D}} \subseteq \mathcal{D}_y = \{y \in \mathbb{R}^K \mid \mathbf{1}_K^\top y = b^\top v\}$ yielding $\min_{y \in \widetilde{\mathcal{D}}} y^\top \boldsymbol{G} y \geq \min_{y \in \mathcal{D}_y} y^\top \boldsymbol{G} y$. However, as shown by Proposition 3.3.8, if $y^* \in \mathcal{D}_y$ solves the aggregate problem, i.e., $y^* \in \operatorname*{argmin}_{y \in \mathcal{D}_y} y^\top \boldsymbol{G} y$, then there exists a matrix $\widetilde{\boldsymbol{Q}}$ such that $y^* = \widetilde{\boldsymbol{Q}} v$, i.e., $y^* \in \widetilde{\mathcal{D}}$. Hence,

$$\widetilde{y}^\top \boldsymbol{Q} \widetilde{y} = \min_{y \in \widetilde{\mathcal{D}}} \; y^\top \boldsymbol{G} y = \min_{y \in \mathcal{D}_y} \; y^\top \boldsymbol{G} y = (y^*)^\top \boldsymbol{G} y^*,$$

i.e., $\widetilde{y} = \boldsymbol{Q}^* v$ solves the aggregate problem (3.14).

- Second, we prove the direction (ii)⇒ (i): Let $y^* = \boldsymbol{Q}^* v \in \operatorname{argmin}_{y \in \mathcal{D}_y} y^\top \boldsymbol{G} y$ solve the aggregate problem. Since $\min_{y \in \widetilde{\mathcal{D}}} y^\top \boldsymbol{G} y \geq \min_{y \in \mathcal{D}_y} y^\top \boldsymbol{G} y$, with $\widetilde{\mathcal{D}}$ as defined in the previous step, and since $y^* = \boldsymbol{Q}^* v$ for some $\boldsymbol{Q}^* \in \mathcal{D}$, we have that $y^* = \boldsymbol{Q}^* v \in \operatorname{argmin}_{y \in \widetilde{\mathcal{D}}} y^\top \boldsymbol{G} y$, which, finally, is equivalent to $\boldsymbol{Q}^*$ being f-efficient, see (3.22).

3.6.2.2 Proof of Lemma 3.3.6

The KKT conditions for minimizing $y^\top \boldsymbol{G} y$ subject to $y \in \mathcal{D}_y$ read as

$$\underbrace{\begin{pmatrix} \boldsymbol{G} & \mathbf{1}_K \\ \mathbf{1}_K^\top & 0 \end{pmatrix}}_{=:\boldsymbol{M}} \cdot \begin{pmatrix} y \\ \lambda \end{pmatrix} = \begin{pmatrix} \mathbf{0}_K \\ b^\top v \end{pmatrix}. \tag{3.23}$$

The inverse of the KKT matrix $\boldsymbol{M}$ is by blockwise inversion (see, e.g., Proposition 2.8.7 in Bernstein (2005)) given by

$$\boldsymbol{M}^{-1} = \begin{pmatrix} \boldsymbol{G}^{-1} - \boldsymbol{G}^{-1}\mathbf{1}_K(\mathbf{1}_K^\top \boldsymbol{G}^{-1}\mathbf{1}_K)^{-1}\mathbf{1}_K^\top \boldsymbol{G}^{-1} & \boldsymbol{G}^{-1}\mathbf{1}_K(\mathbf{1}_K^\top \boldsymbol{G}^{-1}\mathbf{1}_K)^{-1} \\ (\mathbf{1}_K^\top \boldsymbol{G}^{-1}\mathbf{1}_K)^{-1}\mathbf{1}_K^\top \boldsymbol{G}^{-1} & -(\mathbf{1}_K^\top \boldsymbol{G}^{-1}\mathbf{1}_K)^{-1} \end{pmatrix} =: \begin{pmatrix} \boldsymbol{A} & \boldsymbol{B} \\ \boldsymbol{C} & \boldsymbol{D} \end{pmatrix},$$

with $\boldsymbol{A} \in \mathbb{R}^{K \times K}$, $\boldsymbol{B} \in \mathbb{R}^{K \times 1}$, $\boldsymbol{C} \in \mathbb{R}^{1 \times K}$, and $\boldsymbol{D} \in \mathbb{R}$. Note that this inverse matrix exists because, firstly, $\boldsymbol{G}$ is invertible because it is symmetric and positive definite, with inverse given by the Sherman-Morrison formula

$$\boldsymbol{G}^{-1} = \operatorname{Diag}(\tfrac{1}{\sigma^2}) - \frac{\frac{\mu}{\sigma^2}(\frac{\mu}{\sigma^2})^\top}{1 + (\frac{\mu}{\sigma^2})^\top \mu},$$

and, secondly,

$$\mathbf{1}_K^\top \boldsymbol{G}^{-1}\mathbf{1}_K = (\tfrac{1}{\sigma^2})^\top \mathbf{1}_K - \frac{(\mathbf{1}_K^\top \frac{\mu}{\sigma^2})^2}{1 + (\frac{\mu}{\sigma^2})^\top \mu} \neq 0,$$

since with $c := (\frac{1}{\sigma^2})^\top \mathbf{1}_K > 0$

$$\begin{aligned} (\tfrac{1}{\sigma^2})^\top \mathbf{1}_K - \frac{(\mathbf{1}_K^\top \frac{\mu}{\sigma^2})^2}{1 + (\frac{\mu}{\sigma^2})^\top \mu} = 0 \quad &\Leftrightarrow \quad c(1 + (\tfrac{\mu}{\sigma^2})^\top \mu) - (\mathbf{1}_K^\top \tfrac{\mu}{\sigma^2})^2 = 0 \\ &\Leftrightarrow \quad c + c \cdot (\tfrac{\mu}{\sigma})^\top (\tfrac{\mu}{\sigma}) - (\tfrac{\mu}{\sigma})^\top \tfrac{1}{\sigma}(\tfrac{1}{\sigma})^\top \tfrac{\mu}{\sigma} = 0 \\ &\Leftrightarrow \quad (\tfrac{\mu}{\sigma})^\top \underbrace{(\boldsymbol{I} - \tfrac{1}{c} \cdot \tfrac{1}{\sigma}(\tfrac{1}{\sigma})^\top)}_{=:\boldsymbol{E}} \tfrac{\mu}{\sigma} = -1, \end{aligned}$$

and this cannot be fulfilled for any $\frac{\mu}{\sigma} \in \mathbb{R}^K$ since $\boldsymbol{E} \in \mathbb{R}^{K\times K}$ is a positive semidefinite matrix due to its only eigenvalues 0 and 1 (cf. Dattorro (2005), Appendix B.3).

Hence, the f-efficient solution to problem (3.14) is derived from multiplying both sides of equation (3.23) by $\boldsymbol{M}^{-1}$ yielding

$$y^* = \boldsymbol{A}\cdot \boldsymbol{0}_K + \boldsymbol{B}\cdot (b^\top v) = b^\top v \cdot \boldsymbol{G}^{-1}\boldsymbol{1}_K(\boldsymbol{1}_K^\top \boldsymbol{G}^{-1}\boldsymbol{1}_K)^{-1} = \frac{b^\top v}{\boldsymbol{1}_K^\top z} z,$$

where $z := \boldsymbol{G}^{-1}\boldsymbol{1}_K$.

3.6.2.3 Proof of Proposition 3.3.8

We define the matrix

$$\boldsymbol{Q}^p := \left(\tfrac{1}{v_2-v_1}[v_2 q - y^* - (\textstyle\sum_{i=3}^N (v_2-v_i)b_i)e_1^K], \tfrac{1}{v_2-v_1}[y^* - v_1 q - (\textstyle\sum_{i=3}^N (v_i - v_1)b_i)e_1^K], b_3 e_1^K, \dots, b_N e_1^K \right) \in \mathbb{R}^{K\times N}, \tag{3.24}$$

where $e_1^K = (1,0,\dots,0)^\top \in \mathbb{R}^K$. Without loss of generality, we have assumed here that $v_2 \neq v_1$ (cf. Assumption 3.3.3). This matrix satisfies $\boldsymbol{Q}^p \in \mathcal{D}$ as well as $y^* = \boldsymbol{Q}^p v$, for $y^* = \frac{b^\top v}{\boldsymbol{1}_K^\top z} z$, the solution of the aggregate problem (3.14) derived in Lemma 3.3.6:

- $\underline{y^* = \boldsymbol{Q}^p v}$: It holds:

$$\begin{aligned}
(\boldsymbol{Q}^p v)_1 &= \frac{1}{v_2 - v_1}[v_1 v_2 q_1 - y_1^* v_1 - v_1 \sum_{i=3}^N (v_2 - v_i) b_i + y_1^* v_2 - v_1 v_2 q_1 \\
&\quad - v_2 \sum_{i=3}^N (v_i - v_1) b_i] + \sum_{i=3}^N b_i v_i \\
&= \frac{1}{v_2 - v_1}[(v_2 - v_1) y_1^* - (v_2 - v_1) \sum_{i=3}^N b_i v_i] + \sum_{i=3}^N b_i v_i = y_1^*,
\end{aligned}$$

  and for $k = 2,\dots,K$:

$$(\boldsymbol{Q}^p v)_k = \frac{1}{v_2 - v_1}\left(v_1 v_2 q_k - y_k^* v_1 + y_k^* v_2 - v_1 v_2 q_k\right) = y_k^*.$$

- $\underline{\boldsymbol{Q}^p \boldsymbol{1}_N = q}$: We obtain

$$\begin{aligned}
(\boldsymbol{Q}^p \boldsymbol{1}_K)_1 &= \frac{1}{v_2 - v_1}\left(v_2 q_1 - y_1^* - \sum_{i=3}^N (v_2 - v_i) b_i + y_1^* - v_1 q_1 - \sum_{i=3}^N (v_i - v_1) b_i\right) \\
&\quad + \sum_{i=3}^N b_i \\
&= \frac{1}{v_2 - v_1}\left((v_2 - v_1) q_1 + (v_2 - v_1)\sum_{i=3}^N b_i\right) + \sum_{i=3}^N b_i = q_1,
\end{aligned}$$

and for $k = 2, \ldots, K$:

$$(\boldsymbol{Q}^p \mathbf{1}_N)_k = \frac{1}{v_2 - v_1}\left(v_2 q_k - y_k^* + y_k^* - v_1 q_k\right) = q_k.$$

- $\underline{\mathbf{1}_K^\top \boldsymbol{Q}^p = b^\top}$: Obviously, it is $(\mathbf{1}_K^\top \boldsymbol{Q}^p)_i = b_i$, for $i = 3, \ldots, N$. For the first and second entry, it holds that

$$\begin{aligned}
(\mathbf{1}_K^\top \boldsymbol{Q}^p)_1 &= \frac{1}{v_2 - v_1}\left(v_2 \mathbf{1}_K^\top q - \mathbf{1}_K^\top y^* - \sum_{i=3}^{N}(v_2 - v_i) b_i\right) \\
&= \frac{1}{v_2 - v_1}\left(v_2 \sum_{i=1}^{N} b_i - \sum_{i=1}^{N} b_i v_i - \sum_{i=3}^{N} v_2 b_i + \sum_{i=3}^{N} b_i v_i\right) \\
&= \frac{1}{v_2 - v_1}(v_2(b_1 + b_2) - (v_1 b_1 + v_2 b_2)) = b_1,
\end{aligned}$$

where in the first step, we have used that $\sum_{k=1}^{K} q_k = T = \sum_{i=1}^{N} b_i$ and that $\mathbf{1}_K^\top y^* = b^\top v$. Using the same arguments, we obtain

$$\begin{aligned}
(\mathbf{1}_K^\top \boldsymbol{Q}^p)_2 &= \frac{1}{v_2 - v_1}\left(\mathbf{1}_K^\top y^* - v_1 \mathbf{1}_K^\top q - \sum_{i=3}^{N}(v_i - v_1) b_i\right) \\
&= \frac{1}{v_2 - v_1}\left(\sum_{i=1}^{N} b_i - v_1 \sum_{i=1}^{N} b_i v_i - \sum_{i=3}^{N} b_i v_i + \sum_{i=3}^{N} v_1 b_i\right) \\
&= \frac{1}{v_2 - v_1}(b_1 v_1 + b_2 v_2 - (v_1 b_1 + v_1 b_2)) = b_2,
\end{aligned}$$

which completes the proof.

Remark 3.6.1. Due to our two-step solution method proven in Proposition 3.3.5, finding an f-efficient holding matrix $\boldsymbol{Q}^* \in \mathbb{R}^{K \times N}$ is equivalent to solving the linear system

$$\underbrace{\begin{pmatrix}
\mathbf{1}_K^\top & 0 & \cdots & 0 \\
0 & \mathbf{1}_K^\top & \ddots & \vdots \\
\vdots & \ddots & \ddots & 0 \\
0 & \cdots & 0 & \mathbf{1}_K^\top \\
\boldsymbol{I}_K & \boldsymbol{I}_K & \cdots & \boldsymbol{I}_K \\
v_1 \boldsymbol{I}_K & v_2 \boldsymbol{I}_K & \cdots & v_N \boldsymbol{I}_K
\end{pmatrix}}_{=:\boldsymbol{F} \in \mathbb{R}^{2K+N \times KN}} \operatorname{vec}(\boldsymbol{Q}^*) = \begin{pmatrix} b \\ q \\ y^* \end{pmatrix}, \tag{3.25}$$

where $\operatorname{vec}(\boldsymbol{Q}^*) \in \mathbb{R}^{KN}$ denotes the vectorized version of the matrix $\boldsymbol{Q}^*$, obtained by stacking its columns on top of one another. The null space corresponding to the matrix

$\boldsymbol{F}$ is spanned by the $(K-1)(N-2)$ column vectors of the matrix (w.l.o.g. $v_1 \neq v_2$, cf. Assumption 3.3.3)

$$\boldsymbol{O} := \begin{pmatrix} \frac{v_2-v_3}{v_2-v_1}\begin{pmatrix} -\mathbf{1}_{K-1}^\top \\ \boldsymbol{I}_{K-1} \end{pmatrix} & \frac{v_2-v_4}{v_2-v_1}\begin{pmatrix} -\mathbf{1}_{K-1}^\top \\ \boldsymbol{I}_{K-1} \end{pmatrix} & \cdots & \frac{v_2-v_N}{v_2-v_1}\begin{pmatrix} -\mathbf{1}_{K-1}^\top \\ \boldsymbol{I}_{K-1} \end{pmatrix} \\ \frac{v_3-v_1}{v_2-v_1}\begin{pmatrix} -\mathbf{1}_{K-1}^\top \\ \boldsymbol{I}_{K-1} \end{pmatrix} & \frac{v_4-v_1}{v_2-v_1}\begin{pmatrix} -\mathbf{1}_{K-1}^\top \\ \boldsymbol{I}_{K-1} \end{pmatrix} & \cdots & \frac{v_N-v_1}{v_2-v_1}\begin{pmatrix} -\mathbf{1}_{K-1}^\top \\ \boldsymbol{I}_{K-1} \end{pmatrix} \\ \begin{pmatrix} \mathbf{1}_{K-1}^\top \\ -\boldsymbol{I}_{K-1} \end{pmatrix} & \mathbf{0}_{K\times K-1} & \cdots & \mathbf{0}_{K\times K-1} \\ \mathbf{0}_{K\times K-1} & \begin{pmatrix} \mathbf{1}_{K-1}^\top \\ -\boldsymbol{I}_{K-1} \end{pmatrix} & \ddots & \vdots \\ \vdots & \ddots & \ddots & \mathbf{0}_{K\times K-1} \\ \mathbf{0}_{K\times K-1} & \cdots & \mathbf{0}_{K\times K-1} & \begin{pmatrix} \mathbf{1}_{K-1}^\top \\ -\boldsymbol{I}_{K-1} \end{pmatrix} \end{pmatrix} \in \mathbb{R}^{KN\times(K-1)(N-2)}. \tag{3.26}$$

The fact that the linearly independent column vectors of $\boldsymbol{O}$ lie in the null space of $\boldsymbol{F}$ is easily checked via direct calculation; the fact that the dimension of the null space is equal to $(K-1)(N-2)$ follows from a rank-nullity argument given in the proof of Theorem 3.3.9 b) below. Hence, we are able to fully characterize the set of f-efficient holding matrices as

$$\left\{\boldsymbol{Q}^* \in \mathbb{R}^{K\times N} \mid \operatorname{vec}(\boldsymbol{Q}^*) = \operatorname{vec}(\boldsymbol{Q}^p) + \sum_{j=1}^{(K-1)(N-2)} \lambda_j C_j(\boldsymbol{O}),\ \lambda_1,\ldots,\lambda_{(K-1)(N-2)} \in \mathbb{R}\right\},$$

with particular solution $\boldsymbol{Q}^p$ as defined in (3.24) and where $C_j(\boldsymbol{O})$ denotes the j-th column vector of the null space matrix $\boldsymbol{O}$, $j = 1,\ldots,(K-1)(N-2)$.

3.6.2.4 Proof of Theorem 3.3.9

a) The existence of an f-efficient holding matrix for every $N, K \geq 2$ directly follows from Propositions 3.3.8 and 3.3.5. Let $y^* = \frac{b^\top v}{\mathbf{1}_K^\top z} z$, the solution of the aggregate problem (3.14) derived in Lemma 3.3.6 with $z = \boldsymbol{G}^{-1}\mathbf{1}_K$. The mean squared deviation under an f-efficient holding matrix $\boldsymbol{Q}^*$ is given by:

$$\begin{aligned} MSD(\boldsymbol{Q}^*) &= (\boldsymbol{Q}^* v)^\top \boldsymbol{G}(\boldsymbol{Q}^* v) = (y^*)^\top \boldsymbol{G} y^* \\ &= \frac{(b^\top v)^2}{(\mathbf{1}_K^\top z)^2} z^\top \boldsymbol{G} z = \frac{(b^\top v)^2}{(\mathbf{1}_K^\top z)^2} z^\top \boldsymbol{G}\boldsymbol{G}^{-1}\mathbf{1}_K \\ &= \frac{(b^\top v)^2}{(\mathbf{1}_K^\top z)^2}(z^\top \mathbf{1}_K) = \frac{(b^\top v)^2}{\mathbf{1}_K^\top z} = \frac{(b^\top v)^2}{\mathbf{1}_K^\top \boldsymbol{G}^{-1}\mathbf{1}_K}. \end{aligned}$$

b) As outlined above in Remark 3.6.1, finding an f-efficient holding matrix $\boldsymbol{Q}^* \in \mathbb{R}^{K\times N}$ is equivalent to solving the linear system (3.25). We have the following result: The rank of the matrix $\boldsymbol{F}$ is equal to $2K + N - 2$. This can be proven via standard

Gaussian elimination. First, resorting the rows of $\boldsymbol{F}$ and adding the new first K rows multiplied by $-v_1$ to the second K rows yields

$$\begin{pmatrix} \boldsymbol{I}_K & \boldsymbol{I}_K & \cdots & \boldsymbol{I}_K \\ v_1\boldsymbol{I}_K & v_2\boldsymbol{I}_K & \cdots & v_N\boldsymbol{I}_K \\ \mathbf{1}_K^\top & 0 & \cdots & 0 \\ 0 & \mathbf{1}_K^\top & \ddots & \vdots \\ \vdots & \ddots & \ddots & 0 \\ 0 & \cdots & 0 & \mathbf{1}_K^\top \end{pmatrix} \to \begin{pmatrix} \boldsymbol{I}_K & \boldsymbol{I}_K & \cdots & \boldsymbol{I}_K \\ \mathbf{0}_{K\times K} & (v_2-v_1)\boldsymbol{I}_K & \cdots & (v_N-v_1)\boldsymbol{I}_K \\ \mathbf{1}_K^\top & 0 & \cdots & 0 \\ 0 & \mathbf{1}_K^\top & \ddots & \vdots \\ \vdots & \ddots & \ddots & 0 \\ 0 & \cdots & 0 & \mathbf{1}_K^\top \end{pmatrix}.$$

Numbering the rows in this last matrix as $r_1, \ldots, r_{2K+N}$, we observe:

$$r_{2K+1} = \sum_{i=1}^{K} r_i - \sum_{i=2K+2}^{2K+N} r_i$$

and

$$r_{2K+2} = \frac{1}{v_2 - v_1}\left(\sum_{i=K+1}^{2K} r_i - \sum_{i=2K+3}^{2K+N} (v_{i-2K} - v_1) r_i\right),$$

where, as above, w.l.o.g. $v_2 \neq v_1$ (cf. Assumption 3.3.3). Hence, these two rows can be eliminated from the matrix yielding the row-echelon form:

$$\begin{pmatrix} \boldsymbol{I}_K & \boldsymbol{I}_K & \boldsymbol{I}_K & \boldsymbol{I}_K & \cdots & \boldsymbol{I}_K \\ \mathbf{0}_{K\times K} & (v_2-v_1)\boldsymbol{I}_K & (v_3-v_1)\boldsymbol{I}_K & (v_4-v_1)\boldsymbol{I}_K & \cdots & (v_N-v_1)\boldsymbol{I}_K \\ \mathbf{0}_K^\top & \mathbf{0}_K^\top & & \cdots & & \mathbf{0}_K^\top \\ \mathbf{0}_K^\top & \mathbf{0}_K^\top & & \cdots & & \mathbf{0}_K^\top \\ \mathbf{0}_K^\top & \mathbf{0}_K^\top & \mathbf{1}_K^\top & 0 & \cdots & 0 \\ 0 & \cdots & 0 & \mathbf{1}_K^\top & \ddots & \vdots \\ \vdots & \ddots & \vdots & \ddots & \ddots & 0 \\ 0 & \cdots & 0 & \cdots & 0 & \mathbf{1}_K^\top \end{pmatrix},$$

which shows that the matrix $\boldsymbol{F}$ possesses the rank $2K + N - 2$. The rank-nullity theorem now gives rise to the dimension of the null space (a basis is given by the column vectors of the matrix $\boldsymbol{O}$ in Remark 3.6.1 above):

$$KN = \operatorname{rank}(\boldsymbol{F}) + \operatorname{null}(\boldsymbol{F}) \;\Rightarrow\; \operatorname{null}(\boldsymbol{F}) = KN - (2K + N - 2) = (N-2)(K-1),$$

and, hence, the dimension of the null space is zero, i.e., the solution $\boldsymbol{Q}^p$ stated in the proof of Proposition 3.3.8 is unique, if and only if either $K = 1$ or $N = 2$; i.e., if we additionally assume that $K \geq 2$, then this is equivalent to $N = 2$. Finally, the formula for $\boldsymbol{Q}^{N=2}$ directly follows from the definition of $\boldsymbol{Q}^p$ in (3.24).

3.6.2.5 Proof of Theorem 3.3.10

Recall that $\boldsymbol{Q}^{\text{diversified}} = \frac{1}{T} q b^\top = \frac{1}{\mathbf{1}_K^\top q} q b^\top$. Thus, it holds that

$$
\begin{aligned}
& y^* = \boldsymbol{Q}^{\text{diversified}} v \\
\Leftrightarrow \quad & \frac{b^\top v}{\mathbf{1}_K^\top z} \cdot z = \frac{1}{\mathbf{1}_K^\top q} q (b^\top v) \\
\overset{b^\top v \neq 0}{\Leftrightarrow} \quad & \frac{1}{\mathbf{1}_K^\top z} z = \frac{1}{\mathbf{1}_K^\top q} q,
\end{aligned}
$$

i.e., if and only if q and $z = \boldsymbol{G}^{-1} \mathbf{1}_K$ are linearly dependent.

3.6.2.6 Proof of Corollary 3.3.11

- For the proof of statements a) and c), we first observe that if $q_1 = \ldots = q_K$, then

$$
\begin{aligned}
& \frac{1}{\mathbf{1}_K^\top z} z = \frac{1}{\mathbf{1}_K^\top q} q \quad \Leftrightarrow \quad \frac{1}{\mathbf{1}_K^\top z} z = \frac{1}{q_1 \cdot K} q_1 \cdot \mathbf{1}_K \\
\Leftrightarrow \quad & z = \frac{1}{K} \cdot \mathbf{1}_K \mathbf{1}_K^\top z \quad \Leftrightarrow \quad K \cdot z = (\mathbf{1}_K \mathbf{1}_K^\top) z,
\end{aligned}
$$

  i.e., that z is an eigenvector to the eigenvalue K of the all-one matrix $\mathbf{1}_{K \times K} = \mathbf{1}_K \mathbf{1}_K^\top$. This eigenvector is given as $z = c \cdot \mathbf{1}_K$ for a constant $c \in \mathbb{R}$. Hence, $z_k = z_\ell$ for all $k, \ell = 1, \ldots, K$ is equivalent to $\boldsymbol{Q}^{\text{diversified}}$ being f-efficient under the assumption that $q_1 = \ldots = q_K$.

  To prove part a), we now set $\sigma_1^2 = \ldots = \sigma_K^2$. According to the proof of Lemma 3.3.6, the vector z is in this situation given by

$$
z = \boldsymbol{G}^{-1} \mathbf{1}_K = \frac{1}{\sigma_1^2} \cdot \mathbf{1}_K - \frac{(\frac{1}{\sigma_1^2})^2 \cdot \mu^\top \mathbf{1}_K}{1 + \frac{1}{\sigma_1^2 \cdot \mu^\top \mu}} \cdot \mu.
$$

  This means that the condition $z_k = z_\ell$ for all $k, \ell = 1, \ldots, K$ is equivalent to

$$
\begin{aligned}
& z_k = \frac{1}{\sigma_1^2} - \frac{(\frac{1}{\sigma_1^2})^2 \cdot \sum_{j=1}^K \mu_j}{1 + \frac{1}{\sigma_1^2} \cdot \sum_{j=1}^K \mu_j^2} \cdot \mu_k \overset{!}{=} \frac{1}{\sigma_1^2} - \frac{(\frac{1}{\sigma_1^2})^2 \cdot \sum_{j=1}^K \mu_j}{1 + \frac{1}{\sigma_1^2} \cdot \sum_{j=1}^K \mu_j^2} \cdot \mu_\ell = z_\ell \\
\Leftrightarrow \quad & \frac{(\frac{1}{\sigma_1^2})^2 \cdot \sum_{j=1}^K \mu_j}{1 + \frac{1}{\sigma_1^2} \cdot \sum_{j=1}^K \mu_j^2} \cdot \mu_k = \frac{(\frac{1}{\sigma_1^2})^2 \cdot \sum_{j=1}^K \mu_j}{1 + \frac{1}{\sigma_1^2} \cdot \sum_{j=1}^K \mu_j^2} \cdot \mu_\ell \\
\Leftrightarrow \quad & \left(\sum_{j=1}^K \mu_j\right) \cdot \mu_k = \left(\sum_{j=1}^K \mu_j\right) \cdot \mu_\ell,
\end{aligned}
$$

for all $k, \ell = 1, \ldots, K$, i.e., $\mu_k = \mu_\ell$ or $\sum_{j=1}^K \mu_j = 0$. Hence, if $\mu_1 = \ldots = \mu_{K-1}$ and $\mu_K = \mu_1 + \varepsilon$, then, finally, $\boldsymbol{Q}^{\text{diversified}}$ being f-efficient is equivalent to either $\varepsilon = 0$, yielding $\mu_k = \mu_\ell$ for all $k, \ell = 1, \ldots, K$, or $\varepsilon = -K\mu_1$, yielding $\sum_{j=1}^K \mu_j = 0$.

To prove part c), we set $\mu_1 = \ldots = \mu_K$, which (see the proof of Lemma 3.3.6) leads to the vector z given as:

$$z = \boldsymbol{G}^{-1}\mathbf{1}_K = \frac{1}{\sigma^2} - \frac{\mu_1^2 \cdot (\frac{1}{\sigma^2})^\top \mathbf{1}_K}{1 + \mu_1^2 \cdot (\frac{1}{\sigma^2})^\top \mathbf{1}_K} \cdot \frac{1}{\sigma^2}.$$

Thus, the condition $z_k = z_\ell$ for all $k, \ell = 1, \ldots, K$ reads as

$$\begin{aligned} z_k = \left(1 - \frac{\mu_1^2 \cdot \sum_{j=1}^K \frac{1}{\sigma_j^2}}{1 + \mu_1^2 \cdot \sum_{j=1}^K \frac{1}{\sigma_j^2}}\right) \frac{1}{\sigma_k^2} &\overset{!}{=} \left(1 - \frac{\mu_1^2 \cdot \sum_{j=1}^K \frac{1}{\sigma_j^2}}{1 + \mu_1^2 \cdot \sum_{j=1}^K \frac{1}{\sigma_j^2}}\right) \frac{1}{\sigma_\ell^2} = z_\ell \\ \Leftrightarrow \quad \sigma_k^2 = \sigma_\ell^2 & \end{aligned}$$

for all $k, \ell = 1, \ldots, K$. Hence, if $\sigma_1 = \ldots = \sigma_{K-1}$ and $\sigma_K = \sigma_1 + \varepsilon$, this condition is fulfilled if and only if $\varepsilon = 0$.

- For the remaining proof of part b), observe that if $\mu_1 = \ldots = \mu_K$ and $\sigma_1^2 = \ldots = \sigma_K^2$, then

$$z = \boldsymbol{G}^{-1}\mathbf{1}_K = \frac{1}{\sigma_1^2} \cdot \mathbf{1}_K - \frac{(\frac{\mu_1}{\sigma_1^2})^2 \cdot K}{1 + \frac{\mu_1^2}{\sigma_1^2} K} \cdot \mathbf{1}_K,$$

in particular: $z_1 = \ldots = z_K$. Hence:

$$\begin{aligned} \frac{1}{\mathbf{1}_K^\top z} z = \frac{1}{\mathbf{1}_K^\top q} q \quad &\Leftrightarrow \quad \frac{1}{z_1 \cdot K} z_1 \cdot \mathbf{1}_K = \frac{1}{\mathbf{1}_K^\top q} q \\ \Leftrightarrow \quad \mathbf{1}_K \mathbf{1}_K^\top q = K \cdot q & \end{aligned}$$

which is equivalent to q being an eigenvector to the eigenvalue K of the all-one matrix $\mathbf{1}_{K \times K} = \mathbf{1}_K \mathbf{1}_K^\top$, i.e., $q_1 = \ldots = q_K$. Hence, if $q_1 = \ldots = q_{K-1}$ and $q_K = q_1 + \varepsilon$, this condition is equivalent to $\varepsilon = 0$, which completes the proof.

3.6.3 Proofs of Section 3.4

3.6.3.1 Proof of Lemma 3.4.1

First, we derive the explicit formulas for $\boldsymbol{Q}^{2\times2}_{1,1}$ and $d(\boldsymbol{Q}^{2\times2})$ in the special case $N = K = 2$, $q_1 = q_2 = b_1 = b_2 = x$. Note that, here, the unique f-efficient holding matrix is given by

$$\begin{aligned}\boldsymbol{Q}^{2\times2} &= \frac{1}{v_2 - v_1}\begin{pmatrix} v_2 q_1 - y_1^* & y_1^* - v_1 q_1 \\ v_2 q_2 - y_2^* & y_2^* - v_1 q_2\end{pmatrix} \\ &= \frac{x}{(v_2 - v_1)(z_1 + z_2)}\begin{pmatrix} v_2 z_2 - v_1 z_1 & v_2 z_1 - v_1 z_2 \\ v_2 z_1 - v_1 z_2 & v_2 z_2 - v_1 z_1\end{pmatrix},\end{aligned}$$

due to $y^* = x \cdot \frac{v_1+v_2}{z_1+z_2} \cdot z$. Since, $\boldsymbol{Q}^{\text{diversified}} = \frac{x}{2} \cdot \mathbf{1}_{2\times2}$, it holds that

$$\begin{aligned}\boldsymbol{Q}^{2\times2}_{1,1} - \boldsymbol{Q}^{\text{diversified}}_{1,1} &= x \cdot \frac{2v_2 z_2 - 2v_1 z_1 - (v_2 - v_1)(z_1 + z_2)}{2(v_2 - v_1)(z_1 + z_2)} \\ &= x \cdot \frac{v_2 z_2 - v_1 z_1 - v_2 z_1 + v_1 z_2}{2(v_2 - v_1)(z_1 + z_2)} \\ &= x \cdot \frac{(z_2 - z_1)(v_1 + v_2)}{2(v_2 - v_1)(z_1 + z_2)} = \boldsymbol{Q}^{2\times2}_{2,2} - \boldsymbol{Q}^{\text{diversified}}_{2,2},\end{aligned}$$

and

$$\begin{aligned}\boldsymbol{Q}^{2\times2}_{1,2} - \boldsymbol{Q}^{\text{diversified}}_{1,2} &= x \cdot \frac{2v_2 z_1 - 2v_1 z_2 - (v_2 - v_1)(z_1 + z_2)}{2(v_2 - v_1)(z_1 + z_2)} \\ &= x \cdot \frac{v_2 z_1 - v_1 z_2 + v_1 z_1 - v_2 z_2}{2(v_2 - v_1)(z_1 + z_2)} \\ &= x \cdot \frac{(z_1 - z_2)(v_1 + v_2)}{2(v_2 - v_1)(z_1 + z_2)} = \boldsymbol{Q}^{2\times2}_{2,1} - \boldsymbol{Q}^{\text{diversified}}_{2,1}.\end{aligned}$$

Hence,

$$\begin{aligned}d(\boldsymbol{Q}^{2\times2}) = \|\boldsymbol{Q}^{2\times2} - \boldsymbol{Q}^{\text{diversified}}\|_F &= \sqrt{4 \cdot x^2 \cdot \frac{(z_1 - z_2)^2(v_1 + v_2)^2}{4(v_2 - v_1)^2(z_1 + z_2)^2}} \\ &= x \cdot \sqrt{\frac{(z_1 - z_2)^2(v_1 + v_2)^2}{(v_2 - v_1)^2(z_1 + z_2)^2}}. \end{aligned} \tag{3.27}$$

Moreover, a direct calculation of $z = \boldsymbol{G}^{-1}\mathbf{1}_K$ in the 2-by-2-case shows that

$$\boldsymbol{Q}^{2\times2}_{1,1} = x \cdot \frac{v_2(\mu_1^2 + \sigma_1^2 - \mu_1\mu_2) - v_1(\mu_2^2 + \sigma_2^2 - \mu_1\mu_2)}{(v_2 - v_1)(\mu_1^2 + \mu_2^2 - 2\mu_1\mu_2 + \sigma_1^2 + \sigma_2^2)}, \tag{3.28}$$

and that

$$d(\boldsymbol{Q}^{2\times2}) = x \cdot \sqrt{\frac{(\mu_1^2 - \mu_2^2 + \sigma_1^2 - \sigma_2^2)^2(v_1 + v_2)^2}{(v_2 - v_1)^2(\mu_1^2 + \mu_2^2 - 2\mu_1\mu_2 + \sigma_1^2 + \sigma_2^2)^2}}. \tag{3.29}$$

a) Under the conditions $q_1 = q_2 = x$ and $\mu_1 = \mu_2$, it holds that $d(\boldsymbol{Q}^{2\times 2}) = 0$ as a function of σ_1, if and only if $\sigma_1^2 = \sigma_2^2$ (cf. Corollary 3.3.11) and it is strictly positive everywhere else. Hence, we can equivalently analyze the monotonicity behavior of $d(\boldsymbol{Q}^{2\times 2})^2$. According to (3.29), its derivative with respect to σ_1 is given by

$$\frac{\partial}{\partial \sigma_1} d(\boldsymbol{Q}^{2\times 2})^2 = \frac{8\sigma_1\sigma_2^2(\sigma_1^2 - \sigma_2^2)(v_1 + v_2)^2 x^2}{(\sigma_1^2 + \sigma_2^2)^3 (v_1 - v_2)^2} \begin{cases} < 0, & \text{if } \sigma_1^2 < \sigma_2^2, \\ = 0, & \text{if } \sigma_1^2 = \sigma_2^2, \\ > 0, & \text{if } \sigma_1^2 > \sigma_2^2, \end{cases}$$

for $\sigma_1 > 0$ under the given assumptions, which proves the statement.

b) Now assume $x > 0$ and $v_2 > v_1 > 0$. The derivative of (3.28) with respect to σ_1 is given by

$$\begin{aligned} \frac{\partial \boldsymbol{Q}_{1,1}^{2\times 2}}{\partial \sigma_1} &= x \cdot \frac{2\sigma_1(\mu_2^2 + \sigma_2^2 - \mu_1\mu_2)(v_1 + v_2)}{(v_2 - v_1)(\mu_1^2 + \mu_2^2 - 2\mu_1\mu_2 + \sigma_1^2 + \sigma_2^2)^2} \\ &\overset{\mu_1=\mu_2}{=} x \cdot \frac{2\sigma_1\sigma_2^2(v_1 + v_2)}{(\sigma_1^2 + \sigma_2^2)^2(v_2 - v_1)} > 0, \end{aligned}$$

for $\sigma_1 > 0$ under the given assumptions.

3.6.3.2 Proof of Lemma 3.4.2

a) As in the proof of Lemma 3.4.1, $d(\boldsymbol{Q}^{2\times 2})$ as a function of μ_2 is non-negative and, under the given assumptions, strictly positive except for the case $\mu_2 = \mu_1$ (cf. Corollary 3.3.11). Hence, we can again equivalently analyze the monotonicity behavior of the squared distance $d(\boldsymbol{Q}^{2\times 2})^2$. Its derivative with respect to μ_2 is given by

$$\begin{aligned} &\frac{\partial}{\partial \mu_2} d(\boldsymbol{Q}^{2\times 2})^2 \\ &= x^2 \cdot \frac{4(\mu_1^2 - \mu_2^2 + \sigma_1^2 - \sigma_2^2)(-2\mu_2\sigma_1^2 + \mu_1(\mu_1^2 + \mu_2^2 - 2\mu_1\mu_2 + \sigma_1^2 - \sigma_2^2))(v_1 + v_2)^2}{(\mu_1^2 - 2\mu_1\mu_2 + \mu_2^2 + \sigma_1^2 + \sigma_2^2)^3(v_2 - v_1)^2} \\ &\overset{\sigma_1^2=\sigma_2^2,\mu_1=0}{=} x^2 \cdot \frac{8\mu_2^3\sigma_1^2(v_1 + v_2)^2}{(\mu_2^2 + 2\sigma_1^2)^3(v_2 - v_1)^2} \begin{cases} < 0, & \text{if } \mu_2 < 0, \\ = 0, & \text{if } \mu_2 = 0, \\ > 0, & \text{if } \mu_2 > 0, \end{cases} \end{aligned}$$

which proves the lemma.

b) The derivative of (3.28) with respect to μ_2 is given by

$$\frac{\partial}{\partial \mu_2} \boldsymbol{Q}_{1,1}^{2\times 2} = x \cdot \frac{(-2\mu_2\sigma_1^2 + \mu_1(\mu_1^2 + \mu_2^2 - 2\mu_1\mu_2 + \sigma_1^2 - \sigma_2^2))(v_1 + v_2)}{(\mu_1^2 + \mu_2^2 - 2\mu_1\mu_2 + \sigma_1^2 + \sigma_2^2)^2(v_2 - v_1)}$$

$$\stackrel{\sigma_1^2=\sigma_2^2,\mu_1=0}{=} x \cdot \frac{-2\mu_2\sigma_1^2(v_1 + v_2)}{(\mu_2^2 + 2\sigma_1^2)^2(v_2 - v_1)} \begin{cases} > 0, & \text{if } \mu_2 < 0, \\ = 0, & \text{if } \mu_2 = 0, \\ < 0, & \text{if } \mu_2 > 0, \end{cases}$$

under the assumptions $v_2 > v_1 > 0$, $x > 0$, $\sigma_1^2 = \sigma_2^2$, and $\mu_1 = 0$.

3.6.3.3 Proof of Lemma 3.4.3

The derivative of (3.27) with respect to v_2 is given as

$$\frac{\partial}{\partial v_2} d(\boldsymbol{Q}^{2\times 2}) = x \cdot \frac{2v_1}{(v_1 + v_2)(v_1 - v_2)} \cdot \sqrt{\frac{(v_1 + v_2)^2(z_1 - z_2)^2}{(v_2 - v_1)^2(z_1 + z_2)^2}}.$$

Under the given assumptions $x, v_1 > 0$, $|z_1| \neq |z_2|$, and $v_2 \neq v_1$, this term is strictly positive for $v_2 > 0$, if $v_2 < v_1$ and strictly negative if $v_2 > v_1$. This is the statement of the lemma.

3.7 Appendix: Non-Uniqueness of Asset Holdings

We provide an example to show how the interplay between systemic significance and asset riskiness influences the structure of f-efficient holdings. We also discuss the intuition behind the non-uniqueness of holdings when we move from an economy with $N = 2$ banks to one with $N > 2$ banks. Consider an economy with $N = 3$ banks and $K = 3$ assets, where we normalize the total supply of assets within the banking sector and budgets of banks to $q_1 = q_2 = q_3 = b_1 = b_2 = b_3 = x$ with $x := 0.08$. The total supply of each asset is normalized to 1. Asset 1 constitutes the least and asset 3 the most risky asset: $\mu = (0,0,0)^\top$ and $\sigma^2 = (0.15, 0.2, 0.3)^\top$. The three banks are different in their systemic significance parameters $v = (0.15, 0.1, 0.05)^\top$, i.e., bank 1 is the most and bank 3 the least significant to the system. According to Theorem 3.3.9 b), f-efficient holdings in this financial system are not unique. Every f-efficient holding matrix is of the form

$$\boldsymbol{Q}^{*1} + \lambda_1 \begin{pmatrix} 1 & -2 & 1 \\ -1 & 2 & -1 \\ 0 & 0 & 0 \end{pmatrix} + \lambda_2 \begin{pmatrix} 1 & -2 & 1 \\ 0 & 0 & 0 \\ -1 & 2 & -1 \end{pmatrix}, \quad \lambda_1, \lambda_2 \in \mathbb{R}, \tag{3.30}$$

where

$$\boldsymbol{Q}^{*1} = x \cdot \begin{pmatrix} \frac{2}{3} & \frac{1}{3} & 0 \\ \frac{1}{3} & \frac{1}{3} & \frac{1}{3} \\ 0 & \frac{1}{3} & \frac{2}{3} \end{pmatrix}$$

is a particular solution: the f-efficient holding matrix with the smallest Frobenius distance to fully diversified holdings $\boldsymbol{Q}^{\text{diversified}} = x \cdot \frac{1}{3} \cdot \mathbf{1}_{3\times3}$. Hence, $\boldsymbol{Q}^{*1}$ represents a lower bound on how far holdings need to move away from the classical diversification benchmark in order to become f-efficient. Setting $\lambda_1 = x \cdot 1/3$ and $\lambda_2 = -x \cdot 1/6$ in equation (3.30), we obtain a second particular solution:

$$\boldsymbol{Q}^{*2} = x \cdot \begin{pmatrix} \frac{5}{6} & 0 & \frac{1}{6} \\ 0 & 1 & 0 \\ \frac{1}{6} & 0 & \frac{5}{6} \end{pmatrix},$$

which represents those f-efficient holdings with the smallest distance to a fully diverse holding matrix $\boldsymbol{Q}^{\text{diverse}} = x \cdot \boldsymbol{I}_3$. Note, first, that this type of diverse holdings are only defined in the case $N = K$. Second, observe that holdings with the smallest distance to diversity do not maximize the distance to diversification.[14]

The example provides the following insights:

- In both $\boldsymbol{Q}^{*1}$ and $\boldsymbol{Q}^{*2}$, the most risky asset 3 is held in the largest proportion by the least systemically significant bank 3. Conversely, the least risky asset 1 is held in the largest proportion by the most significant bank 1.

  This can be generalized as follows: For every f-efficient holding matrix (see (3.30)), the holdings of the most significant bank 1 in the least risky asset 1 ($x \cdot 2/3 + \lambda_1 + \lambda_2$) are larger than the holdings of the least significant bank 3 in this asset ($\lambda_1 + \lambda_2$). Conversely, for every f-efficient matrix, the holdings of the least significant bank 3 in the most risky asset 3 ($x \cdot 2/3 - \lambda_2$) are larger than bank 1's holdings in this asset ($-\lambda_2$).

- Note that the null space in Equation (3.30) is equivalently written as (cf. Remark 3.6.1 in Appendix 3.6):

$$\lambda_1 \begin{pmatrix} -(v_2-v_3) & v_1-v_3 & -(v_1-v_2) \\ v_2-v_3 & -(v_1-v_3) & v_1-v_2 \\ 0 & 0 & 0 \end{pmatrix} + \lambda_2 \begin{pmatrix} -(v_2-v_3) & v_1-v_3 & -(v_1-v_2) \\ 0 & 0 & 0 \\ v_2-v_3 & -(v_1-v_3) & v_1-v_2 \end{pmatrix}$$

  for $\lambda_1, \lambda_2 \in \mathbb{R}$. Hence, any transfer between two assets in each bank's holdings that is done somewhat proportionally to the differences between the systemic significances (of the other two banks) does not alter the mean squared deviation. This is

[14] Since λ_1, λ_2 in formula (3.30) are unbounded, the distance to diversification within the set of f-efficient holdings is unbounded.

the reason for the uniqueness criterion we found: If there are only two banks in the system, there simply are no "other two banks"and thus there are no transfers which are neutral with respect to the mean squared deviation.

3.8 Appendix: f-Efficient Liquidation Strategies

3.8.1 General Derivation

We want to minimize the mean squared deviation (3.11) as a function of

$$\boldsymbol{\alpha} = \left(\alpha^1 \;\mid\; \cdots \;\mid \alpha^N\right) \in \mathbb{R}^{K\times N}, \text{ for } \alpha^i \in \mathbb{R}^K \text{ with } \mathbf{1}_K^\top \alpha^i = 1 \text{ and } \alpha^i \geq \mathbf{0}_K \;\;, i = 1, \ldots, N.$$

Thus, each bank i is allowed to choose its own personal liquidation strategy α^i and we do not allow for short-selling. In the following lemma, we rewrite the minimization problem as a function of

$$\text{vec}(\boldsymbol{\alpha}) := (\alpha^{1\top}, \ldots, \alpha^{N\top})^\top \in \mathbb{R}^{KN},$$

i.e., $\text{vec}(\boldsymbol{\alpha})$ denotes the vectorization of the matrix $\boldsymbol{\alpha}$.

Lemma 3.8.1. *Minimizing the mean squared deviation as a function of the liquidation strategy matrix $\boldsymbol{\alpha}$ with $\boldsymbol{\alpha} \geq \mathbf{0}$ is equivalent to the following problem:*

$$\min_{\text{vec}(\boldsymbol{\alpha})\in\mathbb{R}^{KN}} \quad \tfrac{1}{2}\,\text{vec}(\boldsymbol{\alpha})^\top (\boldsymbol{C} \otimes \tfrac{Q_{\text{tot}}}{\gamma\circ Q_0^{\text{nb}}} (\tfrac{Q_{\text{tot}}}{\gamma\circ Q_0^{\text{nb}}})^\top)\text{vec}(\boldsymbol{\alpha}) \tag{G}$$

$$s.t. \quad \begin{pmatrix} \mathbf{1}_K^\top & & 0 \\ & \ddots & \\ 0 & & \mathbf{1}_K^\top \end{pmatrix} \text{vec}(\boldsymbol{\alpha}) = \mathbf{1}_N, \quad \text{vec}(\boldsymbol{\alpha}) \geq \mathbf{0}_{KN},$$

where $\boldsymbol{C} = (C^{ij})_{i,j=1,\ldots,N} \in \mathbb{R}^{N\times N}$ with

$$C^{ij} := 2(\boldsymbol{Q}\text{Diag}(\kappa)e^i)^\top (\mu\mu^\top + \text{Diag}(\sigma^2))(\boldsymbol{Q}\text{Diag}(\kappa)e^j),$$

$e^i \in \mathbb{R}^N$ denotes the i'th basis vector (i.e., $e^i_j = 1$ for $j = i$ and zero, otherwise), and $\otimes$ denotes the Kronecker product[15].

[15] For two matrices $\boldsymbol{A} \in \mathbb{R}^{M\times N}, \boldsymbol{B} \in \mathbb{R}^{P\times R}$, the Kronecker product is defined by multiplying every entry of the matrix $\boldsymbol{A}$ by the entire matrix $\boldsymbol{B}$, i.e.,

$$\boldsymbol{A} \otimes \boldsymbol{B} := \begin{pmatrix} A^{11}\boldsymbol{B} & \cdots & A^{1N}\boldsymbol{B} \\ \vdots & \ddots & \vdots \\ A^{M1}\boldsymbol{B} & \cdots & A^{MN}\boldsymbol{B} \end{pmatrix} \in \mathbb{R}^{MP\times NR}.$$

Proof. It holds that $\boldsymbol{Q}\text{Diag}(\kappa)\boldsymbol{\alpha}^\top \frac{Q_{\text{tot}}}{\gamma \circ Q_0^{\text{nb}}} = \boldsymbol{Q}\text{Diag}(\kappa) \cdot (\sum_{i=1}^{N} (\alpha^{i\top} \frac{Q_{\text{tot}}}{\gamma \circ Q_0^{\text{nb}}}) e^i)$. Inserting this expression into formula (3.11) yields

$$
\begin{aligned}
&MSD(\alpha^1, \ldots, \alpha^N) = \\
&\left((\sum_{i=1}^{N} (\alpha^{i\top} \tfrac{Q_{\text{tot}}}{\gamma \circ Q_0^{\text{nb}}})) \boldsymbol{Q}\text{Diag}(\kappa) e^i \right)^\top (\mu\mu^\top + \text{Diag}(\sigma^2)) \left((\sum_{j=1}^{N} (\alpha^{j\top} \tfrac{Q_{\text{tot}}}{\gamma \circ Q_0^{\text{nb}}})) \boldsymbol{Q}\text{Diag}(\kappa) e^j \right) \\
=& \sum_{i=1}^{N} \sum_{j=1}^{N} \left((\alpha^{i\top} \tfrac{Q_{\text{tot}}}{\gamma \circ Q_0^{\text{nb}}}) \boldsymbol{Q}\text{Diag}(\kappa) e^i \right)^\top (\mu\mu^\top + \text{Diag}(\sigma^2)) \left((\alpha^{j\top} \tfrac{Q_{\text{tot}}}{\gamma \circ Q_0^{\text{nb}}}) \boldsymbol{Q}\text{Diag}(\kappa) e^j \right) \\
=& \sum_{i=1}^{N} \sum_{j=1}^{N} \alpha^{i\top} \tfrac{Q_{\text{tot}}}{\gamma \circ Q_0^{\text{nb}}} (\tfrac{Q_{\text{tot}}}{\gamma \circ Q_0^{\text{nb}}})^\top \alpha^j (\boldsymbol{Q}\text{Diag}(\kappa) e^i)^\top (\mu\mu^\top + \text{Diag}(\sigma^2)) (\boldsymbol{Q}\text{Diag}(\kappa) e^j) \\
=& \frac{1}{2} \sum_{i=1}^{N} \sum_{j=1}^{N} \alpha^{i\top} (C^{ij} \cdot \tfrac{Q_{\text{tot}}}{\gamma \circ Q_0^{\text{nb}}} (\tfrac{Q_{\text{tot}}}{\gamma \circ Q_0^{\text{nb}}})^\top) \alpha^j.
\end{aligned}
$$

This proves the formula for the objective function. The linear constraint follows from $\mathbf{1}_K^\top \alpha^i = 1$ for all $i = 1, \ldots, N$. □

The following proposition now provides a locally f-efficient liquidation strategy. Its interpretation is given in Remark 3.8.3.

Proposition 3.8.2. *Let* $m := \max_{k \in \{1,\ldots,K\}} \frac{\gamma_k Q_0^{k,\text{nb}}}{Q_{\text{tot}}^k}$ *denote the maximum entry in the vector* $\frac{\gamma \circ Q_0^{\text{nb}}}{Q_{\text{tot}}}$ *and denote by*

$$k_m = \{k \in \{1, \ldots, K\} \mid \frac{\gamma_k Q_0^{k,\text{nb}}}{Q_{\text{tot}}^k} = m\}$$

the corresponding index set with cardinality $\#k_m$. *For every fixed* $\boldsymbol{Q} \in \mathbb{R}^{K \times N}$, *a local minimizer of the mean squared deviation as a function of the liquidation strategy matrix is given by the matrix* $\boldsymbol{\alpha}^*$ *which is defined by its columns:*

$$\alpha^{ik*} := \begin{cases} \frac{1}{\#k_m}, & \textit{if } k \in k_m, \\ 0, & \textit{otherwise,} \end{cases} \qquad (k = 1, \ldots, K, \quad i = 1, \ldots, N).$$

Proof. It is easily checked that the triplet $(\text{vec}(\boldsymbol{\alpha}^*), \lambda^*, s^*)$, defined as follows, solves the KKT conditions belonging to the optimization problem (G): $\text{vec}(\boldsymbol{\alpha}^*) = (\alpha^{1*\top}, \ldots, \alpha^{N*\top})^\top$ as defined in Proposition 3.8.2, $\lambda^* = (\lambda_1^*, \ldots, \lambda_N^*) \in \mathbb{R}^N$, and $s^* = (s^{1*}, \ldots, s^{N*}) \in \mathbb{R}^{KN}$, where

$$\lambda_i^* = \frac{\sum_{j=1}^N C^{ij}}{m^2}, \quad s^{i*} = \frac{\sum_{j=1}^N C^{ij}}{m} (\frac{Q_{\text{tot}}}{\gamma \circ Q_0^{\text{nb}}} - \frac{1}{m} \mathbf{1}_K), \quad \text{for all } i = 1, \ldots, N.$$

Next, we need to check f-efficiency. Let $g_{ik}(\boldsymbol{\alpha}) := -\alpha^{ik}$ and $h_i(\boldsymbol{\alpha}) := \sum_{k=1}^{K} \alpha^{ik} - 1$ describe the non-negativity and linear conditions of the optimization problem (G), i.e., the conditions translate into $g_{ik}(\boldsymbol{\alpha}) \leq 0$ and $h_i(\boldsymbol{\alpha}) = 0$ for all $i = 1, \ldots, N$ and $k = 1, \ldots, K$. Let $d = (d_1^\top, \ldots, d_N^\top) \in \mathbb{R}^{KN}$, where $d_i \in \mathbb{R}^K$ for all $i = 1, \ldots, N$ and define

$$\mathcal{F}(\boldsymbol{\alpha}) := \{d \neq \mathbf{0} \mid \nabla g_{ik}(\boldsymbol{\alpha})^\top d \begin{cases} = 0, & k \notin k_m \\ \leq 0, & k \in k_m, \end{cases} \text{ and } \nabla h_i(\boldsymbol{\alpha})^\top d = 0,\ \forall i \in \{1, \ldots, N\},\ \forall k \in \{1, \ldots, K\}\}.$$

Applying the second order sufficiency conditions (cf. Theorem 5.2 in Freund (2016)), the KKT point $(\mathrm{vec}(\boldsymbol{\alpha}^*), \lambda^*, s^*)$ constitutes a local minimum if for all $d \in \mathcal{F}(\boldsymbol{\alpha}^*)$ it holds that $d^\top (\boldsymbol{C} \otimes (\frac{Q_{\mathrm{tot}}}{\gamma \circ Q_0^{\mathrm{nb}}})(\frac{Q_{\mathrm{tot}}}{\gamma \circ Q_0^{\mathrm{nb}}})^\top) d > 0$. We have

$$\mathcal{F}(\boldsymbol{\alpha}) = \{d \neq \mathbf{0} \mid d_{ik} \begin{cases} = 0, & k \notin k_m \\ \geq 0, & k \in k_m, \end{cases} \text{ and } \sum_{k=1}^{K} d_{ik} = 0,\ \forall i \in \{1, \ldots, N\}\} = \emptyset$$

for all $\boldsymbol{\alpha}$ and, hence, the second order sufficiency condition is always fulfilled. Thus, $(\mathrm{vec}(\boldsymbol{\alpha}^*), \lambda^*, s^*)$ constitutes a local minimum. □

Remark 3.8.3.
- Note that we may characterize liquidity of asset k by its product of elasticity and supply in the nonbanking sector weighted by total supply, i.e., by $\gamma_k \cdot Q_0^{k,\mathrm{nb}} / Q_{\mathrm{tot}}^k$. Proposition 3.8.2 thus shows that the f-efficient liquidation strategy of banks is given by selling solely the most liquid asset. We will refer to this f-efficient strategy as the *most-liquid-strategy*.
- Note that the most-liquid-strategy depends on (the row sums of) the holding matrix $\boldsymbol{Q}$ since it holds that $Q_0^{k,\mathrm{nb}} = 1 - \sum_{i=1}^{N} Q^{ki}$ for all assets $k = 1, \ldots, K$.
- In the special case that we ex ante assume that all banks follow the same liquidation strategy, the most-liquid-strategy even constitutes a global minimizer of the mean squared deviation. This example is analyzed in Appendix 3.8.2.

3.8.2 Liquidation Strategy Example

In this case study, we ex ante assume that all banks act homogeneously in that they liquidate their portfolios in the exact same way. This assumption leads to the following structure of the liquidation strategy matrix:

$$\boldsymbol{\alpha} = (\widetilde{\alpha} \mid \cdots \mid \widetilde{\alpha}),$$

for a vector $\widetilde{\alpha} \in \mathbb{R}^K$, with $\mathbf{1}^\top \widetilde{\alpha} = 1$, specifying the banks' liquidation of each asset. For the mean squared deviation, this leads to the equation

$$MSD(\widetilde{\alpha}, \boldsymbol{Q}) = (\widetilde{\alpha}^\top \frac{Q_{\mathrm{tot}}}{\gamma \circ Q_0^{\mathrm{nb}}})^2 \cdot (\boldsymbol{Q}\kappa)^\top (\mu\mu^\top + \mathrm{Diag}(\sigma^2))(\boldsymbol{Q}\kappa).$$

For a fixed given holding matrix $\boldsymbol{Q}$, we define an *f-efficient bank-independent liquidation strategy* $\widetilde{\alpha}$ as a minimizer of $MSD(\cdot, \boldsymbol{Q})$ over all $\widetilde{\alpha} \in \mathbb{R}^K_{\geq 0}$ with $\mathbf{1}^\top \widetilde{\alpha} = 1$. We have the following result.

Proposition 3.8.4. *For every fixed $\boldsymbol{Q} \in \mathbb{R}^{K \times N}$, the most-liquid-strategy constitutes a globally f-efficient bank-independent liquidation strategy.*

Proof. Minimizing $MSD(\widetilde{\alpha}, \boldsymbol{Q})$ for a fixed $\boldsymbol{Q}$ over all $\widetilde{\alpha} \in \mathbb{R}^K_{\geq 0}$ with $\mathbf{1}^\top \widetilde{\alpha} = 1$ is equivalent to

$$\begin{aligned} \min_{\widetilde{\alpha} \in \mathbb{R}^K} \quad & \tfrac{1}{2} \widetilde{\alpha}^\top \tfrac{Q_{\mathrm{tot}}}{\gamma \circ Q_0^{\mathrm{nb}}} \left(\tfrac{Q_{\mathrm{tot}}}{\gamma \circ Q_0^{\mathrm{nb}}} \right)^\top \widetilde{\alpha} \\ \text{s.t.} \quad & \mathbf{1}^\top \widetilde{\alpha} = 1, \quad \widetilde{\alpha} \geq \mathbf{0}. \end{aligned} \tag{BI}$$

The KKT conditions for this optimization problem read

$$\mathbf{1}^\top \widetilde{\alpha} = 1, \quad \tfrac{Q_{\mathrm{tot}}}{\gamma \circ Q_0^{\mathrm{nb}}} \left(\tfrac{Q_{\mathrm{tot}}}{\gamma \circ Q_0^{\mathrm{nb}}} \right)^\top \widetilde{\alpha} - \lambda \mathbf{1} - s = \mathbf{0}, \quad \widetilde{\alpha} \geq \mathbf{0}, s \geq \mathbf{0}, \quad \widetilde{\alpha}_k s_k = 0, \ (k = 1, \ldots, K).$$

Let m, k_m, and $\#k_m$ be defined as in Proposition 3.8.2. Direct calculation shows that a solution to the KKT conditions is given by $(\widetilde{\alpha}^*, \lambda^*, s^*)$ defined through

$$\widetilde{\alpha}^*_k := \begin{cases} \frac{1}{\#k_m}, & \text{if } k \in k_m, \\ 0, & \text{otherwise.} \end{cases}, \ (k = 1, \ldots, K), \qquad \lambda^* := \frac{1}{m^2}, \qquad s^* := \frac{1}{m} \left(\frac{Q_{\mathrm{tot}}}{\gamma \circ Q_0^{\mathrm{nb}}} - \frac{1}{m} \mathbf{1} \right).$$

(BI) possesses a convex domain, linear constraints, and a convex objective function, because $\frac{Q_{\mathrm{tot}}}{\gamma \circ Q_0^{\mathrm{nb}}} \left(\frac{Q_{\mathrm{tot}}}{\gamma \circ Q_0^{\mathrm{nb}}} \right)^\top$ is positive semidefinite. Hence, $\widetilde{\alpha}^*$ constitutes a global minimizer of (BI). □

3.9 Appendix: Majorization and Diversity vs. Diversification

In this section, we firstly provide an alternative direct proof for Corollary 3.3.11 using the concept of matrix majorization. Secondly, this concept enables us to illustrate the relation between f-efficiency and diversity vs. diversification for the case of homogeneous asset shocks and budget constraints.

We start with recapitulating a few basic definitions and results from vector and matrix majorization theory.

For $x \in \mathbb{R}^N$, let $x^\downarrow$ denote the vector obtained by rearranging the components of x in decreasing order. Given two vectors $x, y \in \mathbb{R}^N$, we say that x (vector-)majorizes y, in symbols $x \geq_\vartheta y$, if

$$\sum_{j=1}^{k} x_j^\downarrow \geq \sum_{j=1}^{k} y_j^\downarrow, \quad k = 1, \ldots, N-1 \quad \text{and} \quad \sum_{j=1}^{N} x_j = \sum_{j=1}^{N} y_j.$$

There are many different characterizations of vector majorization in the literature. We need the following (see, e.g., Martínez Pería et al. (2005) and Bhatia (2013)).

Theorem 3.9.1. *For $x, y \in \mathbb{R}^N$, the following statements are equivalent:*

(i) $x \geq_\vartheta y$;

(ii) There exists a doubly stochastic matrix $D \in \mathbb{R}^{N\times N}$ such that $y = Dx$;

(iii) For every convex symmetric function $f : \mathbb{R}^N \to \mathbb{R}$, we have $f(x) \geq f(y)$.

A matrix $\boldsymbol{A} \in \mathbb{R}^{N\times M}$ is defined to (matrix-)majorize a matrix $\boldsymbol{B} \in \mathbb{R}^{N\times M}$, in symbols $\boldsymbol{A} \geq \boldsymbol{B}$, if there exists a doubly stochastic matrix $\boldsymbol{D} \in \mathbb{R}^{N\times N}$ such that $\boldsymbol{DA} = \boldsymbol{B}$. An important relation between matrix and vector majorization is given in the following corollary which is a direct consequence of Theorem 3.9.1 (ii).

Corollary 3.9.2. *Let $\boldsymbol{A}, \boldsymbol{B} \in \mathbb{R}^{N\times M}$. If $\boldsymbol{A} \geq \boldsymbol{B}$, then for all vectors $v \in \mathbb{R}^M$ it holds that $\boldsymbol{A}v \geq_\vartheta \boldsymbol{B}v$.*

As the last ingredient for our alternative proof of Corollary 3.3.11, we need the following lemma.

Lemma 3.9.3. *If $q_1 = \ldots = q_K$, then for every $\boldsymbol{Q} \in \mathcal{D}$, it holds that $\boldsymbol{Q} \geq \boldsymbol{Q}^{\text{diversified}}$.*

Proof. Let $\boldsymbol{Q} \in \mathcal{D}$ and set $\boldsymbol{A} := \frac{1}{K}\mathbf{1}_{K\times K} \in \mathbb{R}^{K\times K}$. Then it holds that

$$\boldsymbol{AQ} = \frac{1}{K}\begin{pmatrix} \mathbf{1}_K^\top \boldsymbol{Q} \\ \vdots \\ \mathbf{1}_K^\top \boldsymbol{Q} \end{pmatrix} = \frac{1}{K}\begin{pmatrix} b^\top \\ \vdots \\ b^\top \end{pmatrix} = \boldsymbol{Q}^{\text{diversified}},$$

in the case that $q_1 = \ldots = q_K$. Since $\boldsymbol{A}$ is obviously doubly stochastic, it follows that $\boldsymbol{Q} \geq \boldsymbol{Q}^{\text{diversified}}$. □

This shows that diversification constitutes a minimal element with respect to the matrix majorization preorder within the set of allocations that satisfy our budget and homogeneous supply constraints. Now we are able to give the alternative proof for the following particular statement of Corollary 3.3.11.

Proposition 3.9.4. *If $q_1 = \ldots = q_K$, $\mu_1 = \ldots = \mu_K$, and $\sigma_1^2 = \ldots = \sigma_K^2$, i.e., all assets are homogeneous in their supplies and shock distributions, then $\boldsymbol{Q}^{\text{diversified}}$ is f-efficient.*

Proof. We define the function $f^{MSD} : \mathbb{R}^N \to \mathbb{R}$ through $f^{MSD}(x) := x^\top(\mu\mu^\top + \mathrm{Diag}(\sigma^2))x$ for $x \in \mathbb{R}^N$. It has the following two properties: First, it is convex since $\mu\mu^\top + \mathrm{Diag}(\sigma^2)$ is positive definite. Second, in the case of homogeneous asset shocks, i.e., if $\mu_1 = \ldots = \mu_K$ and $\sigma_1^2 = \ldots = \sigma_K^2$, f^{MSD} is also symmetric. Thus, we can write the mean squared deviation as a convex, symmetric function of $\boldsymbol{Q}v$ with $v \in \mathbb{R}^N$ being the systemic significance vector:

$$\begin{aligned} MSD(\boldsymbol{Q}) &= (\boldsymbol{Q}\,\mathrm{Diag}(\kappa)\boldsymbol{\alpha}^\top(\tfrac{Q_{\mathrm{tot}}}{\gamma\circ(Q_{\mathrm{tot}}-q)}))^\top(\mu\mu^\top + \mathrm{Diag}(\sigma^2))\boldsymbol{Q}\,\mathrm{Diag}(\kappa)\boldsymbol{\alpha}^\top(\tfrac{Q_{\mathrm{tot}}}{\gamma\circ(Q_{\mathrm{tot}}-q)}) \\ &= f^{MSD}(\boldsymbol{Q}v). \end{aligned}$$

Successively using the majorization properties Corollary 3.9.2 and Theorem 3.9.1 (iii), it follows that

$$\begin{aligned} &\boldsymbol{Q} \geq \boldsymbol{Q}' \quad \Rightarrow \quad (\forall x \in \mathbb{R}^N : \boldsymbol{Q}x \geq_\vartheta \boldsymbol{Q}'x) \quad \Rightarrow \quad \boldsymbol{Q}v \geq_\vartheta \boldsymbol{Q}'v \\ &\Rightarrow \quad f^{MSD}(\boldsymbol{Q}v) \geq f^{MSD}(\boldsymbol{Q}'v) \quad \Rightarrow \quad MSD(\boldsymbol{Q}) \geq MSD(\boldsymbol{Q}'). \end{aligned}$$

This shows that the mean squared deviation preserves the matrix majorization preorder. Hence, its minimal element $\boldsymbol{Q}^{\mathrm{diversified}}$ (cf. Lemma 3.9.3) minimizes the mean squared deviation over all holding matrices satisfying our budget and homogeneous supply constraints. □

Lastly, we study the relation between matrix majorization and the two dimensions of diversity vs. diversification and analyze their impact on f-efficiency. The concept of matrix majorization enables a comparison between holding matrices along these two dimensions. While, according to Lemma 3.9.3, diversification represents a minimal element within the considered set of allocations with respect to matrix majorization, we will now show that diversity constitutes a maximal element.

We define a situation of full diversity for the special case $b_1 = \ldots = b_N = q_1 = \ldots = q_K =: x$ (yielding $K = N$) via a matrix $\boldsymbol{Q}^{\mathrm{diverse}} := x \cdot \boldsymbol{P}$, where $\boldsymbol{P} \in \{0,1\}^{K\times K}$ denotes an arbitrary $K \times K$ permutation matrix. Hence, the matrix $\boldsymbol{Q}^{\mathrm{diverse}}$ describes a situation in which each bank possesses holdings in exactly one asset with no overlapping asset portfolios: all banks are fully diverse, but not at all diversified across assets. We have the following result.

Lemma 3.9.5. *If $q_1 = \ldots = q_K = b_1 = \ldots = b_N =: x$, then for every non-negative $\boldsymbol{Q} \in \mathcal{D}$, it holds that $\boldsymbol{Q}^{\mathrm{diverse}} \geq \boldsymbol{Q}$.*

Proof. Let $\boldsymbol{Q} \in \mathcal{D}$ be non-negative and set $\boldsymbol{A} := \frac{1}{x}\boldsymbol{Q}\boldsymbol{P}^{-1}$. Then it holds that

$$\boldsymbol{A}\boldsymbol{Q}^{\mathrm{diverse}} = \frac{1}{x} \cdot \boldsymbol{Q}\boldsymbol{P}^{-1} \cdot x \cdot \boldsymbol{P} = \boldsymbol{Q}.$$

Since $\boldsymbol{A}$ is doubly stochastic due to $\boldsymbol{Q} \in \mathcal{D}$, it follows that $\boldsymbol{Q}^{\mathrm{diverse}} \geq \boldsymbol{Q}$. □

For homogeneous asset shocks and budget constraints, exploiting the monotonicity of the mean squared deviation with respect to matrix majorization (shown in the proof of Proposition 3.9.4 above), full diversification thus minimizes and full diversity maximizes the mean squared deviation over all non-negative holding matrices in $\mathcal{D}$. This reveals a monotonicity result: The more evenly distributed (or the less concentrated) the holdings in such systems, the higher the f-efficiency.

4 Pricing of Cyber Insurance Contracts in a Network Model

The original version of this chapter was previously published in *ASTIN Bulletin*, 48(3): 1175–1218, 2018, see Fahrenwaldt, Weber, and Weske (2018). Reprinted with permission

Cyber risk has evolved as a major threat to businesses. For instance, Lloyd's of London estimates that the total extent of cyber attacks to businesses worldwide comprises losses of USD 400 billion a year (Gandel (2015)). In addition, the size of exposure to cyber risks might significantly grow in our interconnected world. Although companies seem aware of these threats, recent studies find that relatively few firms have yet built a formal cyber risk management system (Swiss Re/IBM (2016)). Their management of cyber risks consists mostly of ad-hoc self-protection mechanisms such as firewalls and anti-virus software, but very few perform regular cyber risk assessments and possess risk management programs that integrate cyber risk on an institutional level.

Cyber damage may occur accidentally, but might also be purposely caused. As described in Swiss Re/IBM (2016), costs "are no longer confined to coping with lost, stolen or corrupted data, but increasingly include potential damage to a firm's property and reputation, and also the cost associated with business interruption or severe disruption to critical infrastructure". Even if future risk management strategies were able to actively improve protection against the occurrence or impact of cyber events, some residual cyber risks would remain that require insurance solutions.

From an actuarial point of view, cyber risk is challenging in three ways. First, data is not available in the required amount or in the desired granularity to apply standard statistical methods. Second, technology and cyber threats are evolving fast; the cyber environment is highly non-stationary. Third, infectious cyber threats pose a large accumulation risk to an insurance company. The typical insurance independence assumption does not hold and, moreover, there is no geographical distinction between dependent groups as there is, for example, for natural catastrophes. This requires new mathematical models that capture the dependence structure of cyber networks in an appropriate way (see also Swiss Re Institute (2017)).

This is the aim of the present chapter. Causes and channels for cyber losses are diverse.

While an insider attack might cause substantial damage to a particular firm, it might not affect other firms. However, if the originally attacked firm is part of a larger network in which the operations of components depend on each other, consecutive and coupled losses might occur. Another related example are worms, viruses and Trojans that spread across data networks and facilitate attacks throughout the network. Our chapter focuses on cyber threats in networks, i.e., infectious cyber threats.

From an insurance perspective, our main contributions are the following:

(i) To the best of our knowledge, we develop the first *mathematical model of insured losses* generated by infectious cyber threats. Dependence is modeled as an undirected network where each node could represent a firm, a system of computers or a single device; each edge constitutes a possible transmission channel in a network.

(ii) We provide a new methodology to *calculate expected aggregate losses* of a (re-) insurance company. Our method is applicable to a large variety of contract designs including both linear and non-linear functions of the generated losses. The application is illustrated in numerical examples. Thus, our approach can be used for pricing decisions.

(iii) In numerical case studies, we analyze the *role of the network topology*. We find that the insured network structure has a significant impact on the generated losses. This illustrates that the topology of the network is a key ingredient for the pricing of cyber insurance contracts and for cyber risk management in general.

Our model consists of two parts: a stochastic process that captures cyber infections, and a mechanism that randomly generates the actual claims at the infected nodes. To model the claims, we introduce a marked point process. This is in spirit of the collective risk model of insurance (see, e.g., Burnecki et al. (2011)). In contrast to the standard setting, the claims in our model depend on the spread of the cyber threat. The cyber infections are modeled by a susceptible-infected-susceptible (SIS) network process (see, e.g., Section V. in Pastor-Satorras et al. (2015)). For a network of size N, this approach results in a continuous-time Markov chain with a very large state space of size 2^N. In order to cope with the resulting computational challenges, we develop a tractable *mean-field approximation* for the Markov process. Approximations of its moments are derived as solutions to systems of ordinary differential equations (ODEs) (see, e.g., Van Mieghem et al. (2009) and Van Mieghem (2011)). Combining these solutions with our claim model finally yields approximations of the expected insured losses. For this purpose, we develop a polynomial approximation approach to evaluate general, possibly non-linear, claim functions. In the context of SIS-processes we provide the following contributions to the theory of mean-field approximations:

(i) We suggest a general and rigorous framework for mean-field approximations of the moments of the spread process of *arbitrary order* $n \geq 1$. We show that there are two key ingredients defining the approximation: a mean-field function, and a splitting algorithm.

(ii) We analyze two mean-field functions in detail that lead to different schemes: the well-known independent approximation (also called NIMFA approximation, see Van Mieghem et al. (2009)) and a new approximation type: the Hilbert approximation.

(iii) For the first order independent approximation, we derive a time-dependent accuracy result.

(iv) For both approximation types, NIMFA and Hilbert, we provide splitting algorithms and briefly address the question of splitting.

Literature

This chapter connects three different research areas: mathematical modeling of cyber insurance, epidemics on networks, and marked point processes.

Cyber Insurance. The literature on mathematical cyber insurance modeling focuses mainly on simple game-theoretic models. These consider, e.g., the following questions: Does a cyber insurance market exist in equilibrium (Böhme (2005))? Does cyber insurance affect the incentives to self-protection (Bolot and Lelarge (2008)), and how does it influence social welfare (Schwartz and Sastry (2014))? A recent review of such game-theoretic approaches can be found in the survey article Marotta et al. (2015). In contrast to these papers, we model cyber insurance with the aim of simulating and evaluating losses and pricing insurance contracts. To date, cyber loss models are mostly based on deterministic scenarios (see Swiss Re Institute (2017)). In contrast, we derive a stochastic model and develop suitable approximation techniques to explicitly calculate the losses.

Epidemic Models. We use the network-based *susceptible-infected-susceptible (SIS) model*, also known as the *contact process*, to model the spread of the considered cyber threat. This continuous time Markov chain has been extensively analyzed. A key topic in the analysis is the long-term behavior of the system as a function of the model parameter τ—the ratio of the infection to the curing rate. For networks of infinite size, both survival and extinction of the considered threat can occur. For example, in the network $\mathbb{Z}^k$ there exists a critical value τ_c such that for $\tau \leq \tau_c$, the infection dies out, while for $\tau > \tau_c$, the infection survives (cf. Liggett (1985) for the case $k = 1$, and Bezuidenhout and Grimmett (1990) and Liggett (1999), Part I, Section 2, for $k \geq 1$). For networks of finite size, however, the infection will almost surely die out in finite time. This is due to the presence of the absorbing healthy state in the Markov chain. Still, there is a different kind of threshold behavior of the system: There exists a critical value for τ that determines the behavior of the expected extinction time as a function of the network size N. Below this critical value, the expected extinction time increases logarithmically for increasing N; above, it increases exponentially fast (see, e.g., Durrett and Liu (1988) for an analysis of the chain graph $\{1, \ldots, N\}$ and Mountford et al. (2016) for bounds on the expected survival time for the homogeneous tree of bounded degree). For a recent survey paper, including bounds in general graphs, we refer to Nowzari et al. (2016) (Theorems 4 and 5).

In our insurance application, we are mainly interested in the moments of the Markovian spread process. These can be used to approximate expected losses and to compute insurance premiums. Since the exact calculation of these moments requires the solution of a system of $2^N - 1$ ordinary differential equations, we use a lower order mean-field approximation in the sense of Van Mieghem et al. (2009). In contrast to the degree-based mean-field approach (Pastor-Satorras and Vespignani (2001), Boguñá and Pastor-Satorras (2002)) which builds on average degrees, this individual-based approach captures the complete structure of the network. This enables us to *analyze the influence of the network topology* on the spread of the infection and on insured losses.

Van Mieghem et al. (2009) derive a first order independent mean-field approximation called NIMFA. We add an analysis of its accuracy. In contrast to earlier papers (such as Van Mieghem and van de Bovenkamp (2015)), we provide a *time-dependent accuracy criterion* that is able to qualitatively capture the behavior of the approximation error over time, if the parameter τ is sufficiently small. For larger values of τ, however, we observe that first order approximations may lead to substantial errors. In this case, we propose not to use a first, but a *higher order approximation.*

The fact that the mean-field approximation approach can be generalized to higher orders has already been noted previously; we refer to Cator and Van Mieghem (2012) for a second order independent approximation with naive single split, to Mata and Ferreira (2013) for a second order pair-approximation, and to (Pastor-Satorras et al., 2015, p.19) for a recent review. The present chapter provides the first explicit *derivation of a general n-th order mean-field approximation*, i.e., an approximation of the moments of the spread process up to order n. We show that our n-th order mean-field approximation is defined by two main ingredients: a mean-field function, and a splitting algorithm. Our framework comprises the previous contributions Van Mieghem et al. (2009) and Cator and Van Mieghem (2012) as special cases. It is also more general than these papers and enables us to introduce and analyze a new *Hilbert approximation* and *splitting algorithms*.

Marked Point Processes. To model the claims, we use a marked point process. A general introduction to this type of processes as well as the main theoretical results can be found in Jacod (1975), Brémaud (1981), and Last and Brandt (1995). Marked point processes have been applied in many different areas such as credit risk modeling, see, e.g., Bielecki and Rutkowski (2004), survival analysis, see, e.g., (Jacobsen, 2006, Chapter 8), and insurance loss modeling, see, e.g., Burnecki et al. (2011). In this chapter, we build on the latter approach; however, our loss process is additionally coupled with the underlying spread process of the cyber infection. This captures the idea that only infected nodes may suffer losses. A similar approach is used in Giesecke and Weber (2004) and Giesecke and Weber (2006) in the context of liquidity and credit risk.

Outline

The chapter is organized as follows. Section 4.1 presents our exact loss model. Section 4.1.1 introduces the SIS Markov chain as a model of the infection process. Section 4.1.2 describes the marked point process that generates the claims at infected sites. A formula for the expected aggregate losses of a reinsurer is derived. Section 4.2 explains different approximations. Section 4.2.1 presents a polynomial approximation approach to evaluate non-linear claim functions. Section 4.2.2 introduces mean-field approximations of the moments of the spread process. We first analyze first order approximations and the corresponding ODE systems. Second, we define the general n-th order approximation and its two key ingredients: the mean-field function, and the splitting algorithm. Section 4.3 illustrates in numerical case studies how the suggested approach may be applied to the pricing of different insurance contracts. This allows to study the influence of the underlying network topology. Section 4.4 concludes. All proofs can be found in an appendix.

4.1 Exact Loss Model

We consider a cyber threat that spreads via two consecutive channels. First, a vulnerability is created by an infection in a given network of agents. More specifically, each agent (a corporation, a system of computers, or a single device) is represented by a node in the network; each edge constitutes a possible transmission channel of the cyber infection. An edge could be a direct link between individual agents, or a link to a central server that stores data or supplies users with software updates. Second, infected agents are vulnerable to randomly occurring attacks, triggering losses of random size. For example, an infected computer may be attacked by collecting and abusing private information such as credit card or banking information, or by disturbing operations on the computer via ransomware. If agents are insured against cyber damage, insurance claims depend on two different types of stochastic processes: first, the infectious spread process of the vulnerability, and, second, the claim frequency and severity processes.

4.1.1 Spread Process

The cyber network consists of N agents, labeled $1, \ldots, N$. To begin with, we focus in the current chapter on a simple undirected graph. The suggested model could easily be extended to directed and weighted graph structures. Such extensions could provide more realistic models of cyber networks with asymmetric infection channels of different strengths, but their analysis would be more involved, and we thus leave a detailed analysis of complex networks to future research. The undirected network is represented by a symmetric adjacency matrix $A \in \{0,1\}^{N \times N}$, with $a_{ii} = 0$ for all i, where $a_{ij} = 1$ indicates a connection between nodes i and j and $a_{ij} = 0$ signifies that i and j are not directly connected.

To describe the dynamics of the first channel, the infectious spread of vulnerability to cyber events, we use the susceptible-infected-susceptible (SIS) model, as, for example, explained in Section V. of Pastor-Satorras et al. (2015)). At any point in time, each node i can be in one of two states: infected or susceptible. The state of node i at time t is denoted by $X_i(t)$, where $X_i(t) = 1$ indicates that node i is infected at time t and $X_i(t) = 0$ indicates that node i is susceptible to an infection. We assume that each node can be infected by its infected neighbors, but is cured independently of all other nodes in the system. We assume that each node is endowed with an independent exponential clock and changes its state when the exponential clock rings. Letting $\beta > 0$ and $\delta > 0$, the rates of these transitions are given as follows ($i = 1, 2, \ldots, N$):

$$\begin{aligned} X_i &: 0 \to 1 \quad \text{with rate} \quad \beta \sum\nolimits_{j=1}^{N} a_{ij} X_j(t) \\ X_i &: 1 \to 0 \quad \text{with rate} \quad \delta. \end{aligned} \tag{4.1}$$

To be precise, we will from now on work on a probability space $(\Omega, \mathcal{F}, P)$ with filtration $\mathbb{F} = (\mathcal{F}_t)_{t \geq 0}$ that satisfies the usual conditions, i.e., the filtration is right-continuous and $\mathcal{F}_0$ contains all P-null sets, see, e.g., Protter (2004). The process X is a Markov-process with state space $E = \{0,1\}^N$ with càdlàg paths and $X_0 = x \in E$. We assume that X is a Feller process with generator $G : C(E) \to \mathbb{R}$ defined by

$$Gf(x) = \sum_{i=1}^{N} \left(\beta (1 - x_i) \sum_{j=1}^{N} a_{ij} x_j + x_i \delta \right) (f(x^i) - f(x)), \quad x \in E,\ f \in C(E)$$

where $x^i_j = x_j$ for $i \neq j$ and $x^i_i = 1 - x_i$. The family $C(E)$ consists of all functions on E. For details we refer to Liggett (1985).

The continuous-time Markov process X is of pure jump-type with exponential waiting times between jumps. The dimension of the state space E is large, i.e., E has cardinality 2^N. In Section 4.2.2, we derive a tractable mean-field approximation in terms of a system of ordinary differential equations that can be applied to the valuation of cyber insurance.

4.1.2 Claims Processes

In our model of cyber losses and insurance, we assume that the process X does not directly cause any damage. Instead, at each point in time, infected agents are *vulnerable* to cyber attacks, while agents who are not infected are not. For example, infected agents might constitute a botnet that enables a denial-of-service or ransomware attack.

In order to model cyber losses, we assume that the attacks are counted by a process $M := (M(t))_{t \geq 0}$ with values in $\{0, 1, 2, \dots\}$. The corresponding jump times are denoted by $(T_n)_{n \in \mathbb{N}}$. The size of possible losses at each site during an attack is modeled by another N-dimensional process $L := (L(t))_{t \geq 0}$, where $L(t) = (L_1(t), \dots, L_N(t))^\top$. We assume that both M and L are independent from the Markovian spread process X.

To be precise, M is a non-explosive counting process adapted to the filtration $\mathbb{F}$. We suppose that M has a stochastic intensity $(\lambda(t))_{t \geq 0}$, i.e., λ is some non-negative $\mathbb{F}$-predictable process with $M(t \wedge T_n) - \int_0^{t \wedge T_n} \lambda(s) ds$ is a martingale for all $n \in \mathbb{N}$, see Brémaud (1981), T9/p. 28 & T13/p. 31. The loss process L is assumed to be predictable and non-negative.

We consider a (re-)insurance contract covering cyber losses and compute the expected aggregate losses over a fixed time window $[0, T]$ with $T > 0$. We suppose that for any time t the insurance contract is characterized by a function $f(\cdot; \cdot) : \mathbb{R}_+ \times \mathbb{R}^N_+ \to \mathbb{R}_+$ where the first argument refers to time and the second argument to the loss vector generated by a cyber attack. We suppose that f is jointly measurable.

We denote the Hadamard product of vectors (i.e., the multiplication of the components) by $\circ$. At time t, the insurance contract covers $f(t; L(t) \circ X(t))$, if a loss event occurs at time t. Neglecting interest rates or considering discounted quantities, the expected aggregate losses of the contract over the time window $[0, T]$ are thus given by:

$$\begin{aligned} &\mathbb{E}\left[\int_0^T f(t; L(t) \circ X(t)) dM(t)\right] = \mathbb{E}\left[\int_0^T f(t; L(t) \circ X(t-)) dM(t)\right] \\ = \ &\mathbb{E}\left[\int_0^T f(t; L(t) \circ X(t-)) \lambda(t) dt\right] = \mathbb{E}\left[\int_0^T f(t; L(t) \circ X(t)) \lambda(t) dt\right]. \end{aligned} \tag{4.2}$$

The first equality is due to the fact that X and M are independent and never jump at the same time with probability 1. The second equality follows from the predictability of the integrand according to D7/p. 27 in Brémaud (1981). The third equality holds, since the paths of X possess at most countably many jumps on $[0, T]$ and constitute a Lebesgue null set for each path.

The simplest contract f is a proportional insurance, i.e., $f(t; z) = \sum_{i=1}^{N} \alpha_i z_i$. In this case,

$$\mathbb{E}\left[\int_0^T f(t; L(t) \circ X(t)) dM(t)\right] = \int_0^T \sum_{i=1}^{N} \alpha_i \cdot \mathbb{E}[X_i(t)] \cdot \mathbb{E}[L_i(t)\lambda(t)]\, dt, \tag{4.3}$$

where the factorization follows from the independence of X and (M, λ, L).

For a linear claim function, the computation of the expected losses of the insurance contract does not require full knowledge of the dynamics of the spread process X, but only of its expectation, i.e., the first moment. If f is non-linear, but continuous, a polynomial approximation can be used in order to evaluate equation (4.2). This requires knowledge of the evolution of all moments of X up to the degree that is desired for the evaluation. This will be explained in Section 4.2.1.

Due to Kolmogorov's equations, using the fact that the components of X are idempotent and commutative, the moments of X are described by a finite system of ordinary differential equations of order N consisting of $\sum_{i=1}^{N} \binom{N}{i} = 2^N - 1$ equations. For large N, this coupled system of equations of first order becomes intractable[1]. If the order of the polynomial approximation is less N, say n, only moments of X up to order n are needed. However, the ordinary differential equations for these moments depend on higher order moments, i.e., the desired system of equations is not closed. We address this problem in Section 4.2.2 by constructing a mean-field approximation of the dynamics of the desired moments which significantly reduces the dimension of the system of ordinary differential equations.

4.2 Approximations

4.2.1 Polynomial Approximation of Non-Linear Claim Functions

In this section, we discuss a polynomial approximation of the claim function f that facilitates the computation of expected insurance losses (4.2) in the non-linear case. In order to simplify the mathematical analysis, we assume in this chapter that f does not depend on t. We do, however, stress that our analysis can be extended to the time-dependent case at the expense of constructing approximations that are sufficiently regular in time. This requires a more complicated notation. The basic idea of the polynomial approximation is that any

[1] On the computing cluster that we used, we were able to numerically solve the coupled system of ordinary differential equations for networks with $N \leq 13$ agents.

continuous function f can be uniformly approximated by polynomials on any compact set according to the Stone-Weierstraß theorem. We make the following assumptions:

Assumption 4.2.1.

1. The function $f : \mathbb{R}_+^N \to \mathbb{R}_+$ is *decomposable*, i.e., one can write

$$f(x_1,\dots,x_N) = g(\Lambda(x_1,\dots,x_N)),$$

   where $\Lambda : \mathbb{R}_+^N \to \mathbb{R}_+$ is a linear and increasing aggregation function and the function $g : \mathbb{R}_+ \to \mathbb{R}_+$ is continuous and increasing.

2. The function g is bounded on $[0, \|\Lambda(L)\|_\infty)$ where $\|\cdot\|_\infty$ denotes the L^∞-norm.

Example 4.2.2.

1. A first example is a catastrophe excess of loss per risk (Cat XL) contract that covers cyber attacks with priority $a \geq 0$ and limit $b - a > 0$. In this case, insurance losses are described by

$$f^{\text{Cat-XL}}(x_1,\dots,x_N) = g^{\text{Cat-XL}}(\Lambda^\Sigma(x_1,\dots,x_N))$$

   with $\Lambda^\Sigma(x_1,\dots,x_N) = \sum_{i=1}^N x_i$, and $g^{\text{Cat-XL}}(y) = (y-a)^+ - (y-b)^+$. This shows that $f^{\text{Cat-XL}}$ satisfies Assumption 4.2.1.

2. Another example is an excess of loss per risk contract (XL) that covers all individual cyber losses. This is described by

$$f^{\text{XL}}(x_1,\dots,x_N) := \sum_{i=1}^N \left((x_i - a_i)^+ - (x_i - b_i)^+\right),$$

   where $a_i \geq 0$ is the priority of risk i and $b_i - a_i > 0$ its corresponding cover. This function is neither linear nor does it satisfy Assumption 4.2.1. However, with a small trick it fits into both frameworks. To this end, observe that

$$f^{\text{XL}}(L(t) \circ X(t)) = \sum_{i=1}^N \left((L_i(t)X_i(t) - a_i)^+ - (L_i(t)X_i(t) - b_i)^+\right).$$

   Since $X_i(t) \in \{0,1\}$, this function can be rewritten in the following form:

$$f^{\text{XL}}(L(t) \circ X(t)) = \sum_{i=1}^N \hat{L}_i(t)X_i(t) =: \hat{f}^{\text{XL}}(\hat{L}(t) \circ X(t)),$$

where $\hat{L}_i(t) = (L_i(t) - a_i)^+ - (L_i(t) - b_i)^+$ for $i = 1, \dots, N$. Then

$$\hat{f}^{\mathrm{XL}}(x_1, \dots, x_N) = \sum_{i=1}^{N} x_i.$$

For the modified loss size process $\hat{L}$, the function $\hat{f}^{\mathrm{XL}}$ describes a proportional reinsurance. Assumption 4.2.1 is satisfied with $\Lambda = \hat{f}^{\mathrm{XL}}$ and $g(\lambda) = \lambda$ for $\lambda \geq 0$.

Remark 4.2.3. The application of the Stone-Weierstraß theorem does not rely on the existence of a decomposition of f as required in Assumption 4.2.1. The decomposition guarantees that we may work with polynomial approximations in *one dimension*. In this case, simple algorithms for the construction of the unique best approximation are available. In contrast, due to the theorem of Mairhuber-Curtis, finite-dimensional subspaces of the space of continuous functions on a multi-dimensional compact set are not Haar spaces, implying that best approximations are not always unique.

If Assumption 4.2.1 is satisfied, a polynomial approximation can be constructed as follows:

Approximation 4.2.4.

1. Choose a bound $\epsilon > 0$ and the desired degree of the polynomial approximation $d \in \mathbb{N}$.

2. Determine a constant $u \in \mathbb{R}_+$ such that the probability that an aggregated loss (under a total infection) exceeds u is bounded from above by ϵ, i.e.,

$$P(\Lambda(L) > u) \leq \epsilon.$$

3. Find the best uniform approximation $p_d(x) := \sum_{\ell=0}^{d} a_\ell x^\ell$ $(a_0, a_1, \dots, a_d \in \mathbb{R})$ of the function g on the compact interval $[0, u]$ in the space of polynomials up to degree d. We denote the resulting approximation error by

$$\max_{x \in [0,u]} |g(x) - p_d(x)| = \|g - p_d\|_{\infty,[0,u]} =: e_d(g).$$

4. The d-th degree polynomial approximation of $f(L \circ X)$ is given by

$$\bar{f}_d(L \circ X) := \begin{cases} p_d(\Lambda(L \circ X)), & \text{if} \quad \Lambda(L) \leq u, \\ 0, & \text{if} \quad \Lambda(L) > u. \end{cases}$$

Remark 4.2.5. Due to Assumption 4.2.1, there exists a real number m s.t.

$$|f(L \circ X)| = |g(\Lambda(L \circ X))| \leq |g(\Lambda(L))| \leq m$$

for all possible realizations of the random variable L. The L^1-norm of the approximation error for $\bar{f}_d(L \circ X)$ is bounded from above by $e_d(g) + m \cdot \epsilon$. This can easily be verified. Letting $Z = L \circ X$, we obtain that

$$\begin{aligned}
\|f(Z) - \bar{f}_d(Z)\|_{L_1} &= \|[f(Z) - p_d(\Lambda(Z))] \cdot \mathbb{1}_{[0,u]}(\Lambda(L)) + f(Z) \cdot \mathbb{1}_{(u,\infty)}(\Lambda(L))\|_{L_1} \\
&\leq \mathbb{E}[|g(\Lambda(Z)) - p_d(\Lambda(Z))| \cdot \mathbb{1}_{[0,u]}(\Lambda(L))] + \mathbb{E}[|f(Z)| \cdot \mathbb{1}_{(u,\infty)}(\Lambda(L))] \\
&\overset{(\circ)}{\leq} \|g - p_d\|_{\infty,[0,u]} \cdot P(\Lambda(L) \leq u) + m \cdot P(\Lambda(L) > u) \\
&\leq e_d(g) + m \cdot \epsilon,
\end{aligned}$$

observing in step $(\circ)$ that $0 \leq \Lambda(Z) \leq \Lambda(L)$.

Finally, consider an insurance contract $f = g(\Lambda)$ with $\Lambda(x_1, \ldots, x_N) = \sum_{i=1}^N b_i x_i$, $b_1, b_2, \ldots, b_N \geq 0$, and polynomial approximation $p_d(x) := \sum_{\ell=0}^d a_\ell x^\ell$. In this case,

$$\mathbb{E}\left[\int_0^T \bar{f}_d(L(t) \circ X(t)) dM(t)\right] = \int_0^T \mathbb{E}[\bar{f}_d(L(t) \circ X(t)) \cdot \lambda(t)]\, dt.$$

Set $\mathcal{G} := \sigma\{L(t), \lambda(t) : t \leq T\}$, and observe that the process X is independent of $\mathcal{G}$. Thus,

$$\mathbb{E}[\bar{f}_d(L(t) \circ X(t)) \cdot \lambda(t) | \mathcal{G}] = \lambda(t) \cdot \mathbb{E}[\bar{f}_d(L(t) \circ X(t)) | \mathcal{G}]. \tag{4.4}$$

We evaluate the second factor. For simplicity, we suppress the dependence on t in the notation.

$$\begin{aligned}
&\mathbb{E}[\,\bar{f}_d(L \circ X) \mid \mathcal{G}] = \mathbb{E}[\,p_d(\Lambda(L \circ X)) \cdot \mathbb{1}_{[0,u]}(\Lambda(L)) \mid \mathcal{G}] \\
&= \sum_{\ell=0}^d a_\ell \cdot \mathbb{E}[(\Lambda(L \circ X))^\ell \mid \mathcal{G}] \cdot \mathbb{1}_{[0,u]}(\Lambda(L)) = \sum_{\ell=0}^d a_\ell \cdot \mathbb{E}[(\textstyle\sum_{i=1}^N b_i L_i X_i)^\ell \mid \mathcal{G}] \cdot \mathbb{1}_{[0,u]}(\Lambda(L)) \\
&= \mathbb{1}_{[0,u]}(\Lambda(L)) \cdot \Bigg[a_0 + a_1 \sum_{i_1=1}^N b_{i_1} L_{i_1} \mathbb{E}[X_{i_1}] + a_2 \sum_{i_1=1}^N \sum_{i_2=1}^N b_{i_1} b_{i_2} L_{i_1} L_{i_2} \mathbb{E}[X_{i_1} X_{i_2}] \\
&\quad + \ldots + a_d \sum_{i_1=1}^N \sum_{i_2=1}^N \cdots \sum_{i_d=1}^N b_{i_1} b_{i_2} \cdots b_{i_d} \cdot L_{i_1} L_{i_2} \cdots L_{i_d} \cdot \mathbb{E}[X_{i_1} X_{i_2} \cdots X_{i_d}]\Bigg].
\end{aligned}$$

Here, we used the fact that the process L is $\mathcal{G}$-measurable, while X is independent of $\mathcal{G}$. In the next step, we can now use the tower property on the conditional expectations in equation (4.4), i.e., $\mathbb{E}[\mathbb{E}(\cdot|\mathcal{G})] = \mathbb{E}(\cdot)$, to obtain the final result. Thus, in summary, for the purpose of approximating the expected insurance losses we need to calculate

$$\int_0^T \mathbb{E}\left(\mathbb{1}_{[0,u]}(\Lambda(L)) \cdot \lambda(t) \cdot \left[a_0 + a_1 \sum_{i_1=1}^{N} b_{i_1} L_{i_1} \mathbb{E}[X_{i_1}] + a_2 \sum_{i_1=1}^{N} \sum_{i_2=1}^{N} b_{i_1} b_{i_2} L_{i_1} L_{i_2} \mathbb{E}[X_{i_1} X_{i_2}] \right.\right.$$
$$\left.\left. + \ldots + a_d \sum_{i_1=1}^{N} \sum_{i_2=1}^{N} \cdots \sum_{i_d=1}^{N} b_{i_1} b_{i_2} \cdots b_{i_d} \cdot L_{i_1} L_{i_2} \cdots L_{i_d} \cdot \mathbb{E}[X_{i_1} X_{i_2} \cdots X_{i_d}]\right]\right) dt \tag{4.5}$$

The formula shows that full knowledge of the probabilistic evolution of the process X is not required. Instead, an analysis of the dynamics of its moments up to order d suffices to compute the sought quantity. As explained earlier, the corresponding system of ordinary differential equations is obtained from Kolmogorov's equations, but involves $2^N - 1$ equations. A closed system for the required moments with a smaller number of equations can be obtained by a mean-field approximation. This method will be explained in the next section.

Remark 4.2.6.

1. If the network size N is not too large, the polynomial approximation enables a flexible and efficient comparison of different contracts in a given network. The mixed moments of the spread process need to be computed only once. Afterwards, polynomial approximations of different contracts can be evaluated. Since the number of mixed moments up to order d grows like N^d when the number of nodes N increases, polynomial approximations are not efficient anymore for very large networks.

2. In this chapter, approximations of the joint moments of the spread process are computed from an ODE system. The methodology is explained in the next section. Alternatively, joint moments could be computed from Monte Carlo simulations of the spread process. A comparison of the advantages and disadvantages of these competing approaches is beyond the scope of the current chapter and constitutes an interesting topic for future research.

4.2.2 Mean-Field Approximation of Moments

To evaluate formula (4.5), we need to compute the moments $\mathbb{E}[X_{i_1}(t)]$, $\mathbb{E}[X_{i_1}(t)X_{i_2}(t)]$, $\ldots, \mathbb{E}[X_{i_1}(t)X_{i_2}(t)\cdots X_{i_n}(t)]$, $i_1, \ldots, i_n \in \{1, \ldots, N\}$, for the desired $n \leq N$. We construct an approximation of these moments and call the parameter n its *order*. For this purpose, we denote by $z^{(n)}_{i_1 i_2 \ldots i_k}$ the n-th order approximation of the moment $\mathbb{E}[X_{i_1} X_{i_2} \cdots X_{i_k}]$ for $k \leq n$. Observe that both $z^{(n)}_{i_1 i_2 \ldots i_k}$ and $\mathbb{E}[X_{i_1} X_{i_2} \cdots X_{i_k}]$ are functions of t. In order to simplify the notation, we will sometimes drop the variable t in our notation. Since the variables X_i, $i = 1,2,\ldots,n$, are commutative and idempotent, we may assume that the indices $i_1,\ldots,i_k$ are pairwise different and ordered, i.e., $i_1 < i_2 < \ldots < i_k$. Alternatively, the n-th order approximation of all moments of X up to order n can simply be enumerated by index sets $I \subseteq \{1,2,\ldots,N\}$ with cardinality $|I| \leq n$. This will be the convention that we choose. As a final result of our construction, we obtain the n-th order approximation of all moments of X up to order n, i.e.,

$$\left(z_I^{(n)}\right)_{I\subseteq\{1,2,\ldots,N\},\,|I|\leq n}$$

We begin with a detailed description of the first order approximation, explaining two strategies for its construction. This approach is later generalized to n-th order approximations for $n > 1$.

4.2.2.1 First Order

We derive the first order mean-field approximation in detail and analyze its accuracy.

Derivation of the Approximations. The transition rates (4.1) describe the infinitesimal dynamics of $X_i(t)$:

$$\mathbb{E}\left[X_i(t+\Delta t) - X_i(t)|\mathcal{F}_t\right] = ((1 - X_i(t))\beta \sum_{j=1}^{N} a_{ij} X_j(t) - \delta X_i(t))\Delta t + o(\Delta t) \qquad (4.6)$$

A susceptible node is infected by its neighbors at rate β; an infected node is cured at rate δ, independently of the state of the others. Intuitively, dividing by Δt, taking the expectation on both sides and letting $\Delta t \to 0$, we obtain the following exact expression for the derivative of the probability $\mathbb{E}[X_i(t)] = P(X_i(t) = 1)$:

$$\frac{d\mathbb{E}[X_i(t)]}{dt} = -\delta\mathbb{E}[X_i(t)] + \beta \sum_{j=1}^{N} a_{ij}\mathbb{E}[X_j(t)] - \beta \sum_{j=1}^{N} a_{ij}\mathbb{E}[X_i(t)X_j(t)], \qquad (4.7)$$

for $i = 1,\ldots,N$. More precisely, these equations are a consequence of Kolmogorov's forward equation.

The occurrence of the mixed terms $\mathbb{E}[X_i(t)X_j(t)]$ for $i \neq j$ signifies that the dynamics of the first order moments depend on higher order moments. The system of ordinary differential equations (4.7) is not closed. An exact solution requires in addition the dynamics of the second order moments, third order moments, etc. Instead of increasing the number of equations, the aim of the first order mean-field approximation is to keep the number of equations fixed, but to pay the price of obtaining an approximate in lieu of an exact solution.

We choose a suitable function $F : [0,1] \to [0,1]$ and split the mixed terms as

$$\mathbb{E}[X_i(t)X_j(t)] \approx F(\mathbb{E}[X_i(t)]) \cdot F(\mathbb{E}[X_j(t)]).$$

This leads to the following approximation:

$$\frac{d\mathbb{E}[X_i(t)]}{dt} \approx -\delta\mathbb{E}[X_i(t)] + \beta \sum_{j=1}^{N} a_{ij}\mathbb{E}[X_j(t)] - \beta \sum_{j=1}^{N} a_{ij} F(\mathbb{E}[X_i(t)]) \cdot F(\mathbb{E}[X_j(t)]). \tag{4.8}$$

We denote by $z_i^{(1)}(t)$ the corresponding approximation of $\mathbb{E}[X_i(t)]$ and arrive at the following system of ODEs

$$\frac{dz_i^{(1)}(t)}{dt} = -\delta z_i^{(1)}(t) + \beta \sum_{j=1}^{N} a_{ij} z_i^{(1)}(t) - \beta \sum_{j=1}^{N} a_{ij} F(z_i^{(1)}(t)) \cdot F(z_j^{(1)}(t)) \quad (i = 1, \ldots, N). \tag{4.9}$$

This is the *first order mean-field approximation* corresponding to the *mean-field function* F.

Next, we consider two examples of mean-field functions and the resulting first order approximations $z_i^{(1)}(t)$ in more detail.

1. If we choose a mean-field function $F_1(x) = x$, we obtain the first order *independent approximation*, also known as the "N-intertwined mean-field approximation (NIMFA)". This approximation is discussed in detail by Van Mieghem et al. (2009). The approximation factorizes the second order moments as if components were independent:

   $$\mathbb{E}[X_i(t)X_j(t)] \approx F_1(\mathbb{E}[X_i(t)]) \cdot F_1(\mathbb{E}[X_j(t)]) = \mathbb{E}[X_i(t)]\mathbb{E}[X_j(t)].$$

   Since it holds that $\mathbb{E}[X_i(t)X_j(t)] = \mathbb{E}[X_i(t)]\mathbb{E}[X_j(t)] + \mathrm{Cov}(X_i(t), X_j(t))$ with covariance $\mathrm{Cov}(X_i(t), X_j(t)) \geq 0$, as shown in Cator and Van Mieghem (2014), equation (4.8) leads to an upper bound:

   $$\frac{d\mathbb{E}[X_i(t)]}{dt} \leq -\delta\mathbb{E}[X_i(t)] + \beta \sum_{j=1}^{N} a_{ij}\mathbb{E}[X_j(t)] - \beta \sum_{j=1}^{N} a_{ij}\mathbb{E}[X_i(t)]\mathbb{E}[X_j(t)].$$

   The upper bound mean-field approximation $v_i(t) := z_i^{(1)}(t)$ is characterized by the ordinary differential equations

   $$\frac{dv_i(t)}{dt} = -\delta v_i(t) + \beta \sum_{j=1}^{N} a_{ij} v_j(t) - \beta \sum_{j=1}^{N} a_{ij} v_i(t) v_j(t), \quad (i = 1, \ldots, N). \tag{4.10}$$

Setting $V := (v_1, v_2, \ldots, v_N)^\top$, we may rewrite the system in matrix notation:

$$\frac{d}{dt}V = (\beta A - \delta\mathbb{I})V - \beta \operatorname{Diag}(V)AV, \tag{4.11}$$

where $\operatorname{Diag}(V)$ denotes the diagonal matrix with entries $v_1, v_2, \ldots, v_N$ and $\mathbb{I} \in \mathbb{R}^{N\times N}$ denotes the identity matrix.

2. A mean-field function $F_2(x) := \sqrt{x}$ leads to a new type of mean-field approximation. We call this the first order *Hilbert approximation* that is motivated by the following observations. The space of square-integrable random variables $\mathcal{L}^2$, equipped with the scalar product $\langle R,S\rangle := \mathbb{E}[R \cdot S]$ for $R,S \in \mathcal{L}^2$, forms a Hilbert space. The induced norm is denoted by $\|R\| := \sqrt{\langle R,R\rangle} = \sqrt{\mathbb{E}[R^2]}$. The scalar product in Hilbert spaces defines the angle ϕ between vectors:

$$\langle R,S\rangle = \|R\| \cdot \|S\| \cdot \cos\phi.$$

The idea is now to use $\|R\| \cdot \|S\|$ as an approximation for $\langle R,S\rangle$. The term $\|R\| \cdot \|S\|$ is never smaller than $\langle R,S\rangle$. The approximation is good, if the angle of R and S is close to 0°. Applying the approximation to equations (4.7), we obtain

$$\frac{d\mathbb{E}[X_i(t)]}{dt} \geq -\delta\mathbb{E}[X_i(t)] + \beta\sum_{k=1}^{N} a_{ik}\mathbb{E}[X_k(t)] - \beta\sum_{k=1}^{N} a_{ik}\sqrt{\mathbb{E}[X_i(t)]}\sqrt{\mathbb{E}[X_k(t)]}, \tag{4.12}$$

$i = 1,2,\ldots,N$. Setting $w_i(t) := z_i^{(1)}(t)$, this leads to the following mean-field approximation:

$$\frac{dw_i(t)}{dt} = -\delta w_i(t) + \beta\sum_{k=1}^{N} a_{ik}w_k(t) - \beta\sum_{k=1}^{N} a_{ik}\sqrt{w_i(t)}\sqrt{w_k(t)},$$

$i = 1,2,\ldots,N$. Setting $W = (w_1,\ldots,w_N)^\top$ and $\sqrt{W} = (\sqrt{w_1},\ldots,\sqrt{w_N})^\top$, we may rewrite the system in matrix notation:

$$\frac{dW}{dt} = (\beta A - \delta\mathbb{I})W - \beta\operatorname{Diag}(\sqrt{W})A\sqrt{W}. \tag{4.13}$$

Properties of ODE Systems. The following theorem summarizes key properties of the mean-field approximations. Its proof can be found in Appendix 4.5. Let $\mathbf{0} = (0,0,\ldots,0)^\top \in \mathbb{R}^N$ and $\mathbf{1} = (1,1,\ldots,1)^\top \in \mathbb{R}^N$ denote the all-zero and the all-one vector, respectively.

Theorem 4.2.7.

(i) Existence. *For any choice of the parameters δ and β, there exist global solutions of the ODE systems* (4.11) *and* (4.13) *with arbitrary non-negative initial conditions.*

(ii) Uniqueness. *The ODE system* (4.11) *possesses a unique solution in* $C([0,\infty);\mathbb{R}^N)$.

(iii) Sandwich Property. *Let* $W(t)$ *be a solution of* (4.13) *and* $V(t)$ *the solution to* (4.11). *For every initial condition* $V(0) = W(0) = X(0) = v_0 \in [0,1]^N$, *it holds that*

$$\mathbf{0} \leq W(t) \leq \mathbb{E}[X(t)] \leq V(t) \leq \mathbf{1},$$

for all $t \geq 0$, *where the inequalities are interpreted componentwise.*

(iv) Stability. *Let* $\hat{\mu}$ *be the spectral radius of* A *and set* $\tau_c^{(1)} := 1/\hat{\mu}$, *a constant that depends on the underlying network. Define* $\tau = \beta/\delta$. *If* $\tau < \tau_c^{(1)}$, *then the zero solutions* $V \equiv 0$ *and* $W \equiv 0$ *are exponentially stable solutions of* (4.11) *and* (4.13), *i.e., there exist constants* $\alpha, \epsilon, C > 0$ *such that for any solution* z *of* (4.11) *and* (4.13), *respectively, and all* $t \geq 0$

$$|z(t)| \leq Ce^{-\alpha t|z(0)|},$$

if $|z(0)| \leq \epsilon$.

We illustrate the two suggested approximation methodologies in the context of a small cyber network.

Example 4.2.8. We consider a system of $N = 7$ agents that are connected in a cyber network as described in Figure 4.1.

The network is regular, i.e., each node is connected to exactly D other nodes. We choose $D = 4$, $\beta = 0.5$, and $\delta = 2.01$. Then $\tau = \beta/\delta = 0.2488 < 1/D = \tau_c^{(1)}$, thus $V \equiv 0$ and $W \equiv 0$ are exponentially stable according to Theorem 4.2.7 (iv). We assume that initially only node 1 is infected, i.e., $V(0) = W(0) = (1,0,0,0,0,0,0)^\top$. Figure 4.2 shows the aggregate infection probabilities for all nodes (A), i.e., $\sum_{j=1}^N \mathbb{E}[X_j(t)]$, and respectively for all initially healthy nodes (B), here: $\sum_{j=2}^N \mathbb{E}[X_j(t)]$, for the original Markov process together with the corresponding approximations. As explained in Theorem 4.2.7 (iii), these provide lower and upper bounds. For both approximations, the error is quite substantial. As we will see in the following sections, this can be improved by higher order approximations.

$$A := \begin{pmatrix} 0 & 1 & 0 & 0 & 1 & 1 & 1 \\ 1 & 0 & 1 & 1 & 0 & 0 & 1 \\ 0 & 1 & 0 & 1 & 1 & 1 & 0 \\ 0 & 1 & 1 & 0 & 1 & 0 & 1 \\ 1 & 0 & 1 & 1 & 0 & 1 & 0 \\ 1 & 0 & 1 & 0 & 1 & 0 & 1 \\ 1 & 1 & 0 & 1 & 0 & 1 & 0 \end{pmatrix}$$

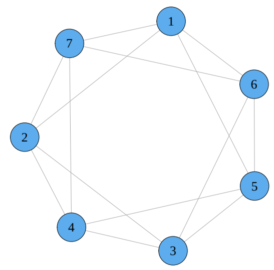

Figure 4.1: A regular network with $N = 7$ nodes and degree $D = 4$.

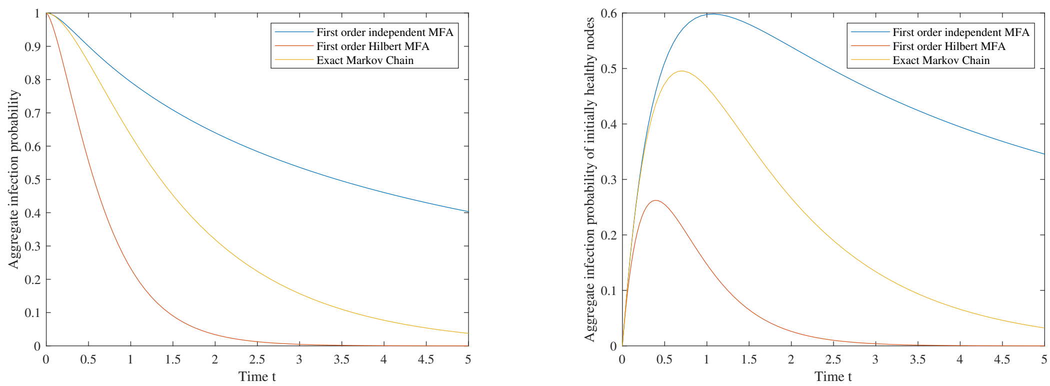

(a) **(b)**

Figure 4.2: Comparison of the aggregate infection probability of all nodes (A) and of initially healthy nodes (B) for the network described in Figure 4.1.

Accuracy Criterion. We derive a time-dependent estimate of the accuracy of the first order independent mean-field approximation. We focus on the correlation matrix as a rough measure for the difference between the exact and approximate dynamics of the $\mathbb{E}[X_i(t)]$.

The first step is to rewrite (4.7) as

$$\frac{d}{dt}\mathbb{E}[X_i(t)] = -\delta\mathbb{E}[X_i(t)] + \beta(1 - \mathbb{E}[X_i(t)]) \sum_{k=1}^{N} a_{ki}\mathbb{E}[X_k(t)] - \beta R_i(t)$$

with error term

$$R_i(t) := \sum_{k=1}^{N} a_{ki}\mathrm{Cov}(X_i(t), X_k(t)).$$

In Van Mieghem and van de Bovenkamp (2015), the authors consider R_i as a measure for the accuracy of the approximation. They investigate numerical examples and analytical criteria to assess the smallness of R_i in different situations. It is clear that in the independent case, yielding $R_i(t) \equiv 0$ for all i, the exact dynamics and the approximation are identical. This is the reason for our choice of the term *independent* approximation. Our result phrases the accuracy of the approximation as a pointwise inequality in the time variable t.

Theorem 4.2.9. *Let $y_i(t) := \mathbb{E}[X_i(t)] - v_i(t)$ and denote by $\hat{\mu}$ the largest eigenvalue of the adjacency matrix A. Then for any $t \geq 0$ we have*

$$||y(t)||^2 \leq e^{(-2\delta+4\beta\hat{\mu}+\beta)t}\beta \int_0^t ||R(s)||^2 ds,$$

where $y(t) = (y_1(t),\ldots,y_N(t))$ and $R(t) = (R_1(t),\ldots,R_N(t))$.

The proof of Theorem 4.2.9 is given in Appendix 4.5. To apply this result, we approximate the norm of the residual term $R(t)$ by

$$||R(t)||^2 = \sum_{i=1}^N \left(\sum_{k=1}^N a_{ki} \mathrm{Cov}(X_i(t), X_k(t)) \right)^2 \leq \frac{1}{16} \sum_{i=1}^N \left(\sum_{k=1}^N a_{ki} \right)^2 \leq \frac{N}{16} \sum_{i=1}^N \sum_{k=1}^N a_{ik} = \frac{N\ell}{8},$$

using Cauchy's inequality and denoting by ℓ the total number of links within the network. Hence, we find the following upper bound for the mean-field approximation error, expressed solely through known characteristics of the given network:

$$\|y(t)\|^2 \leq \frac{\beta N \ell}{8} \cdot te^{(-2\delta+4\beta\hat{\mu}+\beta)t}. \tag{4.14}$$

In the case that $-2\delta + 4\beta\hat{\mu} + \beta < 0$, i.e., for small $\tau = \beta/\delta < \frac{1}{2\hat{\mu}+1/2}$, the approximation error becomes small quite quickly. This corresponds to a high curing rate δ in comparison to the infection rate β. Observe that the stated exponential decay is a useful result for t sufficiently large. Since $N\ell$ can be very large, equation (4.14) does not provide substantial information regarding the approximation error for small t.

Example 4.2.10. We consider the network in Figure 4.1 with fixed infection rate $\beta = 0.5$, but different curing rate δ. The initial state is $V(0) = (1,0,0,0,0,0,0)^\top$, i.e., only node 1 is infected at time zero. Figure 4.3 (a) depicts the exact approximation error $\|y(t)\|^2$. The upper bound from equation (4.14) is shown in Figure 4.3 (b). Although quantitatively strongly different, both figures (a) and (b) exhibit the exponential decay that we proved for the upper bound.

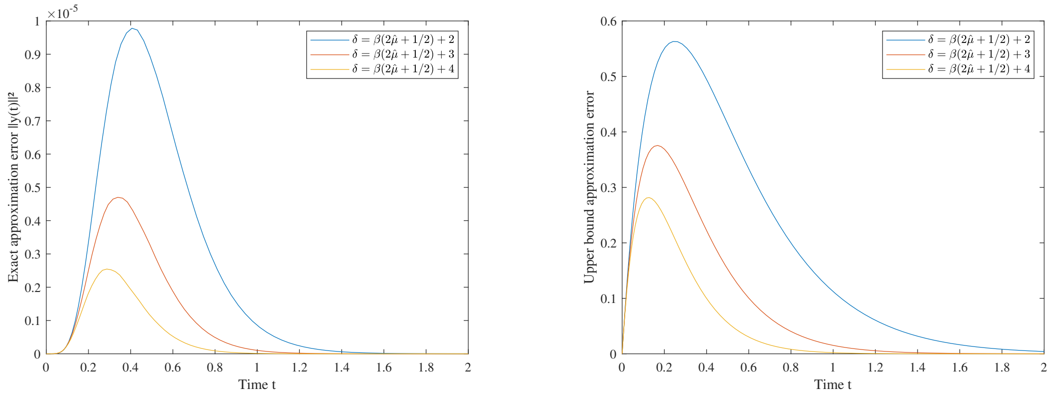

(a) Exact approximation error $\|y(t)\|^2$ **(b)** Upper error bound from (4.14)

Figure 4.3: Exact approximation error and upper bound for different values of the curing rate δ and fixed $\beta = 1/2$ in the regular network A (given in Figure 4.1) with initial state $V(0) = (1,0,0,0,0,0,0)^\top$.

The observation that the approximation error decreases for an increasing curing rate[2] δ is in line with the heuristic arguments of Van Mieghem et al. (2009) who describe a good performance of the first order mean-field approximation for small τ. For intermediate values of τ, however, these authors expect significantly larger first order approximation errors. In addition, if $-2\delta + 4\beta\hat{\mu} + \beta \geq 0$, the upper bounds from Theorem 4.3 and equation (4.14) are not useful anymore, since they grow exponentially in time t. These facts motivate the higher order approximations that we consider later.

Remark 4.2.11. From the point of view of an insurance company, cyber risk is manageable for sufficiently small $\tau = \frac{\beta}{\delta}$. The exact condition $-2\delta + 4\beta\hat{\mu} + \beta < 0 \Leftrightarrow \tau < \frac{1}{2\hat{\mu}+1/2}$ depends on $\hat{\mu}$, i.e., on a characteristic of the underlying network. In this situation, the infection quickly dies out, and the first order mean-field approximation provides an upper bound with known bound for the approximation error. It might thus be used for pricing insurance contracts. For small t, however, the error bound is large and in many cases not very precise, although the approximation might be quite reasonable.

4.2.2.2 n-th Order

In this section, we construct a general n-th order mean-field approximation that has the following two benefits:

- The approximation error of the first order mean-field approximations may be quite

[2] Similar results of decreasing error are found for decreasing infection rate β and spectral radius $\hat{\mu}$.

large for certain parameter choices. The n-th order approximation provides improved approximations for all moments of order $k \leq n$. In particular, it yields improved estimates of single infection probabilities $z_i^{(n)}$ for $i = 1, \ldots, N$.

- On the basis of the n-th order mean-field approximation, expected insurance losses of non-linear claims can be computed as described in Section 4.2.1.

Construction. Fix the order $n \leq N$. By $I \subseteq \{1,2,\ldots,N\}$ we denote a set of indices. We define the product $X_I := \Pi_{i\in I} X_i$. Since the components of X are commutative and idempotent, we may neglect the order of the indices or powers of its components.

The dynamics of all moments are described by coupled ordinary differential equations due to Kolmogorov's forward equations. This system of equations is replaced by a smaller system of equations that involves only approximations of moments up to order n:

(i) Construct an *approximation* for the dynamics of the n-th order moments $\mathbb{E}[X_{i_1} \cdots X_{i_n}]$ in terms of moments up to order n.

(ii) Use the exact relations of the dynamics of $\mathbb{E}[X_{i_1} \cdots X_{i_k}]$ for $1 \leq k \leq n-1$ and the approximation of the n-th order moments to estimate the lower order moments.

The details are as follows:

Step (i): Approximative dynamics of $\mathbb{E}[X_I]$ *for* $|I| = n$. Kolmogorov's forward equation implies that

$$
\begin{aligned}
&\frac{d}{dt}\mathbb{E}[X_{i_1} X_{i_2} \cdots X_{i_n}] \\
=&\mathbb{E}\left[\sum_{l=1}^{n} X_{i_1} \cdots X_{i_{l-1}} \left(-\delta X_{i_l} + \beta(1 - X_{i_l}) \sum_{j_l=1}^{N} a_{i_l j_l} X_{j_l}\right) X_{i_{l+1}} \cdots X_{i_n}\right] \\
=& - n\delta\mathbb{E}\left[X_{i_1} \cdots X_{i_n}\right] + \beta\mathbb{E}\left[\sum_{l=1}^{n}\sum_{j_l=1}^{N} a_{i_l j_l} X_{i_1} \cdots X_{i_{l-1}} X_{j_l} X_{i_{l+1}} \cdots X_{i_n}\right] \\
&- \beta\mathbb{E}\left[\sum_{l=1}^{n}\sum_{j_l=1}^{N} a_{i_l j_l} X_{i_1} \cdots X_{i_n} \cdot X_{j_l}\right].
\end{aligned}
$$

Rewriting this we have the exact expression

$$
\frac{d}{dt}\mathbb{E}[X_I] = -n\delta\mathbb{E}[X_I] + \beta\sum_{i\in I}\sum_{j=1}^{N} a_{ij}\mathbb{E}[X_{I\setminus\{i\}\cup\{j\}}] - \beta\sum_{i\in I}\sum_{j=1}^{N} a_{ij}\mathbb{E}[X_{I\cup\{j\}}]
$$

The expression $\mathbb{E}[X_{I\setminus\{i\}\cup\{j\}}]$ contains at most n factors of X: If $j \notin I \setminus \{i\}$, it contains n factors, and if $j \in I \setminus \{i\}$, it contains $n-1$ factors. Thus, the first sum can be expressed in terms of moments of order less than or equal to n.

Next, consider the term $\mathbb{E}[X_{I\cup\{j\}}]$. If $j \in I$, then $\mathbb{E}[X_{I\cup\{j\}}] = \mathbb{E}[X_I]$. However, if $j \notin I$, the expression contains $n+1$ different indices. This means that the dynamics of the moments up to order n is not described by a closed system of ordinary differential equations. To deal with this difficulty, we extend the idea of the first order mean-field approximation and choose the following two objects:

1. a *mean-field function* $F : [0,1] \to [0,1]$ and

2. a *partition scheme* (I_1, I_2) such that for $j \neq I$ we have $I\cup\{j\} = I_1(I,j)\cup I_2(I,j)$ with $I_1(I,j), I_2(I,j) \neq \emptyset$. Since I is fixed for each equation, we suppress the dependence on I in our notation.

Specific choices of these two key ingredients are addressed in the next section. When they are chosen properly, we approximate the rate of change for the n-th order moments by

$$\begin{aligned}\frac{d}{dt}\mathbb{E}[X_I] \approx& - n\delta\mathbb{E}[X_I] + \beta\sum_{i\in I}\sum_{j=1}^{N} a_{ij}\mathbb{E}\left[X_{I\setminus\{i\}\cup\{j\}}\right] - \beta\sum_{i\in I}\sum_{j=1,j\in I}^{N} a_{ij}\mathbb{E}[X_I] \\ & - \beta\sum_{i\in I}\sum_{j=1,j\notin I}^{N} a_{ij}\cdot F\left(\mathbb{E}[X_{I_1(j)}]\right)\cdot F\left(\mathbb{E}[X_{I_2(j)}]\right). \end{aligned} \tag{4.15}$$

This translates to the ODE

$$\begin{aligned}\dot{z}_I^{(n)} =& - n\delta z_I^{(n)} + \beta\sum_{i\in I}\sum_{j=1}^{N} a_{ij} z^{(n)}_{I\setminus\{i\}\cup\{j\}} - z_I^{(n)}\beta\sum_{i\in I}\sum_{j=1,j\in I}^{N} a_{ij} \\ & - \beta\sum_{i\in I}\sum_{j=1,j\notin I}^{N} a_{ij} F\left(z^{(n)}_{I_1(j)}\right)\cdot F\left(z^{(n)}_{I_2(j)}\right)\end{aligned}$$

describing the approximative dynamics of the n-th order moments.

Step (ii): Exact dynamics of $\mathbb{E}[X_I]$ *for* $|I| = k < n$. For moments of order $k < n$, we write according to Kolmogorov's forward equation

$$\frac{d}{dt}\mathbb{E}[X_I] = -k\delta\mathbb{E}[X_I] + \beta\sum_{i\in I}\sum_{j=1}^{N} a_{ij}\mathbb{E}\left[X_{I\setminus\{i\}\cup\{j\}}\right] - \beta\sum_{i\in I}\sum_{j=1}^{N} a_{ij}\mathbb{E}\left[X_{I\cup\{j\}}\right],$$

and observe that all moments in this exact equation are of order less than or equal to n.

Plugging in the approximations of order n, we obtain the ODE system of the n-th order mean-field approximation:

$$
\left.
\begin{aligned}
|I| = n: \quad \dot{z}_I^{(n)} &= -\left(n\delta + \beta \sum_{i \in I} \sum_{j=1, j \in I}^{N} a_{ij} \right) z_I^{(n)} + \beta \sum_{i \in I} \sum_{j=1}^{N} a_{ij} z_{I \setminus \{i\} \cup \{j\}}^{(n)} \\
&\quad - \beta \sum_{i \in I} \sum_{j=1, j \notin I}^{N} a_{ij} F\left(z_{I_1(j)}^{(n)} \right) \cdot F\left(z_{I_2(j)}^{(n)} \right) \\
|I| = k < n: \quad \dot{z}_I^{(n)} &= -k\delta z_I^{(n)} + \beta \sum_{i \in I} \sum_{j=1}^{N} a_{ij} z_{I \setminus \{i\} \cup \{j\}}^{(n)} - \beta \sum_{i \in I} \sum_{j=1}^{N} a_{ij} z_{I \cup \{j\}}^{(n)},
\end{aligned}
\right\} . \tag{4.16}
$$

The initial condition is the initial configuration of the Markovian system.

Definition 4.2.12. For a mean-field function F and a partition scheme, we define the *n-th order mean-field approximation* as a solution to the ODE system (4.16), i.e.,

$$
\left(z_I^{(n)} \right)_{I \subseteq \{1,2,\ldots,N\},\, |I| \leq n}
$$

Remark 4.2.13. The structure of the ODEs in the n-th order case is analogous to the first order case. The matrix form of the ODE system (4.16) as well as the generalization of the existence and uniqueness results of Theorem 4.2.7 to the n-th order case is discussed in Appendix 4.7.

Approximation Types and Splitting. In this section, we introduce two specific types of higher order mean-field approximations and address the problem of optimally splitting the set $I \cup \{j\}$ for $|I| = n$ and $j \notin I$ consisting of $n+1$ different indices into the two non-empty, disjoint subsets $I_1(j)$ and $I_2(j)$. In contrast to the first order case, this requires a specific choice that may influence the quality of the resulting mean-field approximation. As before, we consider the two mean-field functions $F_1(x) = x$ and $F_2(x) = \sqrt{x}$.

1. The choice of the mean-field function $F_1(x) = x$ leads to the n-th order *independent approximation*. The approximation works as follows: For $j \notin I$

   $$
   \mathbb{E}[X_{I \cup \{j\}}] = \mathbb{E}[X_{I_1(j)}] \cdot \mathbb{E}[X_{I_2(j)}] + \mathrm{Cov}(X_{I_1(j)}, X_{I_2(j)}) \approx \mathbb{E}[X_{I_1(j)}] \cdot \mathbb{E}[X_{I_2(j)}].
   $$

   No error corresponds to a split of $X_{I \cup \{j\}}$ into $X_{I_1(j)}$ and $X_{I_2(j)}$ such that the covariance $\mathrm{Cov}(X_{I_1(j)}, X_{I_2(j)})$ is zero. The factors should thus be as *uncorrelated* as possible.

2. Choosing $F_2(x) = \sqrt{x}$ leads to the n-th order *Hilbert approximation*.

In this case, we set

$$\mathbb{E}[X_{I\cup\{j\}}] = \sqrt{\mathbb{E}[X_{I_1(j)}]} \cdot \sqrt{\mathbb{E}[X_{I_2(j)}]} \cdot \cos\phi \approx \sqrt{\mathbb{E}[X_{I_1(j)}]} \cdot \sqrt{\mathbb{E}[X_{I_2(j)}]},$$

for $j \notin I$. The angle ϕ is defined via the scalar product $\langle R, S\rangle := \mathbb{E}[RS]$ for $R, S \in \mathcal{L}^2$ in the usual Hilbert space. The split is good whenever the angle ϕ between $X_{I_1(j)}$ and $X_{I_2(j)}$ is close to $0°$. This corresponds to highly dependent factors.

A *naive single split* partitions the set $I \cup \{j\}$ into the subsets $I_1(j) = I$ and $I_2(j) = \{j\}$. Note that the sets are enumerated and, thus, the naive single split is uniquely determined. This approach may not always be ideal, if small or strong dependence of the factors is desired in order to keep the error of the approximation small. Hence, we sketch an alternative approach that is based on a measurement of the nodes' distances in the graph.

The graph structure is described by the adjacency matrix $A \in \mathbb{R}^{N\times N}$, i.e., there exists a link between $i, j \in \{1, 2, \ldots, N\}$, if $a_{ij} = a_{ji} = 1$. If two agents are not directly connected, they might be connected indirectly. We define π_{ij} as the length of the shortest path in the graph that connects two agents $i \neq j$, i.e.,

$$\pi_{ij} := \min\{l \in \mathbb{N} : a_{ik_1} = a_{k_1k_2} = a_{k_2k_3} = \cdots = a_{k_{l-1}j} = 1\}.$$

We set $\Pi = (\pi_{ij})_{i,j=1,2,\ldots,N}$ with $\pi_{ii} = 0$ for all $i = 1, 2, \ldots, N$. The splitting algorithm is described by the following pseudocode.

Algorithm 4.2.14.

INPUT An index set I with $|I| = n$ and $j \notin I$ is given.

OUTPUT The output is a partition $I_1(j), I_2(j)$ of $I \cup \{j\}$ constructed as follows:

Step 1 Consider a set of partitions $J_1(j), J_2(j)$ of $I \cup \{j\}$.

Step 2 Choose some $\alpha \in (0, 1)$ and calculate for each partition the following distance measure:

$$m_\alpha(J_1(j), J_2(j)) := \sum_{i\in J_1(j)} \sum_{i'\in J_2(j)} \alpha^{\pi_{ii'}}. \tag{4.17}$$

Step 3 We consider four alternative choices.

a) Minimal single split:
We choose the partition $I_1(j), I_2(j)$ with $|I_2(j)| = 1$ that minimizes m_α.

b) Maximal single split:
We choose the partition $I_1(j), I_2(j)$ with $|I_2(j)| = 1$ that maximizes m_α.

c) **Minimal equal split:**
We choose the partition $I_1(j), I_2(j)$ with $|I_1(j)| = |I_2(j)|$, if $n+1$ is even, or $|I_1(j)| = |I_2(j)| + 1$, if $n + 1$ is odd, that minimizes m_α.

d) **Maximal equal split:**
We choose the partition $I_1(j), I_2(j)$ with $|I_1(j)| = |I_2(j)|$, if $n+1$ is even, or $|I_1(j)| = |I_2(j)| + 1$, if $n + 1$ is odd, that maximizes m_α.

Observe that large values of our distance measure m_α correspond to small graph distances. In line with our heuristic arguments above, we thus apply choices a) and c) to the independent approximation and choices b) and d) to the Hilbert approximation.

Example 4.2.15. To illustrate higher order mean-field approximations, we consider two different networks: the network with adjacency matrix A defined in Figure 4.1 with fixed infection rate $\beta = 1/2$ and curing rate $\delta = 2.01$, and the network with adjacency matrix B defined in Figure 4.4 with $\beta = \delta = 1/2$. For both networks, nodes 1, 3, and 7 are

$$B := \begin{pmatrix} 0 & 1 & 0 & 0 & 1 & 0 & 0 \\ 1 & 0 & 1 & 1 & 0 & 0 & 0 \\ 0 & 1 & 0 & 1 & 0 & 0 & 0 \\ 0 & 1 & 1 & 0 & 0 & 0 & 0 \\ 1 & 0 & 0 & 0 & 0 & 1 & 1 \\ 0 & 0 & 0 & 0 & 1 & 0 & 1 \\ 0 & 0 & 0 & 0 & 1 & 1 & 0 \end{pmatrix}$$

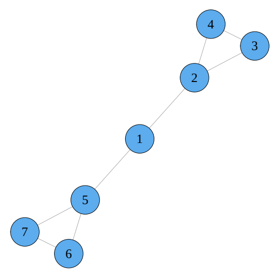

Figure 4.4: A network with $N = 7$ nodes and spectral radius $\hat{\mu} \approx 2.3429$.

initially infected. Figure 4.5 displays the evolution of the aggregate infection probability of initially healthy nodes, i.e., $\sum_{j\in\{2,4,5,6\}} z_j^{(n)}$, for the original Markov chain together with mean-field approximations of order $n = 2, 3, 4$ in both networks under the different splitting choices. We observe that the higher the order of the mean-field approximation, the better is the approximation. In examples (a), (b), and (c), a fourth order mean-field approximation already provides a reasonably good fit to the exact infection probabilities. However, increasing the order of the approximation also substantially increases its computational cost. In comparison to the naive single split, the optimized single split of Algorithm 4.2.14 leads to moderate improvements in all four cases. A split into subsets

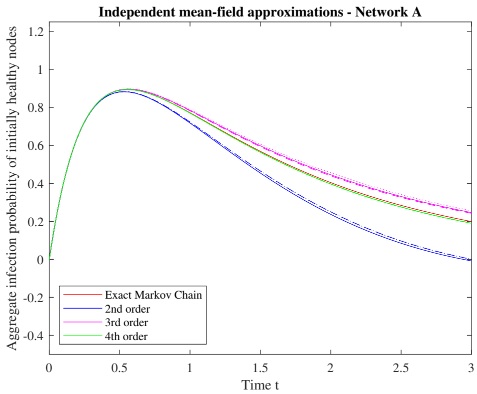

(a) Alg. 4.2.14 a) (dashed), c) (dotted)

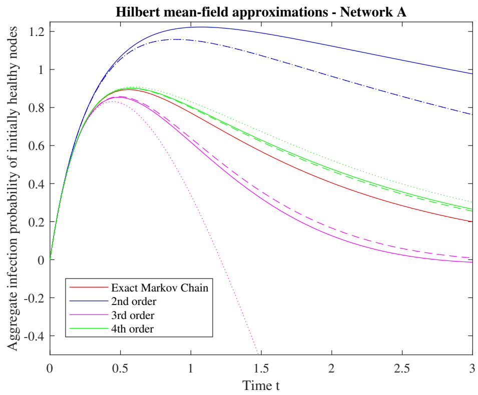

(b) Alg. 4.2.14 b) (dashed), d) (dotted)

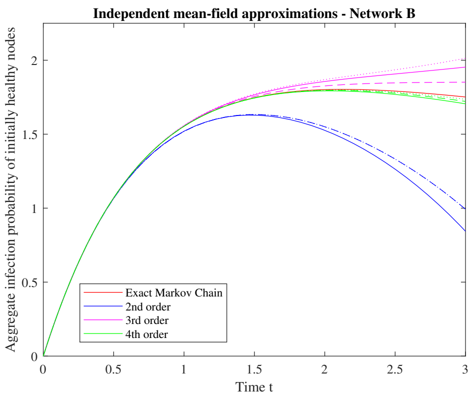

(c) Alg. 4.2.14 a) (dashed), c) (dotted)

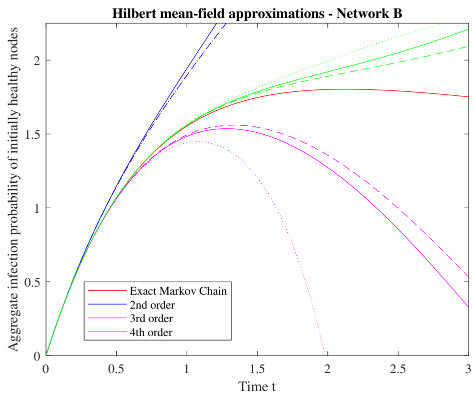

(d) Alg. 4.2.14 b) (dashed), d) (dotted)

Figure 4.5: Aggregate infection probability of initially healthy nodes. Solid lines represent naive single split approximations; dashed lines correspond to the results of Algorithm 4.2.14 ($\alpha = 0.5$) under a single split; dotted lines represent the results of Algorithm 4.2.14 ($\alpha = 0.5$) under an equal split.

of equal size, however, impairs the approximation quality[3] in the cases (a), (b), and (d). In contrast to that, in part (c), the fourth order equal split performs slightly better than the optimized single split. A possible reason for this is the special distance structure for subsets of size three in the network B. This indicates that the structure of the network topology is key to finding a splitting algorithm. Future research should investigate this issue further, analyze how Algorithm 4.2.14 might be improved, e.g., by choosing a better distance measure instead of m_α, and how computational cost and precision can be optimally balanced.

[3]Obviously, the optimized single and equal split coincide for the second order approximations, since sets of cardinality three are split in this case.

4.3 Case Studies

4.3.1 Model Setting

In this section, we compute the expected insurance losses for different insurance contracts in numerical case studies. We consider three network topologies, illustrated in Figure 4.6. All networks consist of $N = 50$ agents or nodes which are all connected to $D = 7$ other

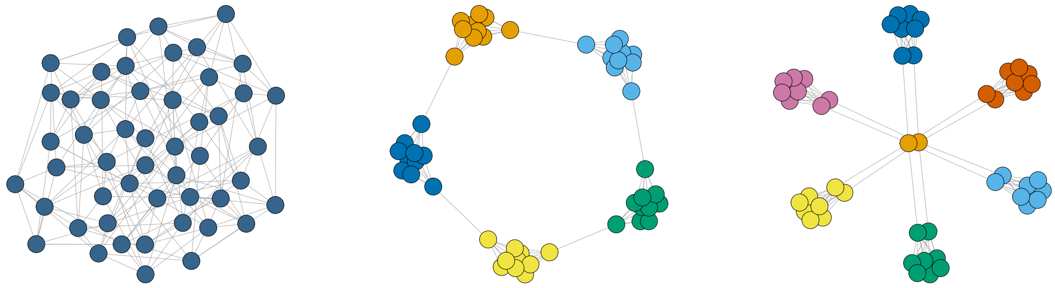

(a) Homogeneous **(b) Clustered** **(c) Star-shaped**

Figure 4.6: Stylized regular network scenarios. Quantities that are kept constant are the number of nodes $N = 50$ and the degree of each node $D = 7$. In particular, this yields a constant total number of edges $ND/2 = 175$ and a constant spectral radius $\hat{\mu} = D = 7$.

nodes. This means that the degree of each node is 7. The number of edges in each of the networks equals $ND/2 = 175$, and the spectral radius of the three corresponding adjacency matrices is $\hat{\mu} = D = 7$.

(a) **Homogeneous network:** The first network that we consider consists of agents of the same type that are homogeneously connected to each other. The corresponding adjacency matrix of this and the other two considered networks can be found in Appendix 4.8. In the homogeneous cyber networks, there is no hierarchy of nodes in terms of data flow and related cyber threats.

(b) **Clustered network:** The key feature of the clustered network is that agents form groups that are closely connected. In contrast, agents within a cluster are less connected to agents from other clusters. This structure might be a more realistic model of cyber networks than a homogeneous network: Consider, e.g., different firms or divisions that are internally densely connected, but less densely connected with other firms or divisions. Qualitatively, the model captures different levels of security for internal and external connections.

(c) **Star-shaped network:** Unlike the clustered network, the star-shaped cyber network possesses a clear hierarchy between central nodes that provide a hub for the data flow, and a number of periphery clusters that are internally homogeneously connected, but apart from the connections via the hub isolated from agents in other clusters.

The cyber networks are the channel for the spread of the cyber infection that makes agents vulnerable to cyber attacks. Cyber attacks affect all vulnerable agents at times that are modeled by a point process. The incurred losses are random. We will provide the parameters of the numerical case studies below.

In this setting, we compute the expected losses for three types of contracts: proportional insurance, excess of loss per risk insurance (XL), and catastrophe excess of loss insurance (Cat-XL). The functions that map physical losses to insured losses were described in equation (4.3) and Example 4.2.2. Exact expected contract losses can be computed according to (4.2). We will apply the mean-field approximation to estimate this quantity.

In our numerical case studies, we use the following parameters. The parameters of the infection dynamics (4.1) are $\beta = 0.5$ and $\delta = \beta \cdot \hat{\mu} + 0.01 = 3.51$. Initially, 10 nodes, i.e., 20% of all nodes, are infected. The location of the initially infected nodes is shown in Figure 4.7. These were sampled from an initial infection that is uniformly distributed across the network. Cyber attacks that cause losses at infected, i.e., vulnerable nodes

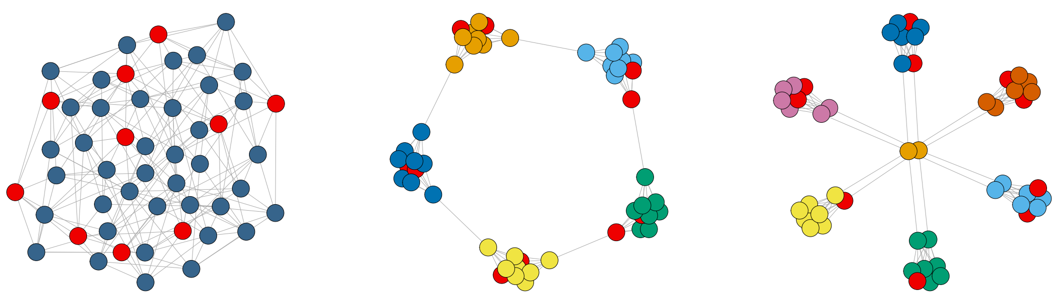

(a) Homogeneous **(b) Clustered** **(c) Star**

Figure 4.7: Infection scenario: The red nodes (3,5,13,15,23,25,33,35,43,45) are initially infected.

occur at the jumps of a homogeneous Poisson process with rate $\lambda = 3$. A cyber event causes a loss at each vulnerable node that is exponentially distributed with mean $\mu = 2$, i.e., with parameter $1/2$. For the insurance contracts, we choose a policy period $T = 3$.

For the numerical simulation we exploit the mean-field approximation to analyze the spread process. In order to generate the losses due to cyber attacks, we use a simple Monte Carlo approach. We simulate 100.000 sample paths of the homogeneous Poisson process and corresponding random losses in the time interval $[0, T]$. For each simulation we compute the integrand of equation (4.5). Averaging over these results yields our Monte Carlo estimator of the expected aggregate losses of the reinsurance company; its standard error is stated in brackets.

4.3.2 Model Results

We comment on the results of the simulation.

4.3.2.1 Infection Probabilities and Mean-Field Approximations

We first analyze the spread process of the cyber infection for the three different network structures. At this stage, we do not consider any cyber losses. We consider the *independent approximation with naive single split*. The aggregate infection probability of initially healthy nodes is a measure of the strength of the infection, i.e.,

$$AP^h_{(n)}(t) := \sum_{i \in \mathcal{H}} z_i^{(n)}(t),$$

where $\mathcal{H}$ denotes the set of initially healthy nodes and n is the order of the mean-field approximation.

Figure 4.8 displays the approximation results for $n = 1, 2, 3, 4$: First, for all networks, the fourth order mean-field approximation and the third order approximation are reasonably close to each other. This indicates that a mean-field approximation of order four provides a relatively good proxy for the exact probability of infection. Second, we find that the infection probability in the homogeneous network tends to be the highest (for $t > 0.5$) while the star exhibits the lowest infection probability. This result will be of key importance for the expected losses of a reinsurance company.

4.3.2.2 Expected Aggregate Losses of the Insurance Company

We now study cyber losses.

Proportional Reinsurance. For simplicity, we consider full insurance; other percentages lead to similar results. The resulting expected aggregate losses (standard errors in paren-

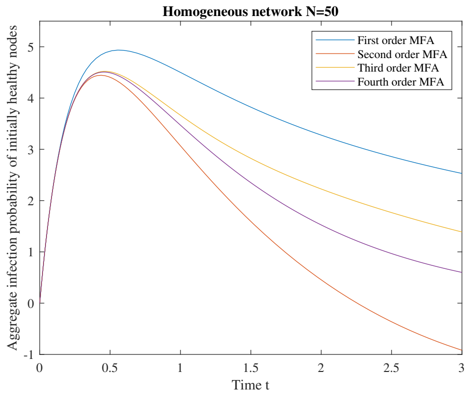

(a) $AP^h_{(n)}(t)$

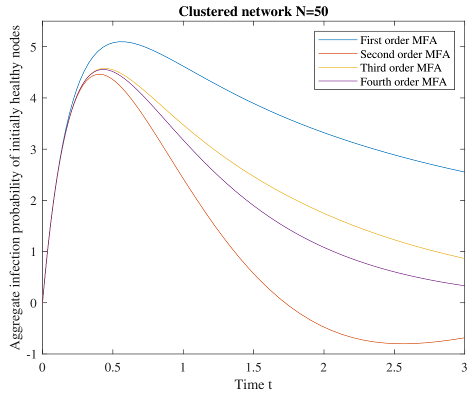

(b) $AP^h_{(n)}(t)$

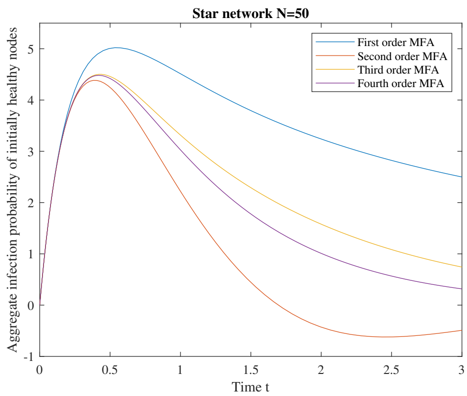

(c) $AP^h_{(n)}(t)$

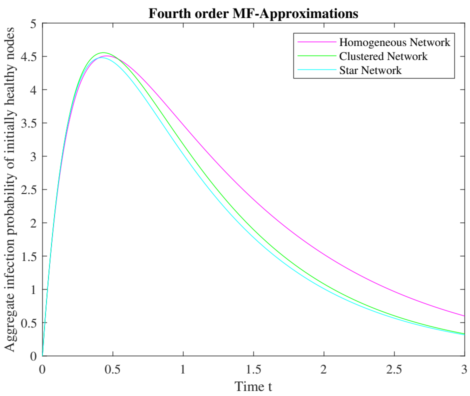

(d) $AP^h_{(4)}(t)$

Figure 4.8: Mean-field approximations of order $n = 1, 2, 3, 4$ for the aggregate infection probability of initially healthy nodes in the homogeneous (a), clustered (b), and star network (c). Part (d) compares the fourth order mean-field approximations for the different network structures.

theses) are shown in Table 4.1. These indicate that the homogeneous network constitutes the highest risk, while the star network exhibits the lowest average losses.

Table 4.1: Proportional insurance

Losses: Total coverage	Homogeneous	Clustered	Star
First order MFA	96.4671 (0.1039)	97.6170 (0.1105)	96.5425 (0.1095)
Second order MFA	51.4911 (0.0836)	39.7776 (0.0797)	39.4127 (0.0782)
Third order MFA	77.8349 (0.0943)	70.6588 (0.0901)	68.0767 (0.0883)
Fourth order MFA	68.0676 (0.0890)	61.3693 (0.0855)	59.9005 (0.0843)

XL. In this case, we assume that the limit per loss is equal to 2. We consider only the lowest tier with priority 0. Using the notation introduced in Example 4.2.2, the random insurance losses are $\sum_{i=1}^{N} \hat{L}_i(t)X_i(t)$ with $\hat{L}_i(t) = L_i(t)^+ - (L_i(t) - 2)^+ = \min\{L_i(t), 2\}$. Apart from the modified losses $\hat{L}_i$ instead of L_i, we are again in the situation of a proportional contract. As expected, the numerical results in Table 4.2 show that the homogeneous network produces the highest expected losses, while the losses are lowest in the star network.

Table 4.2: Excess of loss per risk (XL)

Losses: XL	Homogeneous	Clustered	Star
First order MFA	60.9795 (0.0684)	61.7036 (0.0692)	61.0247 (0.0686)
Second order MFA	32.5475 (0.0522)	25.1401 (0.0497)	24.9105 (0.0488)
Third order MFA	49.2010 (0.0589)	44.6618 (0.0563)	43.0300 (0.0552)
Fourth order MFA	43.0265 (0.0556)	38.7894 (0.0534)	37.8615 (0.0526)

Cat-XL. Finally, we consider an excess of loss per event contract. We consider coverage of the lowest tier, i.e., a priority 0, and choose a cover of 60. Of course, the numerical results in Table 4.3 exhibit again the same ordering of the networks in terms of risk. But, more importantly, the numerical analysis shows very clearly that the first order mean-field approximation is not able to capture this type of contract. Due to its non-linearity, this is not surprising, but the extreme size of the error could not be expected *a priori*. This demonstrates that higher order mean-field approximations are necessary for the computation of the expected insurance losses and are thus also needed for pricing contracts within our model setting.

To be more specific, the contract function of the Cat-XL is given by

$$f^{\text{Cat-XL}}(L(t) \circ X(t)) = g^{\text{Cat-XL}}(\Lambda^{\Sigma}(L(t) \circ X(t))),$$

where $\Lambda^{\Sigma}(x_1, \dots, x_N) := \sum_{i=1}^{N} x_i$, and $g^{\text{Cat-XL}}(y) := (y)^+ - (y - 60)^+ = \min(y, 60)$. We follow Algorithm 4.2.4 and approximate the non-linear claim function $g^{\text{Cat-XL}}$ on a compact interval by a polynomial of chosen degree d.

- *Compact approximation interval.* We choose $\epsilon = 0.05$ and determine a constant $u \in \mathbb{R}_+$ such that
$$P(\Lambda^{\Sigma}(L) > u) \leq \epsilon. \tag{4.18}$$
We use the compact interval $[0, u]$ for the polynomial approximation. Setting $S_t := \Lambda^{\Sigma}(L(t)) = \sum_{i=1}^{N} L_i(t)$, we define $u_t := F_{S_t}^{-1}(1 - \epsilon)$. Since S_t is independent of t and Gamma-distributed with parameters $N = 50$ and $\mu = 2$, we obtain $u = u_t \approx 124.3412$.

- *Polynomial approximation.* For degrees $d \in \{1, 2, 3, 4\}$ we determine the best uniform approximation of $g^{\text{Cat-XL}}$ on $[0, u]$. Figure 4.9 depicts the resulting polynomial approximations for $d \in \{1, 2, 3, 4\}$. The error $e_d(g^{\text{Cat-XL}}) = \|g^{\text{Cat-XL}} - p_d\|_{\infty,[0,u]}$ of the approximations on the interval is $d_1(g^{\text{Cat-XL}}) = 15.5189$, $d_2(g^{\text{Cat-XL}}) = 4.0187$, $d_3(g^{\text{Cat-XL}}) = 3.8741$, and $d_4(g^{\text{Cat-XL}}) = 2.1740$.

According to Section 4.2.1, the total L_1-error is bounded from above by

$$E_d := e_d(g^{\text{Cat-XL}}) + 60 \cdot \epsilon$$

which yields $E_1 \approx 18.5189$, $E_2 \approx 7.0187$, $E_3 \approx 6.8741$, and $E_4 \approx 5.1740$. We combine the polynomial approximations of $g^{\text{Cat-XL}}$ with the fourth order independent mean-field approximation with naive single split. The fourth order approximation is more accurate for lower order moments, but the linear polynomial approximation is of such a low quality that the resulting error is very large. In particular, a first order mean-field approximation is not able to deliver appropriate results for the Cat-XL. The expected losses are given in Table 4.3. We reduced the number of Monte Carlo samples to 10.000 for $d = 1, 2, 3$ and to 1000 for $d = 4$ due to the higher computational complexity.

The fact that the first order approximation performs very badly can be seen by comparing the result to full insurance in Table 4.1. Clearly, full insurance should provide an

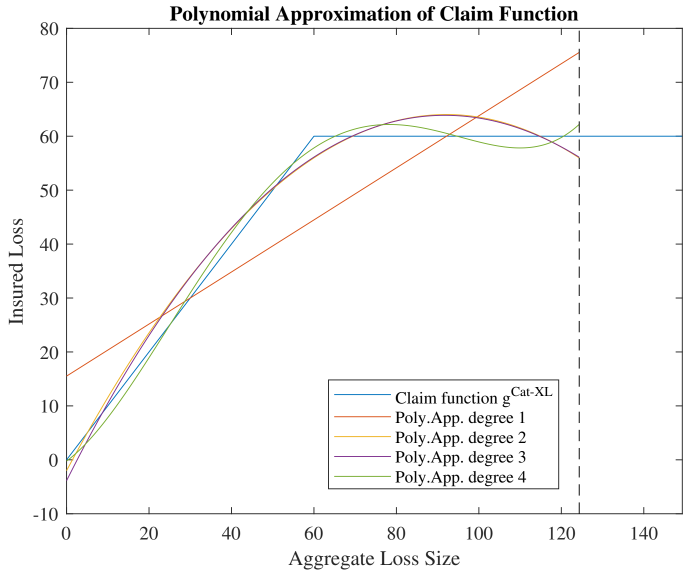

Figure 4.9: Best uniform polynomial approximations of $g^{\text{Cat-XL}}$ for different polynomial degrees in the compact interval $[0, 124.3412]$.

Table 4.3: Excess of loss per event (Cat-XL)

Losses: Cat-XL	Homogeneous	Clustered	Star
$d = 1$	169.6693 (0.5733)	166.6429 (0.5638)	165.9828 (0.5616)
$d = 2$	64.5432 (0.3047)	56.5714 (0.2942)	54.9458 (0.2906)
$d = 3$	52.4555 (0.2867)	44.0598 (0.2796)	42.3615 (0.2764)
$d = 4$	59.2664 (0.8249)	52.8354 (0.7905)	51.0151 (0.7765)

upper bound on the Cat-XL. The polynomial approximation of degree 1 of the Cat-XL is, however, far larger.

Let us finally mention that we considered insurance of all agents in the network and an initial distribution of the infection that was uniformly sampled across the network. This implied a clear ranking of the three network structures in terms of the risk. The spread of the infection will be different, if specific nodes – e.g., the core nodes of the star network – are the origin of the infection. Our model is capable of identifying critical nodes from which the infection spreads. The effect can explicitly be quantified. Another interesting analysis concerns the elimination of links and its impact on aggregate losses. Thereby connections can be identified (and potentially modified) that are critical for the spread of the infection.

Remark 4.3.1. The implementation of the suggested methodology is based on several approximations that lead to approximation errors. First, the claim function is approximated by polynomials. Second, not the exact ODE system is solved, but only a mean-field approximation. Third, further sources of approximation errors are the numerical ODE solver and the Monte Carlo simulation of the processes M and L. This needs to be taken into account when cyber insurance contracts are evaluated.

4.4 Conclusion

We developed a model of cyber losses that are triggered by two underlying risk processes. First, a cyber infection spreads in a network, modeled by an interacting Markov process. Second, infected, i.e., vulnerable agents incur losses due to cyber attacks that occur according to a point process. Due to the large dimension of the system, the computation of expected aggregate insurance losses and pricing of cyber contracts is extremely challenging. We constructed a polynomial approximation for claim functions and higher order mean-field approximations that make these problems tractable. We demonstrated that for non-linear claim functions, higher order polynomial approximations and mean-field approximations are indispensable. We also showed that, if the initial infection is uniformly distributed and all agents in the network are insured, homogeneous networks are the most risky and star networks the least. Our techniques can also be applied to identify critical initial infections and critical links in networks that augment expected losses. A key role is played by the network topology. While this chapter focuses on fixed undirected graphs, future research could investigate more realistic structures such as directed or random graphs.

4.5 Appendix: Proofs

Proof of Theorem 4.2.7

We define the two functions

$$
\begin{aligned}
G_1(x) &:= (\beta A - \delta \mathbb{I})x - \beta \mathrm{Diag}(x) A x, \text{ and} \\
G_2(x) &:= (\beta A - \delta \mathbb{I})x - \beta \mathrm{Diag}(\sqrt{x}) A \sqrt{x},
\end{aligned}
$$

for $x \in \mathbb{R}^N$.

(i) Existence. For G_1, the Picard-Lindelöf theorem (Theorem 4.6.1) used in the proof of (ii) also yields existence of a solution to (4.11).

For G_2, i.e., for the ODE describing the first order Hilbert approximation, we use Theorem 4.6.2 to prove existence of a solution. Define a non-linear map $\bar{G}_2 : \mathbb{R}^N \to \mathbb{R}^N$ by $\bar{G}_2 = (\beta A - \delta \mathbb{I})x - \beta \operatorname{Diag} \sqrt{|x|} A \sqrt{|x|}$ where the absolute value and square root are taken componentwise. Now consider the ODE system $\dot{X}(t) = \bar{G}_2(X(t))$. This enlarges the domain of definition of $\bar{G}_2$ compared to the original function in (4.13), G_2, but does not do any harm for initial conditions in $\mathbb{R}^N_{\geq 0}$.

We now estimate the norm of $\bar{G}_2$. The matrix $A = (a_{ij})_{1 \leq i,j \leq N}$ has zeros on the main diagonal so we find

$$\operatorname{Diag} \sqrt{|x|} A \sqrt{|x|} = \left(\sum_{j \neq 1} a_{1j} \sqrt{|x_1 x_j|}, \ldots, \sum_{j \neq N} a_{Nj} \sqrt{|x_N x_j|} \right)^\top .$$

With $|x_i| \leq ||x||_\infty$ and noting that $a_{ij} \in \{0, 1\}$ we have

$$\sum_{j \neq i} a_{ij} \sqrt{|x_i x_j|} \leq \sum_{j \neq i} ||x||_\infty = (N-1)||x||_\infty.$$

Moreover, $||Ax||_\infty \leq ||A|| \cdot ||x||_\infty$ for the operator norm of A with respect to the l^∞-norm. Thus overall,

$$||\bar{G}_2(x)||_\infty \leq (\beta ||A|| + \delta + N - 1)||x||_\infty.$$

Now let $x_0 \in \mathbb{R}^N$ and choose $r > 0$. The previous inequality translates to

$$||\bar{G}_2(x)||_\infty \leq C(||x_0||_\infty + r).$$

on $B_r(x_0) = \{x \in \mathbb{R}^N : ||x - x_0|| < r\}$ with $C = \beta ||A|| + \delta + N - 1$. Then consider the reciprocal fraction M/r with $M = \sup_{x \in B_r(x_0)} ||\bar{G}_2(x)||$:

$$\frac{M}{r} \leq \frac{C(||x_0||_\infty + r)}{r}.$$

Thus

$$\frac{r}{M} \geq \frac{1}{C} \frac{r}{||x_0||_\infty + r}.$$

Theorem 4.6.2 now shows that existence of a solution to (4.13) holds for any T satisfying the inequality $T < r/M$.

The global existence of a solution now follows from an iteration argument where in the j-th step we have initial condition $x_0^{(j)}$ and radius $r^{(j)}$. Start with any given initial condition $x_0^{(1)} = W(0)$ and set $r^{(1)} = ||x_0^{(1)}||_\infty$. Then by Theorem 4.6.2 there is a solution to (4.13), W, on the time interval $(0, \frac{1}{2C}]$. Repeat this process with the new initial condition $x_0^{(2)} = W(\frac{1}{2C})$ and with $r^{(2)} = ||x_0^{(2)}||_\infty$. This will again have a solution on an interval of length at least $\frac{1}{2C}$. Iterating this process and concatenating the solutions yields a solution on $[0, T]$ for arbitrary T.

(ii) Uniqueness. Let $B_R(\mathbf{0})$ be the open ball of radius R in $\mathbb{R}^N$ endowed with the Euclidean norm. We prove uniqueness using the Picard-Lindelöf theorem (Theorem 4.6.1). Thus, we need to show that there exists a Lipschitz constant $L > 0$ such that

$$||G_1(x_1) - G_1(x_2)||_2 \leq L||x_1 - x_2||_2 \tag{4.19}$$

for all $x_1, x_2 \in B_R(\mathbf{0})$. Then, Theorem 4.6.1 states that the ODE has a unique solution on some small time interval $[0, t_0]$. Since the Lipschitz constant L does not depend on time, the solution exists on the time interval $[0, \infty)$. The solution is smooth by Proposition 6.2 of Taylor (2011) so in particular belongs to $C([0, \infty), \mathbb{R}^N)$.

To prove the Lipschitz condition (4.19), first recall that the operator norm $||A||_{op}$ of a matrix A acting $\mathbb{R}^N \to \mathbb{R}^N$ endowed with the Euclidean norm is given by the spectral radius $\hat{\mu}$ of A. Thus, it follows that the operator norm of $\mathrm{Diag}(x)$ is bounded by $||x||_2$. The claim now follows from a direct calculation. Let $x_1, x_2 \in B_R(\mathbf{0})$. Then

$$\begin{aligned}
&||G_1(x_1) - G_1(x_2)||_2 \\
=&||(\beta A - \delta\mathbb{I})x_1 - \beta\,\mathrm{Diag}(x_1)Ax_1 - (\beta A - \delta\mathbb{I})x_2 + \beta\,\mathrm{Diag}(x_2)Ax_2||_2 \\
=&||(\delta\mathbb{I} - \beta A)(x_1 - x_2) + \beta\,(\mathrm{Diag}(x_1 - x_2)Ax_1 + \beta\,\mathrm{Diag}(x_2)A(x_1 - x_2))\,||_2 \\
\leq&\delta||x_1 - x_2||_2 + \beta||A||_{op}||x_1 - x_2||_2 + \beta||\,\mathrm{Diag}(x_1 - x_2)||_{op}||A||_{op}||x_1||_2 \\
&+ \beta||\,\mathrm{Diag}(x_2)||_{op}||A||_{op}||x_1 - x_2||_2 \\
=&(\delta + \beta\hat{\mu}(1 + 2R)||x_1 - x_2||_2,
\end{aligned}$$

where we used the facts that $||\,\mathrm{Diag}(x_1 - x_2)||_{op} \leq ||x_1 - x_2||_2$ and $||x_i||_2 < R$ for $i = 1, 2$.

(iii) Sandwich Property.

a) First, we prove $W(t) \geq \mathbf{0}$ for all $t \geq 0$. By definition, all components of $W(0)$ are non-negative. Now, by inspection of (4.13), we can immediately deduce that whenever a component, say w_i, at some time t' is zero, then its derivative $\dot{w}_i(t')$ is non-negative. Thus, the trajectory of $w_i(t)$ will be non-negative for some time by the fundamental theorem of calculus. By the continuity of the solution, it follows that $W(t) \geq \mathbf{0}$ for all $t \geq 0$.

b) Second, we prove the lower inequality for the exact dynamics, i.e., $W(t) \leq \mathbb{E}[X(t)]$ for all $t \geq 0$. The proof of the upper inequality $\mathbb{E}[X(t)] \leq V(t)$ is analogous. To begin with, we know that $W(0) = \mathbb{E}[X(0)] = V(0) \in [0, 1]^N$ by definition and that $dW(t)/dt \leq d\mathbb{E}[X(t)]/dt$ (see equation (4.12)). Let $H(t) := \mathbb{E}[X(t)] - W(t)$, i.e., $h_i(t) = \mathbb{E}[X_i(t)] - w_i(t)$ for all $i = 1, \ldots, N$. Then, $dH(t)/dt \geq \mathbf{0}$ for $t \geq 0$ and $H(0) = \mathbf{0}$. Now consider the interval

$[0,t] \subset \mathbb{R}$ for $t > 0$. From the mean-value theorem for vector-valued functions (cf. Matkowski (2012)), it follows that there exist constants $m_1, \ldots, m_N \in [0,t]$ such that:

$$H(t) - H(0) = (t-0) \cdot \left(\frac{dh_1}{dt}(m_1), \ldots, \frac{dh_N}{dt}(m_N)\right)^\top \geq \mathbf{0}.$$

Thus, we have that $H(t) \geq \mathbf{0}$ for all $t \geq 0$, which proves $W(t) \leq \mathbb{E}[X(t)]$ for all $t \geq 0$.

c) Third, we show that $V(t) \leq \mathbf{1}$ for all $t \geq 0$. By definition, all components of $V(0)$ are not larger than 1. Now, by inspection of (4.11), we can immediately deduce that whenever a component at some time t' is 1, e.g., $v_i(t') = 1$, the reaction term vanishes so that $\dot{v}_i(t') = -\delta < 0$. Thus, the function is pushed away from 1 towards 0. By the continuity of the solution, it follows that $V(t) \leq \mathbf{1}$ for all $t \geq 0$.

(iv) Stability. We apply Theorem 4.6.3 to the function G_1. First, $V^* \equiv \mathbf{0}$ is an obvious fix-point of G_1. Second, the Jacobi matrix of G_1 at any point $V \in \mathbb{R}^N$ is given by

$$J_{G_1}(V) = \beta A - \delta \mathbb{I} - \beta \left(\mathrm{Diag}(V)A + \mathrm{Diag}(AV)\right).$$

In particular, at the fix-point $V^* \equiv \mathbf{0}$, the Jacobi matrix reduces to

$$J_{G_1}(\mathbf{0}) = \beta A - \delta \mathbb{I} = -\delta(\mathbb{I} - \tau A),$$

with $\tau = \beta/\delta$. $J_{G_1}(\mathbf{0})$ is real and symmetric and, thus, possesses only real eigenvalues. Let $\lambda_1, \ldots, \lambda_N$ denote the eigenvalues of A. Then, the eigenvalues of $J_{G_1}(0)$ are given by $-\delta(1 - \tau\lambda_i)$ for $i = 1, \ldots, N$. Hence, all eigenvalues of $J_{G_1}(0)$ are negative if and only if $\tau < 1/\max_{1 \leq i \leq N} \lambda_i = 1/\hat{\mu} =: \tau_c^{(1)}$. Thus, in this case, it follows from Theorem 4.6.3 that the fix-point $V^* \equiv \mathbf{0}$ is exponentially stable. Finally, since $W(t) \leq V(t)$ (part (iii)), it follows that the zero solution is also exponentially stable for (4.13).

Proof of Theorem 4.2.9

The difference $y_i(t) = \mathbb{E}[X_i(t)] - v_i(t)$ satisfies the ODE

$$\begin{aligned}\frac{d}{dt} y_i(t) = &- \delta y_i(t) + \beta(1 - y_i(t)) \sum_{k=1}^N a_{ki} y_k(t) \\ &- \beta R_i(t) - \beta y_i(t) \sum_{k=1}^N a_{ki} v_k(t) - \beta v_i(t) \sum_{k=1}^N a_{ki} y_k(t)\end{aligned}$$

with initial condition $y_i(0) = 0$. We want to apply Gronwall's inequality to the l^2-norm $\frac{1}{2}||y(t)||_2^2$. As a first step we note that

$$\begin{aligned}\frac{d}{dt}\frac{1}{2}y_i(t)^2 =& y_i(t)\cdot\frac{d}{dt}y_i(t)\\ =& -\delta y_i(t)^2 + \beta y_i(t)(1-y_i(t))\sum_{k=1}^N a_{ki}y_k(t)\\ &-\beta y_i(t)R_i(t) - \beta y_i(t)^2\sum_{k=1}^N a_{ki}v_k(t) - \beta y_i(t)v_i(t)\sum_{k=1}^N a_{ki}y_k(t).\end{aligned}$$

Summing over all i we obtain

$$\begin{aligned}\frac{d}{dt}\frac{1}{2}||y(t)||^2 =& -\delta||y(t)||^2 + \beta\sum_{i=1}^N y_i(t)(1-y_i(t))\sum_{k=1}^N a_{ki}y_k(t)\\ &-\beta\langle y(t), R(t)\rangle - \beta\sum_{i=1}^N y_i(t)^2\sum_{k=1}^N a_{ki}v_k(t) - \beta\sum_{i=1}^N y_i(t)v_i(t)\sum_{k=1}^N a_{ki}y_k(t)\end{aligned}$$

where $\langle\cdot,\cdot\rangle$ denotes the standard inner product on $\mathbb{R}^N$.

We now estimate the terms on the right hand side. Recall that $\mathbb{E}[X_i(t)]$ and $v_i(t)$ only take values in the interval $[0,1]$ so that also $|y_i(t)| \leq 1$. Denote by $|y(t)|$ the vector $(|y_1(t)|,\dots,|y_N(t)|)$.

- We find that

$$\begin{aligned}\left|\beta\sum_{i=1}^N y_i(t)(1-y_i(t))\sum_{k=1}^N a_{ki}y_k(t)\right| &\leq \beta\sum_{i=1}^N |y_i(t)|\sum_{k=1}^N a_{ki}|y_k(t)|\\ &\leq \beta\langle|y(t)|, A|y(t)|\rangle\\ &\leq \beta||A||_{op}||y(t)||^2\end{aligned}$$

- Clearly, $-\beta\sum_{i=1}^N y_i(t)^2\sum_{k=1}^N a_{ki}v_k(t) \leq 0$.
- It holds that: $-\beta\langle y(t), R(t)\rangle \leq |\beta\langle y(t), R(t)\rangle| \leq \beta||y(t)||||R(t)|| \leq \frac{\beta}{2}||y(t)||^2 + \frac{\beta}{2}||R(t)||^2$
- As for the first term, we find

$$\begin{aligned}\left|\beta\sum_{i=1}^N y_i(t)v_i(t)\sum_{k=1}^N a_{ki}y_k(t)\right| &\leq \beta\sum_{i=1}^N |y_i(t)|\sum_{k=1}^N a_{ki}|y_k(t)|\\ &\leq \beta\langle|y(t)|, A|y(t)|\rangle\\ &\leq \beta||A||_{op}||y(t)||^2\end{aligned}$$

As before, $||A||_{op}$ denotes the operator norm of the matrix A; it is given by the largest eigenvalue $\hat{\mu}$ of A.
Collecting these estimates we arrive at

$$\frac{d}{dt}\frac{1}{2}||y(t)||^2 \leq \left(-\delta + 2\beta||A||_{op} + \frac{\beta}{2}\right)||y(t)||^2 + \frac{\beta}{2}||R(t)||^2$$

or

$$\frac{d}{dt}||y(t)||^2 \leq \left(-2\delta + 4\beta||A||_{op} + \beta\right)||y(t)||^2 + \beta||R(t)||^2$$

We now apply Gronwall's inequality in its differential form for which the sign of the term in brackets is immaterial. This yields

$$||y(t)||^2 \leq e^{\left(-2\delta+4\beta||A||_{op}+\beta\right)t}\beta \int_0^t ||R(s)||^2 ds,$$

as claimed.

4.6 Appendix: Basic ODE Theory

For convenience of the reader, this section contains the basic results from ODE theory used in the proofs of Appendix 4.5. To begin with, we need the following two main results on existence and uniqueness (cf. (Taylor, 2011, Theorem 2.1) and (Hille, 1968, Theorem 2.4.1)).

Theorem 4.6.1 (Picard-Lindelöf-Uniqueness)**.** *Consider the general ODE system*

$$\frac{dy}{dt} = F(t, y), \quad y(t_0) = y_0 \tag{4.20}$$

with $F : \mathrm{Dom}(F) \subset \mathbb{R}^{N+1} \to \mathbb{R}^N$ *defined in a neighborhood of* (t_0, y_0). *Let* $y_0 \in O$ *be an open subset of* $\mathbb{R}^n$ *and* $I \subset \mathbb{R}$ *an interval containing* t_0. *Suppose* F *is continuous on* $I \times O$ *and satisfies the Lipschitz condition:*

$$||F(t, y_1) - F(t, y_2)|| \leq L||y_1 - y_2||,$$

for $t \in I, y_j \in O$. *Then equation* (4.20) *has a unique solution on some* t*-interval containing* t_0.

Theorem 4.6.2 (Peano-Existence)**.** *Suppose* $F(y)$ *is defined and continuous in* $B_r(y_0)$ *where* $B_r(y_0) = \{y \in \mathbb{R}^n : ||y - y_0|| < r\}$ *and suppose that* $||F(y)|| \leq M$ *on* $B_r(y_0)$. *Then the autonomous differential equation* $\frac{dy}{dt} = F(y)$ *with initial condition* y_0 *has at least one solution* y *defined on the time interval* $(-T, T)$ *where* $T < r/M$.

In addition to the key questions of existence and uniqueness, one is also interested in equilibria, i.e., fix-points y^* with $F(t, y^*) = 0$, and their stability, i.e., the behavior of solutions near them. For the autonomous differential system

$$\frac{dy}{dt} = F(y), \quad y(0) = y_0,$$

a fix-point y^* is called *exponentially stable*, if there exist constants $\alpha, \epsilon, C > 0$ such that for all $t \geq 0$

$$|y(t) - y^*| \leq Ce^{-\alpha t|y(0)-y^*|},$$

for any $|y(0) - y^*| \leq \epsilon$ ((Teschl, 2012, Chapter 6.5)). Exponential stability is the strongest type of equilibrium stability and can be proven using the following basic result ((Teschl, 2012, Theorem 6.10)):

Theorem 4.6.3 (Exponential stability via linearization)**.** *Suppose $F \in C^1$ has a fix-point y^* and suppose that all eigenvalues of the Jacobian matrix at y^* have negative real part. Then y^* is exponentially stable.*

4.7 Appendix: Matrix Form of the n-th Order Mean-Field Approximation

Let $M := \sum_{k=1}^{n} \binom{N}{k}$ and denote the n-th order mean-field approximation by

$$z^{(n)} := (z_1^{(n)}, z_2^{(n)}, \ldots, z_N^{(n)}, z_{12}^{(n)}, \ldots, z_{1N}^{(n)}, \ldots, z_{1\cdots n}^{(n)}, \ldots)^\top \in \mathbb{R}^M,$$

i.e., by the vector of solutions to the ODE system (4.16) in lexicographical order. Written in matrix form, (4.16) reads

$$\dot{z}^{(n)} = \underbrace{(\beta A^{(n)} - \delta \mathrm{Diag}(c))z^{(n)}}_{\text{Linear term}} - \beta \underbrace{Q(z^{(n)}; F, \mathrm{Split})}_{\text{Quadratic term}}. \tag{4.21}$$

As in the first order case, the matrix equation is given as the difference of a linear and a quadratic term. Note that the linear term is independent of the mean-field function F and the chosen split, whereas the quadratic term crucially relies on these parameters. We now describe both terms in detail.

Linear term The matrix $A^{(n)} \in \mathbb{R}^{M \times M}$ is a tridiagonal block matrix:

$$A^{(n)} := \begin{bmatrix} D^{1,1} & U^{1,2} & & & & 0 \\ L^{2,1} & D^{2,2} & U^{2,3} & & & \\ & L^{3,2} & D^{3,3} & U^{3,4} & & \\ & & \ddots & \ddots & \ddots & \\ & & & L^{n-1,n-2} & D^{n-1,n-1} & U^{n-1,n} \\ 0 & & & & L^{n,n-1} & D^{n,n} \end{bmatrix}$$

with diagonal blocks

$$\begin{aligned} &D^{k,k} \in \mathbb{R}^{\binom{N}{k} \times \binom{N}{k}} \quad \text{with entries:} \\ &\quad D^{k,k}_{I,I} = A^{(n)}_{I,I} = -\sum_{i \in I} \sum_{j \in I} a_{ij}, \\ &\quad D^{k,k}_{I,I \setminus \{i\} \cup \{j\} (i \in I, j \notin I)} = A^{(n)}_{I,I \setminus \{i\} \cup \{j\} (i \in I, j \notin I)} = a_{ij}, \\ &\text{for } |I| = k, \text{ and } k = 1, \dots, n, \end{aligned}$$

upper diagonal blocks

$$\begin{aligned} &U^{k,k+1} \in \mathbb{R}^{\binom{N}{k} \times \binom{N}{k+1}} \quad \text{with entries:} \\ &\quad U^{k,k+1}_{I,I \cup \{j\} (j \notin I)} = A^{(n)}_{I,I \cup \{j\} (j \notin I)} = -\sum_{i \in I} a_{ij}, \\ &\text{for } |I| = k,\ k = 1, \dots, n-1, \end{aligned}$$

and lower diagonal blocks

$$\begin{aligned} &L^{k,k-1} \in \mathbb{R}^{\binom{N}{k} \times \binom{N}{k-1}} \quad \text{with entries:} \\ &\quad L^{k,k-1}_{I,I \setminus \{i\} (i \in I)} = A^{(n)}_{I,I \setminus \{i\} (i \in I)} = \sum_{j \in I} a_{ij}, \\ &\text{for } |I| = k,\ k = 2, \dots, n. \end{aligned}$$

The matrix $\mathrm{Diag}(c) \in \mathbb{R}^{M \times M}$ is a diagonal matrix with vector $c \in \mathbb{R}^M$ on the diagonal. The vector indicates the cardinality of the underlying index set, i.e., $c_I = k$ if and only if $|I| = k$.

Quadratic term The quadratic term $Q(z^{(n)}; F, \mathrm{Split})$ depends on the mean-field function F and on the chosen split $I \cup \{j\} = I_1(j) \cup I_2(j)$ (for all subsets $I \subseteq \{1, \dots, N\}$ of size $|I| = n$ and all indices $j \in \{1, \dots, N\}$ with $j \notin I$). We denote the split in matrix form by N pairs of matrices

$$(\mathbb{I}_1(1), \mathbb{I}_2(1)), \dots, (\mathbb{I}_1(N), \mathbb{I}_2(N)),$$

where $\mathbb{I}_\ell(j) \in \{0,1\}^{M\times M}$ $(\ell = 1,2)$ is defined by its entries

$$(\mathbb{I}_\ell(j))_{I,J} := \begin{cases} 1, & \text{if } |I| = n, j \notin I, J = I_\ell(j), \\ 0, & \text{otherwise,} \end{cases}$$

i.e., the row of the matrices $\mathbb{I}_1(j)$ and $\mathbb{I}_2(j)$ that corresponds to the set I encodes the subset split of $I \cup \{j\}$, i.e., $I_1(j)$ and $I_2(j)$, respectively. Using this notation for the split, we can write the quadratic term in matrix form as

$$Q(z^{(n)}; F, (\mathbb{I}_1(j), \mathbb{I}_2(j))_{j=1,\dots,N}) = \sum_{j=1}^{N} \mathrm{Diag}\left(\mathbb{I}_1(j) \cdot F(z^{(n)})\right) \cdot C^{(n)}(j) \cdot \mathbb{I}_2(j) \cdot F(z^{(n)}),$$

where,

$$F(z^{(n)}) := (F(z_1^{(n)}), F(z_2^{(n)}), \dots, F(z_N^{(n)}), F(z_{12}^{(n)}), \dots, F(z_{1N}^{(n)}), \dots, F(z_{1\cdots n}^{(n)}), \dots)^\top \in \mathbb{R}^M,$$

and for $j = 1, \dots, N$, the diagonal matrix $C^{(n)}(j) \in \mathbb{R}^{M\times M}$ is defined by its entries

$$(C^{(n)}(j))_{I,I} := \begin{cases} \sum_{i\in I} a_{ij}, & \text{if } |I| = n, j \notin I \\ 0, & \text{otherwise.} \end{cases}$$

Remark 4.7.1. Plugging the derived expression for $Q(z^{(n)}; F, \mathrm{Split})$ into equation (4.21), we immediately see that the matrix equations for the n-th and first order mean-field approximations (cf. equations (4.11) and (4.13)) possess an analogous structure. Hence, the existence of a solution to the n-th order mean-field approximation (for the mean-field functions $F(x) = x$ and $F(x) = \sqrt{x}$) as well as its uniqueness (for $F(x) = x$) follow analogously to the proof of Theorem 4.2.7 (i) and (ii), respectively.

Example 4.7.2. As a concrete example, we consider the quadratic term for the naive single split. Recall that this split is defined by $I_1(j) = I$ and $I_2(j) = j$ for all possible subsets I of size n and indices $j \notin I$. In this case, the matrices $\mathbb{I}_1^{\text{single}}(j)$ become diagonal matrices, i.e.,

$$(\mathbb{I}_1^{\text{single}}(j))_{I,I} = \begin{cases} 1, & \text{if } |I| = n, j \notin I, \\ 0, & \text{otherwise,} \end{cases}$$

and the matrices $\mathbb{I}_2^{\text{single}}(j)$ have non-zero entries only in the lower left corner, i.e.,

$$(\mathbb{I}_2^{\text{single}}(j))_{I,j} = \begin{cases} 1, & \text{if } |I| = n, j \notin I, \\ 0, & \text{otherwise.} \end{cases}$$

This leads to the following quadratic term:

$$\begin{aligned}
Q(z^{(n)}; F, \text{Single Split}) &= \sum_{j=1}^{N} \operatorname{Diag}\left(\mathbb{I}_1^{\text{single}}(j) \cdot F(z^{(n)})\right) \cdot C^{(n)}(j) \cdot \mathbb{I}_2^{\text{single}}(j) \cdot F(z^{(n)}) \\
&= \sum_{j=1}^{N} \operatorname{Diag}\left(F(z^{(n)})\right) \cdot \mathbb{I}_1^{\text{single}}(j) \cdot C^{(n)}(j) \cdot \mathbb{I}_2^{\text{single}}(j) \cdot F(z^{(n)}) \\
&= \operatorname{Diag}\left(F(z^{(n)})\right) \cdot \left(\sum_{j=1}^{N} \mathbb{I}_1^{\text{single}}(j) \cdot C^{(n)}(j) \cdot \mathbb{I}_2^{\text{single}}(j)\right) \cdot F(z^{(n)}) \\
&= \operatorname{Diag}\left(F(z^{(n)})\right) \cdot B^{(n)} \cdot F(z^{(n)}),
\end{aligned}$$

where the first step follows since $\mathbb{I}_1^{\text{single}}(j)$ is diagonal and the matrix $B^{(n)} \in \mathbb{R}^{M \times M}$ is defined by its entries in the lower left corner

$$(B^{(n)})_{I,j} = \begin{cases} \sum_{i \in I} a_{ij}, & \text{if } |I| = n, j \notin I \\ 0, & \text{otherwise.} \end{cases}$$

Note that in this special case, the quadratic term possesses the exact same structure as in the first order case.

4.8 Appendix: Adjacency Matrices

We explicitly give the adjacency matrices for the three example networks depicted in Figure 4.6. The corresponding MATLAB-files are available upon request.

$$A^{\text{Homogeneous}} = \begin{pmatrix}
0 & 0 & 1 & 0 & 0 & 0 & 0 & 0 & 1 & 0 & 0 & 1 & 0 & 0 & 0 & 0 & 0 & 0 & 0 & 0 & 0 & 1 & 0 & 0 & 0 & 0 & 0 & 0 & 0 & 1 & 0 & 0 & 0 & 0 & 0 & 0 & 0 & 0 & 0 & 0 & 1 & 0 & 0 & 0 & 0 & 0 & 0 & 0 & 1 & 0 \\
0 & 0 & 0 & 0 & 0 & 0 & 0 & 0 & 0 & 0 & 0 & 0 & 0 & 1 & 0 & 0 & 0 & 0 & 0 & 0 & 0 & 0 & 0 & 0 & 0 & 0 & 0 & 1 & 0 & 0 & 0 & 0 & 0 & 0 & 1 & 0 & 1 & 1 & 0 & 0 & 0 & 0 & 1 & 1 & 0 & 0 & 0 & 0 & 0 & 0 \\
1 & 0 & 0 & 0 & 0 & 0 & 0 & 1 & 0 & 0 & 0 & 0 & 0 & 0 & 0 & 0 & 0 & 0 & 1 & 0 & 1 & 0 & 1 & 0 & 0 & 1 & 0 & 0 & 0 & 0 & 0 & 0 & 0 & 0 & 0 & 0 & 0 & 0 & 0 & 0 & 0 & 0 & 0 & 1 & 0 & 0 & 0 & 0 & 0 & 0 \\
0 & 0 & 0 & 0 & 0 & 1 & 0 & 1 & 0 & 1 & 0 & 0 & 0 & 0 & 0 & 0 & 0 & 0 & 0 & 0 & 0 & 0 & 0 & 0 & 0 & 0 & 0 & 0 & 0 & 1 & 0 & 0 & 0 & 0 & 1 & 0 & 1 & 0 & 0 & 0 & 0 & 0 & 0 & 1 & 0 & 0 & 0 & 0 & 0 & 0 \\
0 & 0 & 0 & 0 & 0 & 0 & 0 & 0 & 1 & 1 & 0 & 0 & 0 & 0 & 0 & 0 & 0 & 0 & 0 & 1 & 0 & 0 & 0 & 0 & 0 & 0 & 0 & 0 & 1 & 0 & 0 & 0 & 0 & 0 & 0 & 0 & 1 & 0 & 0 & 0 & 0 & 0 & 1 & 0 & 0 & 0 & 0 & 0 & 1 & 0 \\
0 & 0 & 0 & 1 & 0 & 0 & 0 & 0 & 0 & 0 & 0 & 0 & 0 & 0 & 1 & 0 & 0 & 0 & 0 & 0 & 1 & 0 & 0 & 0 & 0 & 0 & 0 & 0 & 1 & 0 & 0 & 0 & 0 & 0 & 0 & 0 & 0 & 0 & 0 & 0 & 0 & 0 & 0 & 1 & 0 & 0 & 1 & 0 & 0 & 1 \\
0 & 0 & 0 & 0 & 0 & 0 & 0 & 0 & 0 & 0 & 0 & 0 & 0 & 0 & 0 & 0 & 0 & 0 & 0 & 1 & 1 & 0 & 1 & 1 & 0 & 0 & 1 & 0 & 0 & 0 & 0 & 0 & 0 & 0 & 0 & 0 & 0 & 0 & 1 & 0 & 1 & 0 & 0 & 0 & 0 & 0 & 0 & 0 & 0 & 0 \\
0 & 0 & 1 & 1 & 0 & 0 & 0 & 0 & 0 & 0 & 1 & 0 & 0 & 0 & 0 & 0 & 1 & 0 & 0 & 0 & 0 & 1 & 0 & 0 & 0 & 0 & 0 & 0 & 0 & 0 & 0 & 0 & 0 & 0 & 0 & 0 & 0 & 0 & 0 & 0 & 0 & 0 & 0 & 0 & 0 & 0 & 1 & 1 & 0 & 0 \\
1 & 0 & 0 & 0 & 1 & 0 & 0 & 0 & 0 & 0 & 0 & 0 & 0 & 0 & 1 & 1 & 0 & 0 & 1 & 0 & 0 & 0 & 0 & 0 & 0 & 0 & 0 & 0 & 0 & 0 & 1 & 0 & 1 & 0 & 0 & 0 & 0 & 0 & 0 & 0 & 0 & 0 & 0 & 0 & 0 & 0 & 0 & 0 & 0 & 0 \\
0 & 0 & 0 & 1 & 1 & 0 & 0 & 0 & 0 & 0 & 0 & 0 & 0 & 0 & 0 & 1 & 0 & 0 & 0 & 0 & 0 & 0 & 0 & 0 & 1 & 1 & 0 & 1 & 0 & 0 & 0 & 0 & 0 & 1 & 0 & 0 & 0 & 0 & 0 & 0 & 0 & 0 & 0 & 0 & 0 & 0 & 0 & 0 & 0 & 0 \\
0 & 0 & 0 & 0 & 0 & 0 & 0 & 1 & 0 & 0 & 0 & 0 & 0 & 0 & 1 & 0 & 0 & 0 & 0 & 1 & 0 & 0 & 0 & 0 & 1 & 1 & 0 & 0 & 0 & 0 & 1 & 0 & 0 & 0 & 0 & 0 & 0 & 0 & 0 & 0 & 0 & 0 & 0 & 0 & 0 & 0 & 0 & 1 & 0 & 0 \\
1 & 0 & 0 & 0 & 0 & 0 & 0 & 0 & 0 & 0 & 0 & 0 & 0 & 0 & 0 & 0 & 0 & 0 & 0 & 0 & 0 & 1 & 0 & 0 & 0 & 1 & 0 & 0 & 0 & 0 & 1 & 0 & 0 & 1 & 0 & 0 & 0 & 0 & 0 & 0 & 1 & 1 & 0 & 0 & 0 & 0 & 0 & 0 & 0 & 0 \\
0 & 0 & 0 & 0 & 0 & 0 & 0 & 0 & 0 & 0 & 0 & 0 & 0 & 0 & 0 & 0 & 0 & 1 & 1 & 0 & 0 & 1 & 0 & 0 & 0 & 0 & 0 & 0 & 0 & 1 & 1 & 0 & 0 & 0 & 0 & 0 & 0 & 0 & 0 & 0 & 0 & 0 & 0 & 0 & 0 & 0 & 1 & 1 & 0 & 0 \\
0 & 1 & 0 & 0 & 0 & 0 & 0 & 0 & 0 & 0 & 0 & 0 & 0 & 0 & 0 & 0 & 1 & 0 & 1 & 0 & 0 & 0 & 0 & 0 & 0 & 1 & 0 & 0 & 0 & 0 & 0 & 0 & 0 & 0 & 0 & 0 & 0 & 1 & 0 & 1 & 0 & 0 & 0 & 0 & 0 & 1 & 0 & 0 & 0 & 0 \\
0 & 0 & 0 & 0 & 0 & 1 & 0 & 0 & 1 & 0 & 1 & 0 & 0 & 0 & 0 & 0 & 0 & 0 & 0 & 0 & 0 & 0 & 0 & 1 & 0 & 0 & 0 & 0 & 0 & 0 & 0 & 0 & 0 & 0 & 0 & 0 & 0 & 1 & 0 & 0 & 0 & 0 & 0 & 0 & 0 & 1 & 0 & 0 & 1 & 0 \\
0 & 0 & 0 & 0 & 0 & 0 & 0 & 0 & 1 & 1 & 0 & 0 & 0 & 0 & 0 & 0 & 0 & 0 & 0 & 0 & 0 & 0 & 0 & 1 & 1 & 0 & 0 & 1 & 0 & 0 & 0 & 0 & 1 & 0 & 0 & 0 & 0 & 0 & 0 & 0 & 0 & 0 & 1 & 0 & 0 & 0 & 0 & 0 & 0 & 0 \\
0 & 0 & 0 & 0 & 0 & 0 & 0 & 1 & 0 & 0 & 0 & 0 & 0 & 1 & 0 & 0 & 0 & 0 & 0 & 0 & 0 & 0 & 0 & 0 & 0 & 0 & 0 & 1 & 0 & 0 & 0 & 0 & 0 & 0 & 0 & 0 & 0 & 0 & 1 & 0 & 0 & 1 & 0 & 0 & 0 & 0 & 1 & 0 & 0 & 1 \\
0 & 0 & 0 & 0 & 0 & 0 & 0 & 0 & 0 & 0 & 0 & 0 & 1 & 0 & 0 & 0 & 0 & 0 & 0 & 0 & 0 & 0 & 0 & 1 & 1 & 0 & 0 & 0 & 1 & 0 & 0 & 0 & 0 & 0 & 0 & 1 & 0 & 0 & 0 & 0 & 0 & 0 & 0 & 0 & 1 & 0 & 0 & 1 & 0 & 0 \\
0 & 0 & 1 & 0 & 0 & 0 & 0 & 0 & 1 & 0 & 0 & 0 & 1 & 1 & 0 & 0 & 0 & 0 & 0 & 0 & 0 & 0 & 0 & 0 & 0 & 0 & 0 & 0 & 1 & 0 & 0 & 0 & 0 & 0 & 0 & 0 & 0 & 0 & 0 & 1 & 0 & 0 & 0 & 0 & 1 & 0 & 0 & 0 & 0 & 0 \\
0 & 0 & 0 & 0 & 1 & 0 & 1 & 0 & 0 & 0 & 1 & 0 & 0 & 0 & 0 & 0 & 0 & 0 & 0 & 0 & 0 & 0 & 0 & 0 & 0 & 0 & 0 & 0 & 0 & 0 & 0 & 0 & 0 & 0 & 0 & 1 & 1 & 0 & 0 & 0 & 0 & 1 & 0 & 0 & 1 & 0 & 0 & 0 & 0 & 0 \\
0 & 0 & 1 & 0 & 0 & 1 & 1 & 0 & 0 & 0 & 0 & 0 & 0 & 0 & 0 & 0 & 0 & 0 & 0 & 0 & 0 & 0 & 0 & 0 & 0 & 0 & 1 & 0 & 0 & 0 & 0 & 0 & 0 & 0 & 1 & 0 & 0 & 0 & 0 & 1 & 0 & 0 & 0 & 0 & 0 & 1 & 0 & 0 & 0 & 0 \\
1 & 0 & 0 & 0 & 0 & 0 & 0 & 1 & 0 & 0 & 0 & 1 & 1 & 0 & 0 & 0 & 0 & 0 & 0 & 0 & 0 & 0 & 0 & 0 & 0 & 0 & 1 & 0 & 0 & 0 & 1 & 0 & 0 & 1 & 0 & 0 & 0 & 0 & 0 & 0 & 0 & 0 & 0 & 0 & 0 & 0 & 0 & 0 & 0 & 0 \\
0 & 0 & 1 & 0 & 0 & 0 & 1 & 0 & 0 & 0 & 0 & 0 & 0 & 0 & 0 & 0 & 0 & 0 & 0 & 0 & 0 & 0 & 0 & 1 & 0 & 0 & 0 & 0 & 0 & 0 & 0 & 1 & 0 & 0 & 0 & 1 & 0 & 1 & 0 & 1 & 0 & 0 & 0 & 0 & 0 & 0 & 0 & 0 & 0 & 0 \\
0 & 0 & 0 & 0 & 0 & 0 & 1 & 0 & 0 & 0 & 0 & 0 & 0 & 0 & 1 & 1 & 0 & 1 & 0 & 0 & 0 & 0 & 1 & 0 & 0 & 0 & 0 & 0 & 0 & 0 & 0 & 0 & 1 & 0 & 0 & 0 & 0 & 0 & 0 & 0 & 0 & 0 & 0 & 1 & 0 & 0 & 0 & 0 & 0 & 0 \\
0 & 0 & 0 & 0 & 0 & 0 & 0 & 0 & 0 & 1 & 1 & 0 & 0 & 0 & 0 & 1 & 0 & 1 & 0 & 0 & 0 & 0 & 0 & 0 & 0 & 0 & 0 & 0 & 0 & 0 & 1 & 0 & 0 & 0 & 0 & 0 & 0 & 0 & 0 & 0 & 0 & 0 & 0 & 0 & 0 & 1 & 0 & 1 & 0 & 0 \\
0 & 0 & 1 & 0 & 0 & 0 & 0 & 0 & 0 & 1 & 1 & 1 & 0 & 1 & 0 & 0 & 0 & 0 & 0 & 0 & 0 & 0 & 0 & 0 & 0 & 0 & 0 & 0 & 0 & 0 & 0 & 0 & 1 & 0 & 0 & 0 & 0 & 0 & 0 & 1 & 0 & 0 & 0 & 0 & 0 & 0 & 0 & 0 & 0 & 0 \\
0 & 0 & 0 & 0 & 0 & 0 & 1 & 0 & 0 & 0 & 0 & 0 & 0 & 0 & 0 & 0 & 0 & 0 & 0 & 0 & 1 & 1 & 0 & 0 & 0 & 0 & 0 & 1 & 0 & 0 & 0 & 0 & 0 & 0 & 0 & 1 & 0 & 1 & 0 & 0 & 0 & 1 & 0 & 0 & 0 & 0 & 0 & 0 & 0 & 0 \\
0 & 1 & 0 & 0 & 0 & 0 & 0 & 0 & 0 & 1 & 0 & 0 & 0 & 0 & 0 & 1 & 1 & 0 & 0 & 0 & 0 & 0 & 0 & 0 & 0 & 0 & 1 & 0 & 0 & 0 & 0 & 0 & 0 & 0 & 0 & 0 & 0 & 0 & 0 & 0 & 1 & 0 & 1 & 0 & 0 & 0 & 0 & 0 & 0 & 0 \\
0 & 0 & 0 & 0 & 1 & 1 & 0 & 0 & 0 & 0 & 0 & 0 & 0 & 0 & 0 & 0 & 0 & 1 & 1 & 0 & 0 & 0 & 0 & 0 & 0 & 0 & 0 & 0 & 0 & 0 & 1 & 0 & 0 & 0 & 0 & 0 & 0 & 0 & 0 & 0 & 1 & 0 & 0 & 0 & 0 & 1 & 0 & 0 & 0 & 0 \\
1 & 0 & 0 & 1 & 0 & 0 & 0 & 0 & 0 & 0 & 0 & 0 & 1 & 0 & 0 & 0 & 0 & 0 & 0 & 0 & 0 & 0 & 0 & 0 & 0 & 0 & 0 & 0 & 0 & 0 & 0 & 0 & 0 & 0 & 0 & 0 & 0 & 0 & 0 & 0 & 0 & 0 & 0 & 1 & 1 & 0 & 1 & 0 & 1 & 0 \\
0 & 0 & 0 & 0 & 0 & 0 & 0 & 0 & 1 & 0 & 1 & 1 & 1 & 0 & 0 & 0 & 0 & 0 & 0 & 0 & 0 & 1 & 0 & 0 & 1 & 0 & 0 & 0 & 1 & 0 & 0 & 0 & 0 & 0 & 0 & 0 & 0 & 0 & 0 & 0 & 0 & 0 & 0 & 0 & 0 & 0 & 0 & 0 & 0 & 0 \\
0 & 0 & 0 & 0 & 0 & 0 & 0 & 0 & 0 & 0 & 0 & 0 & 0 & 0 & 0 & 0 & 0 & 0 & 0 & 0 & 0 & 0 & 1 & 0 & 0 & 0 & 0 & 0 & 0 & 0 & 0 & 0 & 0 & 1 & 0 & 0 & 0 & 0 & 1 & 1 & 0 & 0 & 0 & 0 & 0 & 0 & 1 & 0 & 1 & 1 \\
0 & 0 & 0 & 0 & 0 & 0 & 0 & 0 & 1 & 0 & 0 & 0 & 0 & 0 & 0 & 1 & 0 & 0 & 0 & 0 & 0 & 0 & 0 & 1 & 0 & 1 & 0 & 0 & 0 & 0 & 0 & 0 & 0 & 1 & 0 & 1 & 0 & 0 & 0 & 0 & 0 & 0 & 0 & 0 & 1 & 0 & 0 & 0 & 0 & 0 \\
0 & 0 & 0 & 0 & 0 & 0 & 0 & 0 & 0 & 1 & 0 & 1 & 0 & 0 & 0 & 0 & 0 & 0 & 0 & 0 & 0 & 1 & 0 & 0 & 0 & 0 & 0 & 0 & 0 & 0 & 0 & 1 & 1 & 0 & 1 & 0 & 0 & 0 & 0 & 0 & 0 & 0 & 0 & 0 & 0 & 0 & 0 & 0 & 0 & 1 \\
0 & 1 & 0 & 1 & 0 & 0 & 0 & 0 & 0 & 0 & 0 & 0 & 0 & 0 & 0 & 0 & 0 & 0 & 0 & 0 & 1 & 0 & 0 & 0 & 0 & 0 & 0 & 0 & 0 & 0 & 0 & 0 & 0 & 1 & 0 & 0 & 0 & 0 & 1 & 0 & 0 & 0 & 1 & 0 & 0 & 1 & 0 & 0 & 0 & 0 \\
0 & 0 & 0 & 0 & 0 & 0 & 0 & 0 & 0 & 0 & 0 & 0 & 0 & 0 & 0 & 0 & 0 & 1 & 0 & 1 & 0 & 0 & 1 & 0 & 0 & 0 & 1 & 0 & 0 & 0 & 0 & 0 & 1 & 0 & 0 & 0 & 1 & 0 & 0 & 0 & 0 & 1 & 0 & 0 & 0 & 0 & 0 & 0 & 0 & 0 \\
0 & 1 & 0 & 1 & 1 & 0 & 0 & 0 & 0 & 0 & 0 & 0 & 0 & 0 & 0 & 0 & 0 & 0 & 0 & 1 & 0 & 0 & 0 & 0 & 0 & 0 & 0 & 0 & 0 & 0 & 0 & 0 & 0 & 0 & 0 & 1 & 0 & 0 & 0 & 0 & 0 & 1 & 0 & 0 & 0 & 0 & 0 & 0 & 1 & 0 \\
0 & 1 & 0 & 0 & 0 & 0 & 0 & 0 & 0 & 0 & 0 & 0 & 0 & 1 & 1 & 0 & 0 & 0 & 0 & 0 & 0 & 0 & 1 & 0 & 0 & 0 & 1 & 0 & 0 & 0 & 0 & 0 & 0 & 0 & 0 & 0 & 0 & 0 & 0 & 0 & 1 & 0 & 1 & 0 & 0 & 0 & 0 & 0 & 0 & 0 \\
0 & 0 & 0 & 0 & 0 & 0 & 1 & 0 & 0 & 0 & 0 & 0 & 0 & 0 & 0 & 0 & 1 & 0 & 0 & 0 & 0 & 0 & 0 & 0 & 0 & 0 & 0 & 0 & 0 & 0 & 0 & 1 & 0 & 0 & 1 & 0 & 0 & 0 & 0 & 0 & 0 & 0 & 0 & 0 & 1 & 0 & 0 & 1 & 0 & 1 \\
0 & 0 & 0 & 0 & 0 & 0 & 0 & 0 & 0 & 0 & 0 & 0 & 0 & 1 & 0 & 0 & 0 & 0 & 1 & 0 & 1 & 0 & 1 & 0 & 0 & 1 & 0 & 0 & 0 & 0 & 0 & 1 & 0 & 0 & 0 & 0 & 0 & 0 & 0 & 0 & 0 & 0 & 1 & 0 & 0 & 0 & 0 & 0 & 0 & 0 \\
1 & 0 & 0 & 0 & 0 & 0 & 1 & 0 & 0 & 0 & 0 & 1 & 0 & 0 & 0 & 0 & 0 & 0 & 0 & 0 & 0 & 0 & 0 & 0 & 0 & 0 & 0 & 1 & 1 & 0 & 0 & 0 & 0 & 0 & 0 & 0 & 0 & 1 & 0 & 0 & 0 & 0 & 0 & 0 & 0 & 0 & 0 & 0 & 0 & 1 \\
0 & 0 & 0 & 0 & 0 & 0 & 0 & 0 & 0 & 0 & 0 & 1 & 0 & 0 & 0 & 0 & 1 & 0 & 0 & 1 & 0 & 0 & 0 & 0 & 0 & 0 & 1 & 0 & 0 & 0 & 0 & 0 & 0 & 0 & 0 & 1 & 1 & 0 & 0 & 0 & 0 & 0 & 0 & 0 & 0 & 0 & 0 & 1 & 0 & 0 \\
0 & 1 & 0 & 0 & 1 & 0 & 0 & 0 & 0 & 0 & 0 & 0 & 0 & 0 & 0 & 1 & 0 & 0 & 0 & 0 & 0 & 0 & 0 & 0 & 0 & 0 & 0 & 1 & 0 & 0 & 0 & 0 & 0 & 0 & 1 & 0 & 0 & 1 & 0 & 1 & 0 & 0 & 0 & 0 & 0 & 0 & 0 & 0 & 0 & 0 \\
0 & 1 & 1 & 1 & 0 & 1 & 0 & 0 & 0 & 0 & 0 & 0 & 0 & 0 & 0 & 0 & 0 & 0 & 0 & 0 & 0 & 0 & 0 & 1 & 0 & 0 & 0 & 0 & 0 & 1 & 0 & 0 & 0 & 0 & 0 & 0 & 0 & 0 & 0 & 0 & 0 & 0 & 0 & 0 & 0 & 0 & 0 & 0 & 1 & 0 \\
0 & 0 & 0 & 0 & 0 & 0 & 0 & 0 & 0 & 0 & 0 & 0 & 0 & 0 & 0 & 0 & 0 & 1 & 1 & 1 & 0 & 0 & 0 & 0 & 0 & 0 & 0 & 0 & 0 & 1 & 0 & 0 & 1 & 0 & 0 & 0 & 0 & 0 & 1 & 0 & 0 & 0 & 0 & 0 & 0 & 0 & 0 & 0 & 0 & 1 \\
0 & 0 & 0 & 0 & 0 & 0 & 0 & 0 & 0 & 0 & 0 & 0 & 0 & 1 & 1 & 0 & 0 & 0 & 0 & 0 & 1 & 0 & 0 & 0 & 1 & 0 & 0 & 0 & 1 & 0 & 0 & 0 & 0 & 0 & 1 & 0 & 0 & 0 & 0 & 0 & 0 & 0 & 0 & 0 & 0 & 0 & 1 & 0 & 0 & 0 \\
0 & 0 & 0 & 0 & 0 & 1 & 0 & 1 & 0 & 0 & 0 & 0 & 1 & 0 & 0 & 0 & 1 & 0 & 0 & 0 & 0 & 0 & 0 & 0 & 0 & 0 & 0 & 0 & 0 & 1 & 0 & 1 & 0 & 0 & 0 & 0 & 0 & 0 & 0 & 0 & 0 & 0 & 0 & 0 & 0 & 1 & 0 & 0 & 0 & 0 \\
0 & 0 & 0 & 0 & 0 & 0 & 0 & 1 & 0 & 0 & 1 & 0 & 1 & 0 & 0 & 0 & 0 & 1 & 0 & 0 & 0 & 0 & 0 & 0 & 1 & 0 & 0 & 0 & 0 & 0 & 0 & 0 & 0 & 0 & 0 & 0 & 0 & 0 & 1 & 0 & 0 & 1 & 0 & 0 & 0 & 0 & 0 & 0 & 0 & 0 \\
1 & 0 & 0 & 0 & 1 & 0 & 0 & 0 & 0 & 0 & 0 & 0 & 0 & 0 & 1 & 0 & 0 & 0 & 0 & 0 & 0 & 0 & 0 & 0 & 0 & 0 & 0 & 0 & 0 & 1 & 0 & 1 & 0 & 0 & 0 & 0 & 1 & 0 & 0 & 0 & 0 & 0 & 0 & 1 & 0 & 0 & 0 & 0 & 0 & 0 \\
0 & 0 & 0 & 0 & 0 & 1 & 0 & 0 & 0 & 0 & 0 & 0 & 0 & 0 & 0 & 0 & 1 & 0 & 0 & 0 & 0 & 0 & 0 & 0 & 0 & 0 & 0 & 0 & 0 & 0 & 0 & 1 & 0 & 1 & 0 & 0 & 0 & 0 & 1 & 0 & 1 & 0 & 0 & 0 & 1 & 0 & 0 & 0 & 0 & 0
\end{pmatrix}$$

$$
A^{\text{Clustered}} = \left(\begin{array}{cccccccccccccccccccccccccccccccccccccccccccccccccc}
0 & 0 & 1 & 0 & 1 & 1 & 0 & 1 & 1 & 1 & 1 & 0 & 0 & 0 & 0 & 0 & 0 & 0 & 0 & 0 & 0 & 0 & 0 & 0 & 0 & 0 & 0 & 0 & 0 & 0 & 0 & 0 & 0 & 0 & 0 & 0 & 0 & 0 & 0 & 0 & 0 & 0 & 0 & 0 & 0 & 0 & 0 & 0 & 0 & 0 \\
0 & 0 & 1 & 1 & 1 & 0 & 1 & 1 & 0 & 1 & 0 & 0 & 0 & 0 & 0 & 0 & 0 & 0 & 0 & 0 & 0 & 0 & 0 & 0 & 0 & 0 & 0 & 0 & 0 & 0 & 0 & 0 & 0 & 0 & 0 & 0 & 0 & 0 & 0 & 0 & 0 & 1 & 0 & 0 & 0 & 0 & 0 & 0 & 0 & 0 \\
1 & 1 & 0 & 1 & 0 & 1 & 1 & 1 & 1 & 0 & 0 & 0 & 0 & 0 & 0 & 0 & 0 & 0 & 0 & 0 & 0 & 0 & 0 & 0 & 0 & 0 & 0 & 0 & 0 & 0 & 0 & 0 & 0 & 0 & 0 & 0 & 0 & 0 & 0 & 0 & 0 & 0 & 0 & 0 & 0 & 0 & 0 & 0 & 0 & 0 \\
0 & 1 & 1 & 0 & 1 & 1 & 1 & 0 & 1 & 1 & 0 & 0 & 0 & 0 & 0 & 0 & 0 & 0 & 0 & 0 & 0 & 0 & 0 & 0 & 0 & 0 & 0 & 0 & 0 & 0 & 0 & 0 & 0 & 0 & 0 & 0 & 0 & 0 & 0 & 0 & 0 & 0 & 0 & 0 & 0 & 0 & 0 & 0 & 0 & 0 \\
1 & 1 & 0 & 1 & 0 & 1 & 1 & 1 & 1 & 0 & 0 & 0 & 0 & 0 & 0 & 0 & 0 & 0 & 0 & 0 & 0 & 0 & 0 & 0 & 0 & 0 & 0 & 0 & 0 & 0 & 0 & 0 & 0 & 0 & 0 & 0 & 0 & 0 & 0 & 0 & 0 & 0 & 0 & 0 & 0 & 0 & 0 & 0 & 0 & 0 \\
1 & 0 & 1 & 1 & 1 & 0 & 0 & 1 & 1 & 1 & 0 & 0 & 0 & 0 & 0 & 0 & 0 & 0 & 0 & 0 & 0 & 0 & 0 & 0 & 0 & 0 & 0 & 0 & 0 & 0 & 0 & 0 & 0 & 0 & 0 & 0 & 0 & 0 & 0 & 0 & 0 & 0 & 0 & 0 & 0 & 0 & 0 & 0 & 0 & 0 \\
0 & 1 & 1 & 1 & 1 & 0 & 0 & 1 & 1 & 1 & 0 & 0 & 0 & 0 & 0 & 0 & 0 & 0 & 0 & 0 & 0 & 0 & 0 & 0 & 0 & 0 & 0 & 0 & 0 & 0 & 0 & 0 & 0 & 0 & 0 & 0 & 0 & 0 & 0 & 0 & 0 & 0 & 0 & 0 & 0 & 0 & 0 & 0 & 0 & 0 \\
1 & 1 & 1 & 0 & 1 & 1 & 1 & 0 & 0 & 1 & 0 & 0 & 0 & 0 & 0 & 0 & 0 & 0 & 0 & 0 & 0 & 0 & 0 & 0 & 0 & 0 & 0 & 0 & 0 & 0 & 0 & 0 & 0 & 0 & 0 & 0 & 0 & 0 & 0 & 0 & 0 & 0 & 0 & 0 & 0 & 0 & 0 & 0 & 0 & 0 \\
1 & 0 & 1 & 1 & 1 & 1 & 1 & 0 & 0 & 1 & 0 & 0 & 0 & 0 & 0 & 0 & 0 & 0 & 0 & 0 & 0 & 0 & 0 & 0 & 0 & 0 & 0 & 0 & 0 & 0 & 0 & 0 & 0 & 0 & 0 & 0 & 0 & 0 & 0 & 0 & 0 & 0 & 0 & 0 & 0 & 0 & 0 & 0 & 0 & 0 \\
1 & 1 & 0 & 1 & 0 & 1 & 1 & 1 & 1 & 0 & 0 & 0 & 0 & 0 & 0 & 0 & 0 & 0 & 0 & 0 & 0 & 0 & 0 & 0 & 0 & 0 & 0 & 0 & 0 & 0 & 0 & 0 & 0 & 0 & 0 & 0 & 0 & 0 & 0 & 0 & 0 & 0 & 0 & 0 & 0 & 0 & 0 & 0 & 0 & 0 \\
1 & 0 & 0 & 0 & 0 & 0 & 0 & 0 & 0 & 0 & 0 & 0 & 0 & 1 & 1 & 1 & 1 & 1 & 0 & 1 & 0 & 0 & 0 & 0 & 0 & 0 & 0 & 0 & 0 & 0 & 0 & 0 & 0 & 0 & 0 & 0 & 0 & 0 & 0 & 0 & 0 & 0 & 0 & 0 & 0 & 0 & 0 & 0 & 0 & 0 \\
0 & 0 & 0 & 0 & 0 & 0 & 0 & 0 & 0 & 0 & 0 & 0 & 1 & 1 & 0 & 1 & 1 & 1 & 1 & 0 & 1 & 0 & 0 & 0 & 0 & 0 & 0 & 0 & 0 & 0 & 0 & 0 & 0 & 0 & 0 & 0 & 0 & 0 & 0 & 0 & 0 & 0 & 0 & 0 & 0 & 0 & 0 & 0 & 0 & 0 \\
0 & 0 & 0 & 0 & 0 & 0 & 0 & 0 & 0 & 0 & 0 & 1 & 0 & 1 & 1 & 1 & 1 & 0 & 1 & 1 & 0 & 0 & 0 & 0 & 0 & 0 & 0 & 0 & 0 & 0 & 0 & 0 & 0 & 0 & 0 & 0 & 0 & 0 & 0 & 0 & 0 & 0 & 0 & 0 & 0 & 0 & 0 & 0 & 0 & 0 \\
0 & 0 & 0 & 0 & 0 & 0 & 0 & 0 & 0 & 0 & 1 & 1 & 1 & 0 & 1 & 0 & 0 & 1 & 1 & 1 & 0 & 0 & 0 & 0 & 0 & 0 & 0 & 0 & 0 & 0 & 0 & 0 & 0 & 0 & 0 & 0 & 0 & 0 & 0 & 0 & 0 & 0 & 0 & 0 & 0 & 0 & 0 & 0 & 0 & 0 \\
0 & 0 & 0 & 0 & 0 & 0 & 0 & 0 & 0 & 0 & 1 & 0 & 1 & 1 & 0 & 0 & 1 & 1 & 1 & 1 & 0 & 0 & 0 & 0 & 0 & 0 & 0 & 0 & 0 & 0 & 0 & 0 & 0 & 0 & 0 & 0 & 0 & 0 & 0 & 0 & 0 & 0 & 0 & 0 & 0 & 0 & 0 & 0 & 0 & 0 \\
0 & 0 & 0 & 0 & 0 & 0 & 0 & 0 & 0 & 0 & 1 & 1 & 1 & 0 & 0 & 0 & 1 & 1 & 1 & 1 & 0 & 0 & 0 & 0 & 0 & 0 & 0 & 0 & 0 & 0 & 0 & 0 & 0 & 0 & 0 & 0 & 0 & 0 & 0 & 0 & 0 & 0 & 0 & 0 & 0 & 0 & 0 & 0 & 0 & 0 \\
0 & 0 & 0 & 0 & 0 & 0 & 0 & 0 & 0 & 0 & 1 & 1 & 1 & 0 & 1 & 1 & 0 & 1 & 0 & 1 & 0 & 0 & 0 & 0 & 0 & 0 & 0 & 0 & 0 & 0 & 0 & 0 & 0 & 0 & 0 & 0 & 0 & 0 & 0 & 0 & 0 & 0 & 0 & 0 & 0 & 0 & 0 & 0 & 0 & 0 \\
0 & 0 & 0 & 0 & 0 & 0 & 0 & 0 & 0 & 0 & 1 & 1 & 0 & 1 & 1 & 1 & 1 & 0 & 1 & 0 & 0 & 0 & 0 & 0 & 0 & 0 & 0 & 0 & 0 & 0 & 0 & 0 & 0 & 0 & 0 & 0 & 0 & 0 & 0 & 0 & 0 & 0 & 0 & 0 & 0 & 0 & 0 & 0 & 0 & 0 \\
0 & 0 & 0 & 0 & 0 & 0 & 0 & 0 & 0 & 0 & 0 & 1 & 1 & 1 & 1 & 1 & 0 & 1 & 0 & 1 & 0 & 0 & 0 & 0 & 0 & 0 & 0 & 0 & 0 & 0 & 0 & 0 & 0 & 0 & 0 & 0 & 0 & 0 & 0 & 0 & 0 & 0 & 0 & 0 & 0 & 0 & 0 & 0 & 0 & 0 \\
0 & 0 & 0 & 0 & 0 & 0 & 0 & 0 & 0 & 0 & 1 & 0 & 1 & 1 & 1 & 1 & 1 & 0 & 1 & 0 & 0 & 0 & 0 & 0 & 0 & 0 & 0 & 0 & 0 & 0 & 0 & 0 & 0 & 0 & 0 & 0 & 0 & 0 & 0 & 0 & 0 & 0 & 0 & 0 & 0 & 0 & 0 & 0 & 0 & 0 \\
0 & 0 & 0 & 0 & 0 & 0 & 0 & 0 & 0 & 0 & 0 & 1 & 0 & 0 & 0 & 0 & 0 & 0 & 0 & 0 & 0 & 0 & 0 & 1 & 0 & 1 & 1 & 1 & 1 & 1 & 0 & 0 & 0 & 0 & 0 & 0 & 0 & 0 & 0 & 0 & 0 & 0 & 0 & 0 & 0 & 0 & 0 & 0 & 0 & 0 \\
0 & 0 & 0 & 0 & 0 & 0 & 0 & 0 & 0 & 0 & 0 & 0 & 0 & 0 & 0 & 0 & 0 & 0 & 0 & 0 & 0 & 0 & 1 & 1 & 1 & 1 & 1 & 1 & 0 & 1 & 0 & 0 & 0 & 0 & 0 & 0 & 0 & 0 & 0 & 0 & 0 & 0 & 0 & 0 & 0 & 0 & 0 & 0 & 0 & 0 \\
0 & 0 & 0 & 0 & 0 & 0 & 0 & 0 & 0 & 0 & 0 & 0 & 0 & 0 & 0 & 0 & 0 & 0 & 0 & 0 & 0 & 1 & 0 & 1 & 1 & 1 & 1 & 0 & 1 & 0 & 1 & 0 & 0 & 0 & 0 & 0 & 0 & 0 & 0 & 0 & 0 & 0 & 0 & 0 & 0 & 0 & 0 & 0 & 0 & 0 \\
0 & 0 & 0 & 0 & 0 & 0 & 0 & 0 & 0 & 0 & 0 & 0 & 0 & 0 & 0 & 0 & 0 & 0 & 0 & 0 & 1 & 1 & 1 & 0 & 1 & 1 & 0 & 1 & 0 & 1 & 0 & 0 & 0 & 0 & 0 & 0 & 0 & 0 & 0 & 0 & 0 & 0 & 0 & 0 & 0 & 0 & 0 & 0 & 0 & 0 \\
0 & 0 & 0 & 0 & 0 & 0 & 0 & 0 & 0 & 0 & 0 & 0 & 0 & 0 & 0 & 0 & 0 & 0 & 0 & 0 & 0 & 1 & 1 & 1 & 0 & 0 & 1 & 1 & 1 & 1 & 0 & 0 & 0 & 0 & 0 & 0 & 0 & 0 & 0 & 0 & 0 & 0 & 0 & 0 & 0 & 0 & 0 & 0 & 0 & 0 \\
0 & 0 & 0 & 0 & 0 & 0 & 0 & 0 & 0 & 0 & 0 & 0 & 0 & 0 & 0 & 0 & 0 & 0 & 0 & 0 & 1 & 1 & 1 & 1 & 0 & 0 & 1 & 1 & 1 & 0 & 0 & 0 & 0 & 0 & 0 & 0 & 0 & 0 & 0 & 0 & 0 & 0 & 0 & 0 & 0 & 0 & 0 & 0 & 0 & 0 \\
0 & 0 & 0 & 0 & 0 & 0 & 0 & 0 & 0 & 0 & 0 & 0 & 0 & 0 & 0 & 0 & 0 & 0 & 0 & 0 & 1 & 1 & 1 & 0 & 1 & 1 & 0 & 0 & 1 & 1 & 0 & 0 & 0 & 0 & 0 & 0 & 0 & 0 & 0 & 0 & 0 & 0 & 0 & 0 & 0 & 0 & 0 & 0 & 0 & 0 \\
0 & 0 & 0 & 0 & 0 & 0 & 0 & 0 & 0 & 0 & 0 & 0 & 0 & 0 & 0 & 0 & 0 & 0 & 0 & 0 & 1 & 1 & 0 & 1 & 1 & 1 & 0 & 0 & 1 & 1 & 0 & 0 & 0 & 0 & 0 & 0 & 0 & 0 & 0 & 0 & 0 & 0 & 0 & 0 & 0 & 0 & 0 & 0 & 0 & 0 \\
0 & 0 & 0 & 0 & 0 & 0 & 0 & 0 & 0 & 0 & 0 & 0 & 0 & 0 & 0 & 0 & 0 & 0 & 0 & 0 & 1 & 0 & 1 & 0 & 1 & 1 & 1 & 1 & 0 & 1 & 0 & 0 & 0 & 0 & 0 & 0 & 0 & 0 & 0 & 0 & 0 & 0 & 0 & 0 & 0 & 0 & 0 & 0 & 0 & 0 \\
0 & 0 & 0 & 0 & 0 & 0 & 0 & 0 & 0 & 0 & 0 & 0 & 0 & 0 & 0 & 0 & 0 & 0 & 0 & 0 & 1 & 1 & 0 & 1 & 1 & 0 & 1 & 1 & 1 & 0 & 0 & 0 & 0 & 0 & 0 & 0 & 0 & 0 & 0 & 0 & 0 & 0 & 0 & 0 & 0 & 0 & 0 & 0 & 0 & 0 \\
0 & 0 & 0 & 0 & 0 & 0 & 0 & 0 & 0 & 0 & 0 & 0 & 0 & 0 & 0 & 0 & 0 & 0 & 0 & 0 & 0 & 1 & 0 & 0 & 0 & 0 & 0 & 0 & 0 & 0 & 0 & 0 & 0 & 0 & 1 & 1 & 1 & 1 & 1 & 1 & 0 & 0 & 0 & 0 & 0 & 0 & 0 & 0 & 0 & 0 \\
0 & 0 & 0 & 0 & 0 & 0 & 0 & 0 & 0 & 0 & 0 & 0 & 0 & 0 & 0 & 0 & 0 & 0 & 0 & 0 & 0 & 0 & 0 & 0 & 0 & 0 & 0 & 0 & 0 & 0 & 0 & 0 & 1 & 1 & 1 & 1 & 1 & 0 & 1 & 1 & 0 & 0 & 0 & 0 & 0 & 0 & 0 & 0 & 0 & 0 \\
0 & 0 & 0 & 0 & 0 & 0 & 0 & 0 & 0 & 0 & 0 & 0 & 0 & 0 & 0 & 0 & 0 & 0 & 0 & 0 & 0 & 0 & 0 & 0 & 0 & 0 & 0 & 0 & 0 & 0 & 0 & 1 & 0 & 1 & 1 & 0 & 1 & 0 & 1 & 1 & 1 & 0 & 0 & 0 & 0 & 0 & 0 & 0 & 0 & 0 \\
0 & 0 & 0 & 0 & 0 & 0 & 0 & 0 & 0 & 0 & 0 & 0 & 0 & 0 & 0 & 0 & 0 & 0 & 0 & 0 & 0 & 0 & 0 & 0 & 0 & 0 & 0 & 0 & 0 & 0 & 0 & 1 & 1 & 0 & 1 & 1 & 1 & 1 & 1 & 0 & 0 & 0 & 0 & 0 & 0 & 0 & 0 & 0 & 0 & 0 \\
0 & 0 & 0 & 0 & 0 & 0 & 0 & 0 & 0 & 0 & 0 & 0 & 0 & 0 & 0 & 0 & 0 & 0 & 0 & 0 & 0 & 0 & 0 & 0 & 0 & 0 & 0 & 0 & 0 & 0 & 1 & 1 & 1 & 1 & 0 & 1 & 0 & 1 & 1 & 0 & 0 & 0 & 0 & 0 & 0 & 0 & 0 & 0 & 0 & 0 \\
0 & 0 & 0 & 0 & 0 & 0 & 0 & 0 & 0 & 0 & 0 & 0 & 0 & 0 & 0 & 0 & 0 & 0 & 0 & 0 & 0 & 0 & 0 & 0 & 0 & 0 & 0 & 0 & 0 & 0 & 1 & 1 & 0 & 1 & 1 & 0 & 1 & 1 & 0 & 1 & 0 & 0 & 0 & 0 & 0 & 0 & 0 & 0 & 0 & 0 \\
0 & 0 & 0 & 0 & 0 & 0 & 0 & 0 & 0 & 0 & 0 & 0 & 0 & 0 & 0 & 0 & 0 & 0 & 0 & 0 & 0 & 0 & 0 & 0 & 0 & 0 & 0 & 0 & 0 & 0 & 1 & 1 & 1 & 1 & 0 & 1 & 0 & 1 & 0 & 1 & 0 & 0 & 0 & 0 & 0 & 0 & 0 & 0 & 0 & 0 \\
0 & 0 & 0 & 0 & 0 & 0 & 0 & 0 & 0 & 0 & 0 & 0 & 0 & 0 & 0 & 0 & 0 & 0 & 0 & 0 & 0 & 0 & 0 & 0 & 0 & 0 & 0 & 0 & 0 & 0 & 1 & 0 & 0 & 1 & 1 & 1 & 1 & 0 & 1 & 1 & 0 & 0 & 0 & 0 & 0 & 0 & 0 & 0 & 0 & 0 \\
0 & 0 & 0 & 0 & 0 & 0 & 0 & 0 & 0 & 0 & 0 & 0 & 0 & 0 & 0 & 0 & 0 & 0 & 0 & 0 & 0 & 0 & 0 & 0 & 0 & 0 & 0 & 0 & 0 & 0 & 1 & 1 & 1 & 1 & 1 & 0 & 0 & 1 & 0 & 1 & 0 & 0 & 0 & 0 & 0 & 0 & 0 & 0 & 0 & 0 \\
0 & 0 & 0 & 0 & 0 & 0 & 0 & 0 & 0 & 0 & 0 & 0 & 0 & 0 & 0 & 0 & 0 & 0 & 0 & 0 & 0 & 0 & 0 & 0 & 0 & 0 & 0 & 0 & 0 & 0 & 1 & 1 & 1 & 0 & 0 & 1 & 1 & 1 & 1 & 0 & 0 & 0 & 0 & 0 & 0 & 0 & 0 & 0 & 0 & 0 \\
0 & 0 & 0 & 0 & 0 & 0 & 0 & 0 & 0 & 0 & 0 & 0 & 0 & 0 & 0 & 0 & 0 & 0 & 0 & 0 & 0 & 0 & 0 & 0 & 0 & 0 & 0 & 0 & 0 & 0 & 0 & 0 & 1 & 0 & 0 & 0 & 0 & 0 & 0 & 0 & 0 & 0 & 0 & 1 & 1 & 1 & 1 & 1 & 1 & 0 \\
0 & 1 & 0 & 0 & 0 & 0 & 0 & 0 & 0 & 0 & 0 & 0 & 0 & 0 & 0 & 0 & 0 & 0 & 0 & 0 & 0 & 0 & 0 & 0 & 0 & 0 & 0 & 0 & 0 & 0 & 0 & 0 & 0 & 0 & 0 & 0 & 0 & 0 & 0 & 0 & 0 & 0 & 1 & 0 & 1 & 1 & 1 & 0 & 1 & 1 \\
0 & 0 & 0 & 0 & 0 & 0 & 0 & 0 & 0 & 0 & 0 & 0 & 0 & 0 & 0 & 0 & 0 & 0 & 0 & 0 & 0 & 0 & 0 & 0 & 0 & 0 & 0 & 0 & 0 & 0 & 0 & 0 & 0 & 0 & 0 & 0 & 0 & 0 & 0 & 0 & 0 & 1 & 0 & 1 & 1 & 1 & 1 & 0 & 1 & 1 \\
0 & 0 & 0 & 0 & 0 & 0 & 0 & 0 & 0 & 0 & 0 & 0 & 0 & 0 & 0 & 0 & 0 & 0 & 0 & 0 & 0 & 0 & 0 & 0 & 0 & 0 & 0 & 0 & 0 & 0 & 0 & 0 & 0 & 0 & 0 & 0 & 0 & 0 & 0 & 0 & 1 & 0 & 1 & 0 & 1 & 1 & 0 & 1 & 1 & 1 \\
0 & 0 & 0 & 0 & 0 & 0 & 0 & 0 & 0 & 0 & 0 & 0 & 0 & 0 & 0 & 0 & 0 & 0 & 0 & 0 & 0 & 0 & 0 & 0 & 0 & 0 & 0 & 0 & 0 & 0 & 0 & 0 & 0 & 0 & 0 & 0 & 0 & 0 & 0 & 0 & 1 & 1 & 1 & 1 & 0 & 0 & 1 & 1 & 0 & 1 \\
0 & 0 & 0 & 0 & 0 & 0 & 0 & 0 & 0 & 0 & 0 & 0 & 0 & 0 & 0 & 0 & 0 & 0 & 0 & 0 & 0 & 0 & 0 & 0 & 0 & 0 & 0 & 0 & 0 & 0 & 0 & 0 & 0 & 0 & 0 & 0 & 0 & 0 & 0 & 0 & 1 & 1 & 1 & 1 & 0 & 0 & 1 & 1 & 1 & 0 \\
0 & 0 & 0 & 0 & 0 & 0 & 0 & 0 & 0 & 0 & 0 & 0 & 0 & 0 & 0 & 0 & 0 & 0 & 0 & 0 & 0 & 0 & 0 & 0 & 0 & 0 & 0 & 0 & 0 & 0 & 0 & 0 & 0 & 0 & 0 & 0 & 0 & 0 & 0 & 0 & 1 & 1 & 1 & 0 & 1 & 1 & 0 & 1 & 0 & 1 \\
0 & 0 & 0 & 0 & 0 & 0 & 0 & 0 & 0 & 0 & 0 & 0 & 0 & 0 & 0 & 0 & 0 & 0 & 0 & 0 & 0 & 0 & 0 & 0 & 0 & 0 & 0 & 0 & 0 & 0 & 0 & 0 & 0 & 0 & 0 & 0 & 0 & 0 & 0 & 0 & 1 & 0 & 0 & 1 & 1 & 1 & 1 & 0 & 1 & 1 \\
0 & 0 & 0 & 0 & 0 & 0 & 0 & 0 & 0 & 0 & 0 & 0 & 0 & 0 & 0 & 0 & 0 & 0 & 0 & 0 & 0 & 0 & 0 & 0 & 0 & 0 & 0 & 0 & 0 & 0 & 0 & 0 & 0 & 0 & 0 & 0 & 0 & 0 & 0 & 0 & 1 & 1 & 1 & 1 & 0 & 1 & 0 & 1 & 0 & 1 \\
0 & 0 & 0 & 0 & 0 & 0 & 0 & 0 & 0 & 0 & 0 & 0 & 0 & 0 & 0 & 0 & 0 & 0 & 0 & 0 & 0 & 0 & 0 & 0 & 0 & 0 & 0 & 0 & 0 & 0 & 0 & 0 & 0 & 0 & 0 & 0 & 0 & 0 & 0 & 0 & 0 & 1 & 1 & 1 & 1 & 0 & 1 & 1 & 1 & 0
\end{array}\right)
$$

$$
A^{\text{Star}} = \left(\begin{array}{cccccccccccccccccccccccccccccccccccccccccccccccccc}
0 & 0 & 1 & 1 & 1 & 1 & 1 & 1 & 0 & 0 & 0 & 0 & 0 & 0 & 0 & 0 & 0 & 0 & 0 & 0 & 0 & 0 & 0 & 0 & 0 & 0 & 0 & 0 & 0 & 0 & 0 & 0 & 0 & 0 & 0 & 0 & 0 & 0 & 0 & 0 & 0 & 0 & 0 & 0 & 0 & 0 & 0 & 0 & 1 & 0 \\
0 & 0 & 1 & 1 & 1 & 1 & 1 & 1 & 0 & 0 & 0 & 0 & 0 & 0 & 0 & 0 & 0 & 0 & 0 & 0 & 0 & 0 & 0 & 0 & 0 & 0 & 0 & 0 & 0 & 0 & 0 & 0 & 0 & 0 & 0 & 0 & 0 & 0 & 0 & 0 & 0 & 0 & 0 & 0 & 0 & 0 & 0 & 0 & 0 & 1 \\
1 & 1 & 0 & 1 & 1 & 1 & 1 & 1 & 0 & 0 & 0 & 0 & 0 & 0 & 0 & 0 & 0 & 0 & 0 & 0 & 0 & 0 & 0 & 0 & 0 & 0 & 0 & 0 & 0 & 0 & 0 & 0 & 0 & 0 & 0 & 0 & 0 & 0 & 0 & 0 & 0 & 0 & 0 & 0 & 0 & 0 & 0 & 0 & 0 & 0 \\
1 & 1 & 1 & 0 & 1 & 1 & 1 & 1 & 0 & 0 & 0 & 0 & 0 & 0 & 0 & 0 & 0 & 0 & 0 & 0 & 0 & 0 & 0 & 0 & 0 & 0 & 0 & 0 & 0 & 0 & 0 & 0 & 0 & 0 & 0 & 0 & 0 & 0 & 0 & 0 & 0 & 0 & 0 & 0 & 0 & 0 & 0 & 0 & 0 & 0 \\
1 & 1 & 1 & 1 & 0 & 1 & 1 & 1 & 0 & 0 & 0 & 0 & 0 & 0 & 0 & 0 & 0 & 0 & 0 & 0 & 0 & 0 & 0 & 0 & 0 & 0 & 0 & 0 & 0 & 0 & 0 & 0 & 0 & 0 & 0 & 0 & 0 & 0 & 0 & 0 & 0 & 0 & 0 & 0 & 0 & 0 & 0 & 0 & 0 & 0 \\
1 & 1 & 1 & 1 & 1 & 0 & 1 & 1 & 0 & 0 & 0 & 0 & 0 & 0 & 0 & 0 & 0 & 0 & 0 & 0 & 0 & 0 & 0 & 0 & 0 & 0 & 0 & 0 & 0 & 0 & 0 & 0 & 0 & 0 & 0 & 0 & 0 & 0 & 0 & 0 & 0 & 0 & 0 & 0 & 0 & 0 & 0 & 0 & 0 & 0 \\
1 & 1 & 1 & 1 & 1 & 1 & 0 & 1 & 0 & 0 & 0 & 0 & 0 & 0 & 0 & 0 & 0 & 0 & 0 & 0 & 0 & 0 & 0 & 0 & 0 & 0 & 0 & 0 & 0 & 0 & 0 & 0 & 0 & 0 & 0 & 0 & 0 & 0 & 0 & 0 & 0 & 0 & 0 & 0 & 0 & 0 & 0 & 0 & 0 & 0 \\
1 & 1 & 1 & 1 & 1 & 1 & 1 & 0 & 0 & 0 & 0 & 0 & 0 & 0 & 0 & 0 & 0 & 0 & 0 & 0 & 0 & 0 & 0 & 0 & 0 & 0 & 0 & 0 & 0 & 0 & 0 & 0 & 0 & 0 & 0 & 0 & 0 & 0 & 0 & 0 & 0 & 0 & 0 & 0 & 0 & 0 & 0 & 0 & 0 & 0 \\
0 & 0 & 0 & 0 & 0 & 0 & 0 & 0 & 0 & 0 & 1 & 1 & 1 & 1 & 1 & 1 & 0 & 0 & 0 & 0 & 0 & 0 & 0 & 0 & 0 & 0 & 0 & 0 & 0 & 0 & 0 & 0 & 0 & 0 & 0 & 0 & 0 & 0 & 0 & 0 & 0 & 0 & 0 & 0 & 0 & 0 & 0 & 0 & 1 & 0 \\
0 & 0 & 0 & 0 & 0 & 0 & 0 & 0 & 0 & 0 & 1 & 1 & 1 & 1 & 1 & 1 & 0 & 0 & 0 & 0 & 0 & 0 & 0 & 0 & 0 & 0 & 0 & 0 & 0 & 0 & 0 & 0 & 0 & 0 & 0 & 0 & 0 & 0 & 0 & 0 & 0 & 0 & 0 & 0 & 0 & 0 & 0 & 0 & 0 & 1 \\
0 & 0 & 0 & 0 & 0 & 0 & 0 & 0 & 1 & 1 & 0 & 1 & 1 & 1 & 1 & 1 & 0 & 0 & 0 & 0 & 0 & 0 & 0 & 0 & 0 & 0 & 0 & 0 & 0 & 0 & 0 & 0 & 0 & 0 & 0 & 0 & 0 & 0 & 0 & 0 & 0 & 0 & 0 & 0 & 0 & 0 & 0 & 0 & 0 & 0 \\
0 & 0 & 0 & 0 & 0 & 0 & 0 & 0 & 1 & 1 & 1 & 0 & 1 & 1 & 1 & 1 & 0 & 0 & 0 & 0 & 0 & 0 & 0 & 0 & 0 & 0 & 0 & 0 & 0 & 0 & 0 & 0 & 0 & 0 & 0 & 0 & 0 & 0 & 0 & 0 & 0 & 0 & 0 & 0 & 0 & 0 & 0 & 0 & 0 & 0 \\
0 & 0 & 0 & 0 & 0 & 0 & 0 & 0 & 1 & 1 & 1 & 1 & 0 & 1 & 1 & 1 & 0 & 0 & 0 & 0 & 0 & 0 & 0 & 0 & 0 & 0 & 0 & 0 & 0 & 0 & 0 & 0 & 0 & 0 & 0 & 0 & 0 & 0 & 0 & 0 & 0 & 0 & 0 & 0 & 0 & 0 & 0 & 0 & 0 & 0 \\
0 & 0 & 0 & 0 & 0 & 0 & 0 & 0 & 1 & 1 & 1 & 1 & 1 & 0 & 1 & 1 & 0 & 0 & 0 & 0 & 0 & 0 & 0 & 0 & 0 & 0 & 0 & 0 & 0 & 0 & 0 & 0 & 0 & 0 & 0 & 0 & 0 & 0 & 0 & 0 & 0 & 0 & 0 & 0 & 0 & 0 & 0 & 0 & 0 & 0 \\
0 & 0 & 0 & 0 & 0 & 0 & 0 & 0 & 1 & 1 & 1 & 1 & 1 & 1 & 0 & 1 & 0 & 0 & 0 & 0 & 0 & 0 & 0 & 0 & 0 & 0 & 0 & 0 & 0 & 0 & 0 & 0 & 0 & 0 & 0 & 0 & 0 & 0 & 0 & 0 & 0 & 0 & 0 & 0 & 0 & 0 & 0 & 0 & 0 & 0 \\
0 & 0 & 0 & 0 & 0 & 0 & 0 & 0 & 1 & 1 & 1 & 1 & 1 & 1 & 1 & 0 & 0 & 0 & 0 & 0 & 0 & 0 & 0 & 0 & 0 & 0 & 0 & 0 & 0 & 0 & 0 & 0 & 0 & 0 & 0 & 0 & 0 & 0 & 0 & 0 & 0 & 0 & 0 & 0 & 0 & 0 & 0 & 0 & 0 & 0 \\
0 & 0 & 0 & 0 & 0 & 0 & 0 & 0 & 0 & 0 & 0 & 0 & 0 & 0 & 0 & 0 & 0 & 0 & 1 & 1 & 1 & 1 & 1 & 1 & 0 & 0 & 0 & 0 & 0 & 0 & 0 & 0 & 0 & 0 & 0 & 0 & 0 & 0 & 0 & 0 & 0 & 0 & 0 & 0 & 0 & 0 & 0 & 0 & 1 & 0 \\
0 & 0 & 0 & 0 & 0 & 0 & 0 & 0 & 0 & 0 & 0 & 0 & 0 & 0 & 0 & 0 & 0 & 0 & 1 & 1 & 1 & 1 & 1 & 1 & 0 & 0 & 0 & 0 & 0 & 0 & 0 & 0 & 0 & 0 & 0 & 0 & 0 & 0 & 0 & 0 & 0 & 0 & 0 & 0 & 0 & 0 & 0 & 0 & 0 & 1 \\
0 & 0 & 0 & 0 & 0 & 0 & 0 & 0 & 0 & 0 & 0 & 0 & 0 & 0 & 0 & 0 & 1 & 1 & 0 & 1 & 1 & 1 & 1 & 1 & 0 & 0 & 0 & 0 & 0 & 0 & 0 & 0 & 0 & 0 & 0 & 0 & 0 & 0 & 0 & 0 & 0 & 0 & 0 & 0 & 0 & 0 & 0 & 0 & 0 & 0 \\
0 & 0 & 0 & 0 & 0 & 0 & 0 & 0 & 0 & 0 & 0 & 0 & 0 & 0 & 0 & 0 & 1 & 1 & 1 & 0 & 1 & 1 & 1 & 1 & 0 & 0 & 0 & 0 & 0 & 0 & 0 & 0 & 0 & 0 & 0 & 0 & 0 & 0 & 0 & 0 & 0 & 0 & 0 & 0 & 0 & 0 & 0 & 0 & 0 & 0 \\
0 & 0 & 0 & 0 & 0 & 0 & 0 & 0 & 0 & 0 & 0 & 0 & 0 & 0 & 0 & 0 & 1 & 1 & 1 & 1 & 0 & 1 & 1 & 1 & 0 & 0 & 0 & 0 & 0 & 0 & 0 & 0 & 0 & 0 & 0 & 0 & 0 & 0 & 0 & 0 & 0 & 0 & 0 & 0 & 0 & 0 & 0 & 0 & 0 & 0 \\
0 & 0 & 0 & 0 & 0 & 0 & 0 & 0 & 0 & 0 & 0 & 0 & 0 & 0 & 0 & 0 & 1 & 1 & 1 & 1 & 1 & 0 & 1 & 1 & 0 & 0 & 0 & 0 & 0 & 0 & 0 & 0 & 0 & 0 & 0 & 0 & 0 & 0 & 0 & 0 & 0 & 0 & 0 & 0 & 0 & 0 & 0 & 0 & 0 & 0 \\
0 & 0 & 0 & 0 & 0 & 0 & 0 & 0 & 0 & 0 & 0 & 0 & 0 & 0 & 0 & 0 & 1 & 1 & 1 & 1 & 1 & 1 & 0 & 1 & 0 & 0 & 0 & 0 & 0 & 0 & 0 & 0 & 0 & 0 & 0 & 0 & 0 & 0 & 0 & 0 & 0 & 0 & 0 & 0 & 0 & 0 & 0 & 0 & 0 & 0 \\
0 & 0 & 0 & 0 & 0 & 0 & 0 & 0 & 0 & 0 & 0 & 0 & 0 & 0 & 0 & 0 & 1 & 1 & 1 & 1 & 1 & 1 & 1 & 0 & 0 & 0 & 0 & 0 & 0 & 0 & 0 & 0 & 0 & 0 & 0 & 0 & 0 & 0 & 0 & 0 & 0 & 0 & 0 & 0 & 0 & 0 & 0 & 0 & 0 & 0 \\
0 & 0 & 0 & 0 & 0 & 0 & 0 & 0 & 0 & 0 & 0 & 0 & 0 & 0 & 0 & 0 & 0 & 0 & 0 & 0 & 0 & 0 & 0 & 0 & 0 & 0 & 1 & 1 & 1 & 1 & 1 & 1 & 0 & 0 & 0 & 0 & 0 & 0 & 0 & 0 & 0 & 0 & 0 & 0 & 0 & 0 & 0 & 0 & 1 & 0 \\
0 & 0 & 0 & 0 & 0 & 0 & 0 & 0 & 0 & 0 & 0 & 0 & 0 & 0 & 0 & 0 & 0 & 0 & 0 & 0 & 0 & 0 & 0 & 0 & 0 & 0 & 1 & 1 & 1 & 1 & 1 & 1 & 0 & 0 & 0 & 0 & 0 & 0 & 0 & 0 & 0 & 0 & 0 & 0 & 0 & 0 & 0 & 0 & 0 & 1 \\
0 & 0 & 0 & 0 & 0 & 0 & 0 & 0 & 0 & 0 & 0 & 0 & 0 & 0 & 0 & 0 & 0 & 0 & 0 & 0 & 0 & 0 & 0 & 0 & 1 & 1 & 0 & 1 & 1 & 1 & 1 & 1 & 0 & 0 & 0 & 0 & 0 & 0 & 0 & 0 & 0 & 0 & 0 & 0 & 0 & 0 & 0 & 0 & 0 & 0 \\
0 & 0 & 0 & 0 & 0 & 0 & 0 & 0 & 0 & 0 & 0 & 0 & 0 & 0 & 0 & 0 & 0 & 0 & 0 & 0 & 0 & 0 & 0 & 0 & 1 & 1 & 1 & 0 & 1 & 1 & 1 & 1 & 0 & 0 & 0 & 0 & 0 & 0 & 0 & 0 & 0 & 0 & 0 & 0 & 0 & 0 & 0 & 0 & 0 & 0 \\
0 & 0 & 0 & 0 & 0 & 0 & 0 & 0 & 0 & 0 & 0 & 0 & 0 & 0 & 0 & 0 & 0 & 0 & 0 & 0 & 0 & 0 & 0 & 0 & 1 & 1 & 1 & 1 & 0 & 1 & 1 & 1 & 0 & 0 & 0 & 0 & 0 & 0 & 0 & 0 & 0 & 0 & 0 & 0 & 0 & 0 & 0 & 0 & 0 & 0 \\
0 & 0 & 0 & 0 & 0 & 0 & 0 & 0 & 0 & 0 & 0 & 0 & 0 & 0 & 0 & 0 & 0 & 0 & 0 & 0 & 0 & 0 & 0 & 0 & 1 & 1 & 1 & 1 & 1 & 0 & 1 & 1 & 0 & 0 & 0 & 0 & 0 & 0 & 0 & 0 & 0 & 0 & 0 & 0 & 0 & 0 & 0 & 0 & 0 & 0 \\
0 & 0 & 0 & 0 & 0 & 0 & 0 & 0 & 0 & 0 & 0 & 0 & 0 & 0 & 0 & 0 & 0 & 0 & 0 & 0 & 0 & 0 & 0 & 0 & 1 & 1 & 1 & 1 & 1 & 1 & 0 & 1 & 0 & 0 & 0 & 0 & 0 & 0 & 0 & 0 & 0 & 0 & 0 & 0 & 0 & 0 & 0 & 0 & 0 & 0 \\
0 & 0 & 0 & 0 & 0 & 0 & 0 & 0 & 0 & 0 & 0 & 0 & 0 & 0 & 0 & 0 & 0 & 0 & 0 & 0 & 0 & 0 & 0 & 0 & 1 & 1 & 1 & 1 & 1 & 1 & 1 & 0 & 0 & 0 & 0 & 0 & 0 & 0 & 0 & 0 & 0 & 0 & 0 & 0 & 0 & 0 & 0 & 0 & 0 & 0 \\
0 & 0 & 0 & 0 & 0 & 0 & 0 & 0 & 0 & 0 & 0 & 0 & 0 & 0 & 0 & 0 & 0 & 0 & 0 & 0 & 0 & 0 & 0 & 0 & 0 & 0 & 0 & 0 & 0 & 0 & 0 & 0 & 0 & 0 & 1 & 1 & 1 & 1 & 1 & 1 & 0 & 0 & 0 & 0 & 0 & 0 & 0 & 0 & 1 & 0 \\
0 & 0 & 0 & 0 & 0 & 0 & 0 & 0 & 0 & 0 & 0 & 0 & 0 & 0 & 0 & 0 & 0 & 0 & 0 & 0 & 0 & 0 & 0 & 0 & 0 & 0 & 0 & 0 & 0 & 0 & 0 & 0 & 0 & 0 & 1 & 1 & 1 & 1 & 1 & 1 & 0 & 0 & 0 & 0 & 0 & 0 & 0 & 0 & 0 & 1 \\
0 & 0 & 0 & 0 & 0 & 0 & 0 & 0 & 0 & 0 & 0 & 0 & 0 & 0 & 0 & 0 & 0 & 0 & 0 & 0 & 0 & 0 & 0 & 0 & 0 & 0 & 0 & 0 & 0 & 0 & 0 & 0 & 1 & 1 & 0 & 1 & 1 & 1 & 1 & 1 & 0 & 0 & 0 & 0 & 0 & 0 & 0 & 0 & 0 & 0 \\
0 & 0 & 0 & 0 & 0 & 0 & 0 & 0 & 0 & 0 & 0 & 0 & 0 & 0 & 0 & 0 & 0 & 0 & 0 & 0 & 0 & 0 & 0 & 0 & 0 & 0 & 0 & 0 & 0 & 0 & 0 & 0 & 1 & 1 & 1 & 0 & 1 & 1 & 1 & 1 & 0 & 0 & 0 & 0 & 0 & 0 & 0 & 0 & 0 & 0 \\
0 & 0 & 0 & 0 & 0 & 0 & 0 & 0 & 0 & 0 & 0 & 0 & 0 & 0 & 0 & 0 & 0 & 0 & 0 & 0 & 0 & 0 & 0 & 0 & 0 & 0 & 0 & 0 & 0 & 0 & 0 & 0 & 1 & 1 & 1 & 1 & 0 & 1 & 1 & 1 & 0 & 0 & 0 & 0 & 0 & 0 & 0 & 0 & 0 & 0 \\
0 & 0 & 0 & 0 & 0 & 0 & 0 & 0 & 0 & 0 & 0 & 0 & 0 & 0 & 0 & 0 & 0 & 0 & 0 & 0 & 0 & 0 & 0 & 0 & 0 & 0 & 0 & 0 & 0 & 0 & 0 & 0 & 1 & 1 & 1 & 1 & 1 & 0 & 1 & 1 & 0 & 0 & 0 & 0 & 0 & 0 & 0 & 0 & 0 & 0 \\
0 & 0 & 0 & 0 & 0 & 0 & 0 & 0 & 0 & 0 & 0 & 0 & 0 & 0 & 0 & 0 & 0 & 0 & 0 & 0 & 0 & 0 & 0 & 0 & 0 & 0 & 0 & 0 & 0 & 0 & 0 & 0 & 1 & 1 & 1 & 1 & 1 & 1 & 0 & 1 & 0 & 0 & 0 & 0 & 0 & 0 & 0 & 0 & 0 & 0 \\
0 & 0 & 0 & 0 & 0 & 0 & 0 & 0 & 0 & 0 & 0 & 0 & 0 & 0 & 0 & 0 & 0 & 0 & 0 & 0 & 0 & 0 & 0 & 0 & 0 & 0 & 0 & 0 & 0 & 0 & 0 & 0 & 1 & 1 & 1 & 1 & 1 & 1 & 1 & 0 & 0 & 0 & 0 & 0 & 0 & 0 & 0 & 0 & 0 & 0 \\
0 & 0 & 0 & 0 & 0 & 0 & 0 & 0 & 0 & 0 & 0 & 0 & 0 & 0 & 0 & 0 & 0 & 0 & 0 & 0 & 0 & 0 & 0 & 0 & 0 & 0 & 0 & 0 & 0 & 0 & 0 & 0 & 0 & 0 & 0 & 0 & 0 & 0 & 0 & 0 & 0 & 0 & 1 & 1 & 1 & 1 & 1 & 1 & 1 & 0 \\
0 & 0 & 0 & 0 & 0 & 0 & 0 & 0 & 0 & 0 & 0 & 0 & 0 & 0 & 0 & 0 & 0 & 0 & 0 & 0 & 0 & 0 & 0 & 0 & 0 & 0 & 0 & 0 & 0 & 0 & 0 & 0 & 0 & 0 & 0 & 0 & 0 & 0 & 0 & 0 & 0 & 0 & 1 & 1 & 1 & 1 & 1 & 1 & 0 & 1 \\
0 & 0 & 0 & 0 & 0 & 0 & 0 & 0 & 0 & 0 & 0 & 0 & 0 & 0 & 0 & 0 & 0 & 0 & 0 & 0 & 0 & 0 & 0 & 0 & 0 & 0 & 0 & 0 & 0 & 0 & 0 & 0 & 0 & 0 & 0 & 0 & 0 & 0 & 0 & 0 & 1 & 1 & 0 & 1 & 1 & 1 & 1 & 1 & 0 & 0 \\
0 & 0 & 0 & 0 & 0 & 0 & 0 & 0 & 0 & 0 & 0 & 0 & 0 & 0 & 0 & 0 & 0 & 0 & 0 & 0 & 0 & 0 & 0 & 0 & 0 & 0 & 0 & 0 & 0 & 0 & 0 & 0 & 0 & 0 & 0 & 0 & 0 & 0 & 0 & 0 & 1 & 1 & 1 & 0 & 1 & 1 & 1 & 1 & 0 & 0 \\
0 & 0 & 0 & 0 & 0 & 0 & 0 & 0 & 0 & 0 & 0 & 0 & 0 & 0 & 0 & 0 & 0 & 0 & 0 & 0 & 0 & 0 & 0 & 0 & 0 & 0 & 0 & 0 & 0 & 0 & 0 & 0 & 0 & 0 & 0 & 0 & 0 & 0 & 0 & 0 & 1 & 1 & 1 & 1 & 0 & 1 & 1 & 1 & 0 & 0 \\
0 & 0 & 0 & 0 & 0 & 0 & 0 & 0 & 0 & 0 & 0 & 0 & 0 & 0 & 0 & 0 & 0 & 0 & 0 & 0 & 0 & 0 & 0 & 0 & 0 & 0 & 0 & 0 & 0 & 0 & 0 & 0 & 0 & 0 & 0 & 0 & 0 & 0 & 0 & 0 & 1 & 1 & 1 & 1 & 1 & 0 & 1 & 1 & 0 & 0 \\
0 & 0 & 0 & 0 & 0 & 0 & 0 & 0 & 0 & 0 & 0 & 0 & 0 & 0 & 0 & 0 & 0 & 0 & 0 & 0 & 0 & 0 & 0 & 0 & 0 & 0 & 0 & 0 & 0 & 0 & 0 & 0 & 0 & 0 & 0 & 0 & 0 & 0 & 0 & 0 & 1 & 1 & 1 & 1 & 1 & 1 & 0 & 1 & 0 & 0 \\
0 & 0 & 0 & 0 & 0 & 0 & 0 & 0 & 0 & 0 & 0 & 0 & 0 & 0 & 0 & 0 & 0 & 0 & 0 & 0 & 0 & 0 & 0 & 0 & 0 & 0 & 0 & 0 & 0 & 0 & 0 & 0 & 0 & 0 & 0 & 0 & 0 & 0 & 0 & 0 & 1 & 1 & 1 & 1 & 1 & 1 & 1 & 0 & 0 & 0 \\
1 & 0 & 0 & 0 & 0 & 0 & 0 & 0 & 1 & 0 & 0 & 0 & 0 & 0 & 0 & 0 & 1 & 0 & 0 & 0 & 0 & 0 & 0 & 0 & 1 & 0 & 0 & 0 & 0 & 0 & 0 & 0 & 1 & 0 & 0 & 0 & 0 & 0 & 0 & 0 & 1 & 0 & 0 & 0 & 0 & 0 & 0 & 0 & 0 & 1 \\
0 & 1 & 0 & 0 & 0 & 0 & 0 & 0 & 0 & 1 & 0 & 0 & 0 & 0 & 0 & 0 & 0 & 1 & 0 & 0 & 0 & 0 & 0 & 0 & 0 & 1 & 0 & 0 & 0 & 0 & 0 & 0 & 0 & 1 & 0 & 0 & 0 & 0 & 0 & 0 & 0 & 1 & 0 & 0 & 0 & 0 & 0 & 0 & 1 & 0
\end{array}\right)
$$

Bibliography

D. Acemoglu, A. Ozdaglar, and A. Tahbaz-Salehi. Systemic risk and stability in financial networks. *American Economic Review*, 105(2):564–608, 2015.

T. Adrian and H. S. Shin. Liquidity and leverage. *Journal of Financial Intermediation*, 19(3):418–437, 2010.

T. Adrian and H.S. Shin. Procyclical leverage and value-at-risk. *The Review of Financial Studies*, 27(2):373–403, 2014.

H. Amini, D. Filipović, and A. Minca. Systemic risk with central counterparty clearing. Swiss Finance Institute Research Paper No. 13-34, Swiss Finance Institute, 2013.

H. Amini, D. Filipović, and A. Minca. Uniqueness of equilibrium in a payment system with liquidation costs. *Operations Research Letters*, 44(1):1–5, 2016.

K. Awiszus, A. Capponi, and S. Weber. Market efficient portfolios in a systemic economy. Working Paper, 2020.

N. Beale, D. G. Rand, H. Battey, K. Croxson, R. M. May, and M. A. Nowak. Individual versus systemic risk and the regulator's dilemma. *Proceedings of the National Academy of Sciences*, 108(31):12647–12652, 2011.

D. S. Bernstein. *Matrix Mathematics: Theory, Facts, and Formulas*. Princeton University Press, 2005.

C. Bezuidenhout and G. Grimmett. The critical contact process dies out. *The Annals of Probability*, 18(4):1462–1482, 1990.

R. Bhatia. *Matrix Analysis*. Graduate Texts in Mathematics. Springer New York, 2013.

F. Biagini, J.-P. Fouque, M. Frittelli, and T. Meyer-Brandis. A unified approach to systemic risk measures via acceptance sets. *Mathematical Finance*, 29(1):329–367, 2019.

T. R. Bielecki and M. Rutkowski. *Credit Risk: Modeling, Valuation and Hedging*. Springer Finance. Springer-Verlag, Berlin, Heidelberg, 2004.

M. Boguñá and R. Pastor-Satorras. Epidemic spreading in correlated complex networks. *Physical Review E*, 66:047104, Oct 2002.

R. Böhme. Cyber-insurance revisited. In *Workshop on the Economics of Information Security (WEIS)*, 2005.

J. Bolot and M. Lelarge. A new perspective on internet security using insurance. In *INFOCOM 2008. The 27th Conference on Computer Communications. IEEE*, 2008.

M. Boucinha, S. Holton, and A. Tiseno. Bank equity valuations and credit supply. Working Paper, 2017.

P. Brémaud. *Point Processes and Queues: Martingale Dynamics*. Springer Series in Statistics. Springer-Verlag, New York, Heidelberg, Berlin, 1981.

F. Brioschi, L. Buzzacchi, and M. G. Colombo. Risk capital financing and the separation of ownership and control in business groups. *Journal of Banking and Finance*, 13(4): 747–772, 1989.

M. Brunnermeier and L. Pedersen. Market liquidity and funding liquidity. *The Review of Financial Studies*, 22(6):2201–2238, 2008.

M. K. Brunnermeier. Deciphering the liquidity and credit crunch 2007-2008. *The Journal of Economic Perspectives*, 23(1):77–100, 2009.

M. K. Brunnermeier, M. Sockin, and W. Xiong. China's model of managing its financial system. *Working Paper, Princeton University*, 2018.

K. Burnecki, J. Janczura, and R. Weron. Building loss models. In Cizek P., H́ardle W., and R. Weron, editors, *Statistical Tools for Finance and Insurance*, pages 293–328. Springer-Verlag, Berlin, Heidelberg, 2011.

F. Caccioli, M Shrestha, C. Moore, and J. D. Farmer. Stability analysis of financial contagion due to overlapping portfolios. *Journal of Banking & Finance*, 46:233–245, 2014.

A. Capponi and M. Larsson. Price contagion through balance sheet linkages. *The Review of Asset Pricing Studies*, 5(2):227–253, 2015.

A. Capponi, P.C. Chen, and D. Yao. Liability concentration and systemic losses in financial networks. *Operations Research*, 64(5):1121–1134, 2016.

E. Cator and P. Van Mieghem. Second-order mean-field susceptible-infected-susceptible epidemic threshold. *Physical Review E*, 85(5):056111, 2012.

E. Cator and P. Van Mieghem. Nodal infection in markovian susceptible-infected-susceptible and susceptible-infected-removed epidemics on networks are non-negatively correlated. *Physical Review E*, 89(5):052802, 2014.

C. Chen, G. Iyengar, and C. C. Moallemi. An axiomatic approach to systemic risk. *Management Science*, 59(6):1373–1388, 2013.

N. Chen, X. Liu, and D. D. Yao. An optimization view of financial systemic risk modeling: Network effect and market liquidity effect. *Operations Research*, 64(5):1089–1108, 2016.

Q. Chen, I. Goldstein, and W. Jiang. Payoff complementarities and financial fragility: Evidence from mutual fund outflows. *Journal of Financial Economics*, 97(2):239–262, 2010.

R. Cifuentes, G. Ferrucci, and H. S. Shin. Liquidity risk and contagion. *Journal of the European Economic Association*, 3(2-3):556–566, 2005.

R. Cont and E. Schaaning. Fire sales, indirect contagion and systemic stress testing. Working Paper 02/2017, Norges Bank, 2017.

R. Cont and L. Wagalath. Fire sales forensics: Measuring endogenous risk. *Mathematical Finance*, 26(4):835–866, 2016.

R. Cont, A. Moussa, and E. B. Santos. Network structure and systemic risk in banking systems. In *Handbook on Systemic Risk*, pages 327–368. Cambridge University Press, 2013.

J. Coval and E. Stafford. Asset fire sales (and purchases) in equity markets. *Journal of Financial Economics*, 86(2):479–512, 2007.

B. Craig and G. von Peter. Interbank tiering and money center banks. *Journal of Financial Intermediation*, 23(3):322–347, 2014.

J. Dattorro. *Convex Optimization & Euclidean Distance Geometry*. Meboo Publishing, 2005.

J. Dow and G. Gorton. Stock market efficiency and economic efficiency: Is there a connection? *The Journal of Finance*, 52(3):1087–1129, 1997.

J. Dow and R. Rahi. Informed trading, investment, and welfare. *The Journal of Business*, 76(3):439–454, 2003.

M. Drehmann and N. Tarashev. Measuring the systemic importance of interconnected banks. BIS Working Paper 342, Bank for International Settlements, 2011.

F. Duarte and T. M. Eisenbach. Fire-sale spillovers and systemic risk. *FRB of New York Staff Report*, (645), 2019.

R. Durrett and X.-F. Liu. The contact process on a finite set. *The Annals of Probability*, 16(3):1158–1173, 1988.

L. Eisenberg and T. H. Noe. Systemic risk in financial systems. *Management Science*, 47 (7):236–249, 2001.

M. Elliott, B. Golub, and M. O. Jackson. Financial networks and contagion. *American Economic Review*, 104(10):3115–3153, 2014.

H. Elsinger. Financial networks, cross holdings, and limited liability. Working Papers 156, Österreichische Nationalbank (Austrian Central Bank), 2009.

H. Elsinger, A. Lehar, and M. Summer. Risk assessment for banking systems. *Management Science*, 52(9):1301–1314, 2006.

P. Erdős and A. Rényi. On random graphs, I. *Publicationes Mathematicae (Debrecen)*, 6: 290–297, 1959.

M. A. Fahrenwaldt, S. Weber, and K. Weske. Pricing of cyber insurance contracts in a network model. *ASTIN Bulletin*, 48(3):1175–1218, 2018.

M. Fedenia, J. E. Hodder, and A. J. Triantis. Cross-holdings: Estimation issues, biases, and distortions. *Review of Financial Studies*, 7(1):61–96, 1994.

Z. Feinstein. Financial contagion and asset liquidation strategies. *Operations Research Letters*, 45(2):109–114, 2017.

Z. Feinstein, B. Rudloff, and S. Weber. Measures of systemic risk. *SIAM Journal on Financial Mathematics*, 8(1):672–708, 2017.

T. Fischer. No-arbitrage pricing under systemic risk: Accounting for cross-ownership. *Mathematical Finance*, 24(1):97–124, 2014.

H. Föllmer and A. Schied. *Stochastic Finance - An Introduction in Discrete Time*. De Gruyter, Berlin, 3rd edition, 2011.

H. Föllmer and S. Weber. The Axiomatic Approach to Risk Measurement for Capital Determination. *Annual Review of Financial Economics,*, 7:301–337, 2015.

R. M. Freund. *Optimality conditions for constrained optimization problems*. Massachusetts Institute of Technology, 2016. Lecture Notes.

P. Gai and S. Kapadia. Contagion in financial networks. *Proceedings of the Royal Society A*, 466:2401–2423, 2010.

S. Gandel. Lloyd's CEO: Cyber attacks cost companies $400 billion every year. *Fortune*, 2015. 23 January 2015, http://fortune.com/2015/01/23/cyber-attack-insurance-lloyds/.

K. Giesecke and S. Weber. Cyclical correlations, credit contagion, and portfolio losses. *Journal of Banking and Finance*, 28(12):3009–3036, 2004.

K. Giesecke and S. Weber. Credit contagion and aggregate losses. *Journal of Economic Dynamics and Control*, 30(5):741–767, 2006.

G. Girardi, W. Kathleen, N. Stanislava, L. Pelizzon, and M. Getmansky. Portfolio similarity and asset liquidation in the insurance industry. *Working Paper*, 2019.

P. Glasserman and H. P. Young. How likely is contagion in financial networks? *Journal of Banking and Finance*, 50:383–399, 2015.

I. Goldstein and A. Guembel. Manipulation and the Allocational Role of Prices. *The Review of Economic Studies*, 75(1):133–164, 2008.

D. Greenlaw, J. Hatzius, A. Kashyap, and H.S. Shin. Leveraged losses: Lessons from the mortgage market meltdown. *Proceedings of the U.S. Monetary Policy Forum*, 2008.

R. Greenwood, A. Landier, and D. Thesmar. Vulnerable banks. *Journal of Financial Economics*, 115(3):471–485, 2015.

F. A. Hayek. The use of knowledge in society. *The American Economic Review*, 35(4): 519–530, 1945.

E. Hille. *Lectures on ordinary differential equations*. Addison-Wesley series in mathematics. Addison-Wesley Pub. Co., 1968.

R. A. Horn and C. R. Johnson. *Matrix analysis*. Cambridge University Press, 1985.

R. Ibragimov, D. Jaffee, and J. Walden. Diversification disasters. *Journal of Financial Economics*, 99(2):333–348, 2011.

M. Jacobsen. *Point Process Theory and Applications: Marked Point and Piecewise Deterministic Processes*. Probability and Its Applications. Birkhäuser, Boston, 2006.

J. Jacod. Multivariate point processes: predictable projection, radon-nikodym derivatives, representation of martingales. *Zeitschrift für Wahrscheinlichkeitstheorie und Verwandte Gebiete*, 31(3):235–253, 1975.

C. Jotikasthira, C. Lundblad, and T. Ramadorai. Asset fire sales and purchases and the international transmission of funding shocks. *The Journal of Finance*, 67(6):2015–2050, 2012.

S. Karl and T. Fischer. Cross-ownership as a structural explanation for over- and underestimation of default probability. *Quantitative Finance*, 14(6):1031–1046, 2014.

A. E. Khandani and A. W. Lo. What happened to the quants in august 2007? Evidence from factors and transactions data. *Journal of Financial Markets*, 14(1):1–46, 2011.

G. Last and A. Brandt. *Marked point processes on the real line: The dynamic approach*. Probability and its Applications (New York). Springer-Verlag, New York, 1995.

H. E. Leland. Insider trading: Should it be prohibited? *Journal of Political Economy*, 100 (4):859–887, 1992.

T. M. Liggett. *Interacting particle systems*, volume 276 of *Grundlehren der Mathematischen Wissenschaften*. Springer-Verlag, New York, 1985.

T. M. Liggett. *Stochastic interacting systems: contact, voter and exclusion processes*, volume 324 of *Grundlehren der Mathematischen Wissenschaften*. Springer-Verlag, Berlin, 1999.

A. Marotta, F. Martinelli, S. Nanni, and A. Yautsiukhin. A survey on cyber-insurance. Technical Report IIT TR-17/2015, Istituto di Informatica e Telematica, Consiglio Nazionale delle Richerce, Pisa, 2015.

F. D. Martínez Pería, P. G. Massey, and L. E. Silvestre. Weak matrix majorization. *Linear algebra and its applications*, 403:343–368, 2005.

A. S. Mata and S. C. Ferreira. Pair quenched mean-field theory for the susceptible-infected-susceptible model on complex networks. *EPL (Europhysics Letters)*, 103(4): 48003, 2013.

J. Matkowski. Mean-value theorem for vector-valued functions. *Mathematica Bohemica*, 137(4):415–423, 2012.

T. Mountford, J.-C. Mourrat, D. Valesin, and Q. Yao. Exponential extinction time of the contact process on finite graphs. *Stochastic Processes and their Applications*, 126(7): 1974–2013, 2016.

E. Nier, J. Yang, T. Yorulmazer, and A. Alentorn. Network models and financial stability. *Journal of Economic Dynamics and Control*, 31(6):2033–2060, 2007.

C. Nowzari, V. M. Preciado, and G. J. Pappas. Analysis and control of epidemics: A survey of spreading processes on complex networks. *IEEE Control Syst. Mag.*, 36(1): 26–46, 2016.

R. Pastor-Satorras and A. Vespignani. Epidemic dynamics and endemic states in complex networks. *Physical Review E*, 63:066117, May 2001.

R. Pastor-Satorras, C. Castellano, P. Van Mieghem, and A. Vespignani. Epidemic processes in complex networks. *Reviews of modern physics*, 87(3):925, 2015.

C. Pirrong. *The Economics of Central Clearing: Theory and Practice*. International Swaps and Derivatives Association, 2011.

P. E. Protter. *Stochastic Integration and Differential Equations*, volume 21 of *Applications of Mathematics*. Springer-Verlag, Berlin, Heidelberg, 2004.

L. Raffestin. Diversification and systemic risk. *Journal of Banking & Finance*, 46:85–106, 2014.

L. C. G. Rogers and L. A. M. Veraart. Failure and rescue in an interbank network. *Management Science*, 59(4):882–898, 2013.

G. A. Schwartz and S. S. Sastry. Cyber-insurance framework for large scale interdependent networks. In *Proceedings of the 3rd international conference on High confidence networked systems*, pages 145–154. ACM, 2014.

A. Shleifer and R. W. Vishny. Liquidation values and debt capacity: A market equilibrium approach. *The Journal of Finance*, 47(4):1343–1366, 1992.

A. Shleifer and R. W. Vishny. Fire sales in finance and macroeconomics. *Journal of Economic Perspectives*, 25(1):29–48, March 2011.

J. Staum. Counterparty contagion in context: Contributions to systemic risk. In *Handbook on Systemic Risk*, pages 512–548. Cambridge University Press, 2013.

A. Subrahmanyam and S. Titman. Feedback from stock prices to cash flows. *The Journal of Finance*, 56(6):2389–2413, 2001.

T. Suzuki. Valuing corporate debt : The effect of cross-holdings of stock and debt. *Journal of the Operations Research Society of Japan*, 45(2):123–144, jun 2002.

Swiss Re Institute. Cyber: getting to grisps with a complex risk. sigma 1/2017, 2017.

Swiss Re/IBM. Cyber: in search of resilience in an interconnected world. Technical report, 2016.

A. Tarski. A lattice-theoretical fixpoint theorem and its applications. *Pacific Journal of Mathematics*, 5(2), 1955.

M. E. Taylor. *Partial Differential Equations I: Basic Theory*, volume 115 of *Applied Mathematical Sciences*. Springer-Verlag, New York, second edition, 2011.

G. Teschl. *Ordinary Differential Equations and Dynamical Systems*, volume 140 of *Graduate Studies in Mathematics*. American Mathematical Society, Providence, 2012.

C. Upper. Using counterfactual simulations to assess the danger of contagion in interbank markets. BIS Working Papers 234, Bank for International Settlements, 2007.

C. Upper. Simulation methods to assess the danger of contagion in interbank markets. *Journal of Financial Stability*, 7(3):111–125, 2011.

I. van Lelyveld and D. in 't Veld. Finding the core: Network structure in interbank markets. *Journal of Banking & Finance*, 49:27 – 40, 2014.

P. Van Mieghem. The N-intertwined SIS epidemic network model. *Computing*, 93(2-4): 147–169, 2011.

P. Van Mieghem and R. van de Bovenkamp. Accuracy criterion for the mean-field approximation in susceptible-infected-susceptible epidemics on networks. *Physical Review E*, 91(3):032812, 2015.

P. Van Mieghem, J. Omic, and R. Kooij. Virus spread in networks. *IEEE/ACM Transactions on Networking*, 17(1):1–14, 2009.

W. Wagner. Systemic liquidation risk and the diversity–diversification trade-off. *The Journal of Finance*, 66(4):1141–1175, 2011.

S. Weber and K. Weske. The joint impact of bankruptcy costs, fire sales and cross-holdings on systemic risk in financial networks. *Probability, Uncertainty and Quantitative Risk*, 2(9):1–38, 2017.

List of Figures

1.1 Example networks for the models in the three chapters of this thesis. . . . 2

2.1 Contour plots of the number of defaults for $n = 100$ banks as a function of (a) bankruptcy costs and (b) fire sales, averaged over 1000 simulations of Π. The simulation procedure is explained in Remark 2.3.1. 22

2.2 Number of defaults for $n = 100$ banks as a function of (a) integration and (b) diversification of the cross-holdings matrix C, realized fraction of cross-holdings' market value $\kappa = 0.8$, averaged over 100 simulations of Π, each averaged over 100 simulations of C. The simulation procedure is explained in Remark 2.3.1. 24

2.3 Number of defaults as a function of the realized fraction κ of cross-holdings' market value, varying integration and diversification $d = 10$, averaged over 100 simulations of Π, each averaged over 100 simulations of C. The simulation procedure is explained in Remark 2.3.1. 24

2.4 Standard deviation of the number of defaults for $n = 100$ banks (a) as a function of both parameters of bankruptcy costs for 1000 simulations of Π, and (b) as a function of integration of the cross-holdings matrix C for 100 simulations of Π, each averaged over 100 simulations of C. The simulation procedure is explained in Remark 2.3.1. 25

2.5 Contour plot of the number of defaults for $n = 100$ banks as a function of both parameters of fire sales, ρ and γ, for $\alpha = 0.9$, $\beta = 0.9$, $c = 0.5$, $d = 10$, $\kappa = 0.8$, $\mathbb{I} = \mathbf{1}$ in (a) and $\mathbb{I} = \mathbf{0}$ in (b), averaged over 100 simulations of Π, each averaged over 100 simulations of C. The simulation procedure is explained in Remark 2.3.1. 27

2.6 Contour plot of the price of the illiquid asset for $n = 100$ banks as a function of both parameters of fire sales, ρ and γ, for $\alpha = 0.9$, $\beta = 0.9$, $c = 0.5$, $d = 10$, $\kappa = 0.8$, $\mathbb{I} = \mathbf{1}$ in (a) and $\mathbb{I} = \mathbf{0}$ in (b), averaged over 100 simulations of Π, each averaged over 100 simulations of C. The simulation procedure is explained in Remark 2.3.1. 28

2.7 Average (a) and standard deviation (b) of the number of defaults for $n = 100$ banks as a function of integration c for $d = 10$, and for different bankruptcy costs parametrized by α in an integrated financial system with $\beta = 0.9$, $\gamma = 0.2$, $\rho = 0.02$, $\kappa = 0.8$, $\mathbb{I} = \mathbf{1}$ averaged over 100 simulations of Π, each averaged over 100 simulations of C. The simulation procedure is explained in Remark 2.3.1. 29

2.8 Empirical cumulative distribution functions of the number of defaults in 100 simulations of the relative liabilities matrix Π each averaged over 100 simulations of C, for two integration values $c = 0.3$ and $c = 0.7$ for $\alpha = 0.9$ (a) and $\alpha = 0.925$ (b). 29

2.9 Level sets of the lowest capital adequacy ratio in the banking system $CAR := \min_{i \in \mathcal{N}} CAR_i$ as a function of the buffer δ and the proportion ρ of the illiquid asset in an ENBF-model with $\alpha = 0.925, \beta = 0.9$, and $\gamma = 0.2$. The solid line is the boundary between many (lower right) and few (upper left) defaults. Results are averaged over 100 simulations of Π. The simulation procedure is explained in Remark 2.3.1. 31

2.10 Sample of (a) an Erdős–Rényi random network as described in Section 2.3.1.1 and (b) a core-periphery random network as described in Section 2.3.2.1; here, the highly connected core nodes are highlighted in red. . . . 32

2.11 Contour plots of the number of defaults for $n = 100$ banks as a function of (a) bankruptcy costs and (b) fire sales, conditional on an initial core shock, averaged over 100 simulations of Π, simulated as a core-periphery random network. The simulation procedure is explained in Remark 2.3.1. 34

2.12 Contour plot of the number of defaults for $n = 100$ banks as a function of fire sales in the joint model ($\alpha = 0.9, \beta = 0.9, c = 0.5, d = 10, \kappa = 0.8, \mathbb{I} = \mathbf{1}$), conditional on an initial core default, averaged over 100 simulations of Π, simulated as a core-periphery random network, each averaged over 100 simulations of C simulated as an Erdős–Rényi random network. The simulation procedure is explained in Remark 2.3.1. 35

2.13 Contour plot of the average number of bank defaults as a function of fire sales parameters ρ_{banks} and γ in an ENF-model, averaged over 100 simulations of Π and periphery link choices. The simulation procedure is explained in Remark 2.3.1. 37

2.14 Capital requirements for core and periphery banks as a function of fire sales (varying ρ and fixed $\gamma = 0.2$) (a) separately and (b) together with different levels of bankruptcy costs (varying β and fixed $\alpha = 1$). 38

3.1 f-efficient holdings of bank 1 $\boldsymbol{Q}^{2\times2}_{k,1}$ for assets $k = 1,2$ and distance from diversification, $d(\boldsymbol{Q}^{2\times2}) = \|\boldsymbol{Q}^{2\times2} - \boldsymbol{Q}^{\text{diversified}}\|_F$, as a function of σ_1^2. We fix $\sigma_2^2 = 0.2$, $\mu = (0,0)^\top$, $v = (0.04,0.07)^\top$, $q = b = (0.08,0.08)^\top$. 67
3.2 F-efficient holdings of bank 1 $\boldsymbol{Q}^{2\times2}_{k,1}$ for assets $k = 1,2$ and distance from diversification $d(\boldsymbol{Q}^{2\times2}) = \|\boldsymbol{Q}^{2\times2} - \boldsymbol{Q}^{\text{diversified}}\|_F$ as a function of μ_2 for fixed $\sigma^2 = (0.1,0.2)^\top$, $\mu_1 = 0$, $v = (0.04,0.07)^\top$, $q = b = (0.08,0.08)^\top$. . 68
3.3 F-efficient holdings of bank 1 $\boldsymbol{Q}^{2\times2}_{k,1}$ for assets $k = 1,2$ and distance from diversification $d(\boldsymbol{Q}^{2\times2}) = \|\boldsymbol{Q}^{2\times2} - \boldsymbol{Q}^{\text{diversified}}\|_F$ as a function of systemic significance v_2 for fixed $\sigma^2 = (0.1,0.2)^\top$, $\mu = (0,0)^\top$, $v_1 = 0.04$, $q = b = (0.08,0.08)^\top$. 70
3.4 Isosurface plot of the Frobenius distance $d(\boldsymbol{Q}^{\min})$ from diversification for the f-efficient holding matrix $\boldsymbol{Q}^{\min}$ with the smallest distance to diversification. We vary the systemic significance parameters v_1, v_2, and v_3, and keep fixed shock characteristics, i.e., $\mu = (0.1,0.125,0.15)^\top$ and $\sigma^2 = (0.1,0.15625,0.225)^\top$. To ensure comparability with the results of Section 3.4.1, we choose $q_k = b_i = 0.08$, $i,k = 1,2,3$, and normalize the total supply of each asset to 1. 71
3.5 Probability density function estimates (a) and box plots (b) of market inefficiency $MC^e - MC^f$ for f-efficient ($\boldsymbol{Q}^{*,\cdot}$) and fully diversified ($\boldsymbol{Q}^{\text{diversified}}$) holdings, generated from 100,000 samples of $Z \sim \mathcal{N}_{10}(\mu, \text{Diag}((\sigma^\cdot)^2))$, in the three considered scenarios: (L) liquidity, (I) intermediate crisis, and (H) high risk high illiquidity. 75

4.1 A regular network with $N = 7$ nodes and degree $D = 4$. 113
4.2 Comparison of the aggregate infection probability of all nodes (A) and of initially healthy nodes (B) for the network described in Figure 4.1. 113
4.3 Exact approximation error and upper bound for different values of the curing rate δ and fixed $\beta = 1/2$ in the regular network A (given in Figure 4.1) with initial state $V(0) = (1,0,0,0,0,0,0)^\top$. 115
4.4 A network with $N = 7$ nodes and spectral radius $\hat{\mu} \approx 2.3429$. 120
4.5 Aggregate infection probability of initially healthy nodes. Solid lines represent naive single split approximations; dashed lines correspond to the results of Algorithm 4.2.14 ($\alpha = 0.5$) under a single split; dotted lines represent the results of Algorithm 4.2.14 ($\alpha = 0.5$) under an equal split. . 121
4.6 Stylized regular network scenarios. Quantities that are kept constant are the number of nodes $N = 50$ and the degree of each node $D = 7$. In particular, this yields a constant total number of edges $ND/2 = 175$ and a constant spectral radius $\hat{\mu} = D = 7$. 122

4.7 Infection scenario: The red nodes (3,5,13,15,23,25,33,35,43,45) are initially infected. 123

4.8 Mean-field approximations of order $n = 1, 2, 3, 4$ for the aggregate infection probability of initially healthy nodes in the homogeneous (a), clustered (b), and star network (c). Part (d) compares the fourth order mean-field approximations for the different network structures. 125

4.9 Best uniform polynomial approximations of $g^{\text{Cat-XL}}$ for different polynomial degrees in the compact interval $[0, 124.3412]$. 128

List of Tables

2.1 Extension parameters 21

3.1 Statistics from the Monte Carlo simulation used to estimate the exact market capitalization. The Frobenius distance $d(\boldsymbol{Q}^{*,\cdot})$ measures the difference between diversified and f-efficient holdings. The last two columns present the numbers relative to the liquidity scenario. 76

4.1 Proportional insurance 126
4.2 Excess of loss per risk (XL) 126
4.3 Excess of loss per event (Cat-XL) 128

Publications

- The work presented in Chapter 2 of this thesis was previously published as *The Joint Impact of Bankruptcy Costs, Fire Sales and Cross-Holdings on Systemic Risk in Financial Networks* in *Probability, Uncertainty and Quantitative Risk*, 2(9):1–38, 2017 (joint work with Stefan Weber).
- The work presented in Chapter 3 is based on the working paper *Market Efficient Portfolios in a Systemic Economy* (joint work with Agostino Capponi and Stefan Weber).
- The work presented in Chapter 4 was previously published as *Pricing of Cyber Insurance Contracts in a Network Model* in *ASTIN Bulletin*, 48(3): 1175–1218, 2018 (joint work with Matthias A. Fahrenwaldt and Stefan Weber).

Acknowledgment

First and foremost, I wish to thank my supervisor Prof. Dr. Stefan Weber: for giving me the possibility to write this thesis in the first place, for providing an interdisciplinary, innovative, and inspiring working environment at the Institute of Probability and Statistics and the House of Insurance at Leibniz Universität Hannover, and for the instructive, supportive, strongly motivating, and always enthusiastic guidance throughout each stage of the PhD process.

Further, I would like to thank the members of my thesis committee: Prof. Dr. Agostino Capponi, Prof. Dr. Ralf Korn, and Prof. Dr. Luitgard A. M. Veraart for reviewing my thesis, and Prof. Dr. Marc Steinbach for taking the chair of the examination board.

Special thanks go to Prof. Dr. Agostino Capponi and Prof. Dr. Matthias A. Fahrenwaldt for two fruitful collaborations that led to the results building the basis of the third and fourth chapter of this thesis, see Awiszus, Capponi, and Weber (2020) and Fahrenwaldt, Weber, and Weske (2018), respectively.

Moreover, it is a great pleasure for me to thank the wonderful colleagues I met along the way. In particular, I wish to thank my friends and colleagues Sören Bettels, Dr. Anna-Maria Hamm, and Marcel Kleiber for sharing offices, ideas, comments, and many great times during the development of this thesis.

Lastly, I wish to thank my family, and especially my father, for all the love and support.